Analyse und Vergleich der Feinstrukturen von enzymatisch und fermentativ hergestellten, bakteriellen Homoexopolysacchariden

Dissertation

zur Erlangung des Doktorgrades der Naturwissenschaften
(Dr. rer. nat.)

der

Naturwissenschaftlichen Fakultät II

Chemie, Physik und Mathematik

der Martin-Luther-Universität

Halle-Wittenberg

vorgelegt von

Luise Sophia Ernst

Gutachter: Prof. Dr. Daniel Wefers, Martin-Luther-Universität Halle-Wittenberg
                     Prof. Dr. Mirko Bunzel, Karlsruher Institut für Technologie

Verteidigung: 27. September 2024

Inhaltsverzeichnis

Abkürzungsverzeichnis

CAZy	*Carbohydrate active enzymes* Datenbank
DMSO	Dimethylsulfoxid
DMAc	*N,N*-Dimethylacetamid
DSM	Deutsche Sammlung von Mikroorganismen und Zellkulturen GmbH (Leibniz-Institut in Braunschweig)
EC	*Enzyme commission*
EPS	Exopolysaccharide
FID	Flammenionisationsdetektor
Fru*f*	Fructofuranose
FS	Fructansucrase
GBD	Glucanbindedomäne
GC	Gaschromatographie
GH	*Glycoside Hydrolase*
Glc*p*	Glucopyranose
GS	Glucansucrase
GTF	Glucosyltransferase
HoEPS	Homoexopolysaccharide
HPAEC	Hochleistungsanionenaustauschchromatographie
HPSEC	Hochleistungsgrößenausschlusschromatographie
MALLS	Mehrwinkellaserlichtstreuung
MAS	*Magic angle spinning*
MMB	4-Methylmorpholinboran
MS	Massenspektrometrie
NMR	Kernspinresonanz
NRRL	*Agricultural Research Service Culture Collection* (Stammsammlung des *National Center for Agricultural Utilization Research* in Peoria, Illinois, USA)
PAD	Gepulste amperometrische Detektion
PMAA	Partiell methylierte Alditolacetate
RI	Brechungsindex
SMUT	*Streptococcus mutans*
SSAL	*Streptococcus salivarius*
TFA	Trifluoressigsäure
XRD	Röntgendiffraktion

1 Einleitung

Milch- und Essigsäurebakterien sind in unserer Umgebung weit verbreitet und spielen zum Beispiel in fermentierten Lebensmitteln oder der Zahnplaque eine wichtige Rolle. Viele von ihnen bilden extrazelluläre Polysaccharide (Exopolysaccharide, EPS), wobei je nach Biosyntheseweg und Monosaccharidzusammensetzung zwischen Homoexopolysacchariden (HoEPS) und Heteroexopolysacchariden unterschieden wird. Letztere haben einen aufwendigeren Syntheseweg und geringere Ausbeuten als HoEPS (Bowen *et al*., 2018; Lynch *et al*., 2018; Wünsche & Schmid, 2023; Yassunaka Hata *et al*., 2023). Die meisten HoEPS werden aus Saccharose (β-D-Fructofuranosyl-(2,1)-α-D-Glucopyranosid) durch die extrazellulären Enzyme Fructansucrase (FS) und Glucansucrase (GS) gebildet. FS synthetisieren unter Freisetzung von Glucose Fructane, welche aus β-D-Fructofuranose-Einheiten (Fru*f*) aufgebaut sind. GS bilden unter Freisetzung von Fructose Glucane, die aus α-D-Glucopyranose-Einheiten (Glc*p*) bestehen (Jakob *et al.*, 2019; Leemhuis *et al.*, 2013; van Hijum *et al*., 2006). Grundsätzlich werden Fructane in Inuline (2,1-Fru*f*) und Levane (2,6-Fru*f*) unterteilt, die an Position *O*6 bzw. *O*1 verzweigt sein können (Ni *et al*., 2019; Öner *et al*., 2016). Die am weitesten verbreiteten bakteriellen α-Glucane werden nach dem im Rückgrat vorwiegend vorliegenden Verknüpfungstyp als Dextrane (1,6-Verknüpfungen) und Mutane (1,3-Verknüpfungen) bezeichnet. Sie können je nach Verknüpfungstyp im Rückgrat an Position *O*2, *O*3, *O*4 oder *O*6 verzweigt sein (Monsan *et al*., 2001). Neben diesen grundlegenden Strukturmerkmalen unterscheiden sich HoEPS in ihren Feinstrukturen. Durch die verschiedenen Verknüpfungstypen und Verzweigungen in unterschiedlichen Anteilen, Längen und Verteilungen können HoEPS komplexe Strukturen aufweisen, wobei manche HoEPS Abschnitte mit unterschiedlicher Struktur besitzen. Zudem variiert die Molekülgrößenverteilung und Wasserlöslichkeit von HoEPS (Monsan *et al*., 2001). Weiterhin wurde für wasserunlösliche α-Glucane die Ausbildung von starren, kristallähnlichen Bereichen beschrieben (Kobayashi *et al*., 2017; Ogawa *et al*., 1994). Obwohl HoEPS lediglich aus einer Art Monosaccharid bestehen, sind ihre Strukturen bis heute nur in Teilen verstanden. Dies liegt unter anderem an analytischen Herausforderungen, aber auch an der Varianz der einzelnen HoEPS-Strukturen in Abhängigkeit ihrer Herkunft. Zur detaillierten Strukturaufklärung von HoEPS ist eine Kombination verschiedener Analysemethoden nötig (Côté *et al*., 1999; Kusumi *et al.*, 2023; Münkel *et al*., 2019), wobei Ergebnisse, die mit unterschiedlichen Methoden ermittelt wurden, selten direkt vergleichbar sind. Manche Bakterienstämme produzieren mehreren Sucrasen und sind daher in der Lage, diverse HoEPS zu synthetisieren (van Hijum *et al*., 2006). In ihren natürlichen Vorkommen bestimmt die Kombination aus Bakterien und ihren Enzymen die Synthese und die Strukturen der HoEPS, während im Labor einzelne Bakterienstämme und Enzyme zur Synthese von HoEPS verwendet werden können. Dennoch sind derzeit kaum vergleichende Untersuchungen verschiedener HoEPS vorhanden.

Für die Bakterien haben HoEPS vielfältige Funktionen, die bis heute nicht vollständig verstanden sind. Als strukturgebender Teil des Biofilms dienen HoEPS den Bakterien vermutlich zur Anhaftung an Oberflächen und als Schutz vor Umwelteinflüssen. Daneben wird diskutiert, ob HoEPS als extrazelluläre Kohlenhydratreserve dienen (Caggianiello *et al.*, 2016; Dogsa *et al.*, 2013; Koczan *et al.*, 2009; Laue *et al.*, 2006). In der menschlichen Mundhöhle stellen besonders wasserunlösliche Glucane aber auch Fructane einen Virulenzfaktor bei der Kariesentstehung dar. Sie ermöglichen kariogenen Bakterien wie *Streptococcus mutans* die Adhäsion an der Zahnoberfläche und das Einstellen einer für sie optimalen Mikroumgebung (Bowen & Koo, 2011; Chakraborty *et al.*, 2022; Ebisu *et al.*, 1975; Hotz *et al.*, 1972; Koo *et al.*, 2013; Rozen *et al.*, 2001; Takahashi & Nyvad, 2008; Tsumori & Kuramitsu, 1997; Wenham *et al.*, 1981). Neben der unerwünschten Rolle in der Kariesentstehung haben HoEPS auch für den Menschen nützliche Eigenschaften. Wasserunlösliche Glucane könnten (chemisch modifiziert) als neue bio-basierte Materialien, wie beispielsweise Fasern und Filme, verwendet werden (Fukata *et al.*, 2021; Puanglek *et al.*, 2016, 2017) und viele Anwendungen mit wasserunlöslichen Glucanen werden heutzutage patentiert (Adelman & Behabtu, 2022; Gangoiti *et al.*, 2018; Kim *et al.*, 2023; Nagy *et al.*, 2020). Wie viele Polysaccharide können wasserunlösliche Glucane Gele bilden (Padmanabhan *et al.*, 2003) und es liegen für chemisch modifizierte wasser-unlösliche Glucane Hinweise auf medizinischen Nutzen vor (Boddapati *et al.*, 2020; Buddana *et al.*, 2015). Im Vergleich zu wasserunlöslichen Glucanen sind wasserlösliche Glucane (Dextrane) hinsichtlich ihrer physikochemischen Eigenschaften und Anwendungsmöglich-keiten besser erforscht (Li *et al.*, 2020) und werden seit Jahrzenten als Blutplasmaersatz verwendet (Grönwall & Ingelman, 1945; Moffitt, 1975). Außerdem können Dextrane als Verdickungsmittel und Stabilisator in Konfitüre und Eiscreme verwendet werden und die Festigkeit von Joghurt steigern (Benhouna *et al.*, 2019; Nachtigall *et al.*, 2023; Zannini *et al.*, 2016). Daneben können sie das Brotvolumen erhöhen, Brotalterung vermindern und das Backen glutenfreien Brots vereinfachen (Galle *et al.*, 2012; Katina *et al.*, 2009; Wang *et al.*, 2021). Ernährungsphysiologisch sind bakterielle Glucane Ballaststoffe, deren präbiotische Eigenschaften mehrfach gezeigt wurden (Amaretti *et al.*, 2020; Das *et al.*, 2014; Kim *et al.*, 2022; Kothari *et al.*, 2015; Tingirikari *et al.*, 2014). Auch die physikochemischen Eigenschaften von Levanen sind vielversprechend für den Einsatz in Lebensmitteln (Xu *et al.*, 2018b). So erhöhten Levane von Essigsäurebakterien in Weizenbrot das Volumen, verbesserten die Textur und verzögerten das Altbackenwerden (Jakob *et al.*, 2012, 2013). In Joghurt konnten Levane als Stabilisatoren dienen (Xu *et al.*, 2022a). Daneben fungieren Levane in Lebensmitteln als Ballaststoffe (Adamberg *et al.*, 2015; Bello *et al.*, 2001; Cheng *et al.*, 2021; Xu *et al.*, 2023) und könnten in der Medizin vielseitig eingesetzt werden (Bouallegue *et al.*, 2020; de Siqueira *et al.*, 2020; Gamal *et al.*, 2021; Lee *et al.*, 2023; Pei *et al.*, 2020; Sarilmiser *et al.*, 2015; Srikanth *et al.*, 2015a, 2015b; Taylan *et al.*, 2019). Für pflanzliche Inuline sind gleichermaßen viele gesundheitlich positive Eigenschaften bekannt (Qin *et al.*, 2023; Shoaib *et al.*, 2016), während sie für bakterielle Inuline bisher nicht untersucht sind. Anders als pflanzliche Inuline werden bakterielle Inuline (noch) nicht industriell eingesetzt. Dabei haben mikrobielle Inuline durch ihre deutlich höheren Molekulargewichte andere Eigenschaften wie zum Beispiel erhöhte Löslich-keit, Gelbildung und Lagerstabilität als pflanzliche Inuline (Ni *et al.*, 2019, 2020).

Für jegliche Anwendung ist es von Vorteil, dass bakterielle α-Glucane und β-Fructane mit vergleichsweise wenig Ressourcen- und Energieaufwand synthetisierbar sind. So werden zur Synthese in wässriger Umgebung lediglich Saccharose und Bakterienkulturen oder isolierte Enzyme benötigt (Li *et al*., 2020). Gerade für den Einsatz in Lebensmitteln haben HoEPS gegenüber vielen anderen Polysacchariden und Zusatzstoffen einen Vorteil: HoEPS synthetisierende Bakterien werden zur Fermentation von Lebensmitteln verwendet und viele von ihnen besitzen den *generally recognized as safe* (GRAS)-Status der *U.S. Food and Drug Administration* (FDA) und den *qualified presumption of safety* (QPS)-Status der *European Food Safety Authority* (EFSA). Das bedeutet, dass sie bedenkenlos in Lebensmitteln eingesetzt werden können. Eine *in situ* Synthese von erwünschten HoEPS kann den Einsatz von (vom Verbraucher unerwünschten) Zusatzstoffen vermeiden (Zannini *et al*., 2016). Die Eignung von HoEPS für eine bestimmte Anwendung hängt von ihren physikochemischen Eigenschaften ab, die wiederum durch die Strukturen bedingt sind (Hundschell *et al*., 2020a, 2020b; Nachtigall *et al*., 2023). Um diese Zusammenhänge zu verstehen und HoEPS mit gewünschten Eigenschaften gezielt synthetisieren zu können, ist eine möglichst genaue Kenntnis der molekularen Strukturen erforderlich.

2 Theoretische Hintergründe

2.1 Methoden zur Strukturanalytik

Der erste Schritt einer Strukturanalyse von (Ho)EPS ist häufig die Bestimmung der enthaltenen Monosaccharide. Diese erfolgt meist nach saurer Hydrolyse mit Schwefelsäure, Salzsäure, Oxalsäure oder Trifluoressigsäure (TFA) bei erhöhter Temperatur (60 - 130 °C) (Dimler *et al.*, 1954; Franz, 1991). Im Vergleich zu anderen Säuren bietet TFA den Vorteil, dass sie vollständig durch Verdampfung aus dem Reaktionsgemisch entfernt werden kann (Biermann, 1988) und bei der anschließenden Analyse nicht stört. Die optimalen Bedingungen zur vollständigen Hydrolyse aller glycosidischen Bindungen unter minimalem Abbau der freigesetzten Monosaccharide sind nicht für alle HoEPS beschrieben. Grundsätzlich sind zur Hydrolyse von α-Glucanen vergleichsweise harsche Bedingungen nötig. Sie werden zum Beispiel mit 2 M TFA bei 121 °C für 90 min oder 3 M TFA bei 130 °C für 2 h hydrolysiert (Dimler *et al.*, 1954; Fels *et al*., 2018; Tan *et al*., 2022), wonach Fructose in der Regel nicht mehr nachweisbar ist. Für β-Fructane sind mildere Bedingungen, wie 1 M TFA bei 60 oder 70 °C für 30 min, empfehlenswert (Franz, 1991; Pollock & Cairns, 1991). Nach der Hydrolyse erfolgt die Quantifizierung der Monosaccharide häufig über Hochleistungsflüssigchromatographie oder Gaschromatographie (GC). Für GC-Analysen ist der apparative Aufwand vergleichsweise gering, allerdings müssen Monosaccharide für die gaschromatographische Trennung derivatisiert werden. Hierbei sollte eine Reduktion der anomeren Kohlenstoffatome für die gleichzeitige Analyse von Glucanen und Fructanen vermieden werden, da sowohl aus Glucose als auch aus Fructose ein Sorbit-Derivat erhalten wird (Ruiz-Matute *et al.*, 2011). Flüssigchromatographisch können Monosaccharide über Hochleistungsanionenaustauschchromatographie (HPAEC) gekoppelt mit gepulster amperometrischer Detektion (PAD) ohne Derivatisierung quantifiziert werden (Cataldi *et al.*, 2000).

Die ^{1}H- und ^{13}C-Flüssig-Kernspinresonanz (NMR)-Spektroskopie eignet sich, um HoEPS zerstörungsfrei anhand ihrer Hauptverknüpfungstypen zu unterscheiden. Außerdem liefert sie grobe Informationen über die enthaltenen Verzweigungen. Zur detaillierten Strukturaufklärung von EPS eignen sich zweidimensionale Experimente wie *correlated sprectroscopy* (COSY) oder *heteronuclear single quantum coherence* (HSQC)-Experimente (Matulová *et al*., 2011; van Leeuwen *et al*., 2008b). Allerdings lassen sich Strukturelemente, die nur einen kleinen Anteil an der Gesamtstruktur ausmachen, meist nicht nachweisen. Dies liegt neben der zu geringen Empfindlichkeit an Signalüberlappungen durch ähnliche chemische Verschiebungen der Atomkerne in HoEPS. Meistens müssen die genauen chemischen Verschiebungen anhand von bekannten Einheiten (Polysaccharide mit einem Verknüpfungstyp oder Oligosaccharide) bestimmt werden (Münkel *et al*., 2020). Eine erfolgreiche Zuordnung erlaubt Einblicke in die Feinstrukturen von HoEPS, liefert allerdings keine Informationen über die Anordnung der

einzelnen Strukturelemente innerhalb der HoEPS. Außerdem bilden manche EPS Gele oder hoch viskose Lösungen, was zu Signalverbreiterung und damit reduzierter Auflösung führen kann (El Hariri El Nokab & van der Wel, 2020). Für wasserunlösliche Glucane muss zudem individuell ein geeignetes Lösungsmittel gefunden werden (zum Beispiel Dimethylsulfoxid-d_6 (DMSO-d_6) (Choma *et al.*, 2013; Münkel *et al.*, 2019; Puanglek *et al*., 2016) oder NaOD in D_2O (Wang *et al.*, 2007; Wangpaiboon *et al.*, 2020)), in dem die Glucane vollständig gelöst sind und die Viskosität der Lösung nicht zu hoch ist. Dies erschwert die Analyse wasserunlöslicher HoEPS mit Flüssig-NMR-Spektroskopie.

Eine universelle Methode zur Bestimmung der Verknüpfungstypen stellt die Methylierungs-analyse dar, mit der auch in wasserunlöslichen HoEPS alle glycosidischen Bindungen und ihre Anteile ermittelt werden können. Hierzu werden die frei vorliegenden Hydroxygruppen der HoEPS methyliert und die glycosidischen Bindungen hydrolysiert. Anschließend werden die partiell methylierten Monosaccharide unter Deuterium-Markierung des anomeren Kohlen-stoffatoms reduziert und alle durch Hydrolyse und Reduktion frei gewordenen Hydroxygruppen acetyliert. Die Analyse der partiell methylierten Alditolacetate (PMAA) erfolgt gaschromato-graphisch mit massenspektrometrischer und Flammenionisationsdetektion (GC-MS/FID) (Ciucanu & Kerek, 1984; Harris *et al.*, 1984). Die PMAA sind über ihre charakteristischen Fragmentierungsmuster aus der Elektronenstoßionisation identifizierbar. Hierbei werden bevorzugt Bindungen zwischen zwei methoxylierten Kohlenstoffatomen gespalten, wodurch wenige Primärfragmente entstehen, von denen teilweise charakteristische Neutralfragmente abgespalten werden (Björndal *et al.*, 1967). In Ermangelung von PMAA-Standardsubstanzen wird meist die FID zur (semi)quantitativen Auswertung herangezogen, da hierfür Response-faktoren berechenbar sind (Sims *et al*., 2018). Anders als bei der NMR-Spektroskopie werden auch Verknüpfungen mit geringem prozentualem Anteil erfasst, jedoch keine Informationen über die (anomeren) Konfigurationen erhalten. Zudem wird die Methylierungsanalyse nicht immer durchgeführt, da der experimentelle Aufwand vergleichsweise hoch ist. Den Grundstein für die Methylierungsanalyse legten die Alkylierungsverfahren von Purdie & Irvine (1903) sowie Haworth (1915), die von Hakomori (1964) optimiert wurden. Hierbei werden die Kohlenhydrate mit Methyliodid permethyliert, wobei frisch aus DMSO und NaH generierte Methylsulfinyl-carbanionen die Hydroxygruppen deprotonieren. Diese Methode wurde von Ciucanu & Kerek (1984) durch die Verwendung von NaOH als Base für bessere Ausbeuten optimiert. Bis heute werden Polysaccharide im Zuge der Methylierungsanalyse meist nach der Methode von Ciucanu & Kerek (1984) methyliert und dafür zunächst in DMSO gelöst bzw. gequollen und durch NaOH$_{(s)}$ deprotoniert. Nach der Methylierung durch Methyliodid werden sie in der Regel mit TFA hydrolysiert (Carpita *et al*., 1991; Fels *et al*., 2018; van Geel-Schutten *et al*., 1999; Sims *et al.*, 2018). Die freigesetzten partiell methylierten Monosaccharide werden dann durch NaBD$_4$ in alkalischem Milieu reduziert. Die Verwendung von 1-Methylimidazol als Katalysator erlaubt die anschließende Acetylierung der freien Hydroxygruppen durch Acetanhydrid ohne vor-herige Borat-Entfernung (Blakeney *et al.*, 1983; Sims *et al.*, 2018). Mit dieser Methode können alle Derivatisierungsschritte (Abbildung 2.1) in einem Reaktionsgefäß durchgeführt werden, wodurch Analytverluste vermieden werden (Harris *et al.*, 1984).
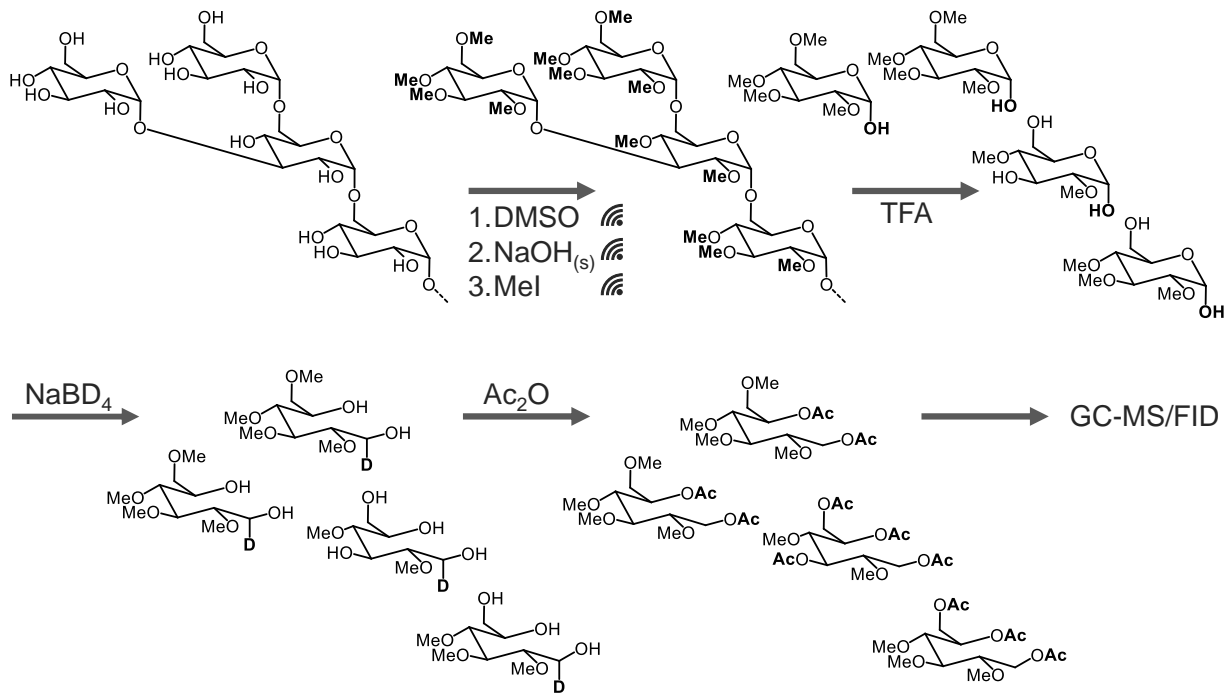
Abbildung 2.1: Schritte der Methylierungsanalyse am Beispiel eines Glucanausschnitts: Quellen/Lösen der Probe in Dimethylsulfoxid (DMSO), Deprotonierung durch NaOH(s), Methylierung durch Methyliodid (MeI) jeweils mit anschließender Ultraschallbehandlung ($\approx$), Hydrolyse durch Trifluoressigsäure (TFA), Reduktion durch NaBD$_4$ und Acetylierung durch Acetanhydrid (Ac$_2$O). Die Analyse der partiell methylierten Alditolacetate erfolgt durch Gaschromatographie mit massenspektrometrischer und Flammenionisationsdetektion (GC-MS/FID).

Durch die vielen Derivatisierungsschritte und die Vielzahl unterschiedlicher HoEPS existieren viele Variablen, die die Ergebnisse der Methylierungsanalyse beeinflussen können. Ein Problem ist die unvollständige Methylierung der Hydroxygruppen, was als Untermethylierung bezeichnet wird und zur Überbestimmung von mehrfach substituierten Einheiten führt. Zur Vermeidung von Untermethylierung werden die Schritte zur Methylierung meist zweimal durchgeführt (Li *et al*., 2012; Sims *et al*., 2018). Das Problem der Untermethylierung besteht vor allem bei in DMSO unlöslichen HoEPS. Zur besseren Quellung werden häufig Ultraschallbehandlungen vor der Derivatisierung, nach Zugabe von NaOH(s) und nach Zugabe von Methyliodid angewandt (Fels *et al*., 2018; Li *et al*., 2012; Wangpaiboon *et al*., 2020). Jedoch ist auch bekannt, dass Ultraschalleinwirkung bei Polysacchariden zu Kettenbrüchen führen kann (Basedow *et al*., 1978; Cui & Zhu, 2021; Huang *et al*., 2015; Kardos & Luche, 2001), was folglich in einer Überbestimmung von terminalen Einheiten resultieren würde. Daneben können die Bedingungen während der Hydrolyse die erhaltenen Ergebnisse beeinflussen. Auch für die Hydrolyse im Rahmen der Methylierungsanalyse ist TFA besonders geeignet, da sie durch Evaporation aus dem Reaktionsgemisch entfernt werden kann, was die anschließende Reduktion durch NaBD$_4$ in alkalischem Milieu vereinfacht (Pettolino *et al.*, 2012; Sims *et al.*, 2018). Im Rahmen der Hydrolyse sollen die glycosidischen Bindungen der methylierten HoEPS vollständig gespalten werden, ohne dass ein Abbau der bereits freigesetzten partiell methylierten Monosaccharide stattfindet. Da Hydrolyserate und Abbaureaktionen von den vorliegenden Polysacchariden (α-/β-Konfiguration, Pyranose/Furanose, Aldose/Ketose) abhängen

(Biermann, 1988), sind je nach HoEPS unterschiedliche Bedingungen nötig (Sims *et al.*, 2018). Für bakterielle α-Glucane wurde im Zuge der Methylierungsanalyse 2 M TFA bei 121 °C für 1,5 - 2 h bzw. bei 125 °C für 1 h oder 2,5 M TFA bei 100 °C für 4 h beschrieben (Fels *et al.*, 2018; Kralj *et al.*, 2004a, 2004b; Maina *et al.*, 2011; Wangpaiboon *et al.*, 2020), während für Fructane 1 M TFA bei 70 °C für 30 min oder 2 M TFA bei 60 °C für 30 min verwendet wurde (Carpita *et al.*, 1991; Pollock *et al.*, 1979). Bei der Reduktion der Ketose Fructose entstehen die zwei Epimere Sorbit und Mannit. Entsprechend entstehen in der Methylierungsanalyse Sorbit- und Mannit-Derivate (Abbildung 2.2). Sind in der Probe Fructane mit 2,6- und 2,1-glycosidischen Bindungen vorhanden, werden neben beiden Sorbit-Derivaten zwei koeluierende Mannit-Derivate erhalten. Letztere unterscheiden sich lediglich in der Position des Deuteriumatoms. Dadurch können sie massenspektrometrisch differenziert, jedoch nicht einzeln über die FID-Peakfläche quantifiziert werden (Kralj *et al.*, 2018; Sims *et al.*, 2018).
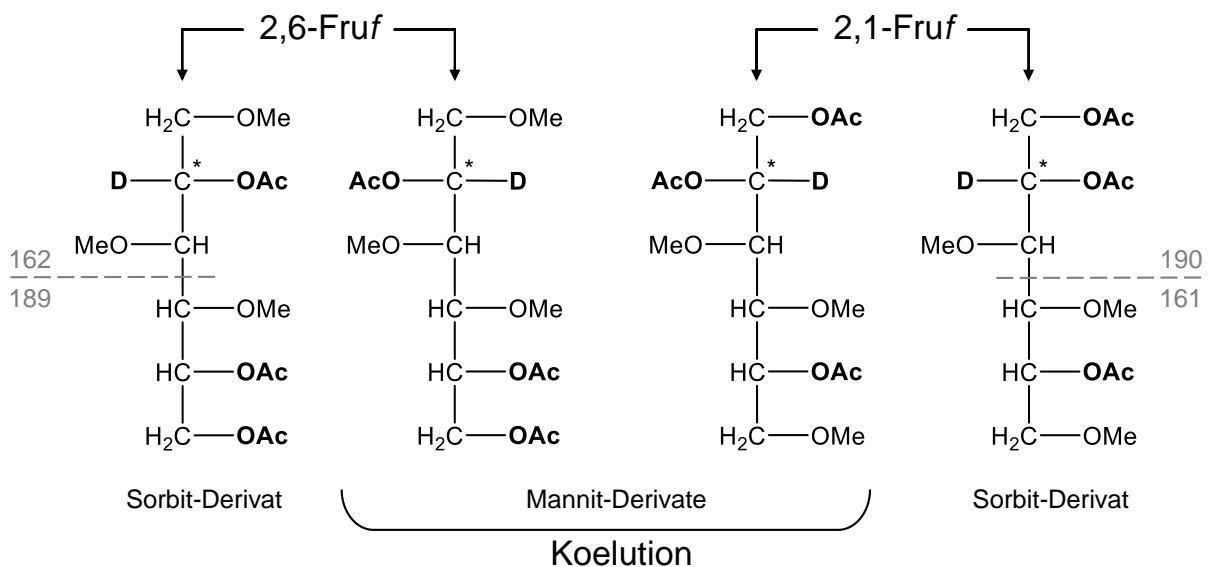
Abbildung 2.2: Partiell methylierte Alditolacetate, die in der Methylierungsanalyse aus 2,6- und 2,1-verknüpfter Fructofuranose (Fru*f*) entstehen. Die durch die Reduktion mit NaBD$_4$ gebildeten Stereozentren sind mit Sternchen (*) markiert. Die Mannit-Derivate von 2,6- und 2,1-Fru*f* koeluieren und können über die Differenz im Masse-zu-Ladungsverhältnis ihrer Fragmente von 1 *m/z* unterschieden werden. Die Masse-zu-Ladungsverhältnisse der Primärfragmente sind beispielhaft an beiden Sorbit-Derivaten eingezeichnet.

Ergänzend zur Methylierungsanalyse können Informationen über die Art der glycosidischen Bindungen und die Feinstrukturen der HoEPS mit Hilfe von *endo*-Hydrolasen erhalten werden (Fels *et al.*, 2018; Katina *et al.*, 2009; Shi *et al.*, 2019; Yi *et al.*, 2015). *Endo*-Fructanasen sowie *endo*-Glucanasen hydrolysieren spezifisch die unverzweigten Abschnitte der HoEPS mit dem entsprechenden Verknüpfungstyp (Inulinasen: β-2,1-Fru*f*, Levanasen: β-2,6-Fru*f*, Dextranasen: α-1,6-Glc*p*, Mutanasen: α-1,3-Glc*p*) und setzen dadurch Mono- und Disaccharide sowie verzweigte Oligo- und Polysaccharide frei. Außerdem können lineare Oligo- und Polysaccharide mit den je nach *endo*-Hydrolase nicht-hydrolysierbaren Verknüpfungstypen freigesetzt werden. Weitere Informationen zu den vorliegenden Poly- und Oligosacchariden können durch den Einsatz von *exo*-Glucosidasen und *exo*-Fructosidasen erhalten werden (Burne *et al.*, 1987;

8

Igarashi *et al*., 1992; Jeza *et al*., 2018; Khalikova *et al*., 2005; Wiater *et al*., 2005). *Debranching*-Enzyme können von Dextranen die Seitenketten an Position *O*2 abspalten (Mitsuishi *et al*., 1980; Miyazaki, 2023), während *debranching*-Enzyme mit anderer Substrat-Spezifität nicht beschrieben sind. Eine geeignete Trennung aller freigesetzten Oligosaccharide bietet die HPAEC, wobei die PAD eine empfindliche und selektive Detektion ermöglicht. Für eine eindeutige Identifizierung und Quantifizierung müssen die jeweiligen Oligosaccharide als Standardsubstanzen vorliegen. Da nur wenige Oligosaccharide aus HoEPS kommerziell erhältlich sind, ist es oft notwendig die verschiedenen Oligosaccharide präparativ zu isolieren und ihre Strukturen aufzuklären. Bisher erfolgte dies hauptsächlich für Oligosaccharide aus Dextranen bzw. Dextran-ähnlichen Glucanen, wobei die NMR-Spektroskopie zur Struktur-aufklärung der Oligosaccharide verwendet wurde (Maina *et al*., 2011; Münkel *et al*., 2019, 2020; Münkel & Wefers, 2019). Mithilfe von MS/MS können ebenfalls Rückschlüsse auf die Oligo-saccharidstrukturen gezogen werden, allerdings ist mit dieser Methode allein meist keine eindeutige Strukturaufklärung möglich (Maina *et al*., 2013; Yi *et al.*, 2015). Viele *endo*-Hydrolasen können aufgrund ihres pH-Optimums im schwach sauren Bereich in Reinstwasser ohne Puffer hydrolysieren, wodurch eine Beeinflussung der anschließenden chromato-graphischen Trennung der Hydrolyseprodukte durch Puffersalze oder deren vorherige Abtrennung vermieden werden kann. Nicht kommerziell erhältliche Hydrolasen können im Labor aus Kulturen der Herkunftsorganismen isoliert oder rekombinant hergestellt werden. Wenn geeignete Enzyme nicht vorliegen, bietet die partielle Säurehydrolyse eine Alternative. Allerdings ist diese weniger spezifisch als die enzymatische Hydrolyse. Auch wenn Unterschiede in der Säurelabilität verschiedener glycosidischer Bindungen existieren und Seitenketten scheinbar bevorzugt hydrolysiert werden (Sidebotham, 1974), werden sehr heterogene Produktspektren erhalten und häufig dominieren Oligosaccharide mit dem Hauptverknüpfungstyp die Chromatogramme der Hydrolysate. Dadurch ist eine vergleichende Analyse der Feinstrukturen verschiedener HoEPS nicht möglich.

Abgesehen von den glycosidischen Bindungen und den Feinstrukturen sind die Größenverteilung und Anordnung der HoEPS-Moleküle wichtige Strukturmerkmale. Zur Bestimmung der Molekülgröße von HoEPS eignet sich die Hochleistungsgrößenausschluss-chromatographie (HPSEC) (Han *et al*., 2021; Isenberg *et al*., 2010; Kim *et al*., 1982; Merienne *et al*., 2000; Nachtigall *et al*., 2023; Ronkart *et al*., 2007). Hierbei werden die Moleküle nach ihrem hydrodynamischen Volumen getrennt und die Bestimmung der Molekulargewichte erfolgt häufig über Vergleichsstandards und Brechungsindex (RI)-Detektion. Alternativ kann das absolute Molekulargewicht über einen zusätzlich zum RI-Detektor angeschlossenen Mehr-winkellaserlichtstreu (MALLS)-Detektor ermittelt werden. Voraussetzung hierfür ist, dass das RI-Inkrement vorher ermittelt wurde und die exakte Probenmenge bekannt ist (Matson *et al*., 2024). Das bedeutet, dass das Polysaccharid möglichst rein vorliegen und vollständig im Eluenten gelöst sein muss, was besonders für wasserunlösliche Polysaccharide eine Herausforderung darstellt. Neben *N,N*-Dimethylacetamid (DMAc) wird in vielen Studien DMSO mit Salzzusätzen als Lösungsmittel für Polysaccharide und Elutionsmittel für die HPSEC verwendet (Merienne *et al*., 2000; Qin *et al*., 2013; Schult *et al*., 2002; Yokoyama *et al*., 1998).

Informationen über starre und bewegliche sowie kristalline Bereiche wasserunlöslicher HoEPS können die Festkörper-NMR-Spektroskopie und die Röntgendiffraktion (XRD) liefern. In ^{13}C-*magic angle spinning* (MAS)-*direct polarization*-NMR-Spektren sind vor allem Peaks der mobilen Atomkerne eines Polysaccharids zu sehen, während in ^{13}C-MAS-*cross polarization*-NMR-Spektren bei kurzer Kontaktzeit Peaks von Atomkernen in starren und bei längerer Kontaktzeit zusätzlich Peaks von Atomkernen in weniger starren, aber nicht beweglichen Regionen zu sehen sind (Perez Garcia *et al*., 2012; Renard & Jarvis, 1999; Wang & Hong, 2016). Darüber hinaus weisen schmale Peaks und eine gute Auflösung in *cross polarization*-NMR-Spektren darauf hin, dass alle chemisch identischen Atomkerne auch ähnliche magnetische Umgebungen haben, was entweder in Kristallen oder in flüssigen Proben (häufig auch hydratisierte, amorphe Polysaccharide) der Fall ist. Bei Letzteren gleicht die Kettenbewegung die unterschiedlichen magnetischen Umgebungen aus (Poulhazan *et al*., 2018). Breite Peaks in *cross polarization*-NMR-Spektren deuten dagegen auf unterschiedliche magnetische Umgebungen hin, was in starren, amorphen Strukturen der Proben der Fall ist (Horn *et al*., 1987). Die aus den Spektren erhaltenen Informationen über die Beweglichkeit lassen sich über die chemischen Verschiebungen der Atomkerne den Einheiten im Polysaccharid zuordnen. Bei ausreichend großen kristallinen Bereichen in HoEPS sind Peaks in Abhängigkeit von der Kristallstruktur bei unterschiedlichen Beugungswinkeln im Röntgendiffraktogramm zu sehen. Dadurch können Strukturunterschiede in den kristallinen Bereichen zwischen verschiedenen HoEPS identifiziert werden. Das Verhältnis von kristallinen zu amorphen Bereichen ist bei Polysacchariden häufig nicht bestimmbar (Seidi *et al*., 2022).

Eine weitere Herausforderung bei der Analyse von HoEPS ist, dass bei fermentativen HoEPS-Synthesen eine Mischung aus Glucanen und Fructanen entstehen kann. Einige Analysen können problemlos aus der Mischung erfolgen (beispielsweise Oligosaccharidanalyse nach enzymatischer Hydrolyse). Bei anderen Methoden ergeben sich Schwierigkeiten, wie Signalüberlappungen in der NMR-Spektroskopie oder unterschiedliche Probenvorbereitungen zur Analyse von Monosacchariden oder Bindungstypen. Hier kann die Trennung von Glucanen und Fructanen hilfreich sein, was in der Literatur jedoch selten beschrieben wurde. Birkhed *et al.* (1979) verwendeten wässrige Ba(OH)$_2$-Lösung zur selektiven Präzipitation von Fructanen aus der Mischung. Andere Autoren nutzten die fraktionierende Präzipitation mit unterschiedlichen Ethanolkonzentrationen, was allerdings nur bei großen Molekulargewichtsunterschieden geeignet und deshalb selten anwendbar ist (Sidebotham, 1974). Alternativ ist ein selektiver Abbau von jeweils einem der HoEPS durch enzymatische Hydrolyse und anschließender Abtrennung der entstandenen Hydrolyseprodukte möglich. Hierfür ist ein vollständiger Abbau zu niedermolekularen Poly-/Oligosacchariden und eine ausreichende Probenmenge Voraussetzung.

2.2 α-Glucane

α-Glucane werden durch GS von Milchsäurebakterien synthetisiert, wobei viele Stämme den Gattungen *Streptococcus, Lactobacillus, Oenococcus, Weissella* und *Leuconostoc* angehören (CAZy, 2024; Kralj *et al*., 2004a; Nachtigall *et al*., 2023; Rühmkorf *et al*., 2013; Tsumuraya & Misaki, 1979; Vuillemin *et al*., 2018). Beim Vorliegen von Saccharose können die Bakterien beachtliche Mengen wasserlöslicher und -unlöslicher α-Glucane bilden.

2.2.1 Glucansucrasen & Glucanhydrolasen

Glucansucrasen (GS, in der Literatur häufig unspezifisch Glucosyltransferase (GTF) genannt) sind extrazelluläre Enzyme, die je nach Art der von ihnen synthetisierten Glucane auch als Dextransucrasen (*enzyme commission* Nummer (EC) 2.4.1.5) und Mutansucrasen (EC 2.4.1.125) bezeichnet werden (Leemhuis *et al*., 2013; van Hijum *et al*., 2006). Anhand ihrer Aminosäuresequenz werden GS von der *Carbohydrate active enzymes* Datenbank (CAZy) in die *Glycoside Hydrolase* (GH) Familie 70 eingeordnet (CAZy, 2024). GH70-Enzyme sind mit GH13- und GH77-Enzymen eng verwandt und bilden mit ihnen den GH-H Clan. Seit 2010 wurden mehrere Kristallstrukturen (gekürzter) GS aufgeklärt (Brison *et al*., 2012; Ito *et al*., 2011; Pijning *et al*., 2008, 2012; Schormann *et al*., 2023; Vujicic-Zagar *et al*., 2010). Die meisten GS haben vier Regionen: Ein Signalpeptid, eine *N*-terminale variable Region mit verschiedenen Aminosäure-Wiederholeinheiten, eine konservierte katalytische Domäne und eine *C*-terminale Glucan-Bindedomäne (GBD) (Leemhuis *et al*., 2013; Meng *et al*., 2016b; Molina *et al*., 2021). Alle GS benötigen Ca^{2+} zur Stabilisierung ihrer Struktur und besitzen drei katalytische Aminosäuren: eine Asparaginsäure als Nukleophil, eine als Säure/Base fungierende Glutaminsäure und eine den Übergangszustand stabilisierende Asparaginsäure. GS katalysieren mit einem „α-*retaining*"-Mechanismus, was bedeutet, dass sich die Glc*p* vor und nach der Reaktion in α-Konfiguration befindet. Dies wird durch ein Zwischenprodukt ermöglicht: Das Sauerstoffatom der glycosidischen Bindung des Substrats Saccharose wird durch Glutaminsäure protoniert, sodass Aspartat nukleophil am anomeren Kohlenstoffatom der Glc*p* angreifen und diese in β-Konfiguration kovalent binden kann. Die Fru*f*-Einheit wird freigesetzt. Glutamat deprotoniert eine Hydroxygruppe am nicht-reduzierenden Ende eines Akzeptormoleküls, sodass das freie Elektronenpaar nukleophil am anomeren Kohlenstoffatom der β-Glc*p*-Einheit angreifen kann. Das Akzeptormolekül verlässt das aktive Zentrum um eine Glc*p*-Einheit verlängert. Neben Saccharose und Glucanen können H_2O oder andere Moleküle mit Hydroxygruppe als Akzeptormoleküle fungieren, was entsprechend zur Hydrolyse des Substrats oder zu einer sogenannten Akzeptorreaktion der GS führt (Leemhuis *et al*., 2013; Molina *et al*., 2021).

Das Zwischenprodukt wird durch mehrere umliegende Aminosäuren so stabilisiert, dass sich die β-gebundene Glc*p*-Einheit an *subsite* (Position) -1 der GS (Nomenklatur nach Davies *et al*., 1997) befindet. Weitere Bindestellen in Richtung nicht-reduzierendem Ende existieren nicht, sodass GS nur eine Glc*p*-Einheit und keine Di- oder Oligosaccharide übertragen. Die Tasche

des aktiven Zentrums und die Aushöhlung der GBD von verschiedenen GS unterscheiden sich. Anders als *subsite* -1 ist *subsite* +1 wenig konserviert, sodass verschiedene GS unterschiedliche Produktspezifitäten haben. Außerdem können Akzeptormoleküle häufig in verschiedener Weise an eine GS binden, sodass diese GS die Bildung von zwei unterschiedlichen glycosidischen Verknüpfungen und Verzweigungen katalysiert (Leemhuis *et al.*, 2013; Molina *et al.*, 2021). Allerdings wurden bislang nur wenige GS beschrieben, die drei lineare Verknüpfungstypen (1,4-, 1,3- und 1,6-Verknüpfungen) synthetisieren können (Funane *et al.*, 2001; Hayacibara *et al.*, 2004; van Leeuwen *et al.*, 2008c). Mutationen in *subsites* +1 und +2 sowie im aktiven Zentrum führen zu unterschiedlichen Verhältnissen der Bindungstypen und Feinstrukturen im Glucan. Die Substitution weniger Aminosäuren reicht, um die Struktur der synthetisierten Glucane grundlegend zu verändern (Gangoiti *et al.*, 2018; Kang *et al.*, 2011; Kralj *et al.*, 2005; Meng *et al.*, 2016a; Münkel *et al.*, 2020; van Leeuwen *et al.*, 2008a; van Leeuwen *et al.*, 2009). Ein Aminosäurerest in *subsite* +2 scheint entscheidenden Einfluss auf das Produkt zu haben: Threonin in Dextransucrasen ist mit der Bildung von 1,6-Verknüpfungen und wasserlöslichen Glucanen assoziiert, während Asparaginsäure in Mutansucrasen mit der Bildung von 1,3-Verknüpfungen und wasserunlöslichen Glucanen verbunden zu sein scheint (Côté & Skory, 2014; Monchois *et al.*, 2000; Schormann *et al.*, 2023; Shimamura *et al.*, 1994). Die GS DEX-N von *Leuconostoc citreum* ABK-1 synthetisiert Glucane, die sich in zwei Fraktionen aufteilen lassen: wasserlösliche, hauptsächlich 1,6-verknüpfte Glucane und wasserunlösliche, 1,3- und 1,6-verknüpfte Glucane (Wangpaiboon *et al.*, 2020). Der Einfluss von *N*-terminalen und *C*-terminalen Domänen auf das Produktspektrum ist bisher nur für einzelne GS untersucht worden und nicht vollständig verstanden (Bechtner *et al.*, 2022; Kralj *et al.*, 2004b; Monchois *et al.*, 1999). Außerdem liegen Hinweise vor, dass die Art der synthetisierten Bindung von der zuvor existierenden glycosidischen Bindung am nicht-reduzierenden Ende abhängen kann (Molina *et al.*, 2019; van Leeuwen *et al.*, 2008a).

Zur Bestimmung der Aktivität von GS werden verschiedene, unterschiedlich genaue Methoden angewandt (Vettori *et al.*, 2011). Eine selten genutzte (beispielsweise von Bechtner *et al.*, 2019; Hellmuth *et al.*, 2008; Hill *et al.*, 2019; Jang *et al.*, 2006), aber sehr aussagekräftige und spezifische Methode ist die Quantifizierung von Glucose, Fructose und Saccharose in der Inkubationslösung. Hieraus lassen sich der Saccharoseumsatz, die Hydrolyse- und die Transferaseaktivität der GS berechnen. GS haben Temperaturoptima im Bereich von 30 - 37 °C, manchmal bis 45 °C, und pH-Optima im Bereich von 5,0 - 6,0 (Côté & Skory, 2012; Kim *et al.*, 2010; Kuramitsu, 1975; Miao *et al.*, 2017; Song *et al.*, 2016). Die Reaktionsbedingungen (Saccharosekonzentration, GS-Konzentration, Temperatur und pH-Wert) während der Glucansynthese beeinflussen neben der Ausbeute und Molekülgröße den Verzweigungsgrad der Produkte (Côté & Robyt, 1983; Côté & Skory, 2015; Falconer *et al.*, 2011; Kim *et al.*, 2003; Schmid *et al.*, 2019). GS können in Lösung oder an Oberflächen gebunden Glucane synthetisieren, was Einfluss auf die Anteile der Bindungstypen im Glucan haben kann (Hayacibara *et al.*, 2004; Kopec *et al.*, 1997; Vacca-Smith *et al.*, 1996). Manche GS benötigen bereits vorhandene Glucane, sog. „Primer-Glucane", um aktiv zu sein (Côté & Skory, 2016; Fukui *et al.*, 1982; Fukushima *et al.*, 1981; Konishi *et al.*, 1999; Simpson *et al.*, 1995).

Außerdem existieren sogenannte *branching*-Sucrasen, die an Position *O*2 oder *O*3 Glucose-Einheiten an Dextrane anfügen (Brison *et al*., 2013; Côté & Robyt, 1983; Passerini *et al.*, 2015; Vuillemin *et al.*, 2016).

Es existieren viele Glucan-spaltende Enzyme, die für die Strukturaufklärung von Glucanen nützlich sind (Kapitel 2.1). Von ihnen werden hier nur die für diese Arbeit relevanten beschrieben: *endo*-Dextranase, *endo*-Mutanase und α-Amylase. *Endo*-Dextranasen (EC 3.2.1.11) werden sowohl von Pilzen als auch Bakterien exprimiert und gehören zu den Familien GH49 (Pilze und Bakterien) und GH66 (nur Bakterien) (CAZy, 2024). Sie hydrolysieren α-1,6-verknüpfte Glc*p*-Einheiten und haben Temperaturoptima im Bereich von 40 - 60 °C und pH-Optima im Bereich von 5,0 - 6,5 (Hiraoka *et al*., 1973; Igarashi *et al*., 2004; Khalikova *et al*., 2005; Pittrof *et al*., 2021; Virgen-Ortíz *et al*., 2015; Volkov *et al*., 2019; Walker & Dewar, 1975; Wanda & Curtiss, 1994). Verschiedene Dextranasen haben unterschiedliche Produktspektren (Pittrof *et al*., 2021; Wang *et al*., 2023). *Endo*-Mutanasen sind α-1,3-Glucanasen (EC 3.2.1.59), die neben Glucose 1,3-verknüpfte Nigero-Oligosaccharide freisetzten. Sie werden von Pilzen, Hefen und Bakterien synthetisiert, wobei die *endo*-Mutanasen von Pilzen und Hefen in GH71 und die von Bakterien in GH87 eingeordnet werden (CAZy, 2024; Pleszczyńska *et al*., 2015). Allgemein haben bakterielle Mutanasen pH-Optima im Bereich von 5,0 - 8,5 und Temperaturoptima im Bereich von 40 - 55 °C (Boddapati & Gummadi, 2023; Buddana *et al*., 2019; Pleszczyńska *et al*., 2015). Bei der Glucansynthese anwesende Dextranasen und/oder Mutanasen beeinflussen die entstehenden Glucane durch ihre Hydrolyseaktivität. Neben Produktmenge und Anteilen an wasserlöslichen und -unlöslichen Glucanen können sich die Morphologie und die Anteile der glycosidischen Bindungen ändern (Hayacibara *et al*., 2004; Inoue *et al*., 1982). Glucane mit konsekutiven α-1,4-Verknüpfungen können durch α-Amylasen in kleinere Oligo- und Polysaccharide hydrolysiert werden. Es sind zahlreiche α-Amylasen bekannt, die in GH13, GH57, GH119 und GH126 eingruppiert werden (Paul *et al*., 2021; Sundarram & Murphy, 2014). Anders als durch *endo*-Dextranasen freigesetzte Oligosaccharide (Kapitel 2.1) wurden durch *endo*-Mutanasen und α-Amylasen freigesetzte verzweigte Oligosaccharide bisher nicht identifiziert und zur Feinstrukturanalyse von bakteriellen α-Glucanen verwendet.

2.2.2 Strukturen von bakteriellen α-Glucanen

Sowohl wasserlösliche als auch wasserunlösliche α-Glucane sind strukturell sehr divers, wobei dieselben Strukturmerkmale in unterschiedlichen Anteilen auftreten können und das Lösungsverhalten mancher Glucane von den vorliegenden Bedingungen abhängen kann. Dennoch ist die Unterscheidung nach Löslichkeit aus praktischen Gründen sinnvoll. Einerseits sind beide Gruppen durch Zentrifugation einfach trennbar und andererseits benötigen sie unterschiedliche analytische Herangehensweisen (Kapitel 2.1).

2.2.2.1 Wasserlösliche α-Glucane

Meistens werden wasserlösliche bakterielle α-Glucane nach den im Polysaccharid-Rückgrat vorliegenden glycosidischen Bindungen in Dextran (≥ 50 % 1,6-verknüpft), Reuteran (1,4- und 1,6-verknüpft) und Alternan (alternierend 1,6- und 1,3-verknüpft) eingeteilt. Im Vergleich zu Dextran sind Alternan und Reuteran selten und werden nur von einzelnen Bakterienstämmen gebildet. Alternan wird neben Dextranen von einigen *Leuconostoc* Stämmen gebildet (Côté & Robyt, 1982; Holt, 2017; Misaki *et al.*, 1980). Reuteran wird von *Limosilactobacillus reuteri* synthetisiert und hat circa 40 % 1,4-, 20 % 1,6- und 10 % 1,4,6-Verknüpfungen (Kralj *et al.*, 2002). Dahingegen werden Dextrane von vielen verschiedenen Bakterienarten synthetisiert, wodurch unterschiedliche Molekülgrößen und Strukturen existieren (Monsan *et al*., 2001; Zannini *et al*., 2016). Es wurden Molekulargewichte im Bereich von 0,1 bis 100 MDa bestimmt (Birkhed *et al*., 1979; Esmaeilnejad-Moghadam *et al*., 2019; Han *et al*., 2014; Llamas-Arriba *et al*., 2019; Shukla *et al*., 2014; Tang *et al*., 2018; Zarour *et al*., 2017). Neben den 1,6-Verknüpfungen können Dextrane auch 1,3-Verknüpfungen enthalten. Die meisten Dextrane weisen Seitenketten an Position *O*3 auf; seltener finden sich Seitenketten an Position *O*2 oder *O*4 sowie Dextrane mit Seitenketten an zwei verschiedenen Positionen.

Dextrane mit Seitenketten an Position *O*3 werden beispielsweise von *Leuconostoc mesenteroides* B-512 gebildet (circa 5 % 1,3,6-Glc*p*-Einheiten). Um die Länge der Seitenketten zu ermitteln, verwendeten Larm *et al.* (1971) einen schrittweisen chemischen Abbau, bei dem über β-Elimination jeweils eine terminale Einheit abspalten wurde. Die Produkte wurden durch Methylierungsanalyse untersucht und die Autoren folgerten, dass 40 % der Seitenketten monomer, 45 % dimer und der Rest oligomer vorliegen (Larm *et al.*, 1971). Diese Methode ist allerdings durch unvollständige Derivatisierungen sehr fehlerbehaftet. Vielversprechender ist die enzymatische Hydrolyse, mit der Taylor *et al.* (1985) Glucane von *Leuconostoc mesenteroides* B-512 und *Streptococcus viridans* NRRL B-3949 untersuchten. Sie isolierten die Produkte nach *endo*-Dextranase-Hydrolyse chromatographisch (C$_{18}$-Säule) und untersuchten die Strukturen der erhaltenen Oligosaccharide mittels α-1,6-Glucosidase und Methylierungsanalyse. Die Ergebnisse wiesen auf Isomalto-Oligosaccharide mit monomeren oder dimeren (1,6-verknüpften) Seitenketten an Position *O*3 hin (Taylor *et al.*, 1985). Eine detailliertere Strukturaufklärung enzymatisch freigesetzter Oligosaccharide führten Maina *et al.* (2011) durch. Sie hydrolysierten Dextrane von *Weissella confusa* VTT E-90392 mit *endo*-Dextranase

und α-Glucosidase und isolierten die entstandenen Tetra- bis Hexasaccharide mittels Gelpermeationschromatographie (Bio-Gel P-2). Die Ergebnisse aus NMR-Spektroskopie, Methylierungsanalyse und MS zeigten, dass es sich um an Position *O*3 substituierte Isomalto-Oligosaccharide mit mono- und dimeren, 1,6-verknüpften Seitenketten handelte (Maina *et al.*, 2011). Die Dextrane von *Liquorilactobacillus hordei* TMW 1.1822 und die (teilweise wasserunlöslichen) Glucane einer GS von *Latilactobacillus curvatus* TMW 1.624 wurden von Münkel & Wefers (2019) untersucht. Nach *endo*-Dextranase-Hydrolyse wurden auch hier Oligosaccharide isoliert (Bio-Gel P-2, PGC-Säule) und ihre Struktur mittels MS und NMR-Spektroskopie aufgeklärt. Es handelte sich um Isomalto-Oligosaccharide mit mono-, di- und trimeren (1,6-verknüpften) Seitenketten an Position *O*3, ähnlich den von Maina *et al.* (2011) isolierten Oligosacchariden. Die unterschiedlichen Peakintensitätsverhältnisse in den HPAEC-PAD-Chromatogrammen der Hydrolysate der Glucane von *Liquorilactobacillus hordei* und *Latilactobacillus curvatus* verdeutlichten, dass die Strukturelemente in unterschiedlichen Verhältnissen vorlagen. Die Glucane von *Liquorilactobacillus hordei* wiesen einen höheren Anteil an oligomeren Seitenketten auf (Münkel & Wefers, 2019). Das Oligosaccharidprofil nach *endo*-Dextranase-Hydrolyse zeigte ebenfalls, dass die Glucane von der GS Lc6255 aus *Leuconostoc citreum* TMW 2.1194 ähnliche Strukturen wie die Glucane von *Latilactobacillus curvatus* besaßen (Münkel *et al.*, 2019). Daneben existieren Dextrane mit Verzweigungen durch 1,4,6-Glc*p*-Einheiten. Die von einer GS aus *Limosilactobacillus reuteri* TMW 1.106 und der GS Lc1785 von *Leuconostoc citreum* TMW 2.1194 synthetisierten Dextrane wurden hinsichtlich ihrer Verzweigungen analysiert. Wie für die an Position *O*3 verzweigten Dextrane wurden die durch *endo*-Dextranase-Hydrolyse freigesetzten Oligosaccharide isoliert und ihre Struktur aufgeklärt. Es handelte sich um unterschiedlich lange Isomalto-Oligosaccharide mit Verzweigungen an Position *O*4. Alle Oligosaccharide aus den Dextranen von *Limosilactobacillus reuteri* hatten eine terminale Glc*p*-Einheit an Position *O*4 gebunden, was demonstrierte, dass die Seitenketten hauptsächlich eine Einheit lang waren. Außerdem wurden Oligosaccharide isoliert, die im Abstand von zwei und drei 1,6-Glc*p*-Einheiten Verzweigungen haben. Dahingegen wurden aus den Glucanen von Lc1785 Isomalto-Oligosaccharide mit dimeren, 1,6-verknüpften Seitenketten an Position *O*4 freigesetzt. Weitere Peaks mit geringerer Intensität in den HPAEC-PAD-Chromatogrammen weisen auf zusätzliche unbekannte Oligosaccharide hin. Das bedeutet, dass neben den bekannten Strukturelementen weitere Strukturelemente vorlagen (Münkel *et al.*, 2019; Münkel & Wefers, 2019). An Position *O*2 verzweigte Dextrane werden von *Leuconostoc mesenteroides* NRRL B-1299 durch eine Kombination mehrerer GS synthetisiert (Fabre *et al.*, 2005; Kobayashi *et al.*, 1984). Zusätzlich wurden Dextrane, die sowohl durch 1,2,6- als auch 1,3,6-Glc*p*-Einheiten verzweigt sind, in der Literatur beschrieben (Maina *et al.*, 2008; Münkel *et al.*, 2019; Slodki *et al.*, 1986).

Dextrane, die neben den 1,6-Verknüpfungen auch 1,3-Verknüpfungen enthalten, sind von zahlreichen Bakterien bekannt (Birkhed *et al.*, 1979; Funane *et al.*, 2001; Pearce *et al.*, 1990), wobei einige dieser Dextrane zusätzlich Verzweigungen durch 1,3,6-Glc*p*-Einheiten besitzen. Verschiedene *Streptococcus*-Arten bilden derartige Dextrane (Birkhed *et al.*, 1979), von denen die Dextrane von *Streptococcus mutans* UA159 näher untersucht wurden. Die Glucane und

die aus ihnen durch partielle Säurehydrolyse freigesetzten und chromatographisch isolierten (Bio-Gel P-2, CarboPac PA-1) Oligosaccharide wurden mittels Methylierungsanalyse und NMR-Spektroskopie analysiert. Es handelte sich um 1,6- und 1,3-verknüpfte Glucane (54 bzw. 18 %) mit Verzweigungen durch 1,3,6-verknüpfte Glc*p*-Einheiten (14 %) (Li *et al*., 2012). Auch wenn die isolierten Oligosaccharide strukturell aufgeklärt wurden (ausschließlich 1,6- und ausschließlich 1,3-verknüpfte Oligosaccharide sowie vier Oligosaccharide mit 1,3- und 1,6-Verknüpfungen), gehen durch die partielle Säurehydrolyse Informationen über ihre Anordnung in den Glucanen verloren (Kapitel 2.1). Dadurch kann beispielsweise nicht bestimmt werden, ob die 1,3-Verknüpfungen in den Seitenketten eines 1,6-verknüpften Rückgrats vorkommen oder ob das Rückgrat aus 1,3- und 1,6-Verknüpfungen besteht.

Wasserlösliche Glucane, die neben 1,6- und 1,3-Verknüpfungen auch 1,4-Verknüpfungen aufweisen, sind selten. Die rekombinant hergestellte GS DSRT5 aus *Leuconostoc mesenteroides* B-512F synthetisiert 90 % wasserunlösliche und nur 10 % wasserlösliche Glucane. Während die wasserunlöslichen Glucane laut Methylierungsanalyse aus 1,3- und 1,6-verknüpfter Glc*p* bestehen, wurden für die wasserlöslichen Glucane 1,3-, 1,4- und 1,6-Verknüpfungen (19, 15 bzw. 41 %) und Verzweigungen durch 1,3,6-Glc*p*-Einheiten (15 %) sowie 1,4,6-Glc*p*-Einheiten (2 %) beschrieben (Funane *et al*., 2001). Hier ist zu beachten, dass die 1,4,6-Glc*p*-Einheiten auch durch Untermethylierung fehlerhaft bestimmt sein können. Daneben wurden Dextrane mit 1,3- und 1,4-Verknüpfungen (jeweils circa 10 %), die durch 1,3,6- und 1,4,6-Glc*p* (jeweils circa 10 %) verzweigt sind, auch von der GS GTF-I von *Streptococcus mutans* beschrieben. Allerdings synthetisiert auch diese GS primär wasserunlösliche Glucane (Hayacibara *et al*., 2004).

2.2.2.2 Wasserunlösliche α-Glucane

Nach derzeitigem Kenntnisstand finden sich unter den α-Glucan produzierenden Bakterien vor allem in den Gattungen *Leuconostoc*, *Lentilactobacillus* und *Streptococcus* Stämme, die wasserunlösliche α-Glucane synthetisieren. Häufig werden 1,3-Glc*p*-Einheiten in Glucanen mit deren Wasserunlöslichkeit in Verbindung gebracht. Die Literaturdaten zeigen jedoch, dass die meisten wasserunlöslichen Glucane sowohl 1,3- als auch 1,6-verknüpft sind, wobei die Anteile an 1,3- und 1,6-Verknüpfungen stark variieren. Es gibt wasserunlösliche Glucane mit weniger als 5 % 1,3-Verknüpfungen (von *Lentilactobacillus hilgardii*; Münkel & Wefers, 2019; Pidoux *et al*., 1990) und fast ausschließlich 1,3-verknüpfte Glucane (von GTF-J aus *Streptococcus salivarius*; Simpson *et al*., 1995; Kobayashi *et al.*, 2017). Dabei werden Glucane, die mehr als 50 % 1,3-Verknüpfungen enthalten, meistens Mutane genannt. Manche Autoren bezeichnen allerdings auch wasserunlösliche Glucane, die weniger als 50 % 1,3-Verknüpfungen enthalten, als Mutane. Wie bei den wasserlöslichen Glucanen wurden wasserunlösliche Glucane, die zusätzlich zu 1,3- und 1,6-Verknüpfungen auch 1,4-Verknüpfungen aufweisen, selten gefunden. Verzweigungen resultieren häufig aus 1,3,6-Glc*p*- und selten aus 1,2,6-Glc*p*-Einheiten. 1,3,4-verknüpfte Glc*p*-Einheiten wurden bisher nicht mit Sicherheit nachgewiesen,

da deren Auftreten ebenfalls auf Artefaktbildung bei der Methylierungsanalyse zurückzuführen sein könnte. Für wasserunlösliche Glucane wurden Verzweigungsgrade bis 20 % beschrieben, wobei Verzweigungsgrade über 10 % selten sind. Daneben existieren vermutlich unverzweigte wasserunlösliche Glucane (Côté *et al*., 1999; Côté & Leathers, 2009; Côté & Skory, 2012; Ebisu *et al*., 1974; Funane *et al*., 2001; Hare *et al*., 1978; Hayacibara *et al*., 2004; Inoue *et al*., 1988; Jeanes *et al*., 1954; Kobayashi *et al*., 2017; Kopec *et al*., 1997; Li *et al*., 2012; Monchois *et al*., 1999; Monsan *et al*., 2001; Münkel & Wefers, 2019; Pearce *et al*., 1990; Slodki *et al*., 1986; Tsumuraya & Misaki, 1979; Wangpaiboon *et al*., 2020; Wiater *et al*., 1999*, 2012*; Zannini *et al*., 2016). Die Strukturen von 1,3- und 1,6-verknüpften Glucanen mit Verzweigungen durch 1,3,6-Glc*p*-Einheiten sind in Abbildung 2.3 dargestellt.
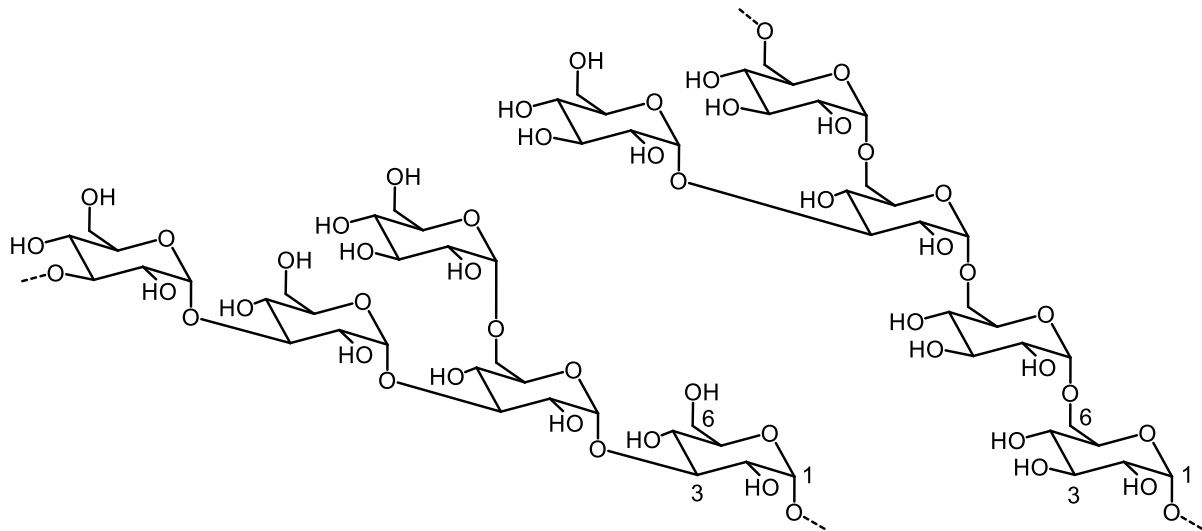
Abbildung 2.3: Strukturausschnitte bisher beschriebener wasserunlöslicher α-Glucane, die von Bakterien gebildet werden (Côté *et al*., 1999; Münkel & Wefers, 2019; Münkel *et al*., 2019).

Hauptsächlich 1,6-verknüpfte wasserunlösliche Glucane mit 3 - 6 % 1,3-Glc*p* und 6 - 7 % 1,3,6-Glc*p* wurden von *Lentilactobacillus hilgardii* beschrieben (Münkel & Wefers, 2019; Pidoux *et al*., 1990). Die HPAEC-PAD-Analyse der durch *endo*-Dextranase-Hydrolyse freigesetzten Oligosaccharide demonstrierte, dass die 1,6-verknüpften Abschnitte dieser Glucane eine ähnliche Feinstruktur aufwiesen wie die Glucane von *Latilactobacillus curvatus*, die keine 1,3-Verknüpfungen enthielten (Kapitel 2.2.2.1; Münkel & Wefers, 2019). Möglicherweise befanden sich die 1,3-Verknüpfungen der *Lentilactobacillus hilgardii* Glucane in den wasserunlöslichen, nicht mittels HPAEC-PAD bestimmten Hydrolyseprodukten, wie es für ähnliche Glucane bereits gezeigt wurde (Fels *et al*., 2018).

1,3- und 1,6-verknüpfte wasserunlösliche Glucane sind von *Leuconostoc* und *Streptococcus* bekannt, wobei nur wenige Glucane detailliert untersucht wurden. Die wasserunlöslichen Glucane der GS DEX-N von *Leuconostoc citreum* ABK-1 wiesen 30 % 1,3-Verknüpfungen und 60 % 1,6-Verknüpfungen sowie 4 % 1,3,6-Verknüpfungen auf. Die Ergebnisse der HPAEC-PAD-Analyse der Produkte aus partieller Säurehydrolyse deuteten darauf hin, dass sowohl konsekutiv 1,3- als auch konsekutiv 1,6-verknüpfte Abschnitte vorlagen (Wangpaiboon *et al*.,

2020). Die Glucane der GS Lc1215 und Lc2135 von *Leuconostoc citreum* TMW 2.1194 hatten neben 1,6-Verknüpfungen 24 bzw. 13 % 1,3-Verknüpfungen und 4 bzw. 3 % 1,3,6-Glc*p*-Einheiten. Die Glucane von Lc2135 wiesen zusätzlich 2 % 1,2,6-Glc*p*-Einheiten auf. Die 1,3-Glc*p*-Einheiten in den Glucanen beider GS lagen in kontinuierlichen Blöcken vor, worauf die HPAEC-PAD-Analyse der durch partielle Säurehydrolyse freigesetzten Oligosaccharide hinwies (Münkel *et al*., 2019). Die 1,6-verknüpften Abschnitte wurden durch *endo*-Dextranase hydrolysiert und die von Münkel & Wefers (2019) isolierten Isomalto-Oligosaccharide identifiziert (Kapitel 2.2.2.1). Dies bedeutet, dass die Glucane beider GS mono-, di- und trimere (1,6-verknüpfte) Seitenketten an Position *O*3 der 1,6-verknüpften Abschnitte aufwiesen. Außerdem lagen die Strukturelemente in ähnlichen Verhältnissen wie in den wasserlöslichen Glucanen vor (Kapitel 2.2.2.1). Daneben gab es Hinweise, dass sich auch die 1,2,6-Glc*p*-Einheiten in 1,6-verknüpften Abschnitten befanden (Münkel *et al*., 2019). Ähnliche wasserunlösliche Glucane einer *Leuconostoc mesenteroides* NRRL B-1355 Mutante analysierten Côté *et al.* (1999). Anders als der *wild type* Stamm *Leuconostoc mesenteroides* NRRL B-1355, der wasserlösliche Alternane und Dextrane synthetisiert, bildet die Mutante wasserunlösliche Glucane. Diese waren hauptsächlich 1,6-verknüpft (46 %) und wiesen zusätzlich 1,3-Verknüpfungen (12 %) sowie Verzweigungen durch 1,3,6-Glc*p*-Einheiten (7 %) und 1,2,6-Glc*p*-Einheiten (12 %) auf. Sie wurden mit Hilfe von schrittweiser enzymatischer Hydrolyse durch *endo*-Dextranase, *endo*-Alternanase und Dextran-1,2-*debranching*-Hydrolase sowie HPSEC, NMR-Spektroskopie und Methylierungsanalyse untersucht. Durch *endo*-Dextranase-Hydrolyse entstand neben wasserlöslichen Oligo- und Polysacchariden eine wasserunlösliche Fraktion. In der wasserunlöslichen Fraktion waren die 1,3-Verknüpfungen (50 %) angereichert, während in den wasserlöslichen Polysacchariden 3 % 1,3-Verknüpfungen und in der Oligosaccharid-Fraktion 9 % 1,3-Verknüpfungen blieben. Die wasserlöslichen Polysaccharide wurden anschließend mit der Dextran-1,2-*debranching*-Hydrolase inkubiert und die resultierenden Polysaccharide mit *endo*-Dextranase vollständig zu Oligosacchariden hydrolysiert. Dieser Ansatz gab Aufschluss über die Verteilung der glycosidischen Bindungen in den Glucanen. Es lagen längere lineare Abschnitte mit 1,6-Verknüpfungen vor, wobei die 1,2,6-Verknüpfungen in 1,6-verknüpften Bereichen waren. Die 1,3,6-Verknüpfungen befanden sich in 1,3-verknüpften Abschnitten (Côté *et al*., 1999). Dies scheint ein Unterschied zu den wasserunlöslichen Glucanen der beiden GS von *Leuconostoc citreum* zu sein, allerdings ist durch die verschiedenen Analysemethoden kein direkter Vergleich möglich. Côté *et al.* (1999) vermuteten, dass es sich bei den wasserunlöslichen Glucanen der *Leuconostoc mesenteroides* NRRL B-1355 Mutante um Pfropf-Copolymere (*graft copolymers*; Rückgrat aus einem Verknüpfungstyp, Seitenketten aus anderem Verknüpfungstyp) handeln könnte. Später untersuchten Côté & Leathers (2009) den nach *endo*-Dextranase wasserunlöslichen, 1,3-Glc*p*-reichen Rückstand mit Hilfe von *exo*-Mutanase und *endo*-Dextranase genauer. Die Ergebnisse bestätigten, dass linear 1,3-verknüpfte und 1,6-verknüpfte Abschnitte vorlagen (Côté & Leathers, 2009).

Pearce *et al.* (1990) analysierten wasserunlösliche Glucane von verschiedenen *Leuconostoc* und *Streptococcus* Stämmen mittels Methylierungsanalyse und fanden sehr unterschiedliche

Anteile an 1,3- bzw. 1,6-Verknüpfungen. Nach *endo*-Mutanase- und *endo*-Dextranase-Hydrolyse betrachteten sie den Anteil an solubilisierten Glucanen und die Menge an freigesetzter Glucose. Die Ergebnisse legten nahe, dass 1,3-verknüpfte Abschnitte für die Wasserunlöslichkeit verantwortlich sind, denn durch *endo*-Mutanase-Hydrolyse wurden unlösliche Glucane löslich (Pearce *et al.*, 1990). Auch für *Streptococcus mutans* wurden wasserunlösliche Glucane mit 1,3- und 1,6-verknüpften Abschnitten beschrieben (Davis *et al.*, 1986; Ebisu *et al.*, 1974). Inzwischen wurden von *Streptococcus mutans* drei genetisch unterschiedliche Arten von GS identifiziert, von denen zwei wasserunlösliche Glucane bilden: GTF-I (auch bezeichnet als GTF-B) und GTF-SI (auch bezeichnet als GTF-C) synthetisieren zu 20 % wasserlösliche und zu 80 % -unlösliche Glucane. Die wasserunlöslichen Glucane beider GS weisen 1,3-, 1,6- und 1,3,6-Verknüpfungen in unterschiedlichen Anteilen auf. Die wasserunlöslichen Glucane der GTF-SI enthalten neben den 1,3- und 1,6-Verknüpfungen auch erhebliche Anteile (> 5 %) an 1,4-verknüpfter Glc*p* und sind damit die einzigen beschriebenen wasserunlöslichen Glucane mit drei verschiedenen linearen Verknüpfungstypen, die von einer unmodifizierten GS synthetisiert werden (Hanada & Kuramitsu, 1988, 1989; Hayacibara *et al*., 2004; Kopec *et al*., 1997; Schormann *et al*., 2023; Xu *et al*., 2018a). In den wasserlöslichen Glucanen von GTF-SI wurden hingegen keine 1,4-Verknüpfungen nachgewiesen (Hayacibara *et al*., 2004). Daneben wurden bei der GS GTF180 von *Limosilactobacillus reuteri* drei Aminosäuren so substituiert, dass sie schwer lösliche Glucane mit 12 % 1,4-, 10 % 1,3- und 42 % 1,6-Verknüpfungen bildete (van Leeuwen *et al*., 2008c). Die Verteilungen der drei Verknüpfungstypen sowie der Verzweigungsstellen in den Glucanen sind nicht bekannt. *Streptococcus salivarius* exprimiert vier genetisch verschiedene GS, von denen zwei, GTF-J und GTF-L, wasserunlösliche Glucane bilden. GTF-J bildet hauptsächlich 1,3-Verknüpfungen, während GTF-L sowohl 1,3- als auch 1,6-Verknüpfungen synthetisiert (Simpson *et al*., 1995). Die Glucane der GTF-L wurden von Kusumi *et al.* (2023) mit Hilfe von HPSEC und Flüssig-NMR-Spektroskopie untersucht. Als Lösungsmittel verwendeten sie LiCl/DMSO oder LiCl/DMAc bzw. acetylierten die Glucane, um eine für zweidimensionale NMR-Spektren ausreichende Menge in CDCl$_3$ lösen zu können. Daneben nutzten sie die Smith-Degradation zum Abbau aller nicht 1,3-verknüpften Glc*p*-Einheiten. Bei dieser Methode wird die kovalente Bindung zweier benachbarter Kohlenstoffatome mit freien Hydroxygruppen unter Oxidation der Kohlenstoffatome durch Periodat gespalten. Anschließend werden die entstandenen Aldehydgruppen reduziert und die glycosidischen Bindungen mit Säure hydrolysiert. Die resultierenden 1,3-verknüpften Glucanabschnitte wiesen gemäß HPSEC-Analyse einen Polymerisationsgrad von mehr als 40 auf. Neben 1,3-Verknüpfungen enthielten die Glucane laut NMR-Spektren 1,6-Verknüpfungen sowie 1,3,6-Glc*p* und terminale Glc*p*. Mit Hilfe von *peak deconvolution* und einem Vergleich mit linear 1,3- und 1,6-verknüpften Glucanen folgerten die Autoren, dass die Seitenketten vier 1,6-Glc*p*-Einheiten lang seien. Insgesamt schienen die Glucane Pfropf-Copolymere zu sein (Kusumi *et al.*, 2023). Die Glucane von GTF-J sind (fast) ausschließlich α-1,3-verknüpft (Simpson *et al.*, 1995; Kobayashi *et al.*, 2017) und damit einzigartig. Die GTF-I von *Streptococcus sobrinus* synthetisiert ebenfalls hauptsächlich 1,3-Verknüpfungen, allerdings benötigt sie neben Saccharose Primer-Dextrane als Akzeptormolekül, wodurch gemischt-verknüpfte Glucane entstehen (Fukui *et al.*, 1982; Takehara *et al.*, 1991).

Anders als die Molekulargewichte von wasserlöslichen bakteriellen α-Glucanen wurden die der wasserunlöslichen Glucane selten untersucht. Für die wasserunlöslichen Glucane der GTF-L von *Streptococcus salivarius* bestimmten Kusumi *et al.* (2023) mittels HPSEC in DMAc mit einem Zusatz von 1 % LiCl Molekulargewichte um 1 MDa. Die Morphologien von wasserlöslichen und -unlöslichen Glucanen unterscheiden sich in der Regel (Inoue *et al*., 1982; Yakushiji *et al*., 1981). Wasserunlösliche Glucane können kristalline Bereiche haben, was bisher für native, chemisch und enzymatisch entzweigte sowie chemisch modifizierte α-1,3-Glucane beschrieben wurde (Kobayashi *et al*., 2017; Ogawa *et al*., 1981, 1994). Generell ist für Polysaccharide bekannt, dass sich ihre Kristallstrukturen durch Trocknung ändern (Kobayashi *et al*., 2010, 2013, 2017). So sind für 1,3-verknüpfte Glucane in Abhängigkeit der Anwesenheit von Wassermolekülen unterschiedliche Kristallstrukturen bekannt, wobei in der hydratisierten Form pro Glucose-Einheit ein Wassermolekül enthalten ist (Ogawa *et al*., 1994). Lineare α-1,3-D-Glucanketten haben eine ausgedehnte bandartige Konformation mit antiparalleler Packung (Marchessault & Deslandes, 1981). Kobayashi *et al.* (2017) untersuchten gefriergetrocknete und nicht getrocknete α-1,3-Glucane der GTF-J aus *Streptococcus salivarius* im Vergleich. Die dehydratisierten Glucane hatten eine ungeordnetere Struktur als die hydratisierten Glucane. Die Autoren vermuteten, dass beide dieselben räumlichen Strukturelemente in unterschiedlicher Anordnung enthielten. Die Polysaccharidketten lagen nicht wie bei Cellulose in Faserrichtung vor, sondern waren in kristallinen Bereichen mit fibrillenartiger Struktur gefaltet, die Bündel bildeten. Daneben lag ein geringerer Anteil kristalliner Bereiche mit lammellenartiger Struktur vor. Bis heute wurde die Kristallstruktur nicht vollständig aufgeklärt (Kobayashi *et al*., 2017). Neben den ausschließlich 1,3-verknüpften Glucanen liegt in der Literatur nur ein Hinweis auf kristalline Bereiche in gemischt-verknüpften Glucanen durch die Untersuchung von Wangpaiboon *et al.* (2020) vor. In den wasserunlöslichen Glucanen der GS DEX-N bildeten die 1,3-verknüpften Abschnitte kristalline Bereiche aus, was die Autoren durch Vergleich von Röntgendiffraktogrammen mit ausschließlich 1,3- und ausschließlich 1,6-verknüpften Glucanen folgerten (Wangpaiboon *et al*., 2020).

2.3 β-Fructane

β-Fructane werden hauptsächlich von Pflanzen und Bakterien gebildet. Vor wenigen Jahren berichteten Kırtel *et al.* (2019) erstmalig, dass auch Archaeen β-Fructane aus Saccharose bilden. Inuline sind eher von Pflanzen als von Mikroorganismen bekannt, während Levane vor allem von Mikroorganismen und nur wenigen Pflanzen (dort auch Phlein genannt) bekannt sind (Ni *et al*., 2021; van den Ende, 2013). Bakterielle Levane werden von Milchsäurebakterien der Gattungen *Streptococcus, Leuconostoc, Fructilactobacillus, Lactobacillus, Oenococcus* und *Weissella*, Essigsäurebakterien der Gattungen *Acetobacter* und *Gluconacetobacter* sowie Bakterien weiterer Gattungen gebildet (Dimopoulou *et al*., 2016; Ebisu *et al*., 1975; Hancock *et al*., 1976; Malang *et al*., 2015; Öner *et al*., 2016; Tieking *et al*., 2005; Visnapuu *et al*., 2011; Zikmanis *et al*., 2020). Mikrobielle Inuline werden sowohl von Pilzen (*Aspergillus*) als auch von Bakterien synthetisiert, wobei von Milchsäurebakterien der Gattungen *Lactobacillus* und *Weissella* fermentativ hergestelltes Inulin und durch Inulosucrasen von *Streptococcus* und *Leuconostoc* enzymatisch produziertes Inulin untersucht wurden (Anwar *et al*., 2008; Ebisu *et al*., 1975; Heyer & Wendenburg, 2001; Malang *et al*., 2015; Ni *et al*., 2019; Ortiz-Soto *et al*., 2004; Ozimek *et al*., 2006; Zikmanis *et al*., 2020).

2.3.1 Fructansucrasen & Fructanhydrolasen

FS gehören zur GH68 Familie und übertragen analog zu GS (Kapitel 2.2.1) die Fru*f*-Einheit von Saccharose oder Raffinose auf eine wachsende Fructankette, H_2O oder einen anderes Akzeptormolekül mit Hydroxygruppe. Grundsätzlich haben auch FS ein Signalpeptid, eine variable *N*-terminale Region, ein konserviertes katalytisches Zentrum und eine *C*-terminale Region, die bei manchen FS eine Zellwandbindedomäne enthält. Trotz der Gemeinsamkeiten haben FS und GS keine Sequenzähnlichkeit (van Hijum *et al*., 2006). Kristallstrukturen von FS zeigen, dass sie eine fünfblättrige β-Propeller-Struktur enthalten, in der sich die drei katalytischen Aminosäuren befinden (Martínez-Fleites *et al*., 2005; Meng & Fütterer, 2003; Ni *et al*., 2019; Pijning *et al*., 2011; Strube *et al*., 2011; Wuerges *et al*., 2015; Xu *et al*., 2022b). Diese sind wie bei den GS zwei Asparaginsäurereste und ein Glutaminsäurerest. Der Reaktionsmechanismus der FS entspricht dem der GS, außer dass Fru*f* übertragen wird. Wie GS benötigen manche FS Ca^{2+}, um ihre Struktur zu stabilisieren (Lammens *et al*., 2009; Meng & Fütterer, 2003, 2008; Ozimek *et al*., 2004, 2005; Pons *et al*., 2004). Nach den von ihnen synthetisierten Fructanen werden FS in Levansucrasen (EC 2.4.1.10) und Inulosucrasen (EC 2.4.1.9) eingeteilt (van Hijum *et al*., 2006). FS scheinen in den von ihnen synthetisierten glycosidischen Bindungen spezifischer als GS. Für die Art der synthetisierten Bindung sind Regionen außerhalb der dem aktiven Zentrum nahen *subsites* verantwortlich (Pijning *et al*., 2011). Derzeit existieren nur für Oligosaccharide bzw. die frühe Phase der Fructansynthese Hinweise, dass eine Levansucrase 2,1- und 2,6-Bindungen katalysieren kann (Okuyama *et al*., 2021). Wie FS Verzweigungen synthetisieren ist unklar, es bestehen jedoch Hinweise, dass die *C*-terminale Domäne eine Rolle spielt (Chambert *et al*., 1992).

Während zahlreiche GS und Levansucrasen bekannt sind (CAZy, 2024; Hill *et al*., 2019; Ortiz-Soto *et al*., 2019), wurden bisher nur wenige bakterielle Inulosucrasen beschrieben (Anwar *et al*., 2008; Kralj *et al*., 2018; Ni *et al*., 2018; Ortiz-Soto *et al*., 2004; Ozimek *et al*., 2006). Manche Levan- und Inulosucrasen bilden hauptsächlich Oligosaccharide, während andere Enzyme hauptsächlich Polysaccharide mit hohem Molekulargewicht synthetisieren. Daneben hängt die Produktspezifität der einzelnen FS auch von den vorliegenden Reaktionsbedingungen und der Enzymkonzentration ab (Kralj *et al*., 2018; Ortiz-Soto *et al*., 2019; Ozimek *et al*., 2006; Porras-Domínguez *et al*., 2014, 2015). Die Aktivitätsbestimmung der FS erfolgt analog zu der der GS (Kapitel 2.2.1). Auch hier kann über getrennte Quantifizierung von Glucose, Fructose und Saccharose die Gesamt-, Hydrolyse- und Transferaseaktivität bestimmt werden (Hill *et al*., 2019; Jang *et al*., 2006; Ortiz-Soto *et al*., 2004). Levansucrasen und Inulosucrasen haben pH-Optima im Bereich von 3,5 - 7,0 (Alméciga-Díaz *et al*., 2011; Anwar *et al*., 2010; Del Moral *et al*., 2008; Frasch *et al*., 2017; Han, 2009; Liu *et al*., 2017; Olvera *et al*., 2007; Ortiz-Soto *et al*., 2004; Tieking *et al*., 2005; van Hijum *et al*., 2002*, 2003, 2004*; Waldherr *et al*., 2008). Ihre Temperaturoptima liegen höher als die der GS. Levansucrasen haben Optima im Bereich von 35 - 55 °C (Anwar *et al*., 2010; Liu *et al*., 2017; Olvera *et al*., 2007; Tieking *et al*., 2005; van Hijum *et al*., 2004; Waldherr *et al*., 2008) und Inulosucrasen im Bereich von 50 - 55 °C (Anwar *et al*., 2008, 2010; Frasch *et al*., 2017; van Hijum *et al*., 2003).

Auch wenn die Sequenzhomologie gering ist, haben GH68-Enzyme ähnliche Strukturen wie GH32-Enzyme (Meng & Fütterer, 2003) und beide Enzymfamilien bilden den GH-J Clan. Anders als GH68-Enzyme polymerisieren die bisher beschriebenen GH32-Enzyme Fructose ausschließlich zu Oligosacchariden und ihnen dient primär Wasser als Akzeptormolekül (Lammens *et al*., 2009). Zu den GH32-Enzymen gehören, neben pflanzlichen Fructosyltransferasen und anderen (*exo*-)Fructohydrolasen, auch *endo*-Inulinasen (EC 3.2.1.7) und *endo*-Levanasen (EC 3.2.1.65) aus Bakterien (Lammens *et al*., 2009; Márquez-López *et al*., 2023; Zhang *et al*., 2019). Dabei können die Produktprofile unterschiedlicher *endo*-Levanasen verschieden sein (Hövels *et al*., 2021; Lekakarn *et al*., 2022; Mardo *et al*., 2017; Miasnikov, 1997; Porras-Domínguez *et al*., 2014). Während die Levanase BT1760 von *Bacteroides thetaiotaomicron* vor allem Levantriose und Levanbiose sowie vergleichsweise wenig Fructose und Levantetraose aus unverzweigtem pflanzlichem Levan freisetzt, bildet LevB2286 von *Azotobacter chroococcum* neben wenig Fructose Levanbiose und Levan-Oligosaccharide bis zu einem Polymerisationsgrad von 6 (Hövels *et al*., 2021; Mardo *et al*., 2017). Außerdem kann das Produktprofil von *endo*-Levanasen vom hydrolysierten Levan abhängen, wobei *endo*-Levanasen spezifisch 2,6-glycosidische Bindungen spalten und Inulin kein geeignetes Substrat ist (Hövels *et al*., 2021; Lekakarn *et al*., 2022; Mardo *et al*., 2017; Porras-Domínguez *et al*., 2014). Levanasen haben Temperaturoptima im Bereich von 35 - 45 °C und pH-Optima bei ungefähr 6 (Dahech *et al*., 2013; Hövels *et al*., 2021; Jensen *et al*., 2016; Mardo *et al*., 2017; Porras-Domínguez *et al*., 2014). Inulinasen haben Temperaturoptima im Bereich von 35 - 70 °C und pH-Optima von 4,5 - 7,5 (Singh *et al*., 2017; Yousefi-Mokri *et al*., 2019). Anders als Levanasen werden Inulinasen heutzutage zur großtechnischen Produktion von Fructooligosacchariden verwendet (Singh *et al*., 2016, 2020).

2.3.2 Strukturen von bakteriellen β-Fructanen

Zahlreiche, meist fermentativ hergestellte Levane unterschiedlicher Bakterien wurden mittels Infrarot- und NMR-Spektroskopie, Methylierungsanalyse, enzymatischer Hydrolyse und HPSEC identifiziert. Einige Studien beschreiben Verzweigungen von Levanen, wobei mithilfe unterschiedlicher Varianten der Methylierungsanalyse 2,1,6-verknüpfte Fru*f*-Einheiten in Anteilen von 3 - 22 % bestimmt wurden (Birkhed *et al*., 1979; Bouallegue *et al*., 2020; Dawes *et al*., 1966; Haddar *et al*., 2021; Han & Clarke, 1990; Hancock *et al*., 1976; Hundschell *et al*., 2020a; Lewis *et al*., 1967; Lindberg *et al*., 1973; Marshall & Weigel, 1980a; Matulová *et al*., 2011; Shukla & Goyal, 2013; Simms *et al*., 1990). Dabei besaßen die fermentativ hergestellten Levane verschiedener *Leuconostoc mesenteroides* Stämme mit circa 20 % die höchsten Verzweigungsgrade (Lewis *et al*., 1967; Lindberg *et al*., 1973), während fermentativ hergestellte Levane verschiedener *Bacillus*-Arten 5 - 12 % Verzweigungen aufwiesen (Bouallegue *et al*., 2020; Haddar *et al*., 2021; Han & Clarke, 1990). Für Levane verschiedener *Streptococcus salivarius* Stämme wurden mit 11 - 15 % 2,1,6-Fru*f*-Einheiten mehr Verzweigungen als für Levane von *Streptococcus mutans* (6 %) beschrieben (Birkhed *et al*., 1979; Hancock *et al*., 1976; Simms *et al*., 1990). Anders als mit der Methylierungsanalyse wurden mit Hilfe der NMR-Spektroskopie keine Verzweigungen in Levanen von *Leuconostoc* und *Bacillus* detektiert (Matulová *et al*., 2011; Shukla & Goyal, 2013), was an der geringen Empfindlichkeit der NMR-Spektroskopie für Strukturelemente mit geringem Anteil (Kapitel 2.1) liegen könnte. Trotz der vielen Daten aus Methylierungsanalysen liegen nur wenige Studien zur Länge und keine Studie zur Verteilung der Verzweigungen vor. Hier könnte eine Analyse der Produkte nach Hydrolyse mit spezifischen Enzymen Aufschluss geben. Bislang wurden *exo*-β-Fructosidasen, *endo*-Inulinasen und *endo*-Levanasen analytisch vor allem in Kombination eingesetzt, um den Gehalt an Fructanen zu bestimmen (McCleary *et al*., 2019; Shi *et al*., 2019). Shi *et al.* (2019) verwendeten *endo*-Levanase sowie *endo*- und *exo*-Inulinase, um selektiv den Levangehalt in Teigmatrix zu bestimmen. Porras-Domínguez *et al.* (2014) hydrolysierten dagegen verschiedene Levane mit *endo*-Levanase und untersuchten die Produkte mit HPAEC-PAD. Die Ergebnisse wiesen auf mehrere Produkte hin, wovon die Autoren lediglich Fructose und Levanbiose identifizieren konnten. Außerdem zeigten die Chromatogramme der verschiedenen Levan-Hydrolysate unterschiedliche Produktprofile. Zur Strukturanalyse von fermentativ durch *Serratia* produzierten Levanen verwendeten Kojima *et al.* (1993) Hydrolysen durch zwei *exo*-β-Fructosidasen und analysierten die entstandenen Produkte mittels Gelpermeationschromatographie (Bio-Gel P2) und Dünnschichtchromatographie. In Kombination mit ^{13}C-NMR-Spektroskopie zeigten sie, dass die Levane verzweigt vorlagen. Für Levane von *Streptococcus salivarius* wurden auf Basis von *exo*-β-Fructosidase-Hydrolysen unterschiedlicher Dauer und Methylierungsanalysen mehrere Einheiten lange Seitenketten und eine baumartige Struktur vorgeschlagen (Hancock *et al*., 1976; Marshall & Weigel, 1980a, 1980b).

Auch von bakteriellen Inulinen sind Feinstrukturen unbekannt. Inuline wurden bisher lediglich grundlegend mit Infrarot- und eindimensionaler NMR-Spektroskopie sowie Methylierungs- analyse untersucht (Anwar *et al*., 2008; Birkhed *et al*., 1979; Ebisu *et al*., 1975; Malang *et al*., 2015; Ni *et al*., 2018). Verzweigungen durch 2,1,6-Fru*f*-Einheiten wurden nur für wenige bakterielle Inuline mittels Methylierungsanalyse identifiziert (Birkhed *et al*., 1979; Ebisu *et al*., 1975; van Hijum *et al*., 2002). Vallejo-García *et al.* (2019) hydrolysierten Inuline von *Leuconostoc citreum* CW28 mit einer *endo*-Inulinase. Die HPAEC-PAD-Analyse zeigte eine Vielzahl verschiedener, größtenteils unbekannter Oligosaccharide im Hydrolysat (Vallejo- García *et al*., 2019). Allerdings wurde die Analyse der Produkte nach enzymatischer Hydrolyse bisher nicht zur Strukturaufklärung der bakteriellen Inuline verwendet. Für pflanzliche Inuline wurden *endo*-Inulinase-Hydrolysen bereits zur Strukturanalyse verwendet und lineare Inulo- Oligosaccharide isoliert (Ronkart *et al*., 2007). In Abbildung 2.4 sind vermutlich existierende Strukturausschnitte der bakteriellen β-Fructane gezeigt.
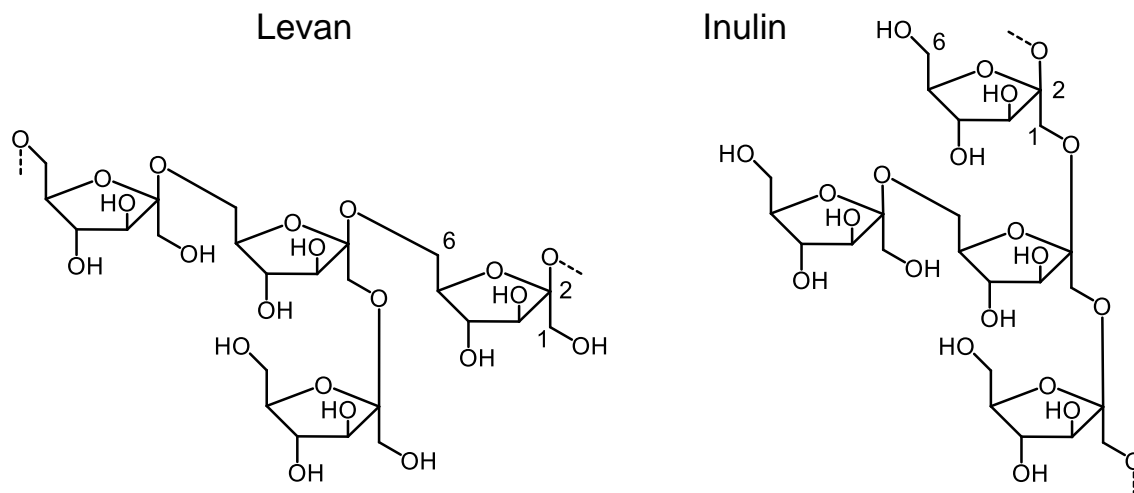
Abbildung 2.4: Mögliche Strukturausschnitte der bakteriellen Fructane Levan und Inulin (Bouallegue *et al*., 2020; Haddar *et al*., 2021; van Hijum *et al*., 2002).

Pflanzliche Fructane haben mit maximal 15 kDa geringere Molekulargewichte als bakterielle Fructane (Ni *et al*., 2024). Für letztere wurden Molekulargewichte im Bereich von 10 bis 10^6 kDa bestimmt (Anwar *et al*., 2008; Bouallegue *et al*., 2020; Hundschell *et al*., 2020b; Kojima *et al*., 1993; Olvera *et al*., 2007; Runyon *et al*., 2014; Shukla & Goyal, 2013; van Hijum *et al*., 2002). Während Levane wasserlöslich sind, können Inuline schwer löslich bis wasserunlöslich sein. Ebisu *et al.* (1975) beschrieben Inuline von *Streptococcus*-Bakterien, die bei Raumtemperatur wasserunlöslich sind und sich erst bei 60 °C lösten. Sowohl Inuline als auch Levane nehmen in Lösung unterschiedliche Konformationen an, wobei auch die Hauptkonformation, eine Helix- Struktur, häufig nur über wenige Furanose-Einheiten existiert. Die Flexibilität der Fructane ist vergleichbar mit der Flexibilität von Polysacchariden aus 1,6-verknüpften Pyranose-Einheiten, während 1,4-verknüpfte Pyranose-Einheiten deutlich starrer sind (Nester & Plazinski, 2019, 2020).

2.4 Problemstellung

Derzeit existieren viele Review-Artikel zu allgemeinen Strukturen, Einsatzmöglichkeiten und Synthesen von HoEPS, aber nur wenige ausführliche Strukturcharakterisierungen. Dadurch sind die umfassenden Strukturen unklar und Feinstrukturelemente nur von wenigen HoEPS bekannt (vgl. Kapitel 2.2.2 & 2.3.2). Dabei sind die Art der glycosidischen Bindungen, aber auch ihre Anteile und Verteilungen im HoEPS, die Seitenkettenverteilung und -länge sowie die Molekülgröße wichtige Strukturparameter, die die physikochemischen Eigenschaften der HoEPS bestimmen. Entsprechend ist das Wissen über ihre Strukturen für alle Einsatzbereiche der HoEPS, aber auch zur Verhinderung ihrer unerwünschten Vorkommen essentiell.

Insbesondere bei bakteriellen Fructanen werden Vorkommen und Anteil von Verzweigungen selten betrachtet (Kapitel 2.3.2), jedoch wird ein Einfluss der Verzweigungen auf die physikochemischen Eigenschaften der Fructane vermutet (Combie & Öner, 2018). Manche Bakterienstämme besitzen verschiedene Sucrasen und synthetisieren sowohl wasserlösliche Glucane als auch Fructane, was für die Strukturanalyse eine Herausforderung darstellt, die in der Literatur kaum Beachtung findet (Kapitel 2.1). Zu einzelnen, vor allem wasserlöslichen, Glucanen existieren umfassende Strukturanalysen und es wurden vergleichende Untersuchungen verschiedener Glucane mit einzelnen Analysemethoden durchgeführt. Diese fehlen jedoch für wasserunlösliche α-Glucane, was insofern von Bedeutung ist, als die Ergebnisse je nach Analysemethode bzw. Probenaufarbeitung variieren können. Dadurch sind die bisherigen Ergebnisse weitgehend nicht vergleichbar. Zudem ist derzeit wenig zu den Feinstrukturen wasserunlöslicher α-Glucane bekannt. Für die Ausbildung geordneter bzw. kristallähnlicher Bereiche scheinen konsekutive α-1,3-Verknüpfungen ein wichtiger Faktor zu sein. Hierbei wurden bisher insbesondere ausschließlich 1,3-verknüpfte Glucane untersucht (Kapitel 2.2.2.2), jedoch sollten gemischt-verknüpfte Glucane ebenfalls diesbezüglich untersucht werden.

Herausforderungen in der Strukturaufklärung liegen wie für alle Polysaccharide in der Analytik, wobei eine Kombination verschiedener Ansätze für umfangreiche Einblicke erforderlich ist. Besonders an HoEPS angepasste und spezifische Methoden sind wertvoll, allerdings wurden hierzu nur wenige Arbeiten (Matulová *et al*., 2011, Maina *et al*., 2008, 2014, van Leeuwen *et al*., 2008b; Striegel *et al.*, 2009) publiziert. Die Verwendung von Enzymen zur spezifischen Hydrolyse von HoEPS zeigt großes Potential, wurde bisher jedoch nur vereinzelt eingesetzt (Côté *et al*., 1999; Maina *et al*., 2011; Münkel & Wefers, 2019; Porras-Domínguez *et al.*, 2014). Für wasserunlösliche Glucane lassen sich Methoden, die für wasserlösliche HoEPS entwickelt wurden, nur bedingt anwenden. So kann die schlechte Löslichkeit bzw. Quellbarkeit vieler wasserunlöslicher Glucane in DMSO bei der Methylierungsanalyse in Untermethylierung resultieren. Daneben ist unbekannt, inwiefern die hierbei angewandten Ultraschallbehandlungen zu Artefaktbildung führen können (Kapitel 2.1). Für flüssigchromatographische Ansätze wie die HPSEC müssen die Glucane in geeigneten Lösungsmitteln möglichst vollständig gelöst

werden. Hierbei besteht eine Schwierigkeit darin, dass nicht alle wasserunlöslichen Glucane das gleiche Lösungsverhalten zeigen. Entsprechend wurde das Molekulargewicht von bakteriellen, wasserunlöslichen α-Glucanen bisher kaum betrachtet (Kapitel 2.2.2.2). Ein weiterer Ansatz ist die Untersuchung der wasserunlöslichen Glucane als Feststoff mit Methoden wie XRD oder Festkörper-NMR-Spektroskopie, wozu jedoch wenig Literatur (Kobayashi *et al*., 2017) vorliegt.

3 Zielstellung

Die von Milch- und Essigsäurebakterien produzierten HoEPS, α-Glucane und β-Fructane, haben in vielen Anwendungen großes Potential (Kapitel 1). Hierfür spielen die vielfältigen Strukturen eine wichtige Rolle, sodass sie eingehend untersucht werden sollten. Allerdings mangelt es an angepassten Analysemethoden zur Untersuchung von HoEPS und in vergangenen Studien wurden lediglich einzelne HoEPS detailliert analysiert oder mehrere HoEPS mit Hilfe einzelner Analysemethoden verglichen. Daneben ist zu den Feinstrukturen von insbesondere wasserunlöslichen HoEPS wenig bekannt (Kapitel 2.2.2 & 2.3.2). Vor diesem Hintergrund ist das Ziel dieser Dissertation, die derzeitigen Kenntnisse über HoEPS-Strukturen durch umfassende Analysen verschiedener HoEPS zu erweitern. Ausgangspunkt hierfür ist die Anpassung bestehender Analysemethoden (Kapitel 2.1) an HoEPS, vor allem wasserunlösliche Glucane, und die Entwicklung neuer Ansätze. Um möglichst strukturell diverse HoEPS betrachten zu können, sollen einerseits von verschiedenen Bakterien fermentativ gebildete HoEPS analysiert werden, wobei die möglichst umfassende Analyse aller gebildeten EPS im Fokus steht. Andererseits sollen auch von rekombinant hergestellten GS synthetisierte wasserunlösliche Glucane detailliert untersucht werden. Neben den GS werden zur spezifischen HoEPS-Hydrolyse die Enzyme *endo*-Mutanase und *endo*-Levanase in *E. coli* heterolog exprimiert und isoliert.

Zunächst erfordert die Methylierungsanalyse als universelle Methode zur Bestimmung der Anteile aller glycosidischen Bindungen in Polysacchariden eine Adaption für HoEPS. Hierbei wird der Einfluss von verschiedenen im Zuge der Methylierung eingesetzten Ultraschallbehandlungen und Hydrolysebedingungen (Dauer, Säurekonzentration, Temperatur) auf die erhaltenen Anteile der glycosidischen Bindungen betrachtet. Außerdem soll ermittelt werden, inwieweit Mischungen aus wasserlöslichen Glucanen und Fructanen ohne vorherige Auftrennung beider HoEPS analysiert werden können.

Bei der Kariesentstehung wichtige HoEPS sind wasserunlösliche α-Glucane von *Streptococcus* Bakterien. Daher sollen mit Hilfe von rekombinant gewonnenen GS strukturell unterschiedliche wasserunlösliche α-Glucane synthetisiert und untersucht werden. Hierzu dienen neben der Methylierungsanalyse Hydrolysen durch *endo*-Dextranase und *endo*-Mutanase. Die Molekülgrößen der wasserunlöslichen Glucane vor und nach enzymatischer Hydrolyse sollen mittels HPSEC-RI in geeignetem Lösungsmittel bestimmt werden, was Aufschluss über die Verteilungen der glycosidischen Bindungen geben soll. Zusätzliche Einblicke in die Feinstrukturen werden durch die Analyse der enzymatisch freigesetzten Oligosaccharide mit HPAEC-PAD/MS angestrebt. Das Vorliegen und, sofern möglich, die Struktur von kristallinen Bereichen sollen mit Festkörperanalysemethoden geprüft werden, wobei besonders gemischt-verknüpfte Glucane interessieren.

Manche Bakterien bilden diverse HoEPS, sodass hier ausgewählte Milchsäurebakterienstämme zur fermentativen Synthese von sowohl wasserlöslichen als auch wasserunlöslichen HoEPS verwendet werden sollen. Nach separater Aufreinigung beider HoEPS-Gruppen mithilfe einer anzupassenden Methode besteht die Besonderheit in der Strukturuntersuchung aller entstandenen Glucane und Fructane. Die wasserunlöslichen Glucane werden mit Methylierungsanalyse und HPSEC-RI grundlegend charakterisiert. Zusätzlich sollen sie mit *endo*-Dextranase hydrolysiert und die freigesetzten Oligosaccharide mit HPAEC-PAD analysiert werden, um Informationen über potenziell enthaltene 1,6-verknüpfte Abschnitte und Verzweigungen in diesen zu erhalten. Die nach *endo*-Dextranase-Hydrolyse wasserunlöslichen Rückstände werden im Vergleich zu den unmodifizierten Glucanen mittels Methylierungsanalyse und HPSEC-RI untersucht. Außerdem sollen 1,3-verknüpfte Abschnitte mit *endo*-Mutanase hydrolysiert und die freigesetzten Oligosaccharide mit HPAEC-PAD/MS analysiert werden. Von den wasserlöslichen HoEPS sollen zunächst die Anteile an enthaltenen Glucanen und Fructanen durch Monosaccharidbestimmung ermittelt werden. Mithilfe der Methylierungsanalyse werden die Verknüpfungen in beiden HoEPS bestimmt. Die Molekülgrößen der wasserlöslichen HoEPS vor und nach *endo*-Dextranase-Hydrolyse werden mit HPSEC-RI ermittelt. Daneben werden die durch *endo*-Dextranase-Hydrolyse freigesetzten Oligosaccharide mittels HPAEC-PAD untersucht. Über die Feinstrukturen der gebildeten Fructane soll die *endo*-Levanase-Hydrolyse mit HPAEC-PAD/MS-Analyse der freigesetzten Oligosaccharide Aufschluss geben. Ergänzend sollen Fructane von bisher nicht für Fructanbildung bekannten Bakterien strukturcharakterisiert werden. Hierzu dienen neben der NMR-Spektroskopie ebenfalls die Methylierungsanalyse, HPSEC-RI und *endo*-Levanase-Hydrolyse.

4 Ergebnisse & Diskussion

4.1 Anpassung der Methylierungsanalyse an bakterielle Homoexopolysaccharide

Für aussagekräftige Ergebnisse, das heißt eine präzise und richtige Ermittlung der Anteile jedes Verknüpfungstyps im Polysaccharid, müssen die Derivatisierungsschritte der Methylierungsanalyse an das zu untersuchende Polysaccharid angepasst sein. Insbesondere die zur besseren Quellung von in DMSO unlöslichen Polysacchariden angewandten Ultraschallbehandlungen und die Bedingungen während der sauren Hydrolyse der permethylierten Polysaccharide können kritische Einflussfaktoren sein (Kapitel 2.1). Da eine Anpassung an bakterielle HoEPS in der Literatur nicht beschrieben war, wurden die Ultraschallbehandlungen und Hydrolysebedingungen bei Methylierungsanalysen von drei ausgewählten Modell-HoEPS variiert. Die wasserunlöslichen Modellglucane wurden mit Hilfe der GS Lc1215 aus *Leuconostoc citreum* hergestellt und enthielten neben terminalen Glc*p*-Einheiten 1,3-, 1,6- und 1,3,6-verknüpfte Glc*p* (Münkel *et al*., 2019), sodass sie für wasserunlösliche Glucane repräsentativ sind (Kapitel 2.2.2.2). Die wasserlöslichen Modellglucane wurden durch eine GS von *Limosilactobacillus reuteri* synthetisiert und enthielten neben 1,6- und 1,4,6-Verknüpfungen geringe Anteile (1 %) 1,4- und 1,3,6-Verknüpfungen (Münkel *et al*., 2020). Als Vertreter für Levane dienten die fermentativ hergestellten Levane von *Gluconobacter albidus*, die neben terminalen und 2,6-verknüpften Fru*f*-Einheiten circa 3 % verzweigte 2,1,6-Fru*f*-Einheiten aufwiesen (Hundschell *et al*., 2020a).

Zunächst wurden die Ultraschallbehandlungen vor der Derivatisierung (1), nach Zugabe von NaOH$_{(s)}$ (2) und nach Zugabe von Methyliodid (3) in verschiedenen Kombinationen eingesetzt und jeweils die Anteile der PMAA bestimmt. Sollte eine Ultraschallbehandlung zu Kettenbrüchen führen, würde das in einer Reduktion des Molekulargewichts resultieren und durch erhöhte Anteile an terminalen Einheiten sichtbar werden. Bei optimalen Ergebnissen wird für hochmolekulare Polysaccharide ein 1:1-Verhältnis von verzweigten zu terminalen Einheiten erwartet. Allerdings muss die Probe hierfür frei von niedermolekularen Sacchariden, wie beispielsweise Verunreinigungen aus der HoEPS-Synthese, sein. Nach Anwendung der verschiedenen Kombinationen an Ultraschallbehandlungen waren bei den wasserunlöslichen Modellglucanen starke Unterschiede in den Anteilen der glycosidischen Bindungen, besonders terminale Glc*p* und 1,6-Glc*p,* sichtbar (Abbildung 4.1A). Zur Minimierung der Überbestimmung der terminalen Einheiten und Abweichung innerhalb der Doppelbestimmung erwiesen sich die Ultraschallbehandlungen zum Lösen bzw. Quellen der Glucane (1 & 2) als entscheidend. Die Ultraschallbehandlung nach Zugabe des Methyliodids (3) kann dagegen entfallen. Diese Ergebnisse stehen im Gegensatz zu den Ergebnissen für die wasserlöslichen Modellglucane, bei denen die Ultraschallbehandlung keinen Einfluss auf die Anteile der glycosidischen

Bindungen hatte (Abbildung 4.1B). Da wasserlösliche Glucane auch in DMSO gut löslich sind, liegen folgende Erklärungen nahe: Wasserunlösliche Glucane sollten gut in DMSO gequollen werden, was die Ultraschallbehandlungen unterstützen. Außerdem ist die vollständige Deprotonierung Voraussetzung für eine vollständige Methylierung, wobei die Ultraschall-behandlungen den Angriff der Hydroxidionen am gequollenen Glucan erleichtern. Einmal gequollen und deprotoniert ist keine Ultraschallbehandlung mehr nötig, da die deprotonierten Glucane gut mit dem Überschuss an Methyliodid reagieren.

Wie bei den wasserlöslichen Modellglucanen, hatten die Ultraschallbehandlungen keinen Einfluss auf die Anteile der glycosidischen Bindungen der Modelllevane. Demnach lagen beide wasserlöslichen HoEPS für eine vollständige Deprotonierung und Methylierung ausreichend gelöst vor. Außerdem zeigen die Ergebnisse beider HoEPS, dass die Ultraschallbehandlungen nicht in merklichem Ausmaß zu Kettenbrüchen führen. Die Untersuchungen dieser Arbeit verdeutlichen erstmals, dass Ultraschallbehandlungen die Ergebnisse der Methylierungs-analyse von HoEPS nicht negativ beeinflussen, sondern für die Deprotonierung von in DMSO unlöslichen α-Glucanen und damit für aussagekräftige Ergebnisse notwendig sind. Diese Erkenntnis kann ebenfalls für andere in DMSO unlösliche Polysaccharide von Bedeutung sein.
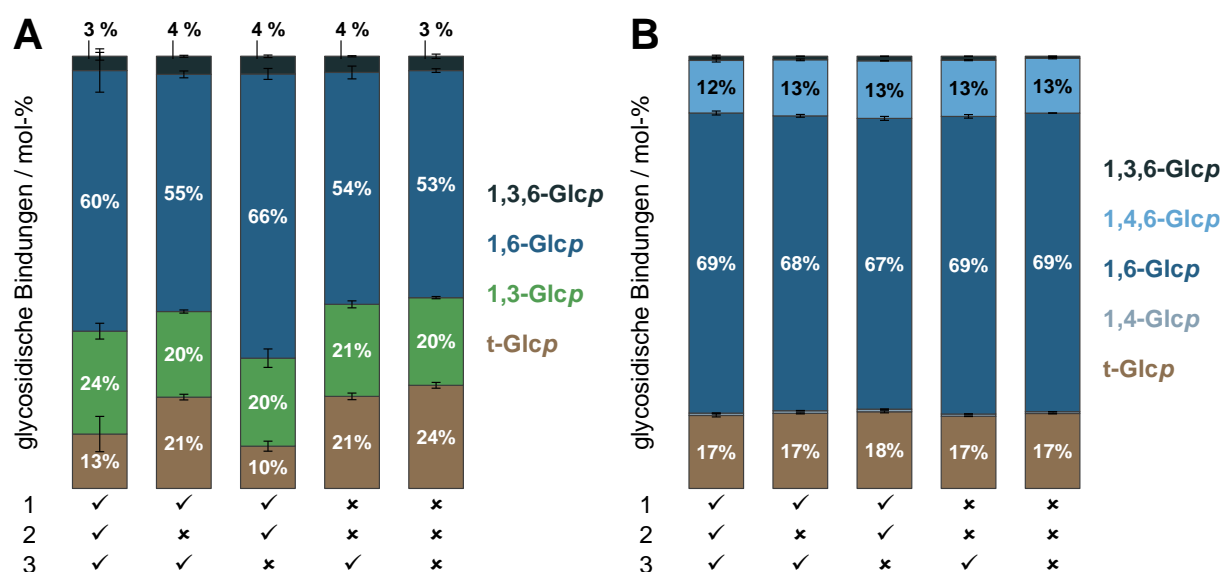
Abbildung 4.1: Anteile der glycosidischen Bindungen in den wasserunlöslichen (A) und wasser-löslichen (B) Modellglucanen in Abhängigkeit von der Anwendung verschiedener Kombinationen der Ultraschallbehandlungen 1, 2 & 3 während der Methylierungsanalyse in Doppelbestimmung. Ultraschallbehandlung 1: während des Quellens in DMSO, Ultraschallbehandlung 2: nach Zugabe von NaOH(s), Ultraschallbehandlung 3: nach Zugabe von Methyliodid, Kreuz: keine Ultraschallbehandlung, Haken: Ultraschallbehandlung, t: terminal, Glc*p*: Glucopyranose, die Zahlen geben die Position der *O*-Substitution an.

Da die optimalen Hydrolysebedingungen vom vorliegenden Polysaccharid abhängen (Kapitel 2.1) und sich permethylierte Polysaccharide während der TFA-Hydrolyse anders verhalten könnten als underivatisierte Polysaccharide, wurden verschiedene Hydrolysebedingungen im Zuge der Methylierungsanalyse angewendet und die Ergebnisse verglichen. Hierbei wurden

die für Glucane beschriebenen Bedingungen (2 M TFA, 121 °C für 60 und 90 min, Kapitel 2.1), mildere Bedingungen (1 M TFA bei 121 °C für 90 min) und die für Fructane häufig verwendeten Bedingungen (1 M TFA bei 70 °C für 30 min, Kapitel 2.1) untersucht. Nach Hydrolyse der permethylierten wasserlöslichen und -unlöslichen Modellglucane mit 2 M TFA bei 121 °C für 60 oder 90 min wurden alle erwarteten PMAA detektiert. Für beide Hydrolysedauern (60 und 90 min) wurden ähnliche Ergebnisse erhalten. Jedoch war bei den wasserunlöslichen Glucanen der Anteil detektierter 1,3-Glc*p* nach 90 min Hydrolysedauer geringfügig höher als nach 60 min, was für eine höhere Stabilität der 1,3-Verknüpfungen im Vergleich zu 1,6-Verknüpfungen spricht. Für beide Modellglucane war 1 M TFA ungeeignet: Nach Hydrolyse mit 1 M TFA bei 70 °C für 30 min wurden keine von Glucose abgeleiteten PMAA detektiert und nach Hydrolyse mit 1 M TFA bei 121 °C für 90 min war der Anteil an terminalen Einheiten im Vergleich zum Erwartungswert und zur Anwendung von 2 M TFA erhöht. Diese Ergebnisse weisen darauf hin, dass die terminalen Einheiten im Vergleich zu einfach oder zweifach substituierten Einheiten schon bei milderen Bedingungen (niedrigerer TFA-Konzentration) abgespalten werden und demnach weniger stabil gebunden sind. Für underivatisierte wasserlösliche Glucane zeigte eine kinetische Studie zur Säurehydrolyse ebenfalls, dass die glycosidischen Bindungen am Ende der Polysaccharide schneller hydrolysiert werden (Basedow *et al*., 1978). Da unklar ist, ob permethylierte Glucane mit underivatisierten Glucanen vergleichbar sind, würde eine Untersuchung zum Verlauf der TFA-Hydrolyse von permethylierten Glucanen weiter Aufschluss zu den optimalen Bedingungen geben. Es ist jedoch davon auszugehen, dass keine Hydrolysebedingungen existieren, bei denen terminale und verzweigte Einheiten gleichermaßen vollständig freigesetzt und nicht abgebaut werden. Dennoch wären Informationen zur Diskriminierung der einzelnen Strukturelemente bei unterschiedlichen Hydrolysebedingungen hilfreich, um die Richtigkeit der Ergebnisse der Methylierungsanalyse besser einschätzen zu können.

Für die Modelllevane wurden nach Hydrolyse mit 1 M TFA (70 °C für 30 min und 121 °C für 90 min) 10 % terminale Fru*f* und 7 % 2,1,6-Fru*f* bestimmt, während nach Hydrolyse mit 2 M TFA (121 °C für 60 und 90 min) weniger terminale als verzweigte Einheiten vorlagen. Nach Verwendung von 2 M TFA bei 121 °C für 60 min fanden auch andere Autoren mehr verzweigte als terminale Fru*f*-Einheiten (Haddar *et al*., 2021; Xu *et al*., 2022a). Dies ist nicht mit dem strukturellen Aufbau von Levanen vereinbar und bestätigt, dass terminale Einheiten bevorzugt abgespalten und bei harscheren Hydrolysebedingungen im weiteren Verlauf der Hydrolyse abgebaut werden. Die Detektion von PMAA aus den Modelllevanen nach Hydrolyse mit 2 M TFA bei 121 °C demonstrierte jedoch, dass permethylierte Levane stabiler sind als underivatisierte, da underivatisierte Levane unter diesen Bedingungen vollständig abgebaut werden (Kapitel 2.1). Zur Verfolgung der Hydrolyse des Levan-Rückgrats wurden die Hydrolyseprodukte der permethylierten Modelllevane nach unterschiedlichen Hydrolyse-bedingungen (1 M TFA bei 70 °C, für 10, 20 oder 30 min sowie 2 M TFA bei 121 °C für 30, 60 oder 90 min) in DMSO gelöst und mittels HPSEC gekoppelt mit einem UV/VIS- und einem RI-Detektor analysiert. Nach manchen Hydrolysebedingungen traten gelbe bis bräunliche Färbungen der Reaktionslösungen auf, weshalb zusätzlich zur RI-Detektion die Messung der

Lichtabsorption bei 420 nm erfolgte. Die Ergebnisse zeigten, dass nach allen Hydrolyse-bedingungen niedermolekulare Produkte mit Elutionsvolumina ähnlich dem Elutionsvolumen von Fructose entstanden und dass die hochmolekularen Levane vollständig hydrolysiert wurden. Zusätzlich trat vor allem nach den Hydrolysen mit 2 M TFA ein früh eluierender Peak auf. Dieser stammte von hochmolekularen Substanzen, die Licht mit einer Wellenlänge von 420 nm absorbierten und somit die Gelbfärbung verursachten. Vermutlich wurden diese Produkte durch Kondensations- und Dehydratisierungsreaktionen von zuvor hydrolytisch freigesetzter, teilweise methylierter Fructose gebildet. Für underivatisierte Fructose wurde die Bildung von gelben polymeren Substanzen im Sauren beschrieben (Krol, 1978; Silberman, 1961), zu den Reaktionsprodukten von methylierten Fructanen oder methylierter Fructose in Anwesenheit von Säure liegen jedoch keine Studien vor. Die polymeren Substanzen traten mit geringerer Peakintensität auch nach den Hydrolysen mit 1 M TFA auf, was darauf hindeutet, dass ihre Bildung nicht vollständig vermieden werden kann. Jedoch konnte durch die HPSEC-Messungen gezeigt werden, dass die milderen Bedingungen (1 M TFA, 70 °C, 20 oder 30 min) einen akzeptablen Kompromiss zwischen Freisetzung und Abbau der Fructose darstellen. Um die Polymerisation von freigesetzter Fructose während der Säurebehandlung zu verringern, sind reduzierende Bedingungen während der Hydrolyse vielversprechend. Dadurch könnten die partiell methylierten Monosaccharide unmittelbar nach ihrer Freisetzung direkt zu den in saurer Umgebung stabileren Alditolen reduziert werden (Stevenson & Furneaux, 1991). Deshalb wurde die Säurehydrolyse der Modelllevane in Anwesenheit des Reduktionsmittels 4-Methylmorpholinboran (MMB) mit verschiedenen TFA-Konzentrationen, Dauern und Tempe-raturen durchgeführt. In ersten Versuchen wurde über die Deuteriummarkierung jedoch nach-gewiesen, dass eine zweite Reduktion durch $NaBD_4$ nach der Hydrolyse notwendig ist, um alle partiell methylierten Monosaccharide zu reduzieren. Dabei wurde der Großteil der partiell methylierten Monosaccharide erst durch $NaBD_4$ reduziert. Zwar wurde für underivatisierte Fructose die vollständige Reduktion durch MMB beschrieben (Garegg *et al*., 1988), allerdings spielen auch hier Unterschiede zwischen underivatisierter und teilweise methylierter Fructose sowie Unterschiede in den Hydrolysebedingungen eine Rolle. Der Einsatz von MMB brachte unter den verwendeten Bedingungen keinen Vorteil, da die verschiedenen PMAA in den gleichen Verhältnissen vorlagen wie nach einer TFA-Hydrolyse ohne MMB. Dennoch könnten die verwendeten Herangehensweisen, HPSEC und reduktive Bedingungen während der Hydrolyse, auf die Untersuchung anderer Polysaccharide übertragen werden.

Die unterschiedlichen optimalen Hydrolysebedingungen für Glucane und Levane erschweren die gleichzeitige Bestimmung der glycosidischen Bindungen beider HoEPS aus ihrer Mischung, wie sie bei fermentativen HoEPS-Synthesen erhalten werden kann. Um die arbeitsintensive und verlustbehaftete Isolierung von Glucanen bzw. Levanen (Kapitel 2.1) zu vermeiden, wurde im nächsten Schritt untersucht, ob die Anwesenheit des jeweils anderen HoEPS die jeweiligen Ergebnisse für Glucane und Levane beeinflusst. Ziel war hier, die Anteile der glycosidischen Bindungen in beiden HoEPS richtig, das heißt wie nach Analyse der Einzel-HoEPS, zu quantifizieren. Zur Bestimmung der Anteile an Levan und Glucan in ihrer Mischung ist die Monosaccharidbestimmung besser geeignet als die Methylierungsanalyse (Kapitel 2.1).

Eine definierte 50/50 (w/w)-Mischung aus Modelllevanen und wasserlöslichen Modellglucanen wurde nach Methylierungsanalyse mit verschiedenen Hydrolysebedingungen (1 M TFA bei 70 °C für 30 min sowie bei 121 °C für 90 min; 2 M TFA bei 121 °C für 60 und 90 min; 3 M TFA bei 121 °C für 90 min) analysiert (Abbildung 4.2). Für Modelllevane wurden nach Hydrolyse der Mischung mit 1 M TFA bei 70 °C für 30 min im Vergleich zur Einzelsubstanz (Abbildung 4.2 links) ähnliche Ergebnisse erhalten, ohne dass aus Glucanen stammende PMAA im Chromatogramm sichtbar waren. Entsprechend konnten die wasserlöslichen Modellglucane nach Hydrolyse mit 3 M TFA bei 121 °C für 90 min bestimmt werden, da störende PMAA aus Levanen nur 2 % der gesamten PMAA ausmachten. Alle PMAA beider Modell-HoEPS wurden nach Hydrolyse mit 1 M TFA bei 121 °C für 90 min sowie nach 2 M TFA bei 121 °C für 60 und 90 min nachgewiesen. Allerdings erschwerte hier die partielle Peaküberlappung der PMAA von 2,1,6-Fru*f* und 1,3,6-Glc*p* die Quantifizierung und die Reproduzierbarkeiten unterschieden sich stark. Nach Hydrolyse mit 2 M TFA bei 121 °C für 60 min war die Abweichung innerhalb der Doppelbestimmung für beide Modell-HoEPS gering, allerdings waren die PMAA aus Levanen (20 %) im Vergleich zu denen aus wasserlöslichen Glucanen unterrepräsentiert (80 %). Dennoch ermöglichen diese Hydrolysebedingungen die Identifizierung und gute Abschätzung der Anteile der glycosidischen Bindungen beider Modell-HoEPS, sodass mit ihnen einen Überblick über die in einer Probe vorliegenden HoEPS erhalten werden kann.
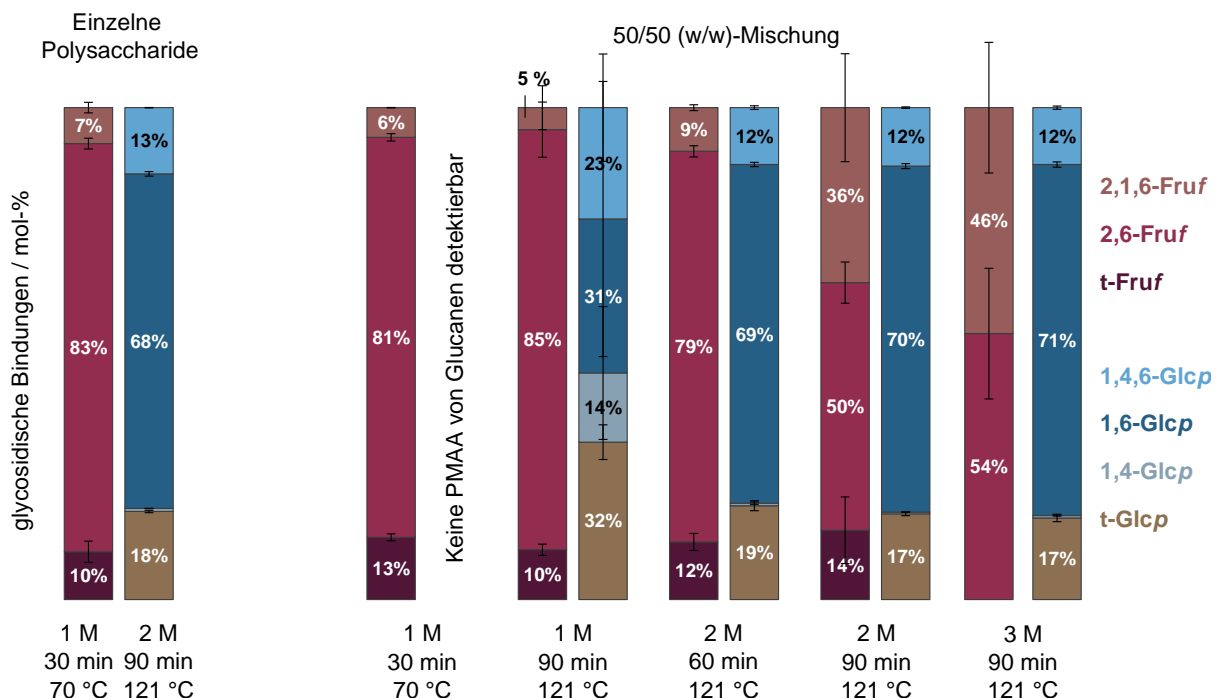
Abbildung 4.2: Anteile der glycosidischen Bindungen in den Modelllevanen und wasserlöslichen Modellglucanen in Abhängigkeit unterschiedlicher Hydrolysebedingungen während der Methylierungsanalyse der 50/50 (w/w)-Mischung beider Polysaccharide in Doppelbestimmung. Die Hydrolysebedingungen (Trifluoressigsäure-Konzentration (M), Dauer (min) und Temperatur (°C)) sind unter den Balken angegeben. Zum Vergleich sind links die Ergebnisse für die einzelne Polysaccharide (linker Balken Levane, rechter Balken Glucane) nach jeweils optimalen Hydrolysebedingungen gezeigt. Fru*f*: Fructofuranose, Glc*p*: Glucopyranose, t: terminal, die Zahlen geben die Position der *O*-Substitution an.

Zusammengefasst konnten an die verschiedenen HoEPS angepasste Bedingungen für die Methylierungsanalyse ermittelt werden. Außerdem konnte gezeigt werden, dass aus der Analyse von HoEPS-Mischungen Informationen über die enthaltenen HoEPS und deren Anteile an glycosidischen Bindungen erhalten werden können. Die gewonnenen Erkenntnisse erlauben eine genaue Analyse der glycosidischen Bindungen in den enzymatisch und fermentativ hergestellten HoEPS dieser Arbeit. Daneben können zukünftig weitere Polysaccharide mit Hilfe der hier verwendeten Ansätze untersucht und weitere Einblicke in die ablaufenden Reaktionen gewonnen werden, was zum besseren Verständnis der Vorgänge während der Derivatisierung beitragen kann.

4.2 Wasserunlösliche α-Glucane von *Streptococcus*-Glucansucrasen

Während die Rolle der wasserunlöslichen Glucane, die durch GS von *Streptococcus*-Bakterien gebildet werden, bei der Entstehung von Plaque und Karies gut untersucht wurde (Kapitel 1), ist über die Feinstrukturen der Glucane einzelner GS wenig bekannt (Kapitel 2.2.2.2). Daher wurden zur systematischen und detaillierten Untersuchung von wasserunlöslichen *Streptococcus*-Glucanen fünf ausgewählte GS rekombinant hergestellt und zur Glucan-synthese eingesetzt: SMUT1101 und SMUT1102 von *Streptococcus mutans* DSM 20523 (NCTC 10449, ATCC 25175) sowie SSAL4540, SSAL4545 und SSAL4550 von *Streptococcus salivarius* DSM 20560 (NCTC 8618, ATCC 7073). Da die GS beider Stämme bisher nicht untersucht wurden, wurden ihre GS durch Aminosäuresequenzvergleich den bereits bekannten GS von *Streptococcus mutans* und *salivarius* (Kapitel 2.2.2.2) zugeordnet. SMUT1101 wurde als GTF-SI und SMUT1102 als GTF-I identifiziert, die beide 1,3- und 1,6-verknüpfte Glucane synthetisieren. Dahingegen wurde SSAL4550 als GTF-K zur Synthese 1,6-verknüpfter Glucane und SSAL4545 als GTF-J zur Synthese 1,3-verknüpfter, teilweise kristalliner Glucane verwendet, um die Strukturvielfalt der wasserunlöslichen Glucane abzudecken. Außerdem wurde die GS SSAL4540 hergestellt, die gemäß Aminosäure-sequenzvergleich zu keiner der vier bekannten GS von *Streptococcus salivarius* passt und deshalb neuartige Glucane synthetisieren könnte. Die Glucansynthese erfolgte in mit $CaCl_2$-versetzter Saccharoselösung bei 37 °C. Die wasserunlöslichen Glucane wurden abzentrifugiert und mit Wasser gewaschen. Sie wurden weder getrocknet noch eingefroren, um ihre nativen räumlichen Strukturen zu erhalten und sie mit Hilfe verschiedener Analysemethoden (Methylierungsanalyse, enzymatische Hydrolyse, HPSEC-RI, XRD, ^{13}C-MAS-NMR-Spektros-kopie) zu charakterisieren.

Die Methylierungsanalyse (Abbildung 4.3) wurde unter Verwendung der an den Modell-glucanen optimierten Bedingungen aus Kapitel 4.1 durchgeführt (Ultraschallbehandlungen 1 & 2, 2 M TFA, 90 min, 121 °C). Für die enzymatischen Hydrolysen wurden *endo*-Dextranase (kommerziell bezogen; *Chaetomium* sp.) und *endo*-Mutanase (rekombinant hergestellt; *Streptococcus salivarius*) verwendet und die freigesetzten Oligosaccharide mittels HPAEC-PAD/MS untersucht. Die von SSAL4550 produzierten Glucane waren ausschließlich α-1,6-verknüpft: In der Methylierungsanalyse wurden < 5 % 1,3- und 1,3,6-Glc*p*-Einheiten bestimmt. Durch *endo*-Dextranase-Hydrolyse wurden Glucose, Isomaltose und Isomaltotriose freigesetzt. Allerdings waren keine an Position *O*3 verzweigten Isomalto-Oligosaccharide nachweisbar und nach *endo*-Mutanase-Hydrolyse wurden keine Oligosaccharide freigesetzt (Abbildung 4.4). Beides spricht dafür, dass die 1,3- und 1,3,6-Glc*p*-Einheiten aus der Methylierungsanalyse Artefakte darstellen.
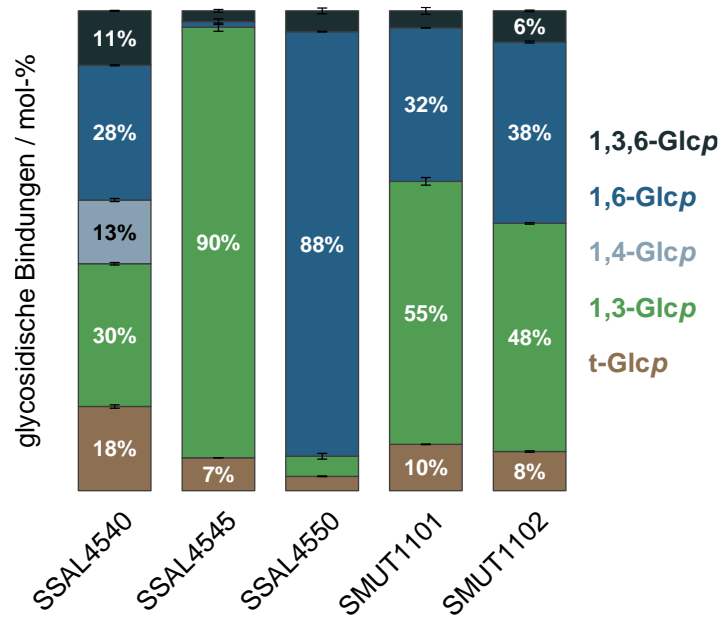
Abbildung 4.3: Anteile der glycosidischen Bindungen der wasserunlöslichen Glucane, die durch die Glucansucrasen SSAL4540, SSAL4545, SSAL4550, SMUT1101 und SMUT1102 synthetisiert wurden. Die glycosidischen Bindungen wurden in Doppelbestimmung durch Methylierungsanalyse bestimmt. t: terminal, Glc*p*: Glucopyranose, die Zahlen geben die Position der *O*-Substitution an.
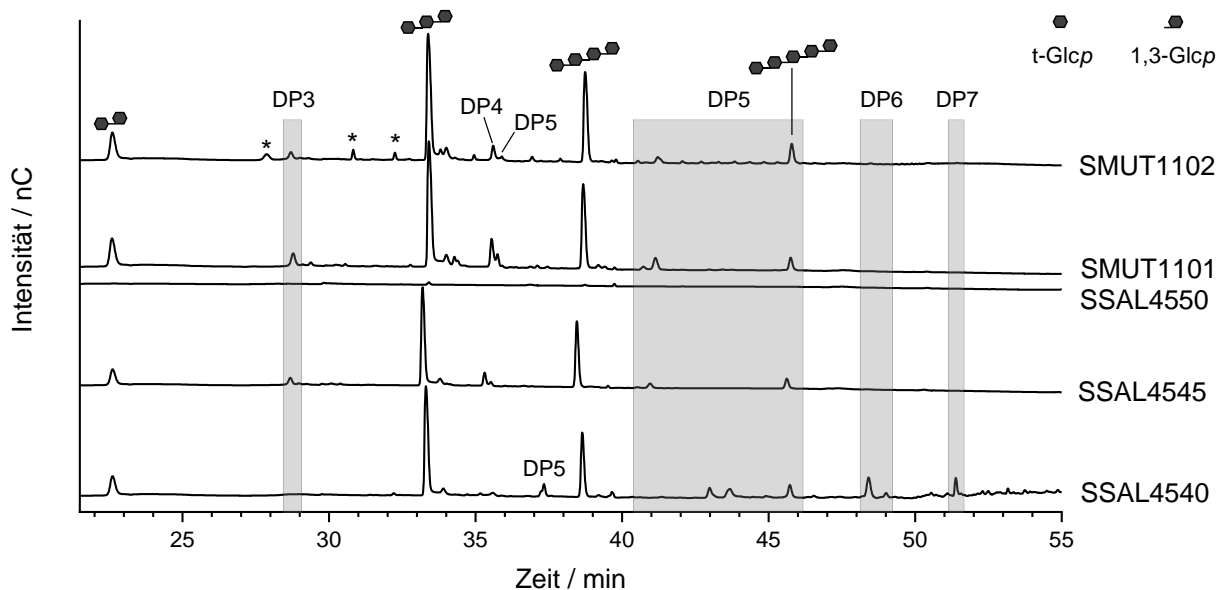
Abbildung 4.4: Chromatogramme (HPAEC-PAD) der *endo*-Mutanase-Hydrolysate der wasserunlöslichen Glucane, die durch die Glucansucrasen SSAL4540, SSAL4545, SSAL4550, SMUT1101 und SMUT1102 synthetisiert wurden. Die Nigero-Oligosaccharide wurden über ihre Retentionszeit identifiziert; die Polymerisationsgrade (DP) der unbekannten Oligosaccharide wurden über die Kopplung mit einem Massenspektrometer bestimmt. Die mit Sternchen (*) markierten Peaks stammten von Isomalto-Oligosacchariden, die auch im Überstand der nicht hydrolysierten Glucansuspension nachweisbar waren. t: terminal, Glc*p*: Glucopyranose, die Zahlen geben die Position der *O*-Substitution an.

Die Ergebnisse der Methylierungsanalyse zeigten, dass die von SSAL4545 produzierten Glucane hauptsächlich 1,3-Verknüpfungen und nur einen geringen Anteil an 1,3,6-verknüpften Einheiten (2 %) aufwiesen. Nach *endo*-Mutanase-Hydrolyse wurden neben ausschließlich α-1,3-verknüpften Nigero-Oligosacchariden weitere Oligosaccharide freigesetzt, für die mit Hilfe der massenspektrometrischen Detektion Polymerisationsgrade von 3 - 7 ermittelt werden

konnten. Die unterschiedlichen Retentionszeiten von Oligosacchariden mit demselben Polymerisationsgrad deuten darauf hin, dass diese Oligosaccharide unterschiedlich verknüpft sind und somit von Verzweigungen stammen. Durch *endo*-Dextranase wurden keine Oligosaccharide freigesetzt. Die Strukturen der von SSAL4550 und SSAL4545 gebildeten Glucane passen zu den für GTF-K und GTF-J Glucane in der Literatur beschriebenen Strukturen (Kobayashi *et al*., 2017; Kusumi *et al*., 2023; Simpson *et al*., 1995), außer dass die 1,6-verknüpften Glucane wasserunlöslich sind. Dies könnte durch ein höheres Molekulargewicht und/oder die Linearität der Glucane von SSAL4550 begründet sein.

Die von SSAL4540 synthetisierten Glucane enthielten 30 % 1,3-, 13 % 1,4- und 28 % 1,6-verknüpfte Glc*p*-Einheiten und waren durch 11 % 1,3,6-Glc*p*-Einheiten verzweigt. Nach *endo*-Dextranase-Hydrolyse wurden keine Oligosaccharide detektiert, was bedeutet, dass die 1,6-Verknüpfungen für das Enzym nicht zugänglich waren und vermutlich nicht in Blöcken vorlagen. Analog wurden durch α-Amylase keine Oligosaccharide freigesetzt, was zeigte, dass die 1,4-Verknüpfungen für das Enzym nicht zugänglich waren. Durch *endo*-Mutanase-Hydrolyse wurden neben linearen Nigero-Oligosacchariden weitere Oligosaccharide freigesetzt. Im Vergleich zu den Hydrolysaten der anderen Glucane enthielt das Hydrolysat der von SSAL4540 produzierten Glucane zusätzliche Oligosaccharide, die 1,3-, 1,4- und/oder 1,6-Verknüpfungen enthalten könnten. In der Literatur wurden nur wenige wasserunlösliche Glucane mit 1,4-Verknüpfungen beschrieben (Kapitel 2.2.2.2). Hayacibara *et al*. (2004) beschrieben 16 - 25 % 1,4-Verknüpfungen in Glucanen der GTF-C von *Streptococcus mutans*, führten jedoch keine genaueren Strukturanalysen dieser Glucane durch, sodass hier *Streptococcus*-Glucane mit relevanten Anteilen an 1,3-, 1,4- und 1,6-Verknüpfungen erstmalig genauer analysiert wurden. Zudem zeigen die erhaltenen Ergebnisse, dass auch GS aus *Streptococcus salivarius* derartige komplexe Glucane bilden können.

Die von SMUT1101 und SMUT1102 gebildeten Glucane wiesen neben 1,6-Verknüpfungen mit 55 bzw. 48 % hauptsächlich 1,3-Verknüpfungen auf und waren durch 1,3,6-Glc*p*-Einheiten verzweigt. Die Verknüpfungen entsprechen den in der Literatur (Hayacibara *et al*., 2004; Kopec *et al*., 1997) beschriebenen und bestätigen, dass GTF-I (SMUT1101) mehr 1,3-Verknüpfungen synthetisiert als GTF-SI (SMUT1102). Nach *endo*-Mutanase-Hydrolyse wurden alle Oligosaccharide, die auch aus den von SSAL4545 synthetisierten Glucanen freigesetzt wurden, detektiert. Dies wies auf einen ähnlichen Aufbau der 1,3-verknüpften Abschnitte in den von SMUT1101, SMUT1102 und SSAL4545 produzierten Glucanen hin. Die e*ndo*-Dextranase-Hydrolyse der von SMUT1101 und SMUT1102 gebildeten Glucane resultierte in der Freisetzung von Isomalto-Oligosacchariden und an Position *O*3 verzweigten Isomalto-Oligosacchariden mit mono- bis trimeren 1,6-verknüpften Seitenketten, die von Münkel *et al.* (2019) in wasserunlöslichen Glucanen anderer Bakteriengattungen nachgewiesen wurden (Kapitel 2.2.2.2). Dies verdeutlichte, dass in den von SMUT1101 und SMUT1102 synthetisierten Glucanen 1,6-verknüpfte Abschnitte mit Seitenketten aus mehreren Einheiten vorlagen. Unterschiedliche Peakintensitätsverhältnisse der durch beide Hydrolasen entstandenen Oligosac-

charide wiesen auf einen unterschiedlichen strukturellen Aufbau der von SMUT1101 und SMUT1102 gebildeten Glucane hin.

Die Freisetzung von Isomalto-Oligosacchariden und an Position *O*3 verzweigten Isomalto-Oligosacchariden durch *endo*-Dextranase sowie von potenziell verzweigten Nigero-Oligosacchariden durch *endo*-Mutanase aus wasserunlöslichen *Streptococcus*-Glucanen wurde bisher nicht in der Literatur beschrieben. Hydrolasen wurden zur Strukturanalyse von wasserunlöslichen Glucanen von *Streptococcus*-GS verwendet, um den Anteil an Glucan, der nach Hydrolaseinkubation wasserlöslich wurde, zu bestimmen, oder es wurden einzelne Hydrolyseprodukte quantifiziert. In machen Studien wurden auch verschiedene Hydrolyseprodukte mehrerer Glucane verglichen (Hare *et al*., 1978; Hayacibara *et al*., 2004; Kopec *et al*., 1997; Pearce *et al*., 1990; Vacca-Smith *et al*., 1996). Nach Mutanase-Hydrolyse von wasserunlöslichen *Streptococcus*-Glucanen wurden bereits lineare Nigero-Oligosaccharide detektiert (Pleszczyńska *et al*., 2012; Tsumori *et al*., 2011), allerdings wurden keine weiteren Oligosaccharide näher betrachtet. Die Strukturaufklärung der unbekannten Oligosaccharide könnte zukünftig genauere Aussagen über die Glucanstrukturen ermöglichen.

Nach *endo*-Dextranase- und *endo*-Mutanase-Hydrolyse der enzymatisch hergestellten *Streptococcus*-Glucane blieben wasserunlösliche Rückstände zurück, die zusammen mit den unmodifizierten Glucanen mittels HPSEC-RI analysiert wurden. Das Lösungsmittel, in dem sich die meisten wasserunlöslichen Glucane dieser Arbeit lösten, war DMSO mit einem Zusatz von 100 mM LiCl. Hierbei war die Zugabe von LiCl als Feststoff zu in DMSO vorgequollenen Glucanen nötig. Die von SSAL4545, SMUT1101 und SMUT1102 synthetisierten Glucane und ihre Rückstände nach Hydrolyse wurden in DMSO mit 100 mM LiCl gelöst, während sich die von SSAL4550 und SSAL4540 produzierten Glucane nicht lösten und dementsprechend nicht analysiert werden konnten. Zur Abschätzung der Molekulargewichte dienten Standardglucane mit bekannten Molekulargewichten (*dextran blue* (circa 2 MDa); 670, 270, 64,3 und 12 kDa). Anhand der Elugramme (Abbildung 4.5) wurde deutlich, dass die Glucane der drei GS unterschiedliche Größenverteilungen besaßen. Während die von SSAL4545 synthetisierten Glucane eine breite Größenverteilung von circa 2 MDa bis 12 kDa aufwiesen, besaßen die von SMUT1102 produzierten Glucane ein hohes Molekulargewicht von circa 2 MDa. Die von SMUT1101 synthetisierten Glucane enthielten zwei Fraktionen mit circa 2 MDa und weniger als 12 kDa Molekulargewicht. Auch die wasserunlöslichen Rückstände nach *endo*-Dextranase-Hydrolyse wiesen unterschiedliche Molekulargewichtsverteilungen auf. Das Molekulargewicht der von SMUT1102 synthetisierten wasserunlöslichen Glucane wurde durch die Hydrolyse von circa 2 MDa auf 64,3 bis12 kDa verringert, was bedeutet, dass sowohl die nicht-hydrolysierten 1,3-Verknüpfungen als auch die hydrolysierten 1,6-Verknüpfungen in längeren Abschnitten vorlagen. Durch *endo*-Dextranase-Hydrolyse wurde bei den wasserunlöslichen Fraktionen der von SMUT1101 synthetisierten Glucane die relative Peakintensität der höhermolekularen Fraktion verringert. Dementsprechend wurde diese Fraktion teilweise hydrolysiert. Auf die Molekulargewichtsverteilung der von SSAL4545 produzierten Glucane hatte *endo*-Dextranase

hingegen keinen Einfluss, was bestätigte, dass diese Glucane nicht durch *endo*-Dextranase hydrolysiert wurden.
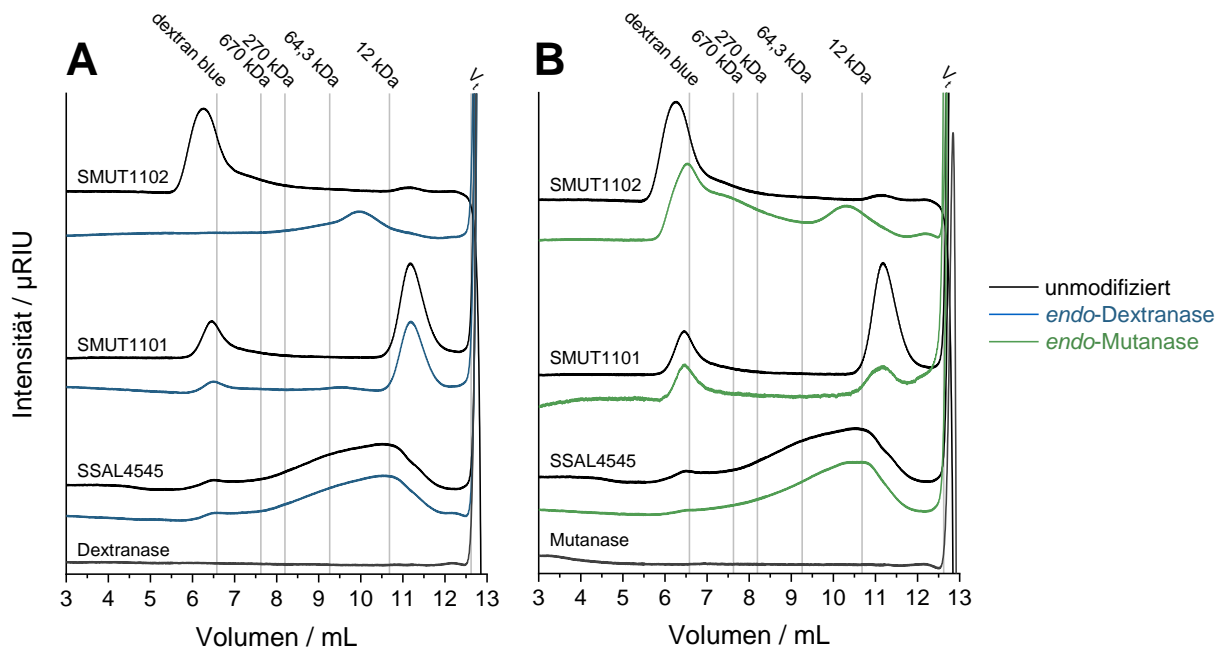
Abbildung 4.5: Elugramme (HPSEC-RI) der wasserunlöslichen Glucane, die durch die Glucan-sucrasen SSAL4545, SMUT1101 und SMUT1102 synthetisiert wurden, sowie ihrer wasser-unlöslichen Produkte nach *endo*-Dextranase- (A) und *endo*-Mutanase-Hydrolyse (B). Die Elutions-volumina der Peakmaxima der Größenstandards (*dextran blue*: circa 2 MDa) und das Elutionsvolumen von Glucose (V$_t$) sind durch Referenzlinien angegeben. Zudem sind die Elugramme der beiden Enzyme ohne Glucan gezeigt.

Auch die Molekulargewichtsverteilungen der wasserunlöslichen Rückstände nach *endo*-Mutanase-Hydrolyse unterschieden sich. Das Elutionsprofil der von SSAL4545 gebildeten wasserunlöslichen Glucane wurde durch die Hydrolyse wenig verändert. Folglich hatte die Freisetzung der wasserlöslichen Oligosaccharide keinen Einfluss auf die Molekular-gewichtsverteilung. Diese unvollständige Hydrolyse durch *endo*-Mutanase war bei den hauptsächlich 1,3-verknüpften Glucanen nicht zu erwarten und könnte an einer begrenzten enzymatischen Zugänglichkeit der Glucane, beispielsweise durch kristalline Bereiche, liegen. Bei den von SMUT1102 synthetisierten Glucanen resultierte die *endo*-Mutanase-Hydrolyse in Produkten mit einer breiteren Größenverteilung und dem Entstehen einer neuen Fraktion im Größenbereich von 64,3 bis 12 kDa. In Kombination mit der *endo*-Dextranase-Hydrolyse wurde deutlich, dass die linear 1,6-verknüpften Abschnitte im Durchschnitt länger waren, als die linear 1,3-verknüpften Abschnitte. Insgesamt wiesen die Ergebnisse auf das Vorliegen von Copolymeren mit 1,6- und 1,3-verknüpften Abschnitten hin. Copolymer-Strukturen mit 1,3- und 1,6-verknüpften Abschnitten wurden bisher für wasserunlösliche Glucane von *Leuconostoc* und von *Streptococcus salivarius* vorgeschlagen (Kapitel 2.2.2.2). Dabei wurde für beide Gattungen jeweils eine GS beschrieben, die copolymere Glucane synthetisiert (Kusumi *et al*., 2023; Wangpaiboon *et al*., 2020), während hier erstmals copolymere α-Glucane einer GS aus *Streptococcus mutans* identifiziert wurden. Bei den von SMUT1101 synthetisierten Glucanen wurde die relative Peakfläche der Fraktion mit geringerem Molekulargewicht durch *endo*-

Mutanase-Hydrolyse reduziert, was darauf hindeutet, dass hier konsekutiv 1,3-verknüpfte Abschnitte vorlagen. Somit lagen bei den von SMUT1101 synthetisierten Glucanen in der höhermolekulareren Fraktion vor allem 1,6-Verknüpfungen und in der niedermolekulareren Fraktion vor allem 1,3-Verknüpfungen vor. Insgesamt bestätigten die HPSEC-Analysen die Ergebnisse der HPAEC und zeigten, dass es sich bei den von SMUT1101 und SMUT1102 produzierten Glucanen um komplexe (Co)Polymere mit unterschiedlicher Struktur handelte. Zusammenfassend konnte durch die HPSEC-RI-Analysen festgestellt werden, dass die von SSAL4545, SMUT1101 und SMUT1102 produzierten wasserunlöslichen α-Glucane sehr unterschiedliche Größenverteilungen aufwiesen. Für die von GTF-L gebildeten gemischt-verknüpften Glucane bestimmten Kusumi *et al.* (2023) ein Molekulargewicht von ca. 1 MDa mit relativ hoher Polydispersität, was zusätzlich darauf hindeutet, dass die Molekulargewichtsverteilungen der Glucane von *Streptococcus*-GS vielfältig sind. Jedoch existiert für die Bestimmung der Molekülgröße von wasserunlöslichen Glucanen keine weitere Literatur (Kapitel 2.2.2.2), sodass diese Arbeit die bisherigen Erkenntnisse deutlich erweitert.

Um Informationen über starre, kristallähnliche Bereiche in den enzymatisch hergestellten, nativen Glucanen zu erhalten, wurden sie mit XRD und ^{13}C-MAS-NMR-Spektroskopie analysiert. Hierfür wurden die Glucane nass und unter Vermeidung von Wasserverdunstung vermessen. In der XRD beugen vergleichsweise große kristalline Strukturen Röntgenstrahlen, was für die von SSAL4545, SMUT1101 und SSAL4540 synthetisierten Glucane beobachtet werden konnte. In den Diffraktogrammen der von SSAL4545 und SMUT1101 produzierten Glucane waren Peaks vorhanden, die in Literatur bereits für lineare α-1,3-verknüpfte Glucane gefunden wurden (Kobayashi *et al*., 2017). Für die von SSAL4540 gebildeten Glucane wurden jedoch bei anderen Winkeln Peaks detektiert, was auf eine andere Kristallstruktur hinweist. Zur weiteren Analyse dieser starren Bereiche wurden die Proben mit ^{13}C-MAS-NMR-Spektroskopie (*cross* und *direct polarization*) untersucht. Die *cross polarization*-NMR-Spektren der von SSAL4545, SMUT1101 und SMUT1102 gebildeten Glucane waren ähnlich und enthielten hauptsächlich Signale, die α-1,3-Glc*p*-Einheiten zugeordnet werden konnten. Dementsprechend lagen in den starren, wenig beweglichen Bereichen hauptsächlich 1,3-Glc*p*-Einheiten vor und die in den von SMUT1101 und SMUT1102 synthetisierten Glucanen enthaltenen 1,6-Glc*p*-Einheiten befanden sich in beweglicheren Abschnitten. Diese Erkenntnis bestätigten die *direct polarization*-NMR-Spektren, in denen zusätzliche Signale auftraten, die α-1,6-Glc*p* zugeordnet wurden. Dass die starren Bereiche der von SMUT1102 gebildeten Glucane in den Diffraktogrammen nicht sichtbar waren, könnte aus ihrer geringen Größe resultieren. Für die von SSAL4540 synthetisierten Glucane waren lediglich im *direct polarization*-NMR-Spektrum, aber nicht im *cross polarization*-NMR-Spektrum Signale vorhanden. Dies deutete entgegen der Ergebnisse aus der XRD darauf hin, dass diese Glucane keine starren Bereiche aufwiesen. Eventuell stammten die Peaks im Diffraktogramm von Verunreinigungen, sodass die Glucane von SSAL4540 als gemischt-verknüpfte Glucane mit drei Verknüpfungstypen zukünftig weiter untersucht werden sollten. Dennoch zeigen die erhaltenen Ergebnisse, dass nicht nur in ausschließlich 1,3-verknüpften sondern auch in gemischt-verknüpften Glucanen von *Streptococcus*-GS starre, kristallähnliche Bereiche

vorliegen. Bisher waren lediglich zu gemischt-verknüpften Glucanen einer GS von *Leuconostoc* Hinweise auf kristalline Bereiche durch XRD-Analysen vorhanden (Kapitel 2.2.2.2). Darüber hinaus erlaubt die MAS-NMR-Spektroskopie erstmalig Einblicke in die Verteilung der Verknüpfungstypen in den beweglichen bzw. starren Bereichen der Glucane.

Die Ergebnisse dieser Arbeit bestätigen die in der Literatur für Glucane von *Streptococcus*-GS beschriebenen Verknüpfungen und zeigen darüber hinaus Einblicke in die Feinstrukturen, was die Kombination der Analysemethoden ermöglicht. Durch die Verwendung einzelner, rekombinant hergestellter GS konnten strukturell diverse wasserunlösliche α-Glucane synthetisiert werden. Die von SSAL4550 synthetisierten Glucane wurden als lineare, 1,6-verknüpfte Glucane identifiziert, die keine starren oder kristallähnlichen Bereiche aufwiesen. Die von SSAL4545 produzierten Glucane waren fast ausschließlich aus 1,3-Verknüpfungen aufgebaut, zeigten eine breite Molekülmassenverteilung und wiesen kristalline Bereiche auf. Bei den von SSAL4540 gebildeten Glucanen handelte es sich um ungewöhnliche, gemischt-verknüpfte Glucane mit drei Verknüpfungstypen. Während die 1,6- und 1,4-Verknüpfungen nicht enzymatisch hydrolysiert wurden, waren längere 1,3-verknüpfte Abschnitte vorhanden, die durch *endo*-Mutanase hydrolysiert wurden. Hier könnte die Identifizierung der unbekannten Oligosaccharide weitere Erkenntnisse über die Struktur liefern. Für diese Glucane konnten keine starren oder kristallähnlichen Bereiche nachgewiesen werden. SSAL4540 und die von ihr gebildeten Glucane sollten weiter untersucht werden, um aufzuklären, wie GS drei Verknüpfungstypen synthetisieren und ob die Glucane ungewöhnliche physikochemische Eigenschaften besitzen. Die von SMUT1101 und SMUT1102 produzierten Glucane besaßen längere 1,3- und längere 1,6-verknüpfte Abschnitte mit Verzweigungen. Außerdem wiesen sie starre, kristallähnliche Bereiche auf, in denen vor allem die 1,3-Glc*p*-Einheiten involviert waren, während sich die 1,6-Glc*p*-Einheiten in beweglicheren Bereichen befanden. Die Glucane beider GS unterschieden sich den enzymatischen Hydrolysen zufolge in ihren Feinstrukturen und besaßen unterschiedliche Molekülgrößenverteilungen. Die von SMUT1101 produzierten Glucane bestanden aus zwei Fraktionen mit unterschiedlicher Größe und Verknüpfungen, während die von SMUT1102 gebildeten Glucane Copolymere waren.

4.3 Fermentativ von *Leuconostoc & Liquorilacto-bacillus* gebildete Homoexopolysaccharide

Bei der fermentativen HoEPS-Synthese können Mischungen aus Glucanen und Fructanen entstehen. Für die Strukturanalyse stellt dies eine Herausforderung dar und in der Vergangenheit wurden nur von einigen *Streptococcus*-Bakterien die gesamten HoEPS vergleichend und umfassend untersucht (Birkhed *et al*., 1979). Deshalb wurden in dieser Arbeit sieben Bakterienstämme der Gattungen *Leuconostoc* und *Liquorilactobacillus* für den Vergleich der (Fein)Strukturen von fermentativ hergestellten, wasserlöslichen und -unlöslichen HoEPS ausgewählt: *Leuconostoc mesenteroides* subsp. *dextranicum* NRRL B-1121 und B-1144, *Leuconostoc mesenteroides* subsp. *mesenteroides* NRRL B-1149, B-1438 und B-1118, *Leuconostoc suionicum* DSM 20241 und *Liquorilactobacillus satsumensis* DSM 16230. Die Bakterien wurden für die HoEPS-Synthese unter identischen Bedingungen in mit Saccharose supplementiertem Medium kultiviert. Anschließend wurden die Kulturen durch Zentrifugation in Überstände mit wasserlöslichen HoEPS sowie Rückstände mit wasserunlöslichen HoEPS und Bakterienzellen getrennt und nach einer angepassten Methode aufgereinigt. Hierbei wurden die wasserlöslichen HoEPS mit Ethanol präzipitiert und zur Abtrennung von Proteinen in 1 M NaOH gelöst und zentrifugiert, während die wasserunlöslichen Rückstände in 1 M NaOH gelöst, zentrifugiert und mit Ethanol präzipitiert wurden. Abschließend wurden alle HoEPS dialysiert und gefriergetrocknet. Die Bakterien aller sieben Stämme synthetisierten sowohl wasserlösliche als auch -unlösliche HoEPS, wobei sich die Gesamtausbeuten deutlich unterschieden. Es wurden zwischen 5 und 22 g HoEPS / L Kultur gebildet. Auch die relativen Ausbeuten an wasserlöslichen und wasserunlöslichen HoEPS variierten. Während Bakterien mancher Stämme hauptsächlich wasserunlösliche HoEPS bildeten (NRRL B-1121, B-1144, B-1118) synthetisierten andere hauptsächlich wasserlösliche HoEPS (NRRL B-1149, DSM 20241). Zur Ausbeutenerhöhung könnten die Kultivierungsbedingungen für einzelne Stämme und HoEPS gezielt optimiert werden, was in der Literatur mehrfach beschrieben wurde (Esmaeilnejad-Moghadam *et al*., 2019; Nabot *et al*., 2022; Sawale & Lele, 2010). Dies lag jedoch nicht im Fokus dieser Arbeit und die Ausbeuten mancher Bakterienstämme (NRRL B-1121 & B-1144, DSM 20241 & 16230) waren auch ohne optimierte Kultivierungsbedingungen bereits vielversprechend.

4.3.1 Wasserunlösliche Glucane

Die wasserunlöslichen HoEPS aller sieben Stämme wurden nach TFA-Hydrolyse und Monosaccharidbestimmung als Glucane identifiziert. Die Ergebnisse der Methylierungsanalyse (Abbildung 4.6) zeigten, dass alle Glucane 1,6-, 1,3-, und 1,3,6-Glc*p*-Einheiten sowie terminale Glc*p*-Einheiten enthielten. Neben 3 - 12 % Verzweigungen machten die 1,6-Verknüpfungen 36 - 68 % und die 1,3-Verknüpfungen 5 - 40 % aus. 1,3- und 1,6-Verknüpfungen sowie Verzweigungen durch 1,3,6-Verknüpfungen sind typisch für wasserunlösliche Glucane (Kapitel 2.2.2.2). Die Anteile der glycosidischen Bindungen in den Glucanen von NRRL B-1121, B-1149,

B-1118 und B-1438 ähneln den in der Literatur beschriebenen (Côté & Skory, 2015; Jeanes *et al*., 1954; Pearce *et al*., 1990; Slodki *et al*., 1986), während sie für die wasserunlöslichen Glucane von NRRL B-1144, DSM 20241 & 16230 bislang nicht beschrieben wurden. Die Ergebnisse für die Glucane der Stämme NRRL B-1144 und DSM 16230 bestätigen zudem, dass auch Glucane mit geringen Anteilen an 1,3-Glc*p* wasserunlöslich sein können. Im Vergleich zu den enzymatisch hergestellten Glucanen (Kapitel 4.2) ist die Varianz in den Bindungstypen gering, dennoch weisen die unterschiedlichen Anteile auf unterschiedliche Feinstrukturen hin.
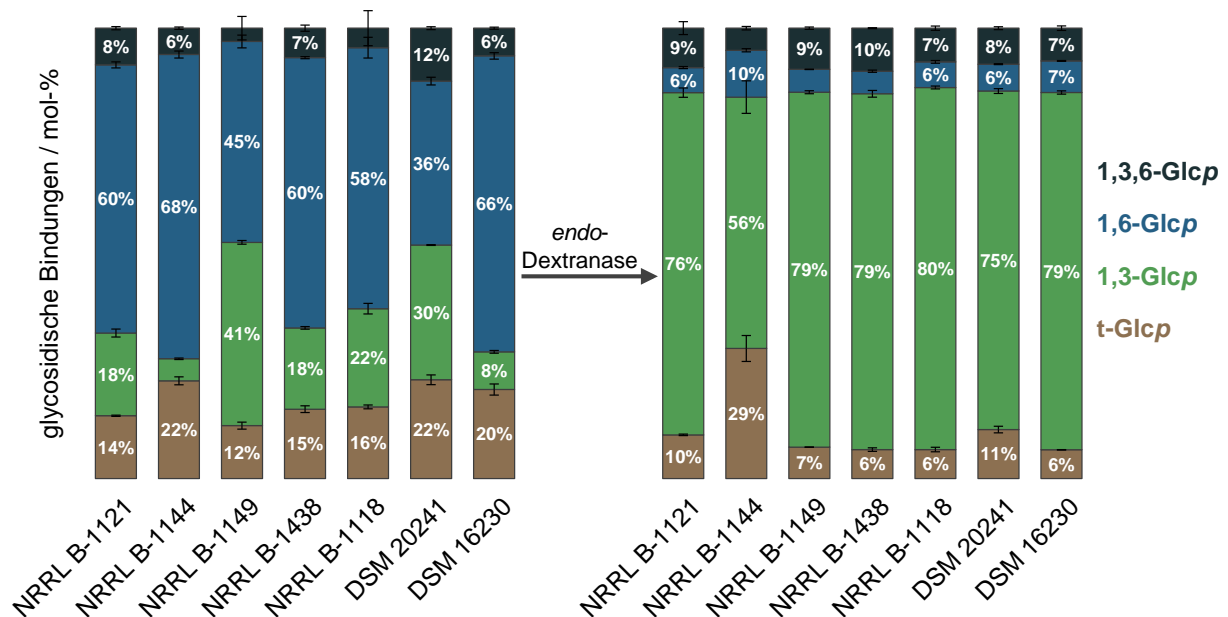
Abbildung 4.6: Anteile der glycosidischen Bindungen in den fermentativ hergestellten wasserunlöslichen Glucanen (links) und ihren wasserunlöslichen Rückständen nach *endo*-Dextranase-Hydrolyse (rechts). Die Glucane wurden von Bakterien der Stämme NRRL B-1121, B-1144, B-1149, B-1438 & B-1118 und DSM 20241 & 16230 synthetisiert. Die glycosidischen Bindungen wurden in Doppelbestimmung durch Methylierungsanalyse bestimmt. t: terminal, Glc*p*: Glucopyranose, die Zahlen geben die Position der *O*-Substitution an.

Um die Verteilung der verschiedenen Verknüpfungstypen zu untersuchen, wurden die wasserunlöslichen Glucane mit *endo*-Dextranase hydrolysiert. Die wasserlöslichen Produkte wurden mittels HPAEC-PAD analysiert. Neben Isomaltose wurden durch *endo*-Dextranase-Hydrolyse unterschiedliche, an Position *O*3 verzweigte Isomalto-Oligosaccharide in ähnlichen Verhältnissen freigesetzt. Diese Isomalto-Oligosaccharide wiesen mono- bis trimere an Position *O*3 gebundene, 1,6-verknüpfte Seitenketten auf. Daraus konnte gefolgert werden, dass in den 1,6-verknüpften Abschnitten der wasserunlöslichen Glucane mehrere Einheiten lange Seitenketten an Position *O*3 gebunden vorlagen. Diese Strukturelemente wurden ebenfalls von Münkel *et al.* (2019) in den wasserunlöslichen Glucanen der *Leuconostoc* GS Lc1215 und Lc2135 sowie von *Lentilactobacillus hilgardii* identifiziert (Kapitel 2.2.2.2). Auch für wasserunlösliche Glucane von *Leuconostoc mesenteroides* NRRL B-1355 gab es in der Literatur Hinweise auf Verzweigungen in den 1,6-verknüpften Abschnitten (Kapitel 2.2.2.2), jedoch wurden keine genaueren Analysen durchgeführt. Insgesamt schienen die Strukturen der 1,6-verknüpften Abschnitte denen von Dextranen zu ähneln (Kapitel 2.2.2.1).

Nach der *endo*-Dextranase-Hydrolyse blieben wasserunlösliche Rückstände zurück, die entsprechend den Ergebnissen der Methylierungsanalyse hauptsächlich aus 1,3-Glc*p* mit 5 - 10 % 1,3,6-Glc*p* bestanden (Abbildung 4.6). 1,6-Glc*p* war nur noch in Anteilen von 5 - 10 % enthalten. Demnach wurden die 1,6-Verknüpfungen fast vollständig hydrolysiert und die 1,6-verknüpften Abschnitte der Glucane waren trotz Wasserunlöslichkeit der Glucane für die *endo*-Dextranase zugänglich. Den HPSEC-RI-Ergebnissen zufolge reduzierte die *endo*-Dextranase-Hydrolyse das Molekulargewicht der wasserunlöslichen Glucane von mehreren MDa auf circa 270 bis 12 kDa (Abbildung 4.7). Folglich waren die 1,3-verknüpften Abschnitte relativ kurz und zwischen 1,6-verknüpften Abschnitten eingebettet. Durch *endo*-Mutanase-Hydrolyse wurden aus den 1,3-verknüpften Abschnitten der nach *endo*-Dextranase-Hydrolyse wasserunlöslichen Rückstände neben linearen Nigero-Oligosacchariden zwei unterschiedlich verknüpfte Pentasaccharide in variierenden Anteilen freigesetzt. Entsprechend wiesen die 1,3-verknüpften Abschnitte der wasserunlöslichen Glucane unterschiedliche Feinstrukturen auf und es konnte bestätigt werden, dass die 1,3-verknüpften Abschnitte verzweigt waren. In der Literatur wurde lediglich die Freisetzung von Nigerose und Nigerotriose durch Mutanase aus zuvor mittels *endo*-Dextranase hydrolysierten wasserunlöslichen Glucanen von *Leuconostoc mesenteroides* B-523 berichtet (Côté & Leathers, 2009). Eine Analyse des Molekulargewichts der Polysaccharide sowie der Größe der verschiedenen Abschnitte erfolgte jedoch nicht, sodass die Ergebnisse dieser Arbeit das Wissen über bakterielle Glucane erweitern und eine Herangehensweise zur Untersuchung weiterer wasserunlöslicher Glucane aufzeigen. Die HPSEC-RI-Analysen dieser Arbeit erlauben den unmittelbaren Vergleich der Molekulargewichtsverteilungen aller untersuchten wasserunlöslichen Glucane. Die Unterschiede in den Molekülgrößen der fermentativ hergestellten Glucane waren im Vergleich zu den durch *Streptococcus*-GS enzymatisch hergestellten wasserunlöslichen Glucanen (Kapitel 4.2) gering. Die Molekülgrößen der Glucane und ihrer nach *endo*-Dextranase-Hydrolyse wasserunlöslichen Rückstände waren bei den fermentativ und den von SMUT1102 produzierten Glucanen ähnlich, was auf Copolymer-Strukturen mit ähnlichen langen Abschnitten hindeutet.

Insgesamt konnte gezeigt werden, dass die wasserunlöslichen Glucane der sieben Bakterienstämme aus 1,6-verknüpften, verzweigten Abschnitten bestanden, die durch vergleichsweise kürzere 1,3-verknüpfte, ebenfalls verzweigte Abschnitte unterbrochen waren. Die isolierten 1,3-verknüpften Abschnitte waren wasserunlöslich und hatten unterschiedliche Feinstrukturen. Trotz der hohen Varianz in den Anteilen der 1,3- und 1,6-verknüpften Abschnitte wiesen die fermentativ hergestellten wasserunlöslichen Glucane ähnliche Strukturen auf. Diese blockartigen Strukturen erinnerten an die Struktur der von SMUT1102 synthetisierten Glucane (Kapitel 4.2) und wurden auf Basis anderer Analysemethoden ebenfalls für weitere Glucane beschrieben (Côté *et al*., 1999; Kusumi *et al*., 2023; Wangpaiboon *et al*., 2020).
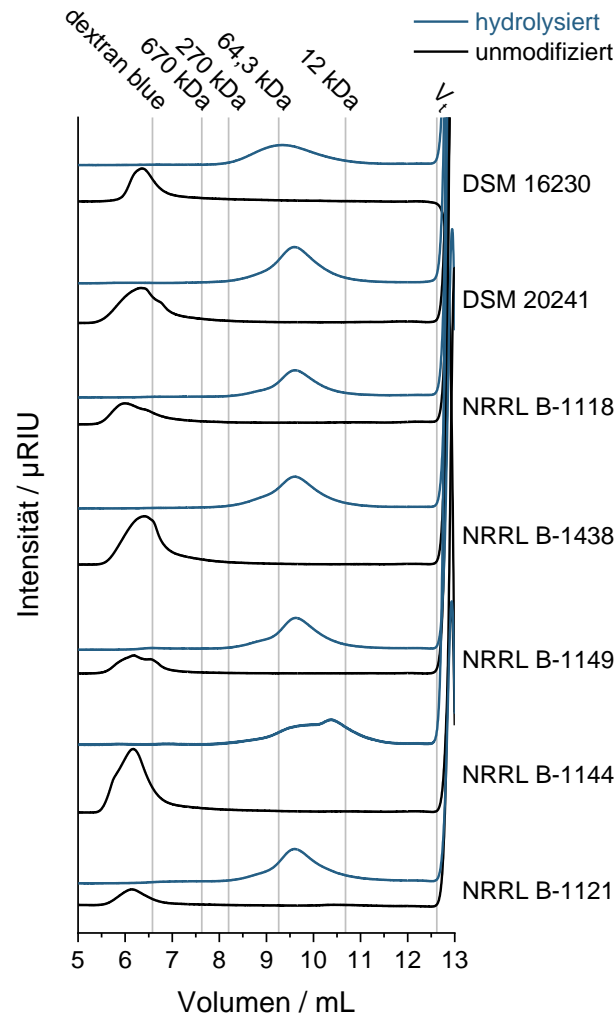
Abbildung 4.7: Elugramme (HPSEC-RI) der fermentativ hergestellten wasserunlöslichen Glucane und ihrer wasserunlöslichen Rückstände nach *endo*-Dextranase-Hydrolyse. Die Glucane wurden von Bakterien der Stämme NRRL B-1121, B-1144, B-1149, B-1438 & B-1118 und DSM 20241 & 16230 synthetisiert. Die Elutionsvolumina der Peakmaxima der Größenstandards (*dextran blue*: circa 2 MDa) und das Elutionsvolumen von Glucose (V_t) sind durch Referenzlinien angegeben.

4.3.2 Wasserlösliche Glucane & Fructane

Neben den wasserunlöslichen Glucanen synthetisierten die Milchsäurebakterien aller sieben Stämme wasserlösliche HoEPS. Die Monosaccharidbestimmung nach TFA-Hydrolyse ergab, dass diese aus Glucanen und Fructanen in unterschiedlichen Anteilen bestanden. Die wasserlöslichen HoEPS der Stämme NRRL B-1149, B-1118 und DSM 20241 waren Fructane (Glucane < 3 %) und DSM 16230 bildete ausschließlich Glucane. Die Stämme NRRL B-1438, B-1121 und B-1144 synthetisierten wasserlösliche Glucane und Fructane. Die chemischen Verschiebungen der Signale in den ^{1}H-NMR-Spektren der HoEPS wiesen darauf hin, dass es sich um 1,6-verknüpfte Glucane und Levane handelte. Zur genaueren Bestimmung der glyco-sidischen Bindungen wurde die Methylierungsanalyse durchgeführt. Mit den Erkenntnissen der Methodenanpassung (Kapitel 4.1) wurden die fermentativ hergestellten HoEPS als Mischung eingesetzt und zweifach analysiert. Nach Hydrolyse mit 1 M TFA bei 70 °C für 30 min wurden die glycosidischen Bindungen der Fructane und nach Hydrolyse mit 3 M TFA bei 121 °C für

90 min die der Glucane bestimmt. Die Ergebnisse zeigten, dass alle Glucane dieselben glycosidischen Bindungen in ähnlichen Anteilen enthielten. Sie bestanden hauptsächlich aus 1,6-Glc*p* (ca. 75 %) und enthielten Verzweigungen durch ca. 10 % 1,3,6-verknüpfte Glc*p*-Einheiten. Demnach handelte es sich bei allen um an Position *O*3 verzweigte Dextrane. Zudem wurden geringe Mengen an 1,3-Verknüpfungen (< 6 %), 1,4-Verknüpfungen (< 1 %) und 1,4,6-Verknüpfungen (< 1 %) gefunden. Die geringen Anteile der 1,4- und 1,4,6-Glc*p*-Einheiten sprachen dafür, dass es sich um Artefakte aus der Aufarbeitung, beispielsweise durch Untermethylierung, handeln könnte. Den Verknüpfungen zufolge lagen typische Dextrane vor (Kapitel 2.2.2.1).

Die Fructane waren aus 2,6-Fru*f*-Einheiten aufgebaut, was bestätigte, dass es sich um Levane handelte. Zusätzlich enthielten sie 2,1,6-verknüpfte Fru*f*-Einheiten in unterschiedlichen Anteilen. Da auch die Anteile an terminalen Fru*f*-Einheiten variierten, wurden zum Vergleich der Levane untereinander die Verzweigungsgrade (Anteil der verzweigten Einheiten an allen Rückgrat-Einheiten) berechnet. Sie variierten zwischen 7 und 24 %, wobei die Levane der Stämme NRRL B-1144 und B-1118 mit über 20 % am stärksten verzweigt waren. Dies bestätigt die Beobachtung aus der Literatur, dass hochverzweigte Levane von *Leuconostoc mesenteroides* produziert werden (Kapitel 2.3.2). Levane mit Verzweigungsgraden > 10 % wurden von Haddar *et al.* (2021), Han & Clarke (1990), Hancock *et al.* (1976) und Marshall & Weigel (1980a) beschrieben und auch zu niedrig verzweigten (< 5 %) Levanen existieren Studien (Bouallegue *et al*., 2020; Hundschell *et al*., 2020a; Shukla & Goyal, 2013). Jedoch resultieren die abweichenden Verzweigungsgrade in den bisherigen Studien aus der Kombination von verschiedenen Analysemethoden und Herkünften der Levane (Bakterien-stamm, fermentative oder enzymatische Synthese und Bedingungen hierbei). Die ver-gleichbaren Ergebnisse dieser Arbeit zeigen hingegen deutlich, dass die Verzweigungsgrade der betrachteten Levane sehr heterogen sind. Für die physikochemischen Eigenschaften sind die unterschiedlichen Verzweigungsgrade der Levane potenziell sehr relevant. Hier spielen jedoch auch die Verteilung und Länge der Seitenketten eine Rolle, was derzeit nur in Ansätzen bekannt ist (Kapitel 2.3.2). Aus diesem Grund wurde eine *endo*-Levanase aus *Bacteroides thetaiotaomicron*, die aus linearem Levan hauptsächlich Levanbiose und Levantriose freisetzt (Kapitel 2.3.1), rekombinant hergestellt und zur Hydrolyse der Levane eingesetzt. Die Hydrolyseprodukte wurden mittels HPAEC-PAD/MS analysiert (Abbildung 4.8). Aus allen Levanen wurden durch *endo*-Levanase dieselben Oligosaccharide in ähnlichen Verhältnissen freigesetzt, was demonstriert, dass die Levane dieselben Strukturelemente in ähnlichen Anteilen enthielten. Mit Hilfe von Standard-Oligosacchariden wurden Levanbiose und Levantriose identifiziert. Daneben waren unbekannte Oligosaccharide vorhanden. Da mehrere unterschiedlich eluierende Oligosaccharide denselben Polymerisationsgrad aufwiesen, handelte es sich um unterschiedlich verknüpfte Oligosaccharide. Das bedeutet, dass neben ausschließlich 2,6-verknüpften Levan-Oligosacchariden auch Oligosaccharide mit 2,1,6- oder 2,1-Verknüpfungen vorlagen. Die Strukturen dieser gemischt-verknüpften Oligosaccharide aus *endo*-Levanase-Hydrolyse sind derzeit nicht bekannt und könnten zukünftig weiterführende Informationen über die Feinstrukturen der Levane liefern. Der hier verfolgte analytische Ansatz

bietet zudem die Möglichkeit die Feinstrukturen unterschiedlicher Levane miteinander zu vergleichen.
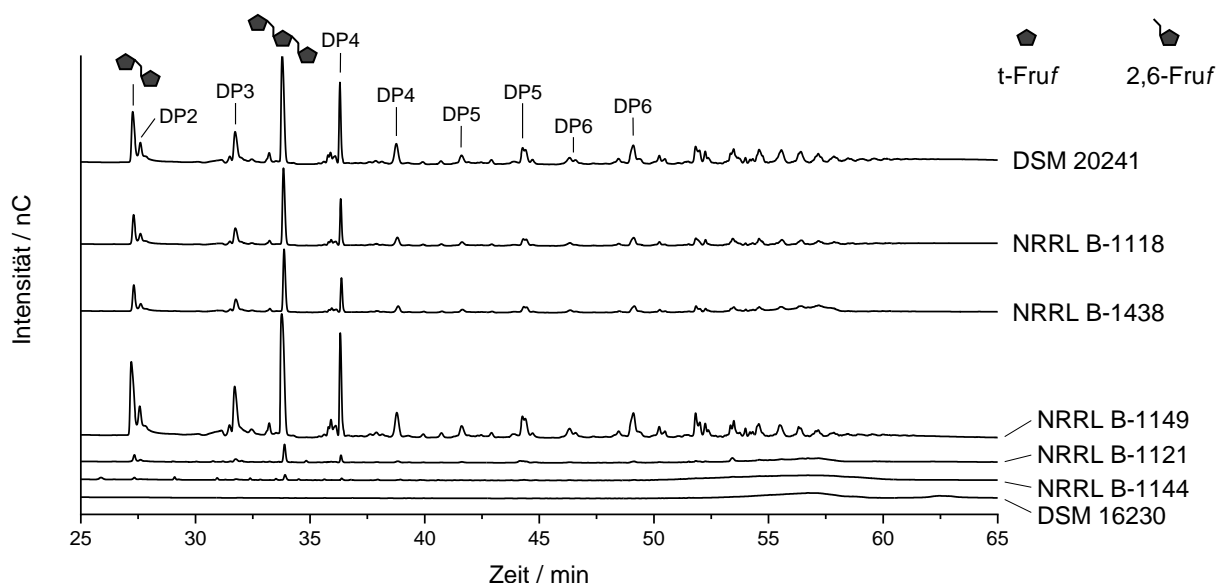
Abbildung 4.8: Chromatogramme (HPAEC-PAD) der *endo*-Levanase-Hydrolysate der wasser-löslichen Homoexopolysaccharide, die fermentativ durch Bakterien von sieben Stämmen (NRRL B-1121, B-1144, B-1149, B-1438 & B-1118 und DSM 20241 & 16230) produziert wurden**.** Levanbiose und Levantriose wurden über ihre Retentionszeit identifiziert. Die Polymerisationsgrade (DP) der unbekannten Oligosaccharide wurden über die Kopplung mit einem Massenspektrometer bestimmt. t: terminal, Fru*f*: Fructofuranose, die Zahlen geben die Position der *O*-Substitution an.

Um genauere Einblicke in die Feinstrukturen der Dextrane zu erhalten, wurden sie mit *endo*-Dextranase hydrolysiert und die erhaltenen Produkte mittels HPAEC-PAD analysiert. Wie bei den wasserunlöslichen Glucanen (Kapitel 4.3.1) entstanden neben Isomaltose unterschiedliche an Position *O*3 verzweigte Isomalto-Oligosaccharide, die das Vorhandensein von Seitenketten unterschiedlicher Länge in allen Dextranen zeigten. Diese Oligosaccharide wurden ebenfalls aus anderen Dextranen von *Liquorilactobacillus*, *Latilactobacillus* und *Weissella* freigesetzt (Kapitel 2.2.2.1). Die Molekülgrößen der wasserlöslichen HoEPS wurden mittels HPSEC-RI bestimmt. Während die Levane hohe Molekulargewichte im Bereich von 2 MDa - 670 kDa aufwiesen, zeigten die wasserlöslichen Glucane eine breite Molekulargewichtsverteilung von 2 MDa bis unter 12 kDa. Die Zuordnung der Peaks zu beiden HoEPS wurde durch *endo*-Dextranase-Hydrolyse bestätigt. Die für Levane bestimmten Molekulargewichte befanden sich im Bereich der für andere Levane bestimmten Molekulargewichte (Kapitel 2.3.2). Dahingegen waren die Molekulargewichte der Glucane im Vergleich zu anderen Glucanen klein (Kapitel 2.2.2.1). In der Literatur liegen wenige Vergleiche der Molekulargewichte von Glucanen und Levanen vor und diese zeigen unterschiedliche Molekulargewichtsverhältnisse beider HoEPS (Fels *et al*., 2018; van Geel-Schutten *et al*., 1999). Die Größen beider HoEPS können außerdem von den vorliegenden Fermentationsbedingungen abhängen. Sowohl für Glucane als auch Levane wurde gezeigt, dass die Kultivierungsbedingungen die Molekular-gewichtsverteilung beeinflussen (Esmaeilnejad-Moghadam *et al*., 2019; Ua-Arak *et al*., 2017; Wu *et al*., 2013).

Insgesamt produzierten die sieben Bakterienstämme unterschiedliche wasserlösliche HoEPS, von denen die Glucane anderen an Position *O*3 verzweigten Dextranen strukturell ähneln. Allerdings besitzen sie eine ungewöhnlich breite Molekülgrößenverteilung. Die ebenfalls entstandenen Levane weisen variierende Verzweigungsgrade (7 - 24 %) und relativ hohe Molekulargewichte auf. Die fermentativ hergestellten HoEPS der sieben Stämme wurden in dieser Arbeit erstmals detailliert untersucht. Je nach Stamm können die fermentativ her-gestellten HoEPS durch ein Zusammenspiel verschiedener GS bzw. FS oder durch einzelne Enzyme synthetisiert werden. Im Genom von *Leuconostoc suionicum* DSM 20241 wurden drei für GH70- und zwei für GH68-Enzyme kodierende Gene identifiziert. Aus der Literatur ist lediglich bekannt, dass dieser Stamm aktive GS exprimiert, wobei die Glucane im Gegensatz zu Akzeptorreaktionen nicht untersucht wurden (Chun *et al*., 2017; Nolte *et al*., 2019). Die fermentative Synthese von wasserunlöslichen Glucanen und Levanen in dieser Arbeit bestätigt die Expression von GS und FS durch DSM 20241. Für *Liquorilactobacillus satsumensis* DSM 16230 wurden mehrere GH70-Enzyme und kein GH68-Enzym vorhergesagt (Sun *et al*., 2015). Für andere *Liquorilactobacillus satsumensis* Stämme ist die Synthese von wasserlöslichen und -unlöslichen Glucanen (durch zwei GS) bereits bekannt (Côté *et al*., 2013; Tan *et al*., 2022). Die Ergebnisse dieser Arbeit zeigen, dass auch DSM 16230 unter den verwendeten Bedingungen wasserlösliche und -unlösliche Glucane synthetisiert und keine aktive FS exprimiert. Für *Leuconostoc mesenteroides* NRRL B-1118 wurden drei für GS und drei für FS kodierende Gene beschrieben und die Produkte einer FS als Levane identifiziert (Olvera *et al*., 2007). Die Glucane zweier GS untersuchten Côté & Skory (2015) näher. Dabei unterschieden sich die Anteile der Verknüpfungen in den Glucanen der beiden einzelnen GS von denen in den Glucanen, die durch die Kombination beider GS entstanden. Eine GS bildete wasserunlösliche Glucane mit 1,3- und 1,6-Verknüpfungen und die andere GS bildete wasserlösliche Glucane mit hohen Anteilen 1,6-Verknüpfungen. Beide GS zusammen synthetisierten den fermentativ hergestellten Glucanen ähnliche Glucane mit 70 % 1,6- und 13 % 1,3-Verknüpfungen (Côté & Skory, 2015), was die Ergebnisse dieser Arbeit bestätigen. In vorangegangenen Studien wurde bereits beschrieben, dass *Leuconostoc mesenteroides* NRRL B-1149 Glucane und Levane produziert (Pearce *et al*., 1990; Seymour & Knapp, 1980; Shukla *et al*., 2010*,* 2011; Shukla & Goyal, 2013; Slodki *et al*., 1986), was in dieser Arbeit ebenfalls bestätigt werden konnte. Für NRRL B-1149, B-1121, B-1144 und B-1438 sind weder GS noch FS bekannt und es ist unklar, wie viele Sucrasen sie besitzen. Insgesamt zeigt die Ähnlichkeit der HoEPS-Strukturen, dass die sieben Bakterienstämme vergleichbare Enzyme oder Enzymkombinationen besitzen. Jedoch deuten Unterschiede, wie die relativen Ausbeuten an Levanen und Glucanen, sowie die unterschiedlichen Verzweigungsgrade der Levane auf verschiedene Enzyme und/oder Enzymaktivitäten bei den verwendeten Fermentationsbedingungen hin. Allgemein ist bekannt, dass die genaue Struktur von Glucanen auch von den Kultivierungsbedingungen abhängen kann (Pidoux *et al*., 1990; Wiater *et al*., 2012). Zudem könnten die HoEPS-Strukturen auch von Glucanasen und Fructanasen, die die Organismen ebenfalls exprimieren, beeinflusst werden (Kapitel 2.2.1 & 2.3.1). Für *Leuconostoc* und *Liquorilactobacillus* sind jedoch weder Levanase noch Mutanase oder Dextranase bzw. ein GH32, GH66 oder GH49 Enzym bekannt (CAZy, 2024).

4.4 Enzymatisch & fermentativ gebildete Fructane

4.4.1 Inuline von *Lactiplantibacillus plantarum*

Heutzutage sind nur wenige bakterielle Inulosucrasen bekannt (Kapitel 2.3.1) und die Strukturen der von ihnen synthetisierten Inuline wurden kaum untersucht (Kapitel 2.3.2). In dieser Arbeit wurden Inuline charakterisiert, die von der erstmals beschriebenen Inulosucrase aus *Lactiplantibacillus plantarum,* LpInu, in Vorarbeiten synthetisiert wurden. Die Inuline wiesen eine breite Molekulargewichtsverteilung von circa 2 MDa bis 12 kDa auf, was mit Hilfe von Dextran-Größenstandards abgeschätzt wurde. Diese breite Verteilung ist ungewöhnlich (vgl. Kapitel 2.3.2), bestätigt aber, dass bakterielle Inuline größer als pflanzliche Inuline (Polymerisationsgrad bis 80, das heißt 13 kDa, Mensink *et al*., 2015) sind. Zusätzlich konnte dies durch ^{1}H-NMR-Spektren bestätigt werden, in denen bei den von LpInu produzierten Inulinen, im Gegensatz zu pflanzlichen Inulinen, keine Peaks terminaler Glucose-Einheiten sichtbar waren. In der Methylierungsanalyse wurden neben terminalen und 2,1-verknüpften Fru*f*-Einheiten 7 % 2,1,6-verknüpfte Fru*f*-Einheiten identifiziert. Verzweigungen in bakteriellen Inulinen wurden bisher selten untersucht. Ebisu *et al.* analysierten Inuline von zwei *Streptococcus mutans* Stämmen mittels Methylierungsanalyse und fanden 3 und 10 % 2,1,6-Fru*f* (Ebisu *et al*., 1975). Für Inuline der Inulosucrase aus *Limosilactobacillus reuteri* 121 beschrieben van Hijum *et al.* 7 % Verzweigungen (t-Fru*f* nicht eingerechnet) (van Hijum *et al*., 2002). Dementsprechend enthalten die von LpInu synthetisierten Inuline ähnliche Anteile an Verzweigungen. Neben den polymeren Inulinen synthetisierte LpInu Oligosaccharide, die mittels HPAEC-PAD analysiert wurden. Neben den linearen Saccharose-Derivaten Kestose, Nystose und Fructosylnystose wurden weitere, unbekannte Oligosaccharide detektiert. Von diesen konnten nur wenige den in pflanzlichem Inulin enthaltenen, linear 2,1-verknüpften Inulo-Oligosacchariden zugeordnet werden, sodass LpInu vermutlich auch verzweigte Fructo-Oligosaccharide bildet. Insgesamt sind die von LpInu gebildeten Oligosaccharide mit den von anderen rekombinanten Inulosucrasen produzierten Oligosacchariden vergleichbar (Anwar *et al*., 2008, 2010; Kralj *et al*., 2018).

4.4.2 Fructane von *Bombella*

Neben den für die Synthese von HoEPS (Levan) bekannten Essigsäurebakterien (Kapitel 2.3) wurde in vorangegangenen Arbeiten auch bei zwei Stämmen der Gattung *Bombella* (*B*.), *B. apis* TMW 2.1884 und *B. mellum* TMW 2.1889, Schleimbildung in Anwesenheit von Saccharose beobachtet. Die EPS des Schleims wurden aus beiden Bakterienkulturen isoliert und im Rahmen dieser Arbeit strukturcharakterisiert. Zur Molekülgrößenbestimmung wurden HPSEC-RI-Messungen durchgeführt und mit Werten aus *asymmetric flow field-flow fractionation* (AF4)-MALLS-Messungen verglichen. Beide Analysemethoden zeigten, dass es sich um hochmolekulare EPS mit Molekulargewichten zwischen 270 kDa und mehreren MDa

handelt. Die EPS der beiden *Bombella* Stämme wiesen dabei unterschiedliche Molekular-gewichtsverteilungen auf. Die Monosaccharidbestimmung nach TFA-Hydrolyse wies auf das Vorliegen von Fructanen hin, während die ^{1}H-NMR-Spektren ergänzend zeigten, dass die EPS Levan-Strukturelemente enthielten. Die Fructane beider *Bombella* Stämme waren durch 7 % 2,1,6-Fru*f*-Einheiten verzweigt, was mit Hilfe der Methylierungsanalyse ermittelt wurde (Abbildung 4.9A). Neben 2,6-Fru*f*-Einheiten wurden auch 8 bzw. 15 % 2,1-Fru*f*-Einheiten identifiziert. Bakterielle Fructane, die sowohl 2,6- als auch 2,1-Fru*f* enthalten, wurden in der Literatur bisher nicht beschrieben. Dies könnte daran liegen, dass die beiden im Rahmen der Methylierungsanalyse erhaltenen Sorbit-Derivate der Fru*f* (Kapitel 2.1) je nach gaschromato-graphischer Trennung der PMAA und Peakintensität koeluieren und deshalb nicht identifiziert wurden. Außerdem wurden in vielen Publikationen lediglich die NMR- und Infrarot-Spektros-kopie zur Identifizierung und gleichzeitiger Strukturaufklärung von bakteriellen Fructanen verwendet (Anwar *et al*., 2008, 2010; Frasch *et al*., 2017; Jathore *et al*., 2012; Liu *et al*., 2017; Malang *et al*., 2015; Matulová *et al*., 2011; Ni *et al*., 2018; Olvera *et al*., 2007). Jedoch können in den NMR-Spektren häufig nur die Hauptverknüpfungstypen identifiziert werden (Kapitel 2.1), wie das Beispiel der Fructane von *Bombella* bestätigt. Deshalb ist es denkbar, dass weitere Fructane mit beiden Verknüpfungstypen existieren. Das gleichzeitige Vorhandensein von 2,6- und 2,1-Fru*f* deutet entweder auf eine Mischung von Levan und Inulin oder Fructan-Copolymere mit 2,6- und 2,1-Verknüpfungen hin. Um Hinweise auf die Anordnung der Struktur-elemente zu erhalten, wurden die Hauptverknüpfungen der Fructane (2,6-Fru*f*) mit *endo*-Levanase hydrolysiert. Die freigesetzten Oligosaccharide wurden mittels HPAEC-PAD/MS analysiert (Abbildung 4.9B). Aus beiden Fructanen wurden neben Fructose, Levanbiose und Levantriose mehrere Oligosaccharide (Polymerisationsgrade von 2 - 7) freigesetzt. Zu unter-schiedlichen Zeiten eluierende Oligosaccharide mit demselben Polymerisationsgrad deuteten darauf hin, dass unterschiedlich verknüpfte Oligosaccharide vorlagen. Der Vergleich mit dem Chromatogramm des Hydrolysats bekannter, 2,6- aber nicht 2,1-verknüpfter Levane von *Gluconobacter albidus* (Hundschell *et al*., 2020a) verdeutlichte, dass dieselben Oligo-saccharide in unterschiedlichen Verhältnissen aus den Fructanen aller drei Essigsäure-bakterienarten freigesetzt wurden. Demnach handelte es sich um 2,6-verknüpfte Levan-Oligosaccharide und gemischt-verknüpfte Oligosaccharide, die vermutlich aus verzweigten 2,6-verknüpften Bereichen und nicht aus den Übergängen von 2,6- zu 2,1-verknüpften Bereichen stammten. Zudem waren die *endo*-Levanase-Hydrolysate der Fructane von *Bom-bella* mit denen der Levane von *Leuconostoc* und *Liquorilactobacillus* (Kapitel 4.3.2) vergleichbar. In allen Hydrolysaten wurden die gleichen Oligosaccharide detektiert, jedoch unterschieden sich die Peakintensitätsverhältnisse und damit die Anteile der einzelnen Oligosaccharide. Der Vergleich der HPSEC-RI-Elugramme der Fructane von *Bombella* vor und nach *endo*-Levanase-Hydrolyse zeigte, dass die hochmolekularen Fraktionen der Fructane beider Stämme zu niedermolekulareren Produkten abgebaut wurden. Im Hydrolysat der Fructane von *B. mellum* war zusätzlich ein Teil höhermolekularer Produkte (circa 670 kDa) vorhanden, bei denen es sich um 2,1-verknüpfte oder alternierend 2,1- und 2,6-verknüpfte Abschnitte des Fructans handeln könnte. Der Abbau der hochmolekularen Fructane und die Bildung von kleineren Polysacchariden spricht für das Vorliegen von Copolymeren. Fructan-

Copolymere mit 2,1- und 2,6-Verknüpfungen sind unbekannt, sodass weitere Analysen die Struktur der *Bombella*-Fructane genauer aufklären sollten.
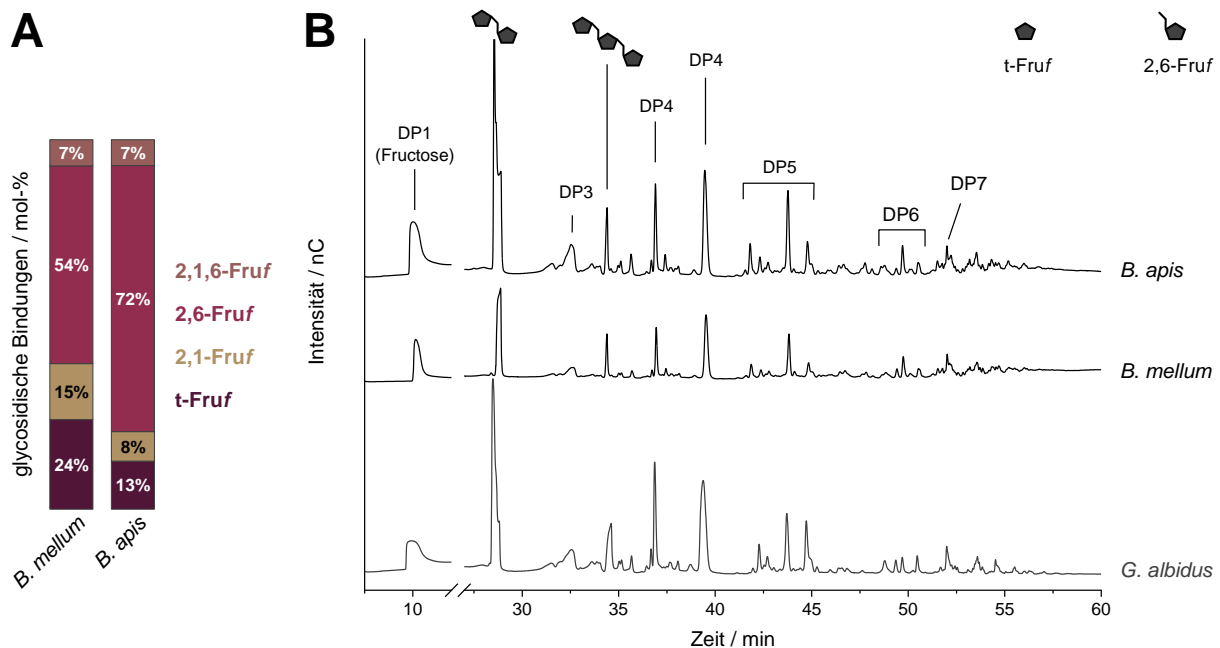
Abbildung 4.9: Anteile der glycosidischen Bindungen in den Fructanen von *Bombella* (*B*.) *mellum* TMW 2.1889 und *B. apis* TMW 2.1884 (A) sowie Chromatogramme (HPAEC-PAD) der *endo*-Levanase-Hydrolysate der Fructane beider *Bombella* Stämme (B). Zusätzlich ist das Chromatogramm des *endo*-Levanase-Hydrolysats der Levane von *Gluconobacter* (*G*.) *albidus*, die keine 2,1-Verknüpfungen enthalten, gezeigt. Fructose, Levanbiose und Levantriose wurden über ihre Retentionszeit identifiziert. Die Polymerisationsgrade (DP) der unbekannten Oligosaccharide wurden über die Kopplung mit einem Massenspektrometer ermittelt. Die glycosidischen Bindungen wurden in Doppelbestimmung durch Methylierungsanalyse bestimmt. t: terminal, Fru*f*: Fructofuranose, die Zahlen geben die Position der *O*-Substitution an.

Neben ihrer Struktur wirft die Synthese der Fructane durch *Bombella* weitere Fragen auf. *Bombella*-Bakterien besitzen keine GH68-Enzyme, sondern lediglich GH32-Enzyme (Jakob *et al*., 2019). Wie in Kapitel 2.3.1 beschrieben, sind GH32-Enzyme nicht dafür bekannt, hoch-molekulare Fructane zu synthetisieren, sondern hauptsächlich Wasser als Akzeptormolekül zu verwenden und Oligosaccharide zu bilden (Lammens *et al*., 2009). In vorangegangenen Arbeiten wurde ermittelt, dass die GH32-Enzyme beider *Bombella* Stämme einen eigenen phylogenetischen Zweig innerhalb der GH32-Familie bilden. Die Fructansynthese durch *Bombella*-Bakterien konnte GH32-Enzymen zugeordnet werden, indem das entsprechende Gen von *B. apis* TMW 2.1884 in Vorarbeiten in *E. coli* kloniert wurde und die durch *E. coli* gebildeten EPS im Vergleich zu den durch *Bombella*-Bakterien synthetisierten EPS analysiert wurden. Die ähnlichen Ergebnisse der Strukturaufklärungen aller EPS zeigen erstmalig, dass GH32-Enzyme auch zur Synthese hochmolekularer Polysaccharide fähig sind. Auf Basis dieser Erkenntnisse ist es möglich, die Besonderheiten der GH32-Enzyme von *Bombella*, also die Bildung hochmolekularer Fructane mit zwei verschiedenen linearen Verknüpfungstypen und Verzweigungen, weiter zu untersuchen.

4.5 Zusammenfassende Diskussion & Ausblick

Durch die Kombination verschiedener Analysemethoden konnten umfassende Informationen über die Strukturen zahlreicher HoEPS erhalten werden. Außerdem ermöglichte die Untersuchung von HoEPS unterschiedlicher Herkunft mit denselben Analysemethoden den direkten Vergleich ihrer (Fein)Strukturen, der aus anderen Studien nur selten möglich war. Als wichtige Methode zur Bestimmung der glycosidischen Bindungen in Polysacchariden wurde die Methylierungsanalyse an HoEPS angepasst. Die Hydrolyse permethylierter Glucane erforderte harschere Bedingungen als die Hydrolyse permethylierter Levane, was bestätigt, dass die glycosidischen Bindungen in Glucanen stabiler sind als in Fructanen. Neben geeigneten Bedingungen für die Hydrolyse der jeweiligen permethylierten HoEPS wurden an einigen Stellen Einblicke in die während der Derivatisierungsschritte ablaufenden Vorgänge erhalten. So konnte die Notwendigkeit von Ultraschallbehandlungen zur Quellung und Deprotonierung von in DMSO unlöslichen Glucanen nachgewiesen werden, während ein Einfluss der Ultraschallbehandlungen auf die Polysaccharidkettenlänge nicht gefunden wurde. In gleicher Weise könnten weitere in DMSO unlösliche Polysaccharide untersucht werden, um auch für sie die Methylierungsanalyse zu verbessern. Daneben zeigten die Untersuchungen der Hydrolyse von Levanen bei verschiedenen Bedingungen, dass sich permethylierte Polysaccharide anders verhalten können als unmodifizierte. Dies sollte für die Methylierungsanalyse weiterer Polysaccharide in Zukunft stärker berücksichtigt werden. Außerdem wurde demonstriert, dass die HPSEC-Analyse wertvolle Informationen über den Reaktionsverlauf der Hydrolyse permethylierter Polysaccharide liefert. Hiermit könnte zukünftig auch näher untersucht werden, ob die glycosidischen Bindungen am Ende permethylierter Glucane schneller als die Bindungen in der Mitte hydrolysiert werden. Zusätzlich konnte in dieser Arbeit erstmals gezeigt werden, unter welchen Bedingungen die einfache Bestimmung einer HoEPS-Mischung einen Überblick über die enthaltenen Glucane und Fructane ermöglicht, während aussagekräftige Ergebnisse für die einzelnen HoEPS durch zweifache Aufarbeitung der Mischung erhalten werden können. Mit diesem Wissen können HoEPS-Mischungen in Zukunft effizienter ohne vorherige Auftrennung analysiert werden.

Mithilfe der angepassten Methylierungsanalyse, enzymatischer Hydrolysen sowie spektroskopischer und chromatographischer Methoden wurden verschiedene fermentativ und enzymatisch synthetisierte HoEPS bzw. HoEPS-Mischungen analysiert. Die Ergebnisse zeigen eindeutig, dass unterschiedliche Strukturen vorliegen. Während die fermentativ hergestellten wasserunlöslichen Glucane untereinander ähnliche Strukturen aufwiesen, waren die Verknüpfungstypen und Feinstrukturen der enzymatisch hergestellten wasserunlöslichen Glucane divers. Glucane beider Gruppen besaßen 1,3- und 1,6-verknüpfte Abschnitte. Von diesen bildeten nur die 1,3-verknüpften Abschnitte starre, kristallähnliche Bereiche aus und die 1,6-verknüpften Abschnitte waren beweglicher, was Festkörperanalysen der enzymatisch hergestellten Glucane zeigten. Da dies in der Literatur nicht bekannt war, sollten Analysen von gemischt-verknüpften Glucanen anderer Herkunft zukünftig das Wissen erweitern. Die

fermentativ hergestellten Glucane sowie die von der GS SMUT1102 produzierten Glucane waren hochmolekulare Copolymere mit längeren 1,6- und 1,3-verknüpften Abschnitten, was durch HPSEC-Analysen der unmodifizierten und enzymatisch hydrolysierten Glucane ermittelt werden konnte. Im Vergleich dazu wiesen die Glucane der GS SMUT1101 zwei Fraktionen unterschiedlichen Molekulargewichts mit längeren 1,6- und kürzeren 1,3- verknüpften Abschnitten auf. Diese Erkenntnisse sind von Bedeutung, da in der Literatur die Molekülgrößen wasserunlöslicher Glucane lediglich vereinzelt und die Längen ihrer Abschnitte nicht beschrieben waren. Über die HPAEC-Analyse enzymatisch freigesetzter Oligosaccharide aus den gemischt-verknüpften Glucanen konnte gezeigt werden, dass Verzweigungen sowohl in 1,3- als auch 1,6-verknüpften Abschnitten existierten. Die Detektion entsprechender Oligosaccharide konnte zudem das Vorliegen von Seitenketten mit mehreren Einheiten in den 1,6-verknüpften Abschnitten nachweisen. Zu den Seitenkettenlängen in den 1,3-verknüpften Abschnitten kann mit den gewonnenen Erkenntnissen keine Aussage getroffen werden, sodass zukünftig die durch *endo*-Mutanase freigesetzten, gemischt-verknüpften Oligosaccharide identifiziert werden sollten. Besonders die weitere Strukturaufklärung der von der GS SSAL4540 synthetisierten Glucane ist aufgrund der unterschiedlichen Verknüpfungstypen und des seltenen Vorkommens derartiger Glucane von großem Interesse. Außerdem konnte durch enzymatische Hydrolysen gezeigt werden, dass wasserunlösliche, vollständig linear 1,6-verknüpfte Glucane und fast ausschließlich 1,3-verknüpfte Glucane von jeweils einer GS synthetisiert werden können.

Die in dieser Arbeit untersuchten wasserlöslichen Glucane hatten ähnliche und bekannte Dextran-Strukturen mit Verzweigungen durch 1,3,6-Glc*p*. Die Seitenketten waren teilweise mehrere Einheiten lang und entsprachen denen, die in anderen Dextranen zuvor gefunden wurden. Daneben wurden diese Strukturelemente in den 1,6-verknüpften Abschnitten der gemischt-verknüpften wasserunlöslichen Glucane identifiziert, was darauf hindeutet, dass diese Abschnitte Dextran-ähnlich aufgebaut sind. Das geringe Vorkommen von 1,3-, 1,4- und 1,4,6-Glc*p* in Dextranen war bereits in der Literatur beschrieben. Allerdings war die Molekular-gewichtsverteilung der untersuchten Dextrane ungewöhnlich breit, was möglicherweise in den verwendeten Kultivierungsbedingungen begründet ist und Einfluss auf die physikochemischen Eigenschaften hat.

In dieser Arbeit wurden zudem Fructane unterschiedlicher Herkunft betrachtet. Neben ver-zweigten bakteriellen Inulinen und Levanen wurden ungewöhnliche gemischt-verknüpfte Fructane identifiziert. Alle untersuchten Fructane hatten im Vergleich zu pflanzlichen Fructanen hohe Molekulargewichte, was andere Verwendungsmöglichkeiten eröffnen kann (Ni *et al*., 2020). Außerdem waren alle Fructane durch 2,1,6-Verknüpfungen verzweigt. Dabei wiesen die Levane unterschiedliche und teilweise hohe Verzweigungsgrade (durchschnittlich fast jede vierte Einheit) auf. Diese Varianz in den Verzweigungsgraden war anhand der bisherigen Literatur anzunehmen, allerdings stammen die Literaturdaten aus unterschiedlichen Analyse-methoden und sind deshalb nicht vergleichbar. Somit verdeutlichen die Ergebnisse dieser Arbeit erstmalig die Heterogenität der Verzweigungsgrade von bakteriellen Levanen. Für alle

Fructane ist der Einfluss ihrer Verzweigungen auf physikochemische und ernährungs-physiologische Eigenschaften unklar (Cheng *et al*., 2021; Liu *et al*., 2020; Xu *et al*., 2018b). Hier könnten die unterschiedlich stark verzweigten Levane dieser Arbeit weiterführende Untersuchungen ermöglichen. Über die Verteilung und Länge der Seitenketten lassen die Ergebnisse dieser Arbeit jedoch keine Aussagen zu und in der Literatur ist dazu für Levan wenig und für Inulin nichts bekannt (Kapitel 2.3.2). Der von Marshall & Weigel (1980a, 1980b) verwendete Ansatz zur Bestimmung von Seitenkettenlängen (*exo*-β-Fructosidase und Methylierungsanalyse) ist relativ ungenau und erlaubt lediglich Rückschlüsse auf die ungefähre Länge der Seitenketten, weshalb er hier nicht verwendet wurde. Hier könnten die durch *endo*-Fructanasen freigesetzten Oligosaccharide Informationen über die Feinstrukturen der Fructane liefern, weshalb die genauen Strukturen der unbekannten durch *endo*-Levanase freigesetzten Oligosaccharide in zukünftigen Arbeiten geklärt werden sollten. Daneben ließe sich der hier verwendete Ansatz, Fructane im Vergleich zu ihren Produkten aus *endo*-Levanase-Hydrolyse mit HPSEC-RI zu analysieren, auf *endo*-Inulinase-Hydrolysate übertragen. Für die Fructane von *Bombella*-Bakterien wurden in dieser Arbeit Hinweise erhalten, dass es sich bei ihnen um Copolymere mit 2,1- und 2,6-verknüpften Abschnitten handeln könnte. Bisher wurden gemischt-verknüpfte Fructane in der Literatur nicht beschrieben, weshalb die Fructane von *Bombella* mit den genannten Möglichkeiten weiter untersucht werden sollten. Zusätzlich könnten die enthaltenen 2,1- und 2,6-verknüpften Abschnitte, beispielsweise nach enzymatischem Abbau, isoliert und einzeln untersucht werden.

Bei allen Ergebnissen ist zu berücksichtigen, dass sowohl bei der fermentativen als auch bei der enzymatischen HoEPS-Synthese unter anderen Bedingungen veränderte Strukturen entstehen könnten. Auch hierzu ist wenig bekannt und es besteht nach wie vor Forschungsbedarf, wobei die in dieser Arbeit (weiter)entwickelten Methoden vielversprechende Optionen für weiterführende Untersuchungen darstellen. Darüber hinaus ist bei den im Rahmen dieser Arbeit fermentativ hergestellten HoEPS die Beteiligung einzelner Enzyme an der Synthese unklar, sodass die rekombinante Herstellung der Sucrasen und die Analyse ihrer jeweiligen Produkte Aufschluss geben kann. Hierfür liefern die Ergebnisse dieser Arbeit eine geeignete Grundlage, auf der beispielsweise gezielt eine FS, die hochverzweigte Levane synthetisiert, identifiziert werden könnte. Da Enzyme nicht nur nach ihrer Aminosäuresequenz und ihrer Struktur, sondern auch nach den von ihnen synthetisierten Produkten eingruppiert werden, ist eine umfassende Analyse der HoEPS sinnvoll. Daneben können die Kenntnisse über die genauen Strukturen der HoEPS zum Verständnis der Produktspezifität von Sucrasen beitragen. Die Strukturanalysen der Glucane von GS aus *Streptococcus* und der *Bombella*-Fructane verdeutlichten, dass manche Unterschiede erst durch Betrachtung der Feinstrukturen und Kombination mehrerer Analysemethoden erkennbar sind. Da über die Feinstrukturen der meisten bisher in der Literatur beschriebenen HoEPS nichts bekannt ist, sollte diesem Aspekt in Zukunft mehr Aufmerksamkeit gewidmet werden. Dabei sollte der Fokus auf der Weiterentwicklung der Methoden zur enzymatischen Freisetzung von Oligo- und Polysacchariden aus (gemischt-verknüpften) HoEPS liegen. Hier ist neben der Analyse der Blocklänge insbesondere die Charakterisierung der durch *endo*-Mutanase und *endo*-Levanase freigesetzten

Oligosaccharide aussichtsreich. Darüber hinaus sollten die kristallähnlichen Bereiche in wasserunlöslichen Glucanen und ihre Auswirkungen auf Enzymzugänglichkeit und physiko-chemische Eigenschaften weiter untersucht werden.

HoEPS haben aufgrund ihrer vielfältigen, steuerbaren Strukturen, aber auch aufgrund ihrer vergleichsweise einfachen Synthese durch ein Enzym (Sucrasen) aus einem einzigen, gut verfügbaren Substrat (Saccharose) hohes Potential für viele industrielle Anwendungen. Vor allem eine mögliche *in situ* Bildung macht sie auch in der Lebensmittelherstellung attraktiv. Aus diesen Gründen lohnt es sich, ihre Synthese, die vorliegenden Strukturen und die gezielte Strukturmodifikation weiter zu erforschen. Beispielsweise können Sucrasen durch *bio-engineering* hinsichtlich Stabilität und Produktspezifität optimiert werden, wenn die Einflüsse der Reaktionsbedingungen und Enzymstrukturen auf die HoEPS-Strukturen verstanden sind. Modifikationen der HoEPS können spezifisch durch Hydrolasen oder *branching*-Sucrasen erfolgen, allerdings sind *branching*-Sucrasen und *debranching*-Enzyme für 1,3-verknüpfte Glucane und Fructane noch unbekannt. In diesem Zusammenhang zeigen die Ergebnisse dieser Arbeit analytische Möglichkeiten auf und liefern für vielfältige HoEPS Grundlagen zur Untersuchung ihrer Struktur-Eigenschaftsbeziehungen.

5 Zusammenfassung

Von Milch- und Essigsäurebakterien gebildete Homoexopolysaccharide (HoEPS) sind in verschiedenen Bereichen, beispielsweise in der Zahnplaque oder fermentierten Lebensmitteln, relevant. Für einen gezielten Einsatz in technischen Anwendungen oder in Lebensmitteln und für ihre Vermeidung in der Zahnplaque ist das Wissen über ihre molekulare Struktur und deren Zusammenhang mit den physikochemischen Eigenschaften essentiell. Bis heute sind hauptsächlich die grundlegenden Strukturen der HoEPS (α-Glucane und β-Fructane) bekannt und Feinstrukturen wurden selten betrachtet. Dies ist unter anderem in analytischen Herausforderungen begründet, weshalb in dieser Dissertation die Strukturen von verschiedenen enzymatisch und fermentativ hergestellten HoEPS mit einer Reihe an separat angepassten und weiterentwickelten Analysemethoden detailliert untersucht wurden.

Als wichtige Methode zur Bestimmung der in Polysacchariden enthaltenen glycosidischen Bindungen wurde die Methylierungsanalyse an bakterielle HoEPS angepasst. Anders als bei wasserlöslichen HoEPS erwiesen sich bei wasserunlöslichen α-Glucanen Ultraschallbehandlungen für eine vollständige Methylierung als wichtig. Daneben benötigten α-Glucane harschere Hydrolysebedingungen (2 M Trifluoressigsäure, 121 °C für 60/90 min) als β-Fructane (1 M Trifluoressigsäure, 70 °C für 30 min). Eine Mischung aus wasserlöslichen α-Glucanen und β-Fructanen kann zur Bestimmung der glycosidischen Bindungen der einzelnen HoEPS ohne Auftrennung verwendet werden, wenn zwei Aufarbeitungen mit jeweils optimalen Hydrolysebedingungen durchgeführt werden.

Neben der Methylierungsanalyse, der Kernspinresonanz (NMR)-Spektroskopie und der Monosaccharidbestimmung wurden die HoEPS und ihre Produkte aus enzymatischen Hydrolysen (*endo*-Levanase, *endo*-Mutanase und *endo*-Dextranase) mittels Hochleistungsanionenaustauschchromatographie gekoppelt mit gepulster amperometrischer und massenspektrometrischer Detektion sowie Hochleistungsgrößenausschlusschromatographie gekoppelt mit Brechungsindexdetektor untersucht.

Zur Untersuchung wasserunlöslicher Glucane wurden fünf Glucansucrasen (GS) von *Streptococcus*-Bakterien rekombinant hergestellt und zur enzymatischen Glucansynthese eingesetzt. Neben linearen 1,6-verknüpften Dextranen und Glucanen mit einem ausschließlich 1,3-verknüpften, schwach verzweigten Rückgrat wurden gemischt-verknüpfte Glucane erhalten. Die Glucane zweier GS waren 1,3-, 1,6- und 1,3,6-verknüpft und wiesen unterschiedliche Molekülgrößenverteilungen und Feinstrukturen auf, was die Analysen der Produkte aus *endo*-Dextranase- und *endo*-Mutanase-Hydrolysen verdeutlichten. Die Glucane der fünften GS enthielten 1,3-, 1,4- und 1,6-Verknüpfungen und hatten damit eine für *Streptococcus salivarius*-Glucane bisher nicht beschriebene Struktur. Mit Hilfe der *endo*-Mutanase-Hydrolyse

konnte gezeigt werden, dass die 1,3-verknüpften Abschnitte im Vergleich zu denen der anderen untersuchten Glucane abweichende Feinstrukturen aufwiesen. Zur Analyse geordneter Strukturen in den Glucanen kamen Röntgendiffraktion und ^{13}C *magic angle spinning* NMR-Spektroskopie zum Einsatz. Für die 1,3-verknüpften sowie 1,3- und 1,6-verknüpften Glucane wurden starre, kristallähnliche Bereiche beobachtet, die aus 1,3-Glucopyranose-Einheiten aufgebaut waren. Die 1,6-Glucopyranose-Einheiten befanden sich in beweglicheren Bereichen. Dies sind die ersten Beobachtungen von kristallähnlichen Bereichen in von *Streptococcus*-GS produzierten gemischt-verknüpften Glucanen und es existierten bisher keine Einblicke in die Verteilung der glycosidischen Bindungen von gemischt-verknüpften Glucanen in ihren starren, kristallähnlichen oder beweglichen Bereichen.

Die HoEPS von sieben Milchsäurebakterienstämmen der Gattungen *Leuconostoc* und *Liquorilactobacillus* wurden fermentativ synthetisiert und wasserunlösliche sowie -lösliche HoEPS getrennt aufgereinigt und analysiert. Die relativen und absoluten Ausbeuten an wasserunlöslichen und -löslichen HoEPS der einzelnen Stämme variierten, wobei die wasserlöslichen HoEPS zu unterschiedlichen Anteilen aus Glucanen und Fructanen bestanden. Die entstandenen wasserunlöslichen Glucane hatten copolymerartige Strukturen mit 1,3- und 1,6-verknüpften Abschnitten, die jeweils durch 1,3,6-Glucopyranose-Einheiten verzweigt waren. Der Anteil an häufig mit Wasserunlöslichkeit in Verbindung gebrachten 1,3-Verknüpfungen variierte von 5 - 40 %. Die wasserlöslichen Glucane waren hauptsächlich 1,6-verknüpft und hatten ähnliche Strukturen, die mit bekannten Strukturen übereinstimmten. Die Glucane besaßen ungewöhnlich breite Molekülgrößenverteilungen. Bei den Fructanen handelte es sich um teilweise stark verzweigte Levane (Verzweigungsgrade 7 - 24 %) mit hohen Molekulargewichten. Durch *endo*-Levanase wurden verschiedene gemischt-verknüpfte Oligosaccharide freigesetzt.

In dieser Arbeit wurden weitere Fructane näher untersucht. Die von einer Inulosucrase synthetisierten Inuline wiesen Verzweigungen und eine breite Molekülgrößenverteilung auf. Ungewöhnliche Fructane mit sowohl 2,1- als auch 2,6-Verknüpfungen und Verzweigungen durch 2,1,6-Fructofuranose-Einheiten besaßen ebenfalls hohe Molekulargewichte und wurden fermentativ von *Bombella* bzw. Enzymen der *Glycoside Hydrolase* Familie 32 dieser Essigsäurebakterien produziert.

Insgesamt unterstreichen die beschriebenen Ergebnisse die Vielfalt der molekularen Strukturen von bakteriellen α-Glucanen und β-Fructanen und verdeutlichen, dass die Kombination angepasster Analysemethoden detaillierte Strukturinformationen liefert. Dementsprechend wurde ein Grundstein für die Ermittlung von Struktur-Wirkungsbeziehungen gelegt, die für eine Anwendung der verschiedenen HoEPS von großer Bedeutung sind.

6 Summary

Homoexopolysaccharides (HoEPS) from lactic and acetic acid bacteria are found, for example, in fermented foods or in human dental plaque. They are of particular interest in food or technical applications where their physico-chemical properties influence their applicability and depend on their molecular structure. The basic structures of HoEPS, α-glucans and β-fructans, are known. However, there are only few studies investigating the fine structures of different HoEPS. Therefore, the aim of this thesis was to characterize different enzymatically and fermentatively synthesized HoEPS in detail using a range of adapted analytical tools.

First, methylation analysis was adjusted for the determination of glycosidic linkages in bacterial HoEPS. Ultrasonic treatments were crucial for complete methylation of water-insoluble glucans, but not necessary for water-soluble HoEPS. Complete hydrolysis of permethylated glucans required 2 M trifluoroacetic acid for 60/90 min at 121 °C, whereas fructans were hydrolyzed in 1 M trifluoroacetic acid for 30 min at 70 °C. Mixtures of water-soluble glucans and fructans can be analyzed without previous separation in two batches using different conditions during hydrolysis.

In addition to methylation analysis, nuclear magnetic resonance (NMR) spectroscopy and monosaccharide analysis, HoEPS and their products from enzymatic hydrolyses (*endo*-levanase, *endo*-mutanase, *endo*-dextranase) were investigated by high performance size exclusion chromatography coupled to refractive index detection (HPSEC-RI) in combination with high performance anion exchange chromatography coupled with pulsed amperometric and mass spectrometric detection (HPAEC-PAD/MS).

Five *Streptococcus* glucansucrases (GS) were selected for enzymatic synthesis of water-insoluble glucans. Glucans with an exclusively 1,3-linked, weakly branched backbone and linear 1,6-linked dextrans were obtained from two GS, whereas three GS synthesized mixed-linkage glucans. The glucans of one GS had an unusual structure with 1,3-, 1,4- and 1,6-linkages. Furthermore, glucans of the remaining two GS were 1,3- and 1,6-linked and branched by 1,3,6-linked glucopyranose units. However, the mixed-linkage glucans had different fine structures as revealed by *endo*-mutanase and *endo*-dextranase hydrolyses followed by HPSEC-RI and HPAEC-PAD/MS analyses. X-ray diffraction and ^{13}C magic angle spinning NMR spectroscopy indicated crystal-like regions in the 1,3-linked glucans as well as in the 1,3- and 1,6-linked glucans. These crystal-like regions were composed of 1,3-linked units while 1,6-linked units were found in the mobile regions. For mixed-linkage *Streptococcus* glucans these are the first reports of crystal-like regions.

For investigation of the overall HoEPS production of lactic acid bacteria seven strains from the genera *Leuconostoc* and *Liquorilactobacillus* were selected. Different yields of fermentatively synthesized water-soluble and water-insoluble HoEPS were obtained, isolated, and analyzed separately. Water-insoluble glucans were copolymers with blocks of 1,3-linkages and blocks of 1,6-linkages. Both block types were branched by 1,3,6-glucopyranose units. 1,3-linkages, which are often associated with water-insolubility, showed varying portions (5 to 40 %). Water-soluble HoEPS consisted of glucans and fructans in different portions. Glucans had similar structures which were comparable to those previously described. They were mainly composed of 1,6-linkages and had a broad molecular size distribution. Besides, fructans were identified as high molecular weight levans. Their degrees of branching varied from 7 to 24 % indicating that some of them were highly branched. *Endo*-levanase hydrolysis liberated different mixed-linkage oligosaccharides.

Other fructans investigated were enzymatically synthesized inulins which were branched and had a broad size distribution. Furthermore, unusual high molecular weight fructans synthesized by glycoside hydrolase family 32 enzymes from acetic acid bacteria had both 2,1- as well as 2,6-linked units and branched 2,1,6-linked units.

Overall, the results of this work emphasize the structural diversity of bacterial α-glucans and β-fructans and demonstrate that the combination of adapted analytical tools reveals detailed information on HoEPS structures. This knowledge of various HoEPS structures will allow an understanding of their physicochemical properties which are of great importance for different applications.

7 Literaturverzeichnis

Adamberg, K.; Tomson, K.; Talve, T.; Pudova, K.; Puurand, M.; Visnapuu, T.; Alamäe, T. & Adamberg, S. (2015): Levan enhances associated growth of *Bacteroides*, *Escherichia*, *Streptococcus* and *Faecalibacterium* in fecal microbiota. *PLOS one,* 10, e0144042.

Adelman, D. J. & Behabtu, N. (2022): Flour- and meal-based food products comprising insoluble α-1,3-glucan. Patent angemeldet am 16.08.2019. US20220322685A1.

Alméciga-Díaz, C. J.; Gutierrez, Á. M.; Bahamon, I.; Rodríguez, A.; Rodríguez, M. A. & Sánchez, O. F. (2011): Computational analysis of the fructosyltransferase enzymes in plants, fungi and bacteria. *Gene,* 484, 26–34.

Amaretti, A.; Bottari, B.; Morreale, F.; Savo Sardaro, M. L.; Angelino, D.; Raimondi, S.; Rossi, M. & Pellegrini, N. (2020): Potential prebiotic effect of a long-chain dextran produced by *Weissella cibaria*: an *in vitro* evaluation. *International Journal of Food Sciences and Nutrition,* 71, 563–571.

Anwar, M. A.; Kralj, S.; Piqué, A. V.; Leemhuis, H.; van der Maarel, M. J. E. C. & Dijkhuizen, L. (2010): Inulin and levan synthesis by probiotic *Lactobacillus gasseri* strains: Characterization of three novel fructansucrase enzymes and their fructan products. *Microbiology,* 156, 1264–1274.

Anwar, M. A.; Kralj, S.; van der Maarel, M. J. E. C. & Dijkhuizen, L. (2008): The probiotic *Lactobacillus johnsonii* NCC 533 produces high-molecular-mass inulin from sucrose by using an inulosucrase enzyme. *Applied and Environmental Microbiology,* 74, 3426–3433.

Basedow, A. M.; Ebert, K. H. & Ederer, H. J. (1978): Kinetic studies on the acid hydrolysis of dextran. *Macromolecules,* 11, 774–781.

Bechtner, J.; Hassler, V.; Wefers, D.; Ehrmann, M. & Jakob, F. (2022): The *C*-terminal domain of *Liquorilactobacillus nagelii* dextransucrase mediates the production of larger dextrans compared to *Liquorilactobacillus hordei*. *Gels,* 8, 171.

Bechtner, J.; Wefers, D.; Schmid, J.; Vogel, R. F. & Jakob, F. (2019): Identification and comparison of two closely related dextransucrases released by water kefir borne *Lactobacillus hordei* TMW 1.1822 and *Lactobacillus nagelii* TMW 1.1827. *Microbiology,* 165, 956–966.

Bello, F. D.; Walter, J.; Hertel, C. & Hammes, W. P. (2001): *In vitro* study of prebiotic properties of levan-type exopolysaccharides from *Lactobacilli* and non-digestible carbohydrates using denaturing gradient gel electrophoresis. *Systematic and Applied Microbiology,* 24, 232–237.

Benhouna, I. S.; Heumann, A.; Rieu, A.; Guzzo, J.; Kihal, M.; Bettache, G.; Champion, D.; Coelho, C. & Weidmann, S. (2019): Exopolysaccharide produced by *Weissella confusa*: Chemical characterisation, rheology and bioactivity. *International Dairy Journal,* 90, 88–94.

Biermann, C. J. (1988): Hydrolysis and other cleavages of glycosidic linkages in polysaccharides. *Advances in Carbohydrate Chemistry and Biochemistry*, 46, 251–271.

Birkhed, D.; Rosell, K. G. & Granath, K. (1979): Structure of extracellular water-soluble polysaccharides synthesized from sucrose by oral strains of *Streptococcus mutans*, *Streptococcus salivarius*, *Streptococcus sanguis* and *Actinomyces viscosus*. *Archives of Oral Biology,* 24, 53–61.

Björndal, H., Lindberg, B. & Svensson, S. (1967): Mass spectrometry of partially methylated alditol acetates. *Carbohydrate Research*, 5, 433-440.

Blakeney, A. B.; Harris, P. J.; Henry, R. J. & Stone, B. A. (1983): A simple and rapid preparation of alditol acetates for monosaccharide analysis. *Carbohydrate Research*, 113, 291-299.

Boddapati, S. & Gummadi, S. N. (2023): Production and application of purified mutanase from novel *Cellulosimicrobium funkei* SNG1 in the *in vitro* biofilm degradation. *Biotechnology and Applied Biochemistry,* 70, 1371–1383.

Boddapati, S.; Rai, R. & Gummadi, S. N. (2020): Structural analysis and antioxidative properties of mutan (water-insoluble glucan) and carboxymethyl mutan from *Streptococcus mutans*. *Process Biochemistry,* 97, 130–139.

Bouallegue, A.; Casillo, A.; Chaari, F.; La Gatta, A.; Lanzetta, R.; Corsaro, M. M.; Bachoual, R. & Ellouz-Chaabouni, S. (2020): Levan from a new isolated *Bacillus subtilis* AF17: Purification, structural analysis and antioxidant activities. *International Journal of Biological Macromolecules,* 144, 316–324.

Bowen, W. H., Burne, R. A., Wu, H. & Koo, H. (2018): Oral biofilms: Pathogens, matrix, and polymicrobial interactions in microenvironments. *Trends in Microbiology*, 26, 229-242.

Bowen, W. H. & Koo, H. (2011): Biology of *Streptococcus mutans*-derived glucosyltransferases: Role in extracellular matrix formation of cariogenic biofilms. *Caries Research,* 45, 69–86.

Brison, Y.; Laguerre, S.; Lefoulon, F.; Morel, S.; Monties, N.; Potocki-Véronèse, G.; Monsan, P. & Remaud-Simeon, M. (2013): Branching pattern of gluco-oligosaccharides and 1.5 kDa dextran grafted by the α-1,2 branching sucrase GBD-CD2. *Carbohydrate Polymers*, 94, 567-576.

Brison, Y.; Pijning, T.; Malbert, Y.; Fabre, É.; Mourey, L.; Morel, S.; Potocki-Véronèse, G.; Monsan, P.; Tranier, S.; Remaud-Siméon, M. & Dijkstra, B. W. (2012): Functional and structural characterization of α-1,2 branching sucrase derived from DSR-E glucansucrase. *Journal of Biological Chemistry,* 287, 7915–7924.

Buddana, S. K.; Amrutha, R. N.; Batchu, U. R.; Penna, S. & Prakasham, R. S. (2019): Mutanase enzyme from *Paracoccus mutanolyticus* RSP02: Characterization and application as a biocontrol agent. *Indian Journal of Microbiology,* 59, 436–444.

Buddana, S. K.; Varanasi, Y. V. N. & Shetty, P. R. (2015): Fibrinolytic, anti-inflammatory and anti-microbial properties of α-1,3-glucans produced from *Streptococcus mutans* (MTCC 497). *Carbohydrate Polymers,* 115, 152–159.

Burne, R. A.; Schilling, K.; Bowen, W. H. & Yasbin, R. E. (1987): Expression, purification, and characterization of an *exo*-β-D-fructosidase of *Streptococcus mutans*. *Journal of Bacteriology,* 169, 4507–4517.

Caggianiello, G.; Kleerebezem, M. & Spano, G. (2016): Exopolysaccharides produced by lactic acid bacteria: from health-promoting benefits to stress tolerance mechanisms. *Applied Microbiology and Biotechnology,* 100, 3877–3886.

Carpita, N. C.; Housley, T. L. & Hendrix, J. E. (1991): New features of plant-fructan structure revealed by methylation analysis and carbon-13 NMR spectroscopy. *Carbohydrate Research,* 217, 127–136.

Cataldi, T. R., Campa, C. & De Benedetto, G. E. (2000): Carbohydrate analysis by high-performance anion-exchange chromatography with pulsed amperometric detection: the potential is still growing. *Fresenius'Journal of Analytical Chemistry*, *368*, 739-758.

CAZy (2024): *Caborhydrate active enzymes* Datenbank, online verfügbar unter http://www.cazy.org/ (zuletzt aufgerufen am: 29.02.2024).

Chakraborty, B.; Zeng, L. & Burne, R. A. (2022): The fruB gene of *Streptococcus mutans* encodes an *endo*-levanase that enhances growth on levan and influences global gene expression. *Microbiology Spectrum,* 10, e0052222.

Chambert, R.; Rain-Guion, M. C. & Petit-Glatron, M. F. (1992): Readthrough of the *Bacillus subtilis* stop codon produces an extended enzyme displaying a higher polymerase activity. *Biochimica et Biophysica Acta - Gene Structure and Expression,* 1132, 145–153.

Cheng, R.; Cheng, L.; Zhao, Y.; Wang, L.; Wang, S. & Zhang, J. (2021): Biosynthesis and prebiotic activity of a linear levan from a new *Paenibacillus* isolate. *Applied Microbiology and Biotechnology,* 105, 769–787.

Choma, A.; Wiater, A.; Komaniecka, I.; Paduch, R.; Pleszczyńska, M. & Szczodrak, J. (2013): Chemical characterization of a water insoluble (1→ 3)-α-D-glucan from an alkaline extract of *Aspergillus wentii*. *Carbohydrate Polymers*, 91, 603-608.

Chun, B. H.; Lee, S. H.; Jeon, H. H.; Kim, D.-W. & Jeon, C. O. (2017): Complete genome sequence of *Leuconostoc suionicum* DSM 20241 provides insights into its functional and metabolic features. *Standards in Genomic Sciences,* 12, 38.

Ciucanu, I. & Kerek, F. (1984): A simple and rapid method for the permethylation of carbohydrates. *Carbohydrate Research,* 131, 209–217.

Combie, J. & Öner, E. T. (2018): From healing wounds to resorbable electronics, levan can fill bioadhesive roles in scores of markets. *Bioinspiration and Biomimetics,* 14, 11001.

Côté, G. L.; Ahlgren, J. A. & Smith, M. R. (1999): Some structural features of an insoluble α-D-glucan from a mutant strain of *Leuconostoc mesenteroides* NRRL B-1355. *Journal of Industrial Microbiology and Biotechnology,* 23, 656–660.

Côté, G. L. & Leathers, T. D. (2009): Insoluble glucans from planktonic and biofilm cultures of mutants of *Leuconostoc mesenteroides* NRRL B-1355. *Applied Microbiology and Biotechnology,* 82, 149–154.

Côté, G. L. & Robyt, J. F. (1982): Isolation and partial characterization of an extracellular glucansucrase from *Leuconostoc mesenteroides* NRRL B-1355 that synthesizes an alternating (1→ 6),(1→ 3)-α-D-glucan. *Carbohydrate Research*, 101, 57-74.

Côté, G. L. & Robyt, J. F. (1983): The formation of α-D-(1→ 3) branch linkages by an exocellular glucansucrase from *Leuconostoc mesenteroides* NRRL B-742. *Carbohydrate Research*, 119, 141-156.

Côté, G. L. & Skory, C. D. (2012): Cloning, expression, and characterization of an insoluble glucan-producing glucansucrase from *Leuconostoc mesenteroides* NRRL B-1118. *Applied Microbiology and Biotechnology,* 93, 2387–2394.

Côté, G. L. & Skory, C. D. (2014): Effects of mutations at threonine-654 on the insoluble glucan synthesized by *Leuconostoc mesenteroides* NRRL B-1118 glucansucrase. *Applied Microbiology and Biotechnology,* 98, 6651–6658.

Côté, G. L. & Skory, C. D. (2015): Water-insoluble glucans from sucrose via glucansucrases. Factors influencing structures and yields. In: Cheng, H. N., Gross, R. A. & Smith, P. B. (Hg.): *Green Polymer Chemistry: Biobased Materials and Biocatalysis*. American Chemical Society, 101–112.

Côté, G. L. & Skory, C. D. (2016): Effect of a single point mutation on the interaction of glucans with a glucansucrase from *Leuconostoc mesenteroides* NRRL B-1118. *Carbohydrate Research,* 428, 57–61.

Côté, G. L.; Skory, C. D.; Unser, S. M. & Rich, J. O. (2013): The production of glucans via glucansucrases from *Lactobacillus satsumensis* isolated from a fermented beverage starter culture. *Applied Microbiology and Biotechnology,* 97, 7265–7273.

Cui, R. & Zhu, F. (2021): Ultrasound modified polysaccharides: A review of structure, physicochemical properties, biological activities and food applications. *Trends in Food Science & Technology,* 107, 491–508.

Cury, J. A.; Rebelo, M. A.; Del Bel Cury, A. A.; Derbyshire, M. T. & Tabchoury, C. P. (2000): Biochemical composition and cariogenicity of dental plaque formed in the presence of sucrose or glucose and fructose. *Caries Research,* 34, 491–497.

Dahech, I.; Ben Ayed, H.; Belghith, K. S.; Belghith, H. & Mejdoub, H. (2013): Microbial production of levanase for specific hydrolysis of levan. *International Journal of Biological Macromolecules,* 60, 128–133.

Das, D.; Baruah, R. & Goyal, A. (2014): A food additive with prebiotic properties of an α-D-glucan from *lactobacillus plantarum* DM5. *International Journal of Biological Macromolecules,* 69, 20–26.

Davies, G. J.; Wilson, K. S. & Henrissat, B. (1997): Nomenclature for sugar-binding subsites in glycosyl hydrolases. *Biochemical Journal,* 321, 557–559.

Davis, H. M.; Hines, H. B. & Edwards, J. R. (1986): Structural elucidation of a water-insoluble glucan produced by a cariogenic oral *Streptococcus*. *Carbohydrate Research,* 156, 69–77.

Dawes, E. A.; Ribbons, D. W. & Rees, D. A. (1966): Sucrose utilization by *Zymomonas mobilis*: Formation of a levan. *Biochemical Journal,* 98, 804–812.

de Siqueira, E. C.; Rebouças, J. d. S.; Pinheiro, I. O. & Formiga, F. R. (2020): Levan-based nanostructured systems: An overview. *International Journal of Pharmaceutics,* 580, 119242.

Del Moral, S.; Olvera, C.; Rodriguez, M. E. & Munguia, A. L. (2008): Functional role of the additional domains in inulosucrase (IslA) from *Leuconostoc citreum* CW28. *BMC Biochemistry,* 9, 6.

Dibdin, G. H. & Shellis, R. P. (1988): Physical and biochemical studies of *Streptococcus mutans* sediments suggest new factors linking the cariogenicity of plaque with its extracellular polysaccharide content. *Journal of Dental Research,* 67, 890–895.

Dimler, R. J., Davis, H. A., Gill, G. J. & Rist, C. E. (1954): Analytical total acid hydrolysis of dextrans. *Analytical Chemistry*, *26*, 1142-1146.

Dimopoulou, M.; Bardeau, T.; Ramonet, P. Y.; Miot-Certier, C.; Claisse, O.; Doco, T.; Petrel, M.; Lucas, P. & Dols-Lafargue, M. (2016): Exopolysaccharides produced by *Oenococcus oeni*: From genomic and phenotypic analysis to technological valorization. *Food Microbiology,* 53, 10–17.

Dogsa, I.; Brloznik, M.; Stopar, D. & Mandic-Mulec, I. (2013): Exopolymer diversity and the role of levan in *Bacillus subtilis* biofilms. *PLOS one,* 8, e62044.

Duarte, S.; Klein, M. I.; Aires, C. P.; Cury, J. A.; Bowen, W. H. & Koo, H. (2008): Influences of starch and sucrose on *Streptococcus mutans* biofilms. *Oral Microbiology and Immunology,* 23, 206–212.

Ebisu, S.; Kato, K.; Kotani, S. & Misaki, A. (1975): Structural differences in fructans elaborated by *Streptococcus mutans* and *Strep. salivarius*. *The Journal of Biochemistry,* 78, 879–887.

Ebisu, S.; Misaki, A.; Kato, K. & Kotani, S. (1974): The structure of water-insoluble glucans of cariogenic *Streptococcus mutans*, formed in the absence and presence of dextranase. *Carbohydrate Research,* 38, 374–381.

El Hariri El Nokab, M. & van der Wel, P. C. A. (2020): Use of solid-state NMR spectroscopy for investigating polysaccharide-based hydrogels: A review. *Carbohydrate Polymers,* 240, 116276.

Esmaeilnejad-Moghadam, B.; Mokarram, R. R.; Hejazi, M. A.; Khiabani, M. S. & Keivaninahr, F. (2019): Low molecular weight dextran production by *Leuconostoc mesenteroides* strains: Optimization of a new culture medium and the rheological assessments. *Bioactive Carbohydrates and Dietary Fibre,* 18, 100181.

Fabre, E.; Bozonnet, S.; Arcache, A.; Willemot, R. M.; Vignon, M.; Monsan, P. & Remaud-Simeon, M. (2005): Role of the two catalytic domains of DSR-E dextransucrase and their involvement in the formation of highly α-1,2 branched dextran. *Journal of Bacteriology*, 187, 296-303.

Falconer, D. J.; Mukerjea, R. & Robyt, J. F. (2011): Biosynthesis of dextrans with different molecular weights by selecting the concentration of *Leuconostoc mesenteroides* B-512FMC dextransucrase, the sucrose concentration, and the temperature. *Carbohydrate Research,* 346, 280–284.

Fels, L.; Jakob, F.; Vogel, R. F. & Wefers, D. (2018): Structural characterization of the exopolysaccharides from water kefir. *Carbohydrate Polymers,* 189, 296–303.

Franz, G. (Hg.) (1991): Polysaccharide. Springer-Verlag Berlin Heidelberg.

Frasch, H. J.; van Leeuwen, S. S. & Dijkhuizen, L. (2017): Molecular and biochemical characteristics of the inulosucrase HugO from *Streptomyces viridochromogenes* DSM40736 (Tü494). *Microbiology,* 163, 1030–1041.

Fukata, Y.; Kimura, S.; Kabe, T.; Gan, H. & Iwata, T. (2021): Manufacture of strong melt-spun fibers derived from α-1,3-glucan esters and determination of their crystal structures and crystalline elastic moduli. *Polymer,* 234, 124225.

Fukui, K.; Moriyama, T.; Miyake, Y.; Mizutani, K. & Tanaka, O. (1982): Purification and properties of glucosyltransferase responsible for water-insoluble glucan synthesis from *Streptococcus mutans*. *Infection and Immunity*, 37, 1-9.

Fukushima, K.; Motoda, R. & Ikeda, T. (1981): Effects of exogenous insoluble glucan primer on insoluble glucan synthesis by *Streptococcus mutans*. *Journal of Dental Research,* 60, 1707–1712.

Funane, K.; Ishii, T.; Matsushita, M.; Hori, K.; Mizuno, K.; Takahara, H.; Kitamura, Y. & Kobayashi, M. (2001): Water-soluble and water-insoluble glucans produced by *Escherichia coli* recombinant dextransucrases from *Leuconostoc mesenteroides* NRRL B-512F. *Carbohydrate Research,* 334, 19–25.

Galle, S.; Schwab, C.; Dal Bello, F.; Coffey, A.; Gänzle, M. G. & Arendt, E. K. (2012): Influence of *in-situ* synthesized exopolysaccharides on the quality of gluten-free sorghum sourdough bread. *International Journal of Food Microbiology,* 155, 105–112.

Gamal, A. A.; Abbas, H. Y.; Abdelwahed, N. A. M.; Kashef, M. T.; Mahmoud, K.; Esawy, M. A. & Ramadan, M. A. (2021): Optimization strategy of *Bacillus subtilis* MT453867 levansucrase and evaluation of levan role in pancreatic cancer treatment. *International Journal of Biological Macromolecules,* 182, 1590–1601.

Gangoiti, J.; Pijning, T. & Dijkhuizen, L. (2018): Biotechnological potential of novel glycoside hydrolase family 70 enzymes synthesizing α-glucans from starch and sucrose. *Biotechnology Advances,* 36, 196–207.

García-Paz, F. d. M.; Martínez-Bahena, S. & Olvera, C. (2022): Structure-function relationship studies of multidomain levansucrases from *Leuconostocaceae* family. *Microorganisms,* 10, 889.

Garegg, P. J.; Lindberg, B.; Konradsson, P. & Kvarnström, I. (1988): Hydrolysis of glycosides under reducing conditions. *Carbohydrate Research,* 176, 145–148.

Gibbons, R. J. & Banghart, S. B. (1967): Synthesis of extracellular dextran by cariogenic bacteria and its presence in human dental plaque. *Archives of Oral Biology,* 12, 11–23.

Grönwall, A. & Ingelman, B. (1945): Dextran as a substitute for plasma. *Nature,* 155, 45.

Haddar, A.; Hamed, M.; Bouallegue, A.; Bastos, R.; Coelho, E. & Coimbra, M. A. (2021): Structural elucidation and interfacial properties of a levan isolated from *Bacillus mojavensis*. *Food Chemistry,* 343, 128456.

Hakomori, S. I. (1964): A rapid permethylation of glycolipid, and polysaccharide catalyzed by methylsulfinyl carbanion in dimethyl sulfoxide. *The Journal of Biochemistry*, 55, 205-208.

Han, J.; Feng, H.; Wang, X.; Liu, Z. & Wu, Z. (2021): Levan from *Leuconostoc citreum* BD1707: production optimization and changes in molecular weight distribution during cultivation. *BMC Biotechnology,* 21, 14.

Han, J.; Hang, F.; Guo, B.; Liu, Z.; You, C. & Wu, Z. (2014): Dextran synthesized by *Leuconostoc mesenteroides* BD1710 in tomato juice supplemented with sucrose. *Carbohydrate Polymers,* 112, 556–562.

Han, W. C. (2009): Production of lactosucrose from sucrose and lactose by a levansucrase from *Zymomonas mobilis*. *Journal of Microbiology and Biotechnology,* 19.

Han, Y. W. & Clarke, M. A. (1990): Production and characterization of microbial levan. *Journal of Agricultural and Food Chemistry,* 38, 393–396.

Hanada, N. & Kuramitsu, H. K. (1988): Isolation and characterization of the *Streptococcus mutans* gtfC gene, coding for synthesis of both soluble and insoluble glucans. *Infection and Immunity,* 56, 1999–2005.

Hanada, N. & Kuramitsu, H. K. (1989): Isolation and characterization of the *Streptococcus mutans* gtfD gene, coding for primer-dependent soluble glucan synthesis. *Infection and Immunity,* 57, 2079–2085.

Hancock, R. A.; Marshall, K. & Weigel, H. (1976): Structure of the levan elaborated by *Streptococcus salivarius* strain 51: an application of chemical-ionisation mass-spectrometry. *Carbohydrate Research,* 49, 351–360.

Hare, M. D.; Svensson, S. & Walker, G. J. (1978): Characterization of the extracellular, water-insoluble α-D-glucans of oral *streptococci* by methylation analysis, and by enzymic synthesis and degradation. *Carbohydrate Research,* 66, 245–264.

Harris, P. J., Henry, R. J., Blakeney, A. B. & Stone, B. A. (1984): An improved procedure for the methylation analysis of oligosaccharides and polysaccharides. *Carbohydrate Research*, *127*, 59-73.

Haworth, W. N. (1915): III. - A new method of preparing alkylated sugars. *Journal of the Chemical Society, Transactions*, 107, 8-16.

Hayacibara, M. F.; Koo, H.; Vacca-Smith, A. M.; Kopec, L. K.; Scott-Anne, K.; Cury, J. A. & Bowen, W. H. (2004): The influence of mutanase and dextranase on the production and structure of glucans synthesized by *streptococcal* glucosyltransferases. *Carbohydrate Research,* 339, 2127–2137.

Hellmuth, H.; Wittrock, S.; Kralj, S.; Dijkhuizen, L.; Hofer, B. & Seibel, J. (2008): Engineering the glucansucrase GTFR enzyme reaction and glycosidic bond specificity: toward tailor-made polymer and oligosaccharide products. *Biochemistry,* 47, 6678–6684.

Heyer, A. G. & Wendenburg, R. (2001): Gene cloning and functional characterization by heterologous expression of the fructosyltransferase of *Aspergillus sydowi* IAM 2544. *Applied and Environmental Microbiology,* 67, 363–370.

Hill, A.; Chen, L.; Mariage, A.; Petit, J.-L.; Berardinis, V. de & Karboune, S. (2019): Discovery of new levansucrase enzymes with interesting properties and improved catalytic activity to produce levan and fructooligosaccharides. *Catalysis Science & Technology,* 9, 2931–2944.

Hiraoka, N.; Tsuji, H.; Fukumoto, J.; Yamamoto, T. & Tsuru, D. (1973): Studies on mold dextranases. Some physicochemical properties and substrate specificity of dextranases obtained from *Aspergillus carneus* and *Penicillium luteum*. *International Journal of Peptide and Protein Research,* 5, 161–169.

Holt, S. M. (2017): Comparative analysis of alternansucrase genes from *Leuconostoc* strains. *Transactions of the Illinois State Academy of Science*, 110.

Horn, F.; Yamamoto, H.; Hirai, A. & Kitamaru, R. (1987): Structural study of amylose polymorphs by cross-polarization-magic-angle spinning, ^{13}C-NMR spectroscopy. *Carbohydrate Research,* 160, 29–40.

Hotz, P.; Guggenheim, B. & Schmid, R. (1972): Carbohydrates in pooled dental plaque. *Caries Research,* 6, 103–121.

Hövels, M.; Kosciow, K. & Deppenmeier, U. (2021): Characterization of a novel *endo*-levanase from *Azotobacter chroococcum* DSM 2286 and its application for the production of prebiotic fructooligosaccharides. *Carbohydrate Polymers,* 255, 117384.

Huang, C.; Miao, M.; Jiang, B.; Cui, S. W.; Jia, X. & Zhang, T. (2015): Polysaccharides modification through green technology: Role of ultrasonication towards improving physicochemical properties of (1,3)(1,6)-α-D-glucans. *Food Hydrocolloids,* 50, 166–173.

Hundschell, C. S.; Braun, A.; Wefers, D.; Vogel, R. F. & Jakob, F. (2020a): Size-dependent variability in flow and viscoelastic behavior of levan produced by *Gluconobacter albidus* TMW 2.1191. *Foods,* 9, 192.

Hundschell, C. S.; Jakob, F. & Wagemans, A. M. (2020b): Molecular weight dependent structure of the exopolysaccharide levan. *International Journal of Biological Macromolecules,* 161, 398–405.

Igarashi, T.; Morisaki, H. & Goto, N. (2004): Molecular characterization of dextranase from *Streptococcus rattus*. *Microbiology and Immunology,* 48, 155–162.

Igarashi, T.; Yamamoto, A. & Goto, N. (1992): Characterization of an *exo*-β-D-fructosidase from *Streptococcus mutans* Ingbritt. *Microbiology and Immunology,* 36, 643–647.

Inoue, M.; Yakushiji, T.; Katsuki, M.; Kudo, N. & Koga, T. (1988): Reduction of the adherence of *Streptococcus sobrinus* insoluble α-D-glucan by *endo*-1,3-α-D-glucanase. *Carbohydrate Research,* 182, 277–286.

Inoue, M.; Yakushiji, T. & Takehara, T. (1982): Ultrastructural changes produced in the oral bacterium *streptococcus mutans* glucans by the action of *endo*-α-1,3-glucanase. *Archives of Oral Biology,* 27, 753–757.

Isenberg, S. L.; Brewer, A. K.; Côté, G. L. & Striegel, A. M. (2010): Hydrodynamic versus size exclusion chromatography characterization of alternan and comparison to off-line MALS. *Biomacromolecules,* 11, 2505–2511.

Ito, K.; Ito, S.; Shimamura, T.; Weyand, S.; Kawarasaki, Y.; Misaka, T.; Abe, K.; Kobayashi, T.; Cameron, A. D. & Iwata, S. (2011): Crystal structure of glucansucrase from the dental caries pathogen *Streptococcus mutans*. *Journal of Molecular Biology,* 408, 177–186.

Jakob, F.; Pfaff, A.; Novoa-Carballal, R.; Rübsam, H.; Becker, T. & Vogel, R. F. (2013): Structural analysis of fructans produced by acetic acid bacteria reveals a relation to hydrocolloid function. *Carbohydrate Polymers,* 92, 1234–1242.

Jakob, F.; Quintero, Y.; Musacchio, A.; Estrada-de los Santos, P.; Hernández, L. & Vogel, R. F. (2019): Acetic acid bacteria encode two levansucrase types of different ecological relationship. *Environmental Microbiology,* 21, 4151–4165.

Jakob, F.; Steger, S. & Vogel, R. F. (2012): Influence of novel fructans produced by selected acetic acid bacteria on the volume and texture of wheat breads. *European Food Research and Technology,* 234, 493–499.

Jakubovics, N. S.; Goodman, S. D.; Mashburn-Warren, L.; Stafford, G. P. & Cieplik, F. (2021): The dental plaque biofilm matrix. *Periodontology 2000,* 86, 32–56.

Jang, K. H.; Jang, E. K.; Kim, S. H.; Kim, I. H.; Kang, S. A.; Koh, I.; Park, Y. I.; Kim, Y. J.; Ha, S. D. & Kim, C. H. (2006): High-level production of low-branched levan from *Pseudomonas aurantiaca* S-4380 for the production of di-β-D-fructofuranose dianhydride IV. *Journal of Microbiology and Biotechnology,* 16, 102–108.

Jathore, N. R.; Bule, M. V.; Tilay, A. V. & Annapure, U. S. (2012): Microbial levan from *Pseudomonas fluorescens*: Characterization and medium optimization for enhanced production. *Food Science and Biotechnology,* 21, 1045–1053.

Jeanes, A.; Haynes, W. C.; Wilham, C.; Rankin, J. C.; Melvin, E. H.; Austin, M. J.; Cluskey, J. E.; Fisher, B. E.; Tsuchiya, H. M. & Rist, C. E. (1954): Characterization and classification of dextrans from ninety-six strains of bacteria. *Journal of the American Chemical Society,* 76, 5041–5052.

Jensen, S. L.; Diemer, M. B.; Lundmark, M.; Larsen, F. H.; Blennow, A.; Mogensen, H. K. & Nielsen, T. H. (2016): Levanase from *Bacillus subtilis* hydrolyses β-2,6 fructosyl bonds in bacterial levans and in grass fructans. *International Journal of Biological Macromolecules,* 85, 514–521.

Jeza, S.; Maseko, S. B. & Lin, J. (2018): Purification and characterization of *exo*-inulinase from *Paenibacillus* sp. d9 strain. *The Protein Journal,* 37, 70–81.

Kang, H. K.; Kimura, A. & Kim, D. (2011): Bioengineering of *Leuconostoc mesenteroides* glucansucrases that gives selected bond formation for glucan synthesis and/or acceptor-product synthesis. *Journal of Agricultural and Food Chemistry,* 59, 4148–4155.

Kardos, N. & Luche, J. L. (2001): Sonochemistry of carbohydrate compounds. *Carbohydrate Research,* 332, 115–131.

Katina, K.; Maina, N. H.; Juvonen, R.; Flander, L.; Johansson, L.; Virkki, L.; Tenkanen, M. & Laitila, A. (2009): *In situ* production and analysis of *Weissella confusa* dextran in wheat sourdough. *Food Microbiology,* 26, 734–743.

Khalikova, E.; Susi, P. & Korpela, T. (2005): Microbial dextran-hydrolyzing enzymes: fundamentals and applications. *Microbiology and Molecular Biology Reviews,* 69, 306–325.

Kim, C. J.; Hamielec, A. E. & Benedek, A. (1982): Characterization of dextrans by size exclusion chromatography using DRI/LALLSP detector system. *Journal of Liquid Chromatography,* 5, 425–441.

Kim, D.; Robyt, J. F.; Lee, S. Y.; Lee, J. H. & Kim, Y. M. (2003): Dextran molecular size and degree of branching as a function of sucrose concentration, pH, and temperature of reaction of *Leuconostoc mesenteroides* B-512FMCM dextransucrase. *Carbohydrate Research,* 338, 1183–1189.

Kim, G.; Bae, J. H.; Cheon, S.; Lee, D. H.; Da Kim, H.; Lee, D.; Park, S. H.; Shim, S.; Seo, J. H. & Han, N. S. (2022): Prebiotic activities of dextran from *Leuconostoc mesenteroides* SPCL742 analyzed in the aspect of the human gut microbial ecosystem. *Food & Function,* 13, 1256–1267.

Kim, K. H. C.; Brun, Y.; Ionescu, L. D.; Londono, J. D.; Mok, J.; Ohane, J. J. & Tong, L. (2023): Highly crystalline α-1,3-glucan. Patent angemeldet am 06.03.2021. US011608388B2.

Kim, Y. M.; Yeon, M. J.; Choi, N. S.; Chang, Y. H.; Jung, M. Y.; Song, J. J. & Kim, J. S. (2010): Purification and characterization of a novel glucansucrase from *Leuconostoc lactis* EG001. *Microbiological Research,* 165, 384–391.

Kırtel, O.; Lescrinier, E.; van den Ende, W. & Toksoy Öner, E. (2019): Discovery of fructans in *Archaea*. *Carbohydrate Polymers,* 220, 149–156.

Kobayashi, K.; Hasegawa, T.; Kusumi, R.; Kimura, S.; Yoshida, M.; Sugiyama, J. & Wada, M. (2017): Characterization of crystalline linear α-1,3-D-glucan synthesized *in vitro*. *Carbohydrate Polymers,* 177, 341–346.

Kobayashi, K.; Kimura, S.; Heux, L. & Wada, M. (2013): Crystal transition between hydrate and anhydrous β-1,3-D-xylan from *Penicillus dumetosus*. *Carbohydrate Polymers,* 97, 105–110.

Kobayashi, K.; Kimura, S.; Togawa, E.; Wada, M. & Kuga, S. (2010): Crystal transition of paramylon with dehydration and hydration. *Carbohydrate Polymers,* 80, 491–497.

Kobayashi, M.; Mitsuishi, Y.; Takagi, S. & Matsuda, K. (1984): Enzymic degradation of water-soluble dextran from *Leuconostoc mesenteroides* NRRL B-1299. *Carbohydrate Research,* 127, 305–317.

Koczan, J. M.; McGrath, M. J.; Zhao, Y. & Sundin, G. W. (2009): Contribution of *Erwinia amylovora* exopolysaccharides amylovoran and levan to biofilm formation: implications in pathogenicity. *Phytopathology,* 99, 1237–1244.

Kojima, I.; Saito, T.; Iizuka, M.; Minamiura, N. & Ono, S. (1993): Characterization of levan produced by *Serratia* sp. *Journal of Fermentation and Bioengineering,* 75, 9–12.

Konishi, N.; Torii, Y.; Yamamoto, T.; Miyagi, A.; Ohta, H.; Fukui, K.; Hanamoto, S.; Matsuno, H.; Komatsu, H.; Kodama, T. & Katayama, E. (1999): Structure and enzymatic properties of genetically truncated forms of the water-insoluble glucan-synthesizing glucosyltransferase from *Streptococcus sobrinus*. *The Journal of Biochemistry,* 126, 287–295.

Koo, H.; Falsetta, M. L. & Klein, M. I. (2013): The exopolysaccharide matrix: A virulence determinant of cariogenic biofilm. *Journal of Dental Research,* 92, 1065–1073.

Kopec, L. K.; Vacca-Smith, A. M. & Bowen, W. H. (1997): Structural aspects of glucans formed in solution and on the surface of hydroxyapatite. *Glycobiology,* 7, 929–934.

Kothari, D.; Tingirikari, J. M. R. & Goyal, A. (2015): *In vitro* analysis of dextran from *Leuconostoc mesenteroides* NRRL B-1426 for functional food application. *Bioactive Carbohydrates and Dietary Fibre,* 6, 55–61.

Kralj, S.; Leeflang, C.; Sierra, E. I.; Kempiński, B.; Alkan, V. & Kolkman, M. (2018): Synthesis of fructooligosaccharides (FosA) and inulin (InuO) by GH68 fructosyltransferases from *Bacillus agaradhaerens* strain WDG185. *Carbohydrate Polymers,* 179, 350–359.

Kralj, S.; van Geel-Schutten, G. H.; Rahaoui, H.; Leer, R. J.; Faber, E. J.; Van Der Maarel, M. J. E. C. & Dijkhuizen, L. (2002): Molecular characterization of a novel glucosyltransferase from *Lactobacillus reuteri* strain 121 synthesizing a unique, highly branched glucan with α-(1→ 4) and α-(1→ 6) glucosidic bonds. *Applied and Environmental Microbiology,* 68, 4283-4291.

Kralj, S.; van Geel-Schutten, G. H.; Dondorff, M. M. G.; Kirsanovs, S.; van der Maarel, M. J. E. C. & Dijkhuizen, L. (2004a): Glucan synthesis in the genus Lactobacillus: Isolation and characterization of glucansucrase genes, enzymes and glucan products from six different strains. *Microbiology,* 150, 3681–3690.

Kralj, S.; van Geel-Schutten, G. H.; van der Maarel, M. J. E. C. & Dijkhuizen, L. (2004b): Biochemical and molecular characterization of *Lactobacillus reuteri* 121 reuteransucrase. *Microbiology,* 150, 2099–2112.

Kralj, S.; van Geel-Schutten, I. G. H.; Faber, E. J.; van der Maarel, M. J. E. C. & Dijkhuizen, L. (2005): Rational transformation of *Lactobacillus reuteri* 121 reuteransucrase into a dextransucrase. *Biochemistry,* 44, 9206–9216.

Krol, B. (1978): Condensation of fructose in acid water-solutions. *Acta Alimentaria Polonica,* 04.

Kuramitsu, H. K. (1975): Characterization of extracellular glucosyltransferase activity of *Streptococcus mutans*. *Infection and Immunity,* 12, 738–749.

Kusumi, R.; Asai, S.; He, Q.; Kobayashi, K.; Kimura, S.; Yoshida, M. & Wada, M. (2023): α-1,3-graft-1,6-D-glucan: Comb-like polysaccharide synthesized *in vitro* with α-1,3/1,6-glucosyltransferase L from *Streptococcus salivarius*. *Carbohydrate Research,* 534, 108969.

Lammens, W.; Le Roy, K.; Schroeven, L.; van Laere, A.; Rabijns, A. & van den Ende, W. (2009): Structural insights into glycoside hydrolase family 32 and 68 enzymes: functional implications. *Journal of Experimental Botany,* 60, 727–740.

Larm, O.; Lindberg, B. & Svensson, S. (1971): Studies on the length of the side chains of the dextran elaborated by *Leuconostoc mesenteroides* NRRL B-512. *Carbohydrate Research*, 20, 39–48.

Laue, H.; Schenk, A.; Li, H.; Lambertsen, L.; Neu, T. R.; Molin, S. & Ullrich, M. S. (2006): Contribution of alginate and levan production to biofilm formation by *Pseudomonas syringae*. *Microbiology*, 152, 2909–2918.

Lee, J. S.; Park, E.; Oh, H.; Choi, W. I. & Koo, H. (2023): Levan nanoparticles with intrinsic Cd44-targeting ability for tumor-targeted drug delivery. *International Journal of Biological Macromolecules,* 234, 123634.

Leemhuis, H.; Pijning, T.; Dobruchowska, J. M.; van Leeuwen, S. S.; Kralj, S.; Dijkstra, B. W. & Dijkhuizen, L. (2013): Glucansucrases: three-dimensional structures, reactions, mechanism, α-glucan analysis and their implications in biotechnology and food applications. *Journal of Biotechnology,* 163, 250–272.

Lekakarn, H.; Bunterngsook, B.; Jaikaew, P.; Kuantum, T.; Wansuksri, R. & Champreda, V. (2022): Functional characterization of recombinant *endo*-levanase (LevBk) from *Bacillus koreensis* HL12 on short-chain levan-type fructooligosaccharides production. *The Protein Journal*, 41, 477-488.

Lewis, B. A.; Cyr, M. & Smith, F. (1967): The constitution of the fructan produced by *Leuconostoc mesenteroides* strain C. *Carbohydrate Research,* 5, 194–201.

Li, B.; Dobruchowska, J. M.; Hoogenkamp, M. A. & Gerwig, G. J. (2012): Structural investigation of an extracellular polysaccharide produced by the cariogenic bacterium *Streptococcus mutans* strain UA159. *Carbohydrate Polymers,* 90, 675–682.

Li, X.; Wang, X.; Meng, X.; Dijkhuizen, L. & Liu, W. (2020): Structures, physico-chemical properties, production and (potential) applications of sucrose-derived α-D-glucans synthesized by glucansucrases. *Carbohydrate Polymers,* 249, 116818.

Lin, Y.; Chen, J.; Zhou, X. & Li, Y. (2021): Inhibition of *Streptococcus mutans* biofilm formation by strategies targeting the metabolism of exopolysaccharides. *Critical Reviews in Microbiology,* 47, 667–677.

Lindberg, B.; Lönngren, J.; Thompson, J. L.; Pessa, M.; van der Hoeven, M. G. & Swahn, C. G. (1973): Methylation studies on levans. *Acta Chem. Scand*., 27, 1819–1821.

Liu, C.; Kolida, S.; Charalampopoulos, D. & Rastall, R. A. (2020): An evaluation of the prebiotic potential of microbial levans from *Erwinia* sp. 10119. *Journal of Functional Foods,* 64, 103668.

Liu, Q.; Yu, S.; Zhang, T.; Jiang, B. & Mu, W. (2017): Efficient biosynthesis of levan from sucrose by a novel levansucrase from *Brenneria goodwinii*. *Carbohydrate Polymers,* 157, 1732–1740.

Llamas-Arriba, M. G.; Puertas, A. I.; Prieto, A.; López, P.; Cobos, M.; Miranda, J. I.; Marieta, C.; Ruas-Madiedo, P. & Dueñas, M. T. (2019): Characterization of dextrans produced by *Lactobacillus mali* CUPV271 and *Leuconostoc carnosum* CUPV411. *Food Hydrocolloids,* 89, 613–622.

Lynch, K. M.; Zannini, E.; Coffey, A. & Arendt, E. K. (2018): Lactic acid bacteria exopolysaccharides in foods and beverages: Isolation, properties, characterization, and health benefits. *Annual Review of Food Science and Technology,* 9, 155–176.

Maina, N. H.; Juvonen, M.; Domingues, R. M.; Virkki, L.; Jokela, J. & Tenkanen, M. (2013): Structural analysis of linear mixed-linkage glucooligosaccharides by tandem mass spectrometry. *Food Chemistry,* 136, 1496–1507.

Maina, N. H.; Pitkänen, L.; Heikkinen, S.; Tuomainen, P.; Virkki, L. & Tenkanen, M. (2014): Challenges in analysis of high-molar mass dextrans: comparison of HPSEC, AsFlFFF and DOSY NMR spectroscopy. *Carbohydrate Polymers*, 99, 199-207.

Maina, N. H.; Tenkanen, M.; Maaheimo, H.; Juvonen, R. & Virkki, L. (2008): NMR spectroscopic analysis of exopolysaccharides produced by *Leuconostoc citreum* and *Weissella confusa*. *Carbohydrate Research,* 343, 1446–1455.

Maina, N. H.; Virkki, L.; Pynnönen, H.; Maaheimo, H. & Tenkanen, M. (2011): Structural analysis of enzyme-resistant isomaltooligosaccharides reveals the elongation of α-1,3-linked branches in *Weissella confusa* dextran. *Biomacromolecules,* 12, 409–418.

Malang, S. K.; Maina, N. H.; Schwab, C.; Tenkanen, M. & Lacroix, C. (2015): Characterization of exopolysaccharide and ropy capsular polysaccharide formation by *Weissella*. *Food Microbiology,* 46, 418–427.

Marchessault, R. H. & Deslandes, Y. (1981): Crystalline conformation of homo- and regular heteroglucan chains. *Carbohydrate Polymers,* 1, 31–38.

Mardo, K.; Visnapuu, T.; Vija, H.; Aasamets, A.; Viigand, K. & Alamäe, T. (2017): A highly active *endo*-Levanase BT1760 of a dominant mammalian gut commensal *Bacteroides thetaiotaomicron* cleaves not only various bacterial levans, but also levan of timothy grass. *PLOS one,* 12, e0169989.

Márquez-López, R. E.; Uc-Chuc, M. A.; Loyola-Vargas, V. M.; Santiago-García, P. A. & López, M. G. (2023): Fructosyltransferases in plants: Structure, function and application: A review. *Carbohydrate Polymer Technologies and Applications,* 6, 100343.

Marshall, K. & Weigel, H. (1980a): Evidence of multiple branching in the levan elaborated by *Streptococcus salivarius* strain 51. *Carbohydrate Research,* 83, 321–326.

Marshall, K. & Weigel, H. (1980b): Extracellular β-D-fructofuranosidase elaborated by *Streptococcus salivarius* strain 51: preparation, and mode of action on a levan and on homologues of inulobiose. *Carbohydrate Research,* 83, 315–320.

Martínez-Fleites, C.; Ortíz-Lombardía, M.; Pons, T.; Tarbouriech, N.; Taylor, E. J.; Arrieta, J. G.; Hernández, L. & Davies, G. J. (2005): Crystal structure of levansucrase from the gram-negative bacterium *Gluconacetobacter diazotrophicus*. *The Biochemical Journal,* 390, 19–27.

Matson, J. B.; Steele, A. Q.; Mase, J. D. & Schulz, M. D. (2024): Polymer characterization by size-exclusion chromatography with multi-angle light scattering (SEC-MALS): a tutorial review. *Polymer Chemistry*, 15, 127-142.

Matulová, M.; Husárová, S.; Capek, P.; Sancelme, M. & Delort, A.-M. (2011): NMR structural study of fructans produced by *Bacillus* sp. 3B6, bacterium isolated in cloud water. *Carbohydrate Research,* 346, 501–507.

McCleary, B. V.; Charmier, L. M. J.; McKie, V. A.; McLoughlin, C. & Rogowski, A. (2019): Determination of fructan (inulin, FOS, levan, and branched fructan) in animal food (animal feed, pet food, and ingredients): Single-laboratory validation, first action 2018.07. *Journal of AOAC International,* 102, 883–892.

Meng, G. & Fütterer, K. (2003): Structural framework of fructosyl transfer in *Bacillus subtilis* levansucrase. *Nature structural Biology,* 10, 935–941.

Meng, G. & Fütterer, K. (2008): Donor substrate recognition in the raffinose-bound E342A mutant of fructosyltransferase *Bacillus subtilis* levansucrase. *BMC Structural Biology,* 8, 16.

Meng, X.; Dobruchowska, J. M.; Pijning, T.; Gerwig, G. J. & Dijkhuizen, L. (2016a): Synthesis of new hyperbranched α-glucans from sucrose by *Lactobacillus reuteri* 180 glucansucrase mutants. *Journal of Agricultural and Food Chemistry,* 64, 433–442.

Meng, X.; Gangoiti, J.; Bai, Y.; Pijning, T.; van Leeuwen, S. S. & Dijkhuizen, L. (2016b): Structure-function relationships of family GH70 glucansucrase and 4,6-α-glucanotransferase enzymes, and their evolutionary relationships with family GH13 enzymes. *Cellular and Molecular Life Sciences,* 73, 2681–2706.

Mensink, M. A.; Frijlink, H. W.; van der Voort Maarschalk, K. & Hinrichs, W. L. J. (2015): Inulin, a flexible oligosaccharide I: Review of its physicochemical characteristics. *Carbohydrate Polymers,* 130, 405–419.

Merienne, S.; Busnel, J. P.; Fricoteaux, F. & Prudhomme, J. C. (2000): Size exclusion chromatography of dextrans in DMSO as eluent. *Journal of Liquid Chromatography & Related Technologies,* 23, 1745–1756.

Miao, M.; Ma, Y.; Jiang, B.; Cui, S. W.; Jin, Z. & Zhang, T. (2017): Characterisations of *Lactobacillus reuteri* SK24.003 glucansucrase: Implications for α-gluco-poly- and oligosaccharides biosynthesis. *Food Chemistry,* 222, 105–112.

Miasnikov, A. N. (1997): Characterization of a novel *endo*-levanase and its gene from *Bacillus* sp. L7. *FEMS Microbiology Letters*, 154, 23-28.

Misaki, A.; Torii, M.; Sawai, T. & Goldstein, I. J. (1980): Structure of the dextran of *Leuconostoc mesenteroides* B-1355. *Carbohydrate Research*, 84, 273-285.

Mitsuishi, Y.; Kobayashi, M. & Matsuda, K. (1980): Dextran α-1,2-debranching enzyme from *Flavobacterium* sp. M-73. Properties and mode of action. *Carbohydrate Research,* 83, 303–313.

Miyazaki, T. (2023): Glycoside hydrolases active on microbial exopolysaccharide α-glucans: structures and function. *Essays in Biochemistry,* 67, 505–520.

Moffitt, E. A. (1975): Blood substitutes. *Canadian Anaesthetists' Society Journal,* 22, 12–19.

Molina, M.; Cioci, G.; Moulis, C.; Séverac, E. & Remaud-Siméon, M. (2021): Bacterial α-glucan and branching sucrases from GH70 family: Discovery, structure-function relationship studies and engineering. *Microorganisms,* 9, 1607.

Molina, M.; Moulis, C.; Monties, N.; Pizzut-Serin, S.; Guieysse, D.; Morel, S.; Cioci, G. & Remaud-Siméon, M. (2019): Deciphering an undecided enzyme: Investigations of the structural determinants involved in the linkage specificity of alternansucrase. *ACS Catalysis,* 9, 2222–2237.

Monchois, V.; Arguello-Morales, M. & Russell, R. R. (1999): Isolation of an active catalytic core of *Streptococcus downei* MFe28 GTF-I glucosyltransferase. *Journal of Bacteriology,* 181, 2290–2292.

Monchois, V.; Vignon, M. & Russell, R. R. (2000): Mutagenesis of asp-569 of glucosyltransferase I glucansucrase modulates glucan and oligosaccharide synthesis. *Applied and Environmental Microbiology,* 66, 1923–1927.

Monsan, P.; Bozonnet, S.; Albenne, C.; Joucla, G.; Willemot, R.-M. & Remaud-Siméon, M. (2001): Homopolysaccharides from lactic acid bacteria. *International Dairy Journal,* 11, 675–685.

Münkel, F.; Bechtner, J.; Eckel, V.; Fischer, A.; Herbi, F.; Jakob, F. & Wefers, D. (2019): Detailed structural characterization of glucans produced by glucansucrases from *Leuconostoc citreum* TMW 2.1194. *Journal of Agricultural and Food Chemistry,* 67, 6856–6866.

Münkel, F.; Fischer, A. & Wefers, D. (2020): Structural characterization of mixed-linkage α-glucans produced by mutants of *Lactobacillus reuteri* TMW 1.106 dextransucrase. *Carbohydrate Polymers,* 231, 115697.

Münkel, F. & Wefers, D. (2019): Fine structures of different dextrans assessed by isolation and characterization of *endo*-dextranase liberated isomalto-oligosaccharides. *Carbohydrate Polymers,* 215, 296–306.

Nabot, M.; Guérin, M.; Sivakumar, D.; Remize, F. & Garcia, C. (2022): Variability of bacterial homopolysaccharide production and properties during food processing. *Biology,* 11.

Nachtigall, C.; Hassler, V.; Wefers, D.; Rohm, H. & Jaros, D. (2023): Dextrans of *Weissella cibaria* DSM14295: Microbial production, structure and functionality. *International Journal of Biological Macromolecules,* 246, 125631.

Nagy, K. D.; Hennessey, S. M.; Brun, Y. & Reichman, M. (2020): Enzymatic production of α-1,3-glucan. Patent angemeldet am 29.11.2018. US010774352B2.

Nester, K. & Plazinski, W. (2019): Deciphering the conformational preferences of furanosides. A molecular dynamics study. *Journal of Biomolecular Structure and Dynamics*, 38, 3359-3370.

Nester, K. & Plazinski, W. (2020): Conformational properties of inulin, levan and arabinan studied by molecular dynamics simulations. *Carbohydrate Polymers,* 240, 116266.

Ni, D.; Xu, W. & Mu, W. (2021): Inulosucrase, an efficient transfructosylation tool for the synthesis of microbial inulin. In: Mu, W., Zhang, W. & Chen, Q. (Hg.): *Novel enzymes for functional carbohydrates production. From scientific research to application in health food industry*. 1. Edition, Springer Nature Singapore, 199–222.

Ni, D.; Xu, W.; Zhu, Y.; Zhang, W.; Zhang, T.; Guang, C. & Mu, W. (2019): Inulin and its enzymatic production by inulosucrase: Characteristics, structural features, molecular modifications and applications. *Biotechnology Advances,* 37, 306–318.

Ni, D.; Zhang, S.; Liu, X.; Zhu, Y.; Xu, W.; Zhang, W. & Mu, W. (2024): Production, effects, and applications of fructans with various molecular weights. *Food Chemistry,* 437, 137895.

Ni, D.; Zhu, Y.; Xu, W.; Bai, Y.; Zhang, T. & Mu, W. (2018): Biosynthesis of inulin from sucrose using inulosucrase from *Lactobacillus gasseri* DSM 20604. *International Journal of Biological Macromolecules,* 109, 1209–1218.

Ni, D.; Zhu, Y.; Xu, W.; Pang, X.; Lv, J. & Mu, W. (2020): Production and physicochemical properties of food-grade high-molecular-weight *Lactobacillus* inulin. *Journal of Agricultural and Food Chemistry,* 68, 5854–5862.

Nolte, J.; Kempa, A.; Schlockermann, A.; Hochgürtel, M. & Schörken, U. (2019): Glycosylation of caffeic acid and structural analogues catalyzed by novel glucansucrases from *Leuconostoc* and *Weissella* species. *Biocatalysis and Agricultural Biotechnology,* 19, 101114.

Ogawa, K.; Okamura, K. & Sarko, A. (1981): Molecular and crystal structure of the regenerated form of α-1,3-D-glucan. *International Journal of Biological Macromolecules,* 3, 31–36.

Ogawa, K.; Yui, T.; Okamura, K. & Misaki, A. (1994): Crystalline features of *Streptococcal* α-1,3-D-glucans of human saliva. *Bioscience, Biotechnology, and Biochemistry,* 58, 1326–1327.

Okuyama, M.; Serizawa, R.; Tanuma, M.; Kikuchi, A.; Sadahiro, J.; Tagami, T.; Lang, W. & Kimura, A. (2021): Molecular insight into regioselectivity of transfructosylation catalyzed by GH68 levansucrase and β-fructofuranosidase. *Journal of Biological Chemistry,* 296, 100398.

Olvera, C.; Centeno-Leija, S. & López-Munguía, A. (2007): Structural and functional features of fructansucrases present in *Leuconostoc mesenteroides* ATCC 8293. *Antonie van Leeuwenhoek,* 92, 11–20.

Öner, E. T.; Hernández, L. & Combie, J. (2016): Review of levan polysaccharide: From a century of past experiences to future prospects. *Biotechnology Advances,* 34, 827–844.

Ortiz-Soto, M. E.; Olivares-Illana, V. & López-Munguía, A. (2004): Biochemical properties of inulosucrase from *Leuconostoc citreum* CW28 used for inulin synthesis. *Biocatalysis and Biotransformation,* 22, 275–281.

Ortiz-Soto, M. E.; Porras-Domínguez, J. R.; Seibel, J. & López-Munguía, A. (2019): A close look at the structural features and reaction conditions that modulate the synthesis of low and high molecular weight fructans by levansucrases. *Carbohydrate Polymers,* 219, 130–142.

Osorio, M. I.; Zúñiga, M. A.; Mendoza, F.; Jaña, G. A. & Jiménez, V. A. (2019): Modulation of glucan-enzyme interactions by domain V in GTF-SI from *Streptococcus mutans*. *Proteins: Structure, Function, and Bioinformatics,* 87, 74–80.

Ozimek, L. K.; Euverink, G. J. W.; van der Maarel, M. J. E. C. & Dijkhuizen, L. (2005): Mutational analysis of the role of calcium ions in the *Lactobacillus reuteri* strain 121 fructosyltransferase (levansucrase and inulosucrase) enzymes. *FEBS Letters,* 579, 1124–1128.

Ozimek, L. K.; Kralj, S.; van der Maarel, M. J. E. C. & Dijkhuizen, L. (2006): The levansucrase and inulosucrase enzymes of *Lactobacillus reuteri* 121 catalyse processive and non-processive transglycosylation reactions. *Microbiology,* 152, 1187–1196.

Ozimek, L. K.; van Hijum, S. A. F. T.; van Koningsveld, G. A.; van der Maarel, M. J. E. C.; van Geel-Schutten, G. H. & Dijkhuizen, L. (2004): Site-directed mutagenesis study of the three catalytic residues of the fructosyltransferases of *Lactobacillus reuteri* 121. *FEBS Letters,* 560, 131–133.

Padmanabhan, P. A.; Kim, D. S.; Pak, D. & Sim, S. J. (2003): Rheology and gelation of water-insoluble dextran from *Leuconostoc mesenteroides* NRRL B-523. *Carbohydrate Polymers,* 53, 459–468.

Passerini, D.; Vuillemin, M.; Ufarté, L.; Morel, S.; Loux, V.; Fontagné-Faucher, C.; Monsan, P.; Remaud-Siméon, M. & Moulis, C. (2015): Inventory of the GH 70 enzymes encoded by *Leuconostoc citreum* NRRL B-1299 – identification of three novel α-transglucosylases. *The FEBS Journal*, 282, 2115-2130.

Paul, J. S.; Gupta, N.; Beliya, E.; Tiwari, S. & Jadhav, S. K. (2021): Aspects and recent trends in microbial α-amylase: A review. *Applied Biochemistry and Biotechnology,* 193, 2649–2698.

Pearce, B. J.; Walker, G. J.; Slodki, M. E. & Schuerch, C. (1990): Enzymic and methylation analysis of dextrans and a-1,3-D-glucans. *Carbohydrate Research,* 203, 229–246.

Pei, F.; Ma, Y.; Chen, X. & Liu, H. (2020): Purification and structural characterization and antioxidant activity of levan from *Bacillus megaterium* PFY-147. *International Journal of Biological Macromolecules,* 161, 1181–1188.

Perez Garcia, M.; Wang, T.; Salazar, A.; Zabotina, O. A. & Hong, M. (2012): Multidimensional solid-state NMR studies of the structure and dynamics of pectic polysaccharides in uniformly ^{13}C-labeled *Arabidopsis* primary cell walls. *Magnetic Resonance in Chemistry,* 50, 539–550.

Pettolino, F. A., Walsh, C., Fincher, G. B. & Bacic, A. (2012): Determining the polysaccharide composition of plant cell walls. *Nature protocols*, 7, 1590-1607.

Pidoux, M.; de Ruiter, G. A.; Brooker, B. E.; Colquhoun, I. J. & Morris, V. J. (1990): Microscopic and chemical studies of a gelling polysaccharide from *Lactobacillus hilgardii*. *Carbohydrate Polymers,* 13, 351–362.

Pijning, T.; Anwar, M. A.; Böger, M.; Dobruchowska, J. M.; Leemhuis, H.; Kralj, S.; Dijkhuizen, L. & Dijkstra, B. W. (2011): Crystal structure of inulosucrase from *Lactobacillus*: insights into the substrate specificity and product specificity of GH68 fructansucrases. *Journal of Molecular Biology,* 412, 80–93.

Pijning, T.; Vujičić-Žagar, A.; Kralj, S.; Dijkhuizen, L. & Dijkstra, B. W. (2012): Structure of the α-1,6/α-1,4-specific glucansucrase GTFA from *Lactobacillus reuteri* 121. *Acta Crystallographica Section F: Structural Biology and Crystallization Communications,* 68, 1448–1454.

Pijning, T.; Vujičić-Žagar, A.; Kralj, S.; Eeuwema, W.; Dijkhuizen, L. & Dijkstra, B. W. (2008): Biochemical and crystallographic characterization of a glucansucrase from *Lactobacillus reuteri* 180. *Biocatalysis and Biotransformation,* 26, 12–17.

Pittrof, S. L.; Kaufhold, L.; Fischer, A. & Wefers, D. (2021): Products released from structurally different dextrans by bacterial and fungal dextranases. *Foods,* 10, 244.

Pleszczyńska, M.; Boguszewska, A.; Tchórzewski, M.; Wiater, A. & Szczodrak, J. (2012): Gene cloning, expression, and characterization of mutanase from *Paenibacillus curdlanolyticus* MP-1. *Protein Expression and Purification,* 86, 68–74.

Pleszczyńska, M.; Wiater, A.; Janczarek, M. & Szczodrak, J. (2015): α-1,3-D-Glucan hydrolases in dental biofilm prevention and control: A review. *International Journal of Biological Macromolecules,* 79, 761–778.

Pollock, C. J. & Cairns, A. J. (1991): Fructan metabolism in grasses and cereals. *Annual Review of Plant Biology,* 42, 77–101.

Pollock, C. J.; Hall, M. A. & Roberts, D. P. (1979): Structural analysis of fructose polymers by gas-liquid chromatography and gel filtration. *Journal of Chromatography A, 171,* 411-415.

Pons, T.; Naumoff, D. G.; Martínez-Fleites, C. & Hernández, L. (2004): Three acidic residues are at the active site of a β-propeller architecture in glycoside hydrolase families 32, 43, 62, and 68. *Proteins: Structure, Function, and Bioinformatics,* 54, 424–432.

Porras-Domínguez, J. R.; Ávila-Fernández, Á.; Miranda-Molina, A.; Rodríguez-Alegría, M. E. & Munguía, A. L. (2015): *Bacillus subtilis* 168 levansucrase (SacB) activity affects average levan molecular weight. *Carbohydrate Polymers,* 132, 338–344.

Porras-Domínguez, J. R.; Ávila-Fernández, Á.; Rodríguez-Alegría, M. E.; Miranda-Molina, A.; Escalante, A.; González-Cervantes, R.; Olvera, C. & López Munguía, A. (2014): Levan-type FOS production using a *Bacillus licheniformis endo*-levanase. *Process Biochemistry,* 49, 783–790.

Poulhazan, A.; Arnold, A. A.; Warschawski, D. E. & Marcotte, I. (2018): Unambiguous *ex situ* and in cell 2D ^{13}C solid-state NMR characterization of starch and its constituents. *International Journal of Molecular Sciences,* 19, 3817.

Puanglek, S.; Kimura, S.; Enomoto-Rogers, Y.; Kabe, T.; Yoshida, M.; Wada, M. & Iwata, T. (2016): *In vitro* synthesis of linear α-1,3-glucan and chemical modification to ester derivatives exhibiting outstanding thermal properties. *Scientific Reports,* 6, 30479.

Puanglek, S.; Kimura, S. & Iwata, T. (2017): Thermal and mechanical properties of tailor-made unbranched α-1,3-glucan esters with various carboxylic acid chain length. *Carbohydrate Polymers,* 169, 245–254.

Purdie, T. & Irvine, J. C. (1903): C. - The alkylation of sugars. *Journal of the Chemical Society, Transactions*, 83, 1021-1037.

Qin, F.; Kes, M. & Christensen, B. E. (2013): A study of bioactive, branched β-1,3-D-glucans in dimethylacetamide/LiCl and dimethyl sulphoxide/LiCl using size-exclusion chromatography with multi-angle light scattering detection. *Journal of Chromatography A,* 1305, 109–113.

Qin, Y. Q.; Wang, L. Y.; Yang, X. Y.; Xu, Y. J.; Fan, G.; Fan, Y. G.; Ren, J. N.; An, Q. & Li, X. (2023): Inulin: properties and health benefits. *Food & Function,* 14, 2948–2968.

Renard, C. M. & Jarvis, M. C. (1999): A cross-polarization, magic-angle-spinning, ^{13}C-NMR study of polysaccharides in sugar beet cell walls. *Plant Physiology,* 119, 1315–1322.

Ronkart, S. N.; Blecker, C. S.; Fourmanoir, H.; Fougnies, C.; Deroanne, C.; van Herck, J.-C. & Paquot, M. (2007): Isolation and identification of inulooligosaccharides resulting from inulin hydrolysis. *Analytica Chimica Acta,* 604, 81–87.

Rozen, R.; Bachrach, G.; Bronshteyn, M.; Gedalia, I. & Steinberg, D. (2001): The role of fructans on dental biofilm formation by *Streptococcus sobrinus*, *Streptococcus mutans*, *Streptococcus gordonii* and *Actinomyces viscosus*. *FEMS Microbiology Letters,* 195, 205–210.

Rühmkorf, C.; Bork, C.; Mischnick, P.; Rübsam, H.; Becker, T. & Vogel, R. F. (2013): Identification of *Lactobacillus curvatus* TMW 1.624 dextransucrase and comparative characterization with *Lactobacillus reuteri* TMW 1.106 and *Lactobacillus animalis* TMW 1.971 dextransucrases. *Food Microbiology,* 34, 52–61.

Ruiz-Matute, A. I., Hernández-Hernández, O., Rodríguez-Sánchez, S., Sanz, M. L. & Martínez-Castro, I. (2011): Derivatization of carbohydrates for GC and GC–MS analyses. *Journal of Chromatography B*, 879, 1226-1240.

Runyon, J. R.; Nilsson, L.; Ulmius, M.; Castro, A.; Ionescu, R.; Andersson, C. & Schmidt, C. (2014): Characterizing changes in levan physicochemical properties in different pH environments using asymmetric flow field-flow fractionation. *Analytical and Bioanalytical Chemistry,* 406, 1597–1605.

Sarilmiser, H. K.; Ates, O.; Ozdemir, G.; Arga, K. Y. & Oner, E. T. (2015): Effective stimulating factors for microbial levan production by *Halomonas smyrnensis* AAD6T. *Journal of Bioscience and Bioengineering,* 119, 455–463.

Sawale, S. D. & Lele, S. S. (2010): Statistical optimization of media for dextran production by *Leuconostoc* sp., isolated from fermented idli batter. *Food Science and Biotechnology,* 19, 471–478.

Schmid, J.; Bechtner, J.; Vogel, R. F. & Jakob, F. (2019): A systematic approach to study the pH-dependent release, productivity and product specificity of dextransucrases. *Microbial Cell Factories,* 18, 153.

Schormann, N.; Patel, M.; Thannickal, L.; Purushotham, S.; Wu, R.; Mieher, J. L.; Wu, H. & Deivanayagam, C. (2023): The catalytic domains of *Streptococcus mutans* glucosyltransferases: a structural analysis. *Acta Crystallographica Section F: Structural Biology Communications*, 119–127.

Schult, T.; Hjerde, T.; Inge Optun, O.; Kleppe, P. J. & Moe, S. (2002): Characterization of cellulose by SEC-MALLS. *Cellulose,* 9, 149–158.

Seidi, F.; Yazdi, M. K.; Jouyandeh, M.; Habibzadeh, S.; Munir, M. T.; Vahabi, H.; Bagheri, B.; Rabiee, N.; Zarrintaj, P. & Saeb, M. R. (2022): Crystalline polysaccharides: A review. *Carbohydrate Polymers,* 275, 118624.

Seymour, F. R. & Knapp, R. D. (1980): Structural analysis of dextrans, from strains of *leuconostoc* and related genera, that contain 3-*O*-α-D-glucosylated α-D-glucopyranosyl residues at the branch points, or in consecutive, linear positions. *Carbohydrate Research,* 81, 105–129.

Shi, Q.; Hou, Y.; Xu, Y.; Mørkeberg Krogh, K. B. R. & Tenkanen, M. (2019): Enzymatic analysis of levan produced by lactic acid bacteria in fermented doughs. *Carbohydrate Polymers,* 208, 285–293.

Shimamura, A.; Nakano, Y. J.; Mukasa, H. & Kuramitsu, H. K. (1994): Identification of amino acid residues in *Streptococcus mutans* glucosyltransferases influencing the structure of the glucan product. *Journal of Bacteriology,* 176, 4845–4850.

Shoaib, M.; Shehzad, A.; Omar, M.; Rakha, A.; Raza, H.; Sharif, H. R.; Shakeel, A.; Ansari, A. & Niazi, S. (2016): Inulin: Properties, health benefits and food applications. *Carbohydrate Polymers,* 147, 444–454.

Shukla, R. & Goyal, A. (2013): Elucidation of structure and biocompatibility of levan from *Leuconostoc mesenteroides* NRRL B-1149. *Current Trends in Biotechnology and Pharmacy,* 7, 635–643.

Shukla, R.; Iliev, I. & Goyal, A. (2010): Purification and characterization of dextransucrase from *Leuconostoc mesenteroides* NRRL B-1149. *Biotechnology & Biotechnological Equipment,* 24, 576–580.

Shukla, R.; Shukla, S.; Bivolarski, V.; Iliev, I.; Ivanova, I. & Goyal, A. (2011): Structural characterization of insoluble dextran produced by *Leuconostoc mesenteroides* NRRL B-1149 in the presence of maltose. *Food Technology and Biotechnology,* 49, 291–296.

Shukla, S.; Shi, Q.; Maina, N. H.; Juvonen, M.; Tenkanen, M. & Goyal, A. (2014): *Weissella confusa* Cab3 dextransucrase: properties and *in vitro* synthesis of dextran and glucooligosaccharides. *Carbohydrate Polymers,* 101, 554–564.

Sidebotham, R. L. (1974): Dextrans. *Advances in carbohydrate chemistry and biochemistry,* 30, 371–444.

Silberman, H. C. (1961): Reactions of sugars in the presence of acids: A paper chromatographic study. *The Journal of Organic Chemistry,* 26, 1967–1969.

Simms, P. J.; Boyko, W. J. & Edwards, J. R. (1990): The structural analysis of a levan produced by *Streptococcus salivarius* SS2. *Carbohydrate Research,* 208, 193–198.

Simpson, C. L.; Cheetham, N. W. H. & Jacques, N. A. (1995): Four glucosyltransferases, GtfJ, GtfK, GtfL and GtfM, from *Streptococcus salivarius* ATCC 25975. *Microbiology,* 141, 1451–1460.

Sims, I. M.; Carnachan, S. M.; Bell, T. J. & Hinkley, S. F. R. (2018): Methylation analysis of polysaccharides: Technical advice. *Carbohydrate Polymers,* 188, 1–7.

Singh, R. S.; Chauhan, K. & Kennedy, J. F. (2017): A panorama of bacterial inulinases: Production, purification, characterization and industrial applications. *International Journal of Biological Macromolecules,* 96, 312–322.

Singh, R. S.; Singh, T.; Hassan, M. & Kennedy, J. F. (2020): Updates on inulinases: Structural aspects and biotechnological applications. *International Journal of Biological Macromolecules*, 164, 193-210.

Singh, R. S.; Singh, R. P. & Kennedy, J. F. (2016): Recent insights in enzymatic synthesis of fructooligosaccharides from inulin. *International Journal of Biological Macromolecules*, 85, 565-572.

Slodki, M. E.; England, R. E.; Plattner, R. D. & Dick, W. E. (1986): Methylation analyses of NRRL dextrans by capillary gas-liquid chromatography. *Carbohydrate Research,* 156, 199–206.

Song, L.; Miao, M.; Jiang, B.; Xu, T.; Cui, S. W. & Zhang, T. (2016): *Leuconostoc citreum* SK24.002 glucansucrase: Biochemical characterisation and *de novo* synthesis of α-glucan. *International Journal of Biological Macromolecules,* 91, 123–131.

Srikanth, R.; Reddy, C. H. S. S. S.; Siddartha, G.; Ramaiah, M. J. & Uppuluri, K. B. (2015a): Review on production, characterization and applications of microbial levan. *Carbohydrate Polymers,* 120, 102–114.

Srikanth, R.; Siddartha, G.; Sundhar Reddy, C. H. S. S.; Harish, B. S.; Janaki Ramaiah, M. & Uppuluri, K. B. (2015b): Antioxidant and anti-inflammatory levan produced from *Acetobacter xylinum* NCIM2526 and its statistical optimization. *Carbohydrate Polymers,* 123, 8–16.

Stevenson, T. T. & Furneaux, R. H. (1991): Chemical methods for the analysis of sulphated galactans from red algae. *Carbohydrate Research,* 210, 277–298.

Striegel, A. M.; Isenberg, S. L. & Côté, G. L. (2009): An SEC/MALS study of alternan degradation during size-exclusion chromatographic analysis. *Analytical and Bioanalytical Chemistry*, 394, 1887-1893.

Strube, C. P.; Homann, A.; Gamer, M.; Jahn, D.; Seibel, J. & Heinz, D. W. (2011): Polysaccharide synthesis of the levansucrase SacB from *Bacillus megaterium* is controlled by distinct surface motifs. *Journal of Biological Chemistry,* 286, 17593–17600.

Sun, Z.; Harris, H. M. B.; McCann, A.; Guo, C.; Argimón, S.; Zhang, W.; Yang, X.; Jeffery, I. B.; Cooney, J. C.; Kagawa, T. F.; Liu, W.; Song, Y.; Salvetti, E.; Wrobel, A.; Rasinkangas, P.; Parkhill, J.; Rea, M. C.; O'Sullivan, O.; Ritari, J.; Douillard, F. P.; Paul Ross, R.; Yang, R.; Briner, A. E.; Felis, G. E.; de Vos, W. M.; Barrangou, R.; Klaenhammer, T. R.; Caufield, P. W.; Cui, Y.; Zhang, H. & O'Toole, P. W. (2015): Expanding the biotechnology potential of *lactobacilli* through comparative genomics of 213 strains and associated genera. *Nature communications,* 6, 8322.

Sundarram, A. & Murphy, T. P. K. (2014): α-Amylase production and applications: a review. *Journal of Applied & Environmental Microbiology,* 2, 166–175.

Takahashi, N. & Nyvad, B. (2008): Caries ecology revisited: Microbial dynamics and the caries process. *Caries Research,* 42, 409–418.

Takehara, T.; Ansai, T.; Kunimori, A.; Yamashita, Y. & Hanada, N. (1991): The extension of α-D-1,3-branch linkages by 1,3-α-D-glucan synthase from *Streptococcus sobrinus*. *FEMS Microbiology Letters*, 83, 69-71.

Tan, L. L.; Ngiam, J. J.; Sim, E. S. Z.; Conway, P. L. & Loo, S. C. J. (2022): *Liquorilactobacillus satsumensis* from water kefir yields α-glucan polysaccharides with prebiotic and synbiotic qualities. *Carbohydrate Polymers,* 290, 119515.

Tang, X.; Liu, N.; Huang, W.; Cheng, X.; Wang, F.; Zhang, B.; Chen, J.; Jiang, H.; Omedi, J. O. & Li, Z. (2018): Syneresis rate, water distribution, and microstructure of wheat starch gel during freeze-thaw process: Role of a high molecular weight dextran produced by *Weissella confusa* QS 813 from traditional sourdough. *Cereal Chemistry,* 95, 117–129.

Taylan, O.; Yilmaz, M. T. & Dertli, E. (2019): Partial characterization of a levan type exopolysaccharide (EPS) produced by *Leuconostoc mesenteroides* showing immunostimulatory and antioxidant activities. *International Journal of Biological Macromolecules,* 136, 436–444.

Taylor, C.; Cheetham, N. W. & Walker, G. J. (1985): Application of high-performance liquid chromatography to a study of branching in dextrans. *Carbohydrate Research,* 137, 1–12.

Tieking, M.; Ehrmann, M. A.; Vogel, R. F. & Gänzle, M. G. (2005): Molecular and functional characterization of a levansucrase from the sourdough isolate *Lactobacillus sanfranciscensis* TMW 1.392. *Applied Microbiology and Biotechnology,* 66, 655–663.

Tingirikari, J. M. R.; Kothari, D. & Goyal, A. (2014): Superior prebiotic and physicochemical properties of novel dextran from *Weissella cibaria* JAG8 for potential food applications. *Food & Function,* 5, 2324–2330.

Tsumori, H. & Kuramitsu, H. (1997): The role of the *Streptococcus mutans* glucosyl-transferases in the sucrose-dependent attachment to smooth surfaces: essential role of the GtfC enzyme. *Oral Microbiology and Immunology,* 12, 274–280.

Tsumori, H.; Shimamura, A.; Sakurai, Y. & Yamakami, K. (2011): Substrate specificity of mutanase of *Paenibacillus humicus* from fermented food. *Journal of Health Science,* 57, 78–81.

Tsumuraya, Y. & Misaki, A. (1979): Structure of the water-insoluble α-D-glucan of *Strepto-coccus salivarius* HHT. *Carbohydrate Research,* 74, 217–225.

Ua-Arak, T.; Jakob, F. & Vogel, R. F. (2017): Fermentation pH modulates the size distributions and functional properties of *Gluconobacter albidus* TMW 2.1191 levan. *Frontiers in Microbiology,* 8, 807.

Vacca-Smith, A. M.; Venkitaraman, A. R.; Quivey, R. G. & Bowen, W. H. (1996): Interactions of *streptococcal* glucosyltransferases with a-amylase and starch on the surface of saliva-coated hydroxyapatite. *Archives of Oral Biology,* 41, 291–298.

Vallejo-García, L. C.; Rodríguez-Alegría, M. E. & López Munguía, A. (2019): Enzymatic process yielding a diversity of inulin-type microbial fructooligosaccharides. *Journal of Agricultural and Food Chemistry,* 67, 10392–10400.

van den Ende, W. (2013): Multifunctional fructans and raffinose family oligosaccharides. *Frontiers in Plant Science,* 4, 247.

van Geel-Schutten, G. H.; Faber, E. J.; Smit, E.; Bonting, K.; Smith, M. R.; ten Brink, B.; Kamerling, J. P.; Vliegenthart, J. F. & Dijkhuizen, L. (1999): Biochemical and structural characterization of the glucan and fructan exopolysaccharides synthesized by the *lactobacillus reuteri* wild-type strain and by mutant strains. *Applied and Environmental Microbiology,* 65, 3008–3014.

van Hijum, S.; van der Maarel, M. & Dijkhuizen, L. (2003): Kinetic properties of an inulosucrase from *Lactobacillus reuteri* 121. *FEBS Letters,* 534, 207–210.

van Hijum, S. A. F. T.; Kralj, S.; Ozimek, L. K.; Dijkhuizen, L. & van Geel-Schutten, I. G. H. (2006): Structure-function relationships of glucansucrase and fructansucrase enzymes from lactic acid bacteria. *Microbiology and molecular biology reviews,* 70, 157–176.

van Hijum, S. A. F. T.; Szalowska, E.; van der Maarel, M. J. E. C. & Dijkhuizen, L. (2004): Biochemical and molecular characterization of a levansucrase from *Lactobacillus reuteri*. *Microbiology,* 150, 621–630.

van Hijum, S. A. F. T.; van Geel-Schutten, G. H.; Rahaoui, H.; van der Maarel, M. J. E. C. & Dijkhuizen, L. (2002): Characterization of a novel fructosyltransferase from *Lactobacillus reuteri* that synthesizes high-molecular-weight inulin and inulin oligosaccharides. *Applied and Environmental Microbiology,* 68, 4390–4398.

van Leeuwen, S. S.; Kralj, S.; Eeuwema, W.; Gerwig, G. J.; Dijkhuizen, L. & Kamerling, J. P. (2009): Structural characterization of bioengineered α-D-glucans produced by mutant glucansucrase GTF180 enzymes of *Lactobacillus reuteri* strain 180. *Biomacromolecules,* 10, 580–588.

van Leeuwen, S. S.; Kralj, S.; van Geel-Schutten, I. H.; Gerwig, G. J.; Dijkhuizen, L. & Kamerling, J. P. (2008a): Structural analysis of the α-D-glucan (EPS180) produced by the *Lactobacillus reuteri* strain 180 glucansucrase GTF180 enzyme. *Carbohydrate Research,* 343, 1237–1250.

van Leeuwen, S. S.; Leeflang, B. R.; Gerwig, G. J. & Kamerling, J. P. (2008b): Development of a ^{1}H NMR structural-reporter-group concept for the primary structural characterisation of α-D-glucans. *Carbohydrate Research,* 343, 1114–1119.

van Leeuwen, S. S.; Kralj, S.; Gerwig, G. J.; Dijkhuizen, L. & Kamerling, J. P. (2008c): Structural analysis of bioengineered α-D-glucan produced by a triple mutant of the glucansucrase GTF180 enzyme from *Lactobacillus reuteri* strain 180: generation of (α1→4) linkages in a native (1→3)(1→6)-α-D-glucan. *Biomacromolecules*, 9, 2251-2258.

Vettori, M. H. P. B.; Mukerjea, R. & Robyt, J. F. (2011): Comparative study of the efficacies of nine assay methods for the dextransucrase synthesis of dextran. *Carbohydrate Research,* 346, 1077–1082.

Virgen-Ortíz, J. J.; Ibarra-Junquera, V.; Escalante-Minakata, P.; Ornelas-Paz, J. d. J.; Osuna-Castro, J. A. & González-Potes, A. (2015): Kinetics and thermodynamic of the purified dextranase from *Chaetomium erraticum*. *Journal of Molecular Catalysis B: Enzymatic,* 122, 80–86.

Visnapuu, T.; Mardo, K.; Mosoarca, C.; Zamfir, A. D.; Vigants, A. & Alamäe, T. (2011): Levansucrases from *Pseudomonas syringae* pv. tomato and *P. chlororaphis* subsp. *aurantiaca*: substrate specificity, polymerizing properties and usage of different acceptors for fructosylation. *Journal of Biotechnology,* 155, 338–349.

Volkov, P. V.; Gusakov, A. V.; Rubtsova, E. A.; Rozhkova, A. M.; Matys, V. Y.; Nemashkalov, V. A. & Sinitsyn, A. P. (2019): Properties of a recombinant GH49 family dextranase heterologously expressed in two recipient strains of *Penicillium* species. *Biochimie,* 157, 123–130.

Vuillemin, M.; Claverie, M.; Brison, Y.; Séverac, E.; Bondy, P.; Morel, S.; Monsan, R.; Moulis, C. & Remaud-Siméon, M. (2016): Characterization of the first α-(1→3) branching sucrases of the GH70 family. *Journal of Biological Chemistry*, 291, 7687-7702.

Vuillemin, M.; Grimaud, F.; Claverie, M.; Rolland-Sabaté, A.; Garnier, C.; Lucas, P.; Monsan, P.; Dols-Lafargue, M.; Remaud-Siméon, M. & Moulis, C. (2018): A dextran with unique rheological properties produced by the dextransucrase from *Oenococcus kitaharae* DSM 17330. *Carbohydrate Polymers,* 179, 10–18.

Vujicic-Zagar, A.; Pijning, T.; Kralj, S.; López, C. A.; Eeuwema, W.; Dijkhuizen, L. & Dijkstra, B. W. (2010): Crystal structure of a 117 kDa glucansucrase fragment provides insight into evolution and product specificity of GH70 enzymes. *Proceedings of the National Academy of Sciences,* 107, 21406–21411.

Waldherr, F. W.; Meissner, D. & Vogel, R. F. (2008): Genetic and functional characterization of *Lactobacillus panis* levansucrase. *Archives of Microbiology,* 190, 497–505.

Walker, G. J. & Dewar, M. D. (1975): The action pattern of *Penicillium lilacinum* dextranase. *Carbohydrate Research,* 39, 303–315.

Wanda, S. Y. & Curtiss, R. (1994): Purification and characterization of *Streptococcus sobrinus* dextranase produced in recombinant *Escherichia coli* and sequence analysis of the dextranase gene. *Journal of Bacteriology,* 176, 3839–3850.

Wang, T.; Deng, L.; Li, S. & Tan, T. (2007): Structural characterization of a water-insoluble (1→3)-α-D-glucan isolated from the *Penicillium chrysogenum*. *Carbohydrate Polymers*, 67, 133-137.

Wang, H.; Lin, Q.; Liu, M.; Ding, W.; Weng, N.; Ni, H.; Lu, J.; Lyu, M. & Wang, S. (2023): Molecular docking and site-directed mutagenesis of GH49 family dextranase for the preparation of high-degree polymerization isomaltooligosaccharide. *Biomolecules,* 13, 300.

Wang, T. & Hong, M. (2016): Solid-state NMR investigations of cellulose structure and interactions with matrix polysaccharides in plant primary cell walls. *Journal of Experimental Botany,* 67, 503–514.

Wang, Y.; Maina, N. H.; Coda, R. & Katina, K. (2021): Challenges and opportunities for wheat alternative grains in breadmaking: *Ex-situ-* versus *in-situ*-produced dextran. *Trends in Food Science & Technology,* 113, 232–244.

Wangpaiboon, K.; Waiyaseesang, N.; Panpetch, P.; Charoenwongpaiboon, T.; Nepogodiev, S. A.; Ekgasit, S.; Field, R. A. & Pichayangkura, R. (2020): Characterisation of insoluble α-1,3-/α-1,6 mixed linkage glucan produced in addition to soluble α-1,6-linked dextran by glucansucrase (DEX-N) from *Leuconostoc citreum* ABK-1. *International Journal of Biological Macromolecules,* 152, 473–482.

Wenham, D. G.; Davies, R. M. & Cole, J. A. (1981): Insoluble glucan synthesis by mutansucrase as a determinant of the cariogenicity of *Streptococcus mutans*. *Journal of general Microbiology,* 127, 407–415.

Wiater, A.; Choma, A. & Szczodrak, J. (1999): Insoluble glucans synthesized by cariogenic *streptococci*: a structural study. *Journal of Basic Microbiology,* 39, 265–273.

Wiater, A.; Pleszczyńska, M.; Próchniak, K. & Szczodrak, J. (2012): Structural diversity of *streptococcal* mutans synthesized under different culture and environmental conditions and its effect on mutanase synthesis. *Molecules,* 17, 11800–11815.

Wiater, A.; Szczodrak, J.; Pleszczynska, M. & Próchniak, K. (2005): Production and use of mutanase from *Trichoderma harzianum* for effective degradation of *streptococcal* mutans. *Brazilian Journal of Microbiology,* 36.

Wu, F. C.; Chou, S. Z. & Shih, I. L. (2013): Factors affecting the production and molecular weight of levan of *Bacillus subtilis* natto in batch and fed-batch culture in fermenter. *Journal of the Taiwan Institute of Chemical Engineers,* 44, 846–853.

Wünsche, J. & Schmid, J. (2023): Acetobacteraceae as exopolysaccharide producers: Current state of knowledge and further perspectives. *Frontiers in Bioengineering and Biotechnology*, 11, 1166618.

Wuerges, J.; Caputi, L.; Cianci, M.; Boivin, S.; Meijers, R. & Benini, S. (2015): The crystal structure of *Erwinia amylovora* levansucrase provides a snapshot of the products of sucrose hydrolysis trapped into the active site. *Journal of Structural Biology,* 191, 290–298.

Xu, M.; Pan, L.; Wang, B.; Zou, X.; Zhang, A.; Zhou, Z. & Han, Y. (2023): Simulated digestion and fecal fermentation behaviors of levan and its impacts on the gut microbiota. *Journal of Agricultural and Food Chemistry,* 71, 1531–1546.

Xu, M.; Pan, L.; Zhou, Z. & Han, Y. (2022a): Structural characterization of levan synthesized by a recombinant levansucrase and its application as yogurt stabilizers. *Carbohydrate Polymers,* 291, 119519.

Xu, R. R.; Yang, W. D.; Niu, K. X.; Wang, B. & Wang, W. M. (2018a): An update on the evolution of glucosyltransferase (Gtf) genes in *Streptococcus*. *Frontiers in Microbiology,* 9, 2979.

Xu, W.; Liu, Q.; Bai, Y.; Yu, S.; Zhang, T.; Jiang, B. & Mu, W. (2018b): Physicochemical properties of a high molecular weight levan from *Brenneria* sp. EniD312. *International Journal of Biological Macromolecules,* 109, 810–818.

Xu, W.; Ni, D.; Hou, X.; Pijning, T.; Guskov, A.; Rao, Y. & Mu, W. (2022b): Crystal structure of levansucrase from the gram-negative bacterium *Brenneria p*rovides insights into its product size specificity. *Journal of Agricultural and Food Chemistry,* 70, 5095–5105.

Xu, W.; Ni, D.; Zhang, W.; Guang, C.; Zhang, T. & Mu, W. (2019): Recent advances in levansucrase and inulosucrase: Evolution, characteristics, and application. *Critical Reviews in Food Science and Nutrition,* 59, 3630–3647.

Yakushiji, T.; Koga, T. & Inoue, M. (1981): Morphology of water-insoluble and -soluble glucans of the dental plaque organism *Streptococcus mutans* AHT and their interaction with the cell surface envelope. *Archives of Oral Biology,* 26, 931–937.

Yassunaka Hata, N. N.; Surek, M.; Sartori, D.; Serrato, R. V. & Spinosa, W. A.(2023): Role of acetic acid bacteria in food and beverages. *Food Technology and Biotechnology*, 61, 85–103.

Yi, L.; Sun, X.; Du, K.; Ouyang, Y.; Wu, C.; Xu, N.; Linhardt, R. J. & Zhang, Z. (2015): UP-HILIC-MS/MS to determine the action pattern of *Penicillium* sp. dextranase. *Journal of the American Society for Mass Spectrometry,* 26, 1174–1185.

Yokoyama, W.; Renner-Nantz, J. J. & Shoemaker, C. F. (1998): Starch molecular mass and size by size-exclusion chromatography in DMSO-LiBr coupled with multiple angle laser light scattering. *Cereal Chemistry,* 75, 530–535.

Yousefi-Mokri, M.; Sharafi, A.; Rezaei, S.; Sadeghian-Abadi, S.; Imanparast, S.; Mogharabi-Manzari, M.; Amanzadeh, Y. & Faramarzi, M. A. (2019): Enzymatic hydrolysis of inulin by an immobilized extremophilic inulinase from the halophile bacterium *Alkalibacillus filiformis*. *Carbohydrate Research,* 483, 107746.

Zannini, E.; Waters, D. M.; Coffey, A. & Arendt, E. K. (2016): Production, properties, and industrial food application of lactic acid bacteria-derived exopolysaccharides. *Applied Microbiology and Biotechnology,* 100, 1121–1135.

Zarour, K.; Llamas, M. G.; Prieto, A.; Rúas-Madiedo, P.; Dueñas, M. T.; de Palencia, P. F.; Aznar, R.; Kihal, M. & López, P. (2017): Rheology and bioactivity of high molecular weight dextrans synthesised by lactic acid bacteria. *Carbohydrate Polymers,* 174, 646–657.

Zhang, W.; Xu, W.; Ni, D.; Dai, Q.; Guang, C.; Zhang, T. & Mu, W. (2019): An overview of levan-degrading enzyme from microbes. *Applied Microbiology and Biotechnology,* 103, 7891–7902.

Zikmanis, P.; Brants, K.; Kolesovs, S. & Semjonovs, P. (2020): Extracellular polysaccharides produced by bacteria of the *Leuconostoc* genus. *World Journal of Microbiology and Biotechnology,* 36, 161.

8 Eigenständigkeitserklärung

Ich erkläre, dass ich diese Dissertation selbstständig und ohne fremde Hilfe verfasst, keine anderen als die von mir angegebenen Quellen und Hilfsmittel benutzt und die den benutzten Werken inhaltlich entnommenen Stellen als solche kenntlich gemacht habe. Daneben erkläre ich, dass die Dissertation bei keiner anderen Fakultät vorliegt bzw. vorgelegen hat.

Halle (Saale), 21. Mai 2024

Luise Sophia Ernst

9 Publikationen

Publikationen in Fachzeitschriften

Ernst, L.; Werner, A. & Wefers, D. (2023): Influence of ultrasonication and hydrolysis conditions in methylation analysis of bacterial homoexopolysaccharides. *Carbohydrate Polymers*, 308, 120643, https://doi.org/10.1016/j.carbpol.2023.120643.

Ernst, L.; Schulz, C.; Petzold, A.; Thurn-Albrecht, T.; Saalwächter, K. & Wefers, D. (2024): Detailed structural characterization of five water-insoluble α-glucans produced by glucansucrases from *Streptococcus* spp. *Carbohydrate Polymers*, 337, 122164, https://doi.org/10.1016/j.carbpol.2024.122164.

Ernst, L.; Offermann, H.; Werner, A. & Wefers, D. (2024): Comprehensive structural characterization of water-soluble and water-insoluble homoexopolysaccharides from seven lactic acid bacteria. *Carbohydrate Polymers*, 323, 121417, https://doi.org/10.1016/j.carbpol.2023.121417.

Sarang, S.; Ernst, L.; Wefers, D. & Kulkarni, R. (2024): Characterization of a novel inulosucrase from *Lactiplantibacillus plantarum*. *Food Chemistry*, 453, 139597, https://doi.org/10.1016/j.foodchem.2024.139597.

Härer, L.; Ernst, L.; Bechtner, J.; Wefers, D. & Ehrmann, M. A. (2023): Glycoside hydrolase family 32 enzymes from *Bombella* spp. catalyze the formation of high molecular weight fructans from sucrose. *Journal of Applied Microbiology,* 134, lxad268, https://doi.org/10.1093/jambio/lxad268.

Vorträge auf Fachtagungen

Ernst, L.; Offermann, H.; Werner, A. & Wefers, D. Untersuchung fermentativ hergestellter Homoexopolysaccharide von Milchsäurebakterien. 32. Arbeitstagung des Regionalverbands Südost der Lebensmittelchemischen Gesellschaft, **23.03.2023**, Halle (Saale), 10.1002/lemi.202352078.

Ernst L.; Offermann H.; Schulz C.; Werner A.; Müller O. & Wefers D. Synthesis and structural characterization of water insoluble α-glucans from lactic acid bacteria. 8th EPNOE International Polysaccharide Conference, **19.09.2023**, Graz (Österreich).

Posterbeiträge auf Fachtagungen

Ernst, L.; Werner, A. & Wefers, D. Anpassung der Methylierungsanalyse für verschiedene bakterielle Homoexopolysaccharide. 50. Deutscher Lebensmittelchemikertag, **19.-21.09.2022**, Hamburg, 10.1002/lemi.202259102.

Ernst, L.; Schulz, C. & D. Wefers. Strukturen wasserunlöslicher, durch *Streptococcus*-Glucansucrasen synthetisierter α-Glucane. 51. Deutsche Lebensmittelchemietage, **21.-23.08.2023**, Bonn, 10.1002/lemi.202359061.

Ernst, L.; Härer, L.; Bechtner, J.; Ehrmann, M. & Wefers, D. Charakterisierung der von zwei *Bombella*-Arten aus Honigbienenstöcken gebildeten Fructane. 51. Deutsche Lebensmittelchemietage, **21.-23.08.2023**, Bonn, 10.1002/lemi.202359062.

Ernst, L.; Schulz, C.; Offermann, H.; Werner, A. & Wefers, D. Enzymatic synthesis of structurally diverse water-insoluble α-glucans from sucrose. Carbohydrate Bioengineering Meeting 15, **5.-8.05.2024**, Gent (Belgien).

Publikation: _Carbohydrate Polymers_, 308, 120643

Influence of ultrasonication and hydrolysis conditions in methylation analysis of bacterial homoexopolysaccharides

Luise Ernst , Annemarie Werner , Daniel Wefers [*]

Institute of Chemistry, Food Chemistry - Functional Food, Martin Luther University Halle-Wittenberg, 06120 Halle (Saale), Germany

ARTICLE INFO

ABSTRACT

Homoexopolysaccharides (HoEPS) such as α-glucans and β-fructans are synthesized by lactic and acetic acid bacteria. Methylation analysis is an important and well-established tool for the structural analysis of these polysaccharides, however, multiple steps are required for polysaccharide derivatization. Because ultrasonication during methylation and the conditions during acid hydrolysis may influence the results, we investigated their role in the analysis of selected bacterial HoEPS. The results reveal that ultrasonication is crucial for water insoluble α-glucan to swell/disperse and deprotonate prior to methylation whereas it is not necessary for water soluble HoEPS (dextran and levan). Complete hydrolysis of permethylated α-glucans requires 2 M trifluoroacetic acid (TFA) for 60/90 min at 121 °C while levan is hydrolyzed in 1 M TFA for 30 min at 70 °C. Nevertheless, levan was also detectable after hydrolysis in 2 M TFA at 121 °C. Thus, these conditions can be used to analyze a levan/ dextran mixture. However, size exclusion chromatography of permethylated and hydrolyzed levan showed degradation and condensation reactions at harsher hydrolysis conditions. Application of reductive hydrolysis with 4-methylmorpholine-borane and TFA did not lead to improved results. Overall, our results demonstrate that conditions used for methylation analysis have to be adjusted for the analysis of different bacterial HoEPS.

1. Introduction

The most important bacterial homoexopolysaccharides (HoEPS) are α-glucans and β-fructans which are enzymatically synthesized by glucansucrases and fructansucrases from sucrose (Leemhuis et al., 2013; Meng et al., 2016; van Hijum et al., 2006; Xu et al., 2019). The most common α-glucan is dextran, which is composed of a backbone of 1,6-linked D-glucopyranoses (Glc_p_) with ramifications at different positions (Monsan et al., 2001; Zannini et al., 2016). Usually dextran is water soluble, however, completely linear α-1,6-linked glucan is water insoluble (Padmanabhan et al., 2003; Pittrof et al., 2021). Furthermore, glucans containing sequences of α-1,3-linked Glc_p_, so-called mutans, are also found to be water insoluble (Côté & Leathers, 2009). β-D-Fructans are mostly water soluble and classified into levan (2,6-linked fructofuranoses (Fru_f_)) and inulin (1,2-linked Fru_f_) (Zannini et al., 2016). Levan and inulin may also be branched at position _O_1 or position _O_6, respectively. To understand the physicochemical properties of bacterial HoEPS, it is important to elucidate their molecular structure.

One part of a complete polysaccharide characterization is the examination of glycosidic linkages by using methylation analysis, which is based on the analysis of partially methylated alditol acetates (PMAAs) by gas chromatography (GC). Polysaccharides are converted into PMAAs by methylation, hydrolysis, reduction with concomitant deuterium labelling of the anomeric carbon atoms, and acetylation. Methylation analysis has its origins in the alkylation procedures of Purdie and Irvine (1903) and Haworth (1915), which were improved by Hakamori (1964) and optimized by Ciucanu and Kerek (1984) in terms of higher permethylation yields. Identification of PMAAs by mass spectrometry (MS) after GC separation was introduced by Björndal et al. (1967) and a one-tube derivatization procedure was developed by Harris et al. (1984). Today, methylation analysis is still a valuable method for the identification and semiquantitative determination of glycosidic linkages (Pettolino et al., 2012; Sims et al., 2018).

A complete permethylation of the analyzed polysaccharides is a

Publikation: *Carbohydrate Polymers*, 308, 120643

L. Ernst et al.

crucial step to obtain meaningful results. Available methylation procedures are diverse and depend on the type of polysaccharide (Ciucanu, 2006; Hanisch, 1994; Jay, 1996). Methylation according to Ciucanu and Kerek (1984) is most commonly used for uncharged polysaccharides. This procedure involves the addition of powdered $NaOH_{(s)}$ and methyl iodide to a solution of the polysaccharide sample in DMSO. To overcome carbohydrate oxidation during methylation, treatment of the polysaccharide with $NaOH_{(s)}$ prior to addition of methyl iodide is important (Needs & Selvendran, 1993). Many authors use ultrasonic treatment for better swelling/dissolution of the polysaccharide and better dispersion of $NaOH_{(s)}$ in DMSO (Fels et al., 2018; Needs & Selvendran, 1993; Nunes & Coimbra, 2001; Pettolino et al., 2012; Wangpaiboon et al., 2020). Unfortunately, ultrasonication is also known to induce polysaccharide degradation and a concomitant decrease of molecular weight (Basedow & Ebert, 1975; Cui & Zhu, 2021; Huang et al., 2015; Kardos & Luche, 2001).

Another critical step in methylation analysis is acid hydrolysis of the extracted and dried permethylated polysaccharides. Several protocols for cleavage of permethylated polysaccharide into partially methylated monosaccharides exist, amongst others formolysis, reductive hydrolysis, and hydrolysis in sulfuric acid or trifluoroacetic acid (TFA) (Hanisch, 1994; Jay, 1996). Hydrolysis in diluted TFA is widely used, because it offers an important practical advantage: TFA can be removed by evaporation prior to reduction with $NaBD_4$ which requires alkaline conditions (Biermann, 1988; Pettolino et al., 2012). By using 1-methylimidazole as a catalyst, the subsequent acetylation of the partially methylated alditols can then be achieved without additional transfer or evaporation steps (Blakeney et al., 1983). Polysaccharide hydrolysis is supposed to cleave all glycosidic linkages without degradation of the liberated monosaccharides. However, the rates of hydrolysis and degradation depend on the type of ring form (pyranose or furanose) as well as the type of glycosidic linkages (e.g. α- or β-glycosidic linkages). Thus, optimal conditions for hydrolysis vary depending on the polysaccharide.

For bacterial HoEPS, different hydrolysis procedures are described in the literature. Permethylated fructans were hydrolyzed with 1 M TFA for 30 min at 70 °C or 2 M TFA for 30 min at 60 °C (Carpita et al., 1991; Pollock et al., 1979) whereas permethylated glucans were hydrolyzed in 2 M TFA for 1,5–2 h at 121 °C, in 2 M TFA for 1 h at 125 °C or 2,5 M TFA for 4 h at 100 °C (Fels et al., 2018; Kralj et al., 2004; Maina et al., 2011; Wangpaiboon et al., 2018). An alternative procedure for the hydrolysis of labile monosaccharides is reductive acid hydrolysis, which can be achieved by the addition of a reducing agent such as 4-methylmorpholine-borane (MMB) to TFA hydrolysis (Garegg et al., 1988; Stevenson & Furneaux, 1991).

Based on the above considerations, we hypothesized that the results obtained from methylation analysis of bacterial HoEPS depend on the conditions used during derivatization. However, a systematic investigation of the influence of different sonication and hydrolysis procedures has not been conducted yet. Therefore, we applied different experimental conditions for methylation analysis of selected bacterial HoEPS and evaluated which conditions are suitable for their analysis.

2. Experimental

2.1. Materials

Levan was produced by fermentation of a sucrose solution with *Gluconobacter albidus* TMW 2.1191 and isolated as described by Hundschell et al. (2020). Water insoluble glucan was synthesized by glucansucrase Lc1215 from *Leuconostoc citreum* TMW 2.1194 (Münkel et al., 2019). Dextran was produced by dextransucrase from *Limosilactobacillus reuteri* TMW 1.106 (Münkel et al., 2020). The 50:50 (w/w)-mixture of levan and dextran was obtained by solubilizing 10 mg of each polysaccharide in ultrapure water, mixing and subsequent lyophilization. If not stated otherwise, all chemicals used were of "p.a." grade or

better and were purchased from Carl Roth (Karlsruhe, Germany), Merck (Darmstadt, Germany), Thermo Fisher Scientific (Waltham, MA USA) and Grüssing GmbH (Filsum, Germany).

2.2. Methylation analysis

The basic protocol for methylation analysis was based on the methylation procedure described by Ciucanu and Kerek (1984), whereas hydrolysis, reduction, and acetylation were based on the procedures described by Albersheim et al. (1967); Carpita et al. (1991) and Blakeney et al. (1983). The procedure was slightly modified as described previously (Fels et al., 2018; Nunes & Coimbra, 2001) and carried out in glass culture tubes with PTFE lined screw caps. Unless stated otherwise, all steps and incubations were carried out under air. About 1 mg of each sample was swollen in 2 mL of dimethyl sulfoxide (DMSO) overnight and subsequently sonicated for 30 min (sonication 1) in an ultrasonic bath (35 kHz, 80 W; Sonorex RK 100H, Brandelin, Berlin, Germany). Ice cubes were occasionally added to the ultrasonic bath to avoid warming of the samples. After sonication, approximately 100 mg of dry $NaOH_{(s)}$ were freshly ground under argon atmosphere and added to the sample solutions/suspensions. Samples were sonicated for 90 min (sonication 2) as described above and subsequently incubated at room temperature for 90 min. Methylation was performed by adding 1 mL of methyl iodide. The reaction mixture was sonicated in the ultrasonic bath for 30 min (sonication 3) and subsequently incubated at room temperature for 30 min. Permethylated polysaccharides were extracted by adding 3 mL of dichloromethane and 5 mL of 0.1 M sodium thiosulfate. The organic layer was washed twice with ultrapure water. The solvent was evaporated and the samples were dried in a vacuum oven at 40 °C overnight. To ensure complete methylation, the methylation procedure was repeated once. The permethylated polysaccharides were hydrolyzed by adding 2 mL of 2 M TFA for 90 min at 121 °C (glucans) and 1 M TFA for 30 min at 70 °C (levan). TFA was removed by evaporation at 60 °C and 20 mg $NaBD_4$ in 2 M aqueous NH_3 (0.3 mL) were added to the residue. The sample was incubated at room temperature for 1 h. Subsequently, the reaction was stopped by adding glacial acetic acid (0.1 mL). For acetylation 3 mL of acetic anhydride and 450 μL of 1-methylimidazole were added under ice-cooling and samples were incubated for 30 min at room temperature. After addition of 3 mL of ultrapure water, PMAAs were extracted into 5 mL of dichloromethane and washed three times with ultrapure water. Residual water was removed by freezing at −20 °C overnight and the organic phase was analyzed as described in Section 2.4.

This standard protocol was varied regarding the ultrasonic treatments and hydrolysis conditions. Different combinations of the three ultrasonic treatments shown in Fig. 1 were used. Either all three sonications were applied or sonications 1 and 2, sonication 2, sonication 3 or
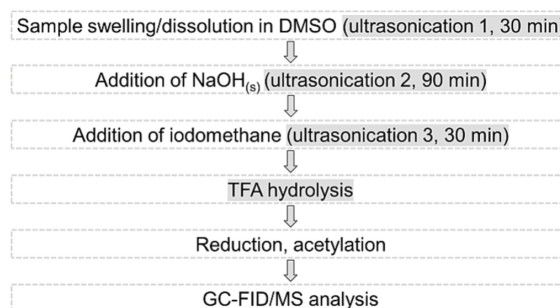
Fig. 1. Schematic derivatization protocol for methylation analysis. Parameters which were varied in this study are marked in gray. DMSO: dimethyl sulfoxide, TFA: trifluoroacetic acid, GC: gas chromatography, FID: flame ionization detector, MS: mass spectrometry.

2

Publikation: *Carbohydrate Polymers*, 308, 120643

L. Ernst et al.

all sonications steps were omitted. When sonication 1 was omitted, samples were vigorously shaken at about 3000 rpm. When sonication 2 of the sample was replaced, freshly ground $NaOH_{(s)}$ was added to 1 mL of DMSO in a separate tube and sonicated for 90 min. The obtained slurry was added to the sample which was dissolved/swollen in 1 mL instead of 2 mL of DMSO. Afterwards the sample with added NaOH dispersion was incubated at room temperature for 90 min. Sonication 3 was replaced by incubating at room temperature for the same duration. To investigate the influence of different hydrolysis conditions, TFA concentration, duration and temperature were varied: 1 M TFA was used at 70 °C for 30 min or at 121 °C for 90 min; 2 M TFA was used at 121 °C for 60 or 90 min; 3 M TFA at 121 °C for 90 min was solely used to hydrolyze the mixture of dextran and levan. All analyses were performed in duplicate.

2.3. Reductive hydrolysis of levan

Samples were methylated as described in the initial protocol and reductively hydrolyzed according to Stevenson and Furneaux (1991): A 80 mg/mL solution of MMB in ultrapure water was freshly prepared (the solution was heated to 50 °C to dissolve MMB). Subsequently, 50 µL of MMB solution and 0.2 mL of TFA were added to the dry methylated polysaccharides. The concentration of the added TFA solution was varied to achieve different final concentrations (0.5 and 1 M TFA). The samples were heated for 5 min to 70 °C or 80 °C (depending on the subsequent hydrolysis at 70 °C or 121 °C, respectively). After cooling to room temperature another 50 µL of MMB solution were added and samples were hydrolyzed for 30 or 60 min at 70 °C or for 90 min at 121 °C. Samples were cooled to room temperature and 100 µL of MMB solution were added. The solvent was removed by evaporation at 50 °C and 150 µL of 2 M NH_3 followed by $NaBD_4$ (20 mg in 0.3 mL 2 M NH_3) were added to ensure complete reduction. After incubating the samples for 1 h at room temperature, acetylation and PMAA extraction were performed as described in Section 2.2.

2.4. Gas chromatographic analysis

PMAAs in dichloromethane were analyzed by GC–MS and GC-FID. GC–MS (HP6890 + 5973, Agilent, Santa Clara, CA, USA) equipped with a VF5-MS column (30 m × 0.25 mm i.d., film thickness 0.25 µm, Agilent) with helium as carrier gas (constant flow at 1 mL/min) was used. Injector temperature was 220 °C and splitless injection was used. The following temperature program was applied: 80 °C held for 2 min; increased with 10 °C/min to 220 °C, held for 25 min; ramped at 40 °C/min to 260 °C, held for 5 min. The transfer line was held at 270 °C and mass spectra were recorded at 70 eV electron impact in full scan. GC (HP5890, Agilent) coupled to FID (HP5850, Agilent) was run under the same conditions as described for GC–MS except that the initial oven temperature was 140 °C (for 1 min). FID temperature was 240 °C. Identification of the PMAAs was based on their characteristic fragmentation patterns, which were interpreted by comparison to literature data (Carpita et al., 1989; CCRC – Complex Carbohydrate Research Center, 2022; Sassaki et al., 2005; Sassaki & Souza, 2013). Relative quantification of the PMAAs was carried out by using the molar response factors described by Sweet et al. (1975).

2.5. High performance size exclusion chromatography of methylated and hydrolyzed levan

Levan and fructose were methylated as described in Section 2.2 with three sonications. Hydrolysis was carried out by using different TFA-concentrations, durations, and temperatures (1 M TFA at 70 °C for 10, 20 and 30 min as well as 2 M TFA at 121 °C for 30, 60 and 90 min). Subsequently, samples were cooled on ice, evaporated and washed with 500 µL of ethanol twice. The washed samples were dried overnight at 40 °C in a vacuum oven, 500 µL of DMSO were added, and samples were

shaken overnight at room temperature. The dissolved samples, as well as untreated fructose and levan were analyzed by high performance size exclusion chromatography coupled to ultraviolet and refractive index detection (HPSEC-UV-RI). An Agilent 1100 Series HPLC with variable wavelength detector (G1316A) and refractive index detector (1260 Infinity II) equipped with an DMSO-Phil-P-150 column (300 × 8 mm, 10 µm, AppliChrom, Oranienburg, Germany) was used. DMSO was used as eluent at a flow rate of 0.2 mL/min and column temperature was 75 °C. The RI detector was operated at 35 °C and UV detection was carried out at 420 nm.

3. Results and discussion

As described above, we assumed that ultrasonication and hydrolysis conditions can influence the results obtained from methylation analysis of bacterial HoEPS. To prove this hypothesis, we used three model HoEPS: A water insoluble α-glucan (produced by a recombinant glucansucrase from *Leuconostoc citreum*), a water soluble dextran (produced by a recombinant glucansucrase from *Limosilactobacillus reuteri*), and a water soluble levan (produced by fermentation with *Gluconobacter albidus*). These polysaccharides were chosen because they are representative for the types of HoEPS formed by lactic and acetic acid bacteria. During methylation analysis, ultrasonication could result in a reduction of molecular weight which would lead to higher portions of terminal units. Thus, we investigated whether an elimination of different ultrasonic treatments results in lower portions of terminal units. Furthermore, appropriate hydrolysis conditions are crucial for correct results: They should result in a complete hydrolysis of the polysaccharides with as little concomitant degradation of liberated monosaccharide units as possible. Therefore, we applied harsh conditions (2 M TFA, 121 °C for 60 and 90 min) which are usually used for all kinds of polysaccharides as well as 1 M TFA at 121 °C for 90 min and mild conditions (1 M TFA, 70 °C for 30 min) which are commonly used for fructans to elucidate how individual conditions influence reproducibility, portions of glycosidic linkages, and the ratio between terminal and branched units. The latter is usually expected to be around 1 and higher portions of terminal than branched units indicate an overestimation (Lindberg et al., 1973; Sims et al., 2018). However, higher portions of terminal units can also result from low molecular weight compounds in the polysaccharide samples or from variations in PMAA stability.

3.1. Ultrasonication

To evaluate the influence of sonication, we applied different combinations of the three ultrasonic treatments shown in Fig. 1 in methylation analysis of the three model HoEPS. The results are shown in Fig. 2 and will be discussed in the following sections.

3.1.1. Water insoluble glucan and dextran

Application of the standard protocol (three ultrasonic treatments) demonstrated that the water insoluble glucan used is composed of 60 % 1,6- and 24 % 1,3-linked Glc*p*. Terminal units account for 13 % and branched units (1,3,6-linked) for 3 %. This high portion of terminal units is most likely due to residual sucrose and/or low molecular weight glucans (Münkel et al., 2019). When different ultrasonication treatments were applied, the portions of the glycosidic linkages clearly varied. Notably, all samples which were derivatized without the second sonication treatment, show higher portions of terminal glucose units. Because the portions of branched units remained unaltered, these results indicated an overestimation of terminal units. The higher portion of terminal units may result from the fact that the low molecular weight compounds present in the sample are easily solubilized without sonication whereas the insoluble glucan is not. Therefore, application of the second ultrasonic treatment seems to be necessary for reliable results. Furthermore, the results suggest that the last ultrasonic treatment which

Publikation: *Carbohydrate Polymers*, 308, 120643

L. Ernst et al.

Fig. 2. Glycosidic linkages (mol-%) of levan (bottom), dextran (center) and water insoluble glucan (top) determined by methylation analysis. Ticks and crosses indicate the application of ultrasonic treatments 1, 2 and 3 (Fig. 1). All analyses were performed in duplicate and mean values with half range uncertainties are shown. Furthermore, schematic structures of the analyzed polysaccharides are shown. t: terminal, Glc*p*: glucopyranose, Fru*f*: fructofuranose, Numbers indicate the position of substitution in the monosaccharide unit.

is applied after addition of methyl iodide can be left out to increase reproducibility (compared to the standard protocol). Thus, dissolving and swelling of the polysaccharides seems to be of greater importance than mixing the suspension during the reaction with methyl iodide.

The results obtained for dextran by applying the standard protocol show that this polysaccharide is mainly composed of 1,6-linkages. Furthermore, 12 % of the monosaccharide units are 1,4,6-linked and a slightly higher portion of terminal units (17 %) were detected besides minor portions ($\leq$1 %) of 1,4- and 1,3,6-linked units. Applying different combinations of the three ultrasonic treatments does not seem to have an influence on the results. Neither portions of the PMAAs nor reproducibility change. Thus, chain disruption of polysaccharides, which would result in higher portions of terminal units, does not occur to a significant extent.

3.1.2. Levan

As expected, the standard protocol demonstrated that levan is mainly 2,6-linked and has about 10 % terminal and 7 % 1,2,6-linked units. The application of different ultrasonic treatments does not seem to have significant influence on the results of methylation analysis. Notably, a slightly better reproducibility is obtained by leaving out at least one of the three ultrasonic treatments. However, our results suggest that

ultrasonication is not a critical step for polysaccharides which are soluble in water and DMSO.

3.2. Hydrolysis

To completely cleave (permethylated) polysaccharides to monomers, appropriate hydrolysis conditions are crucial. Therefore, we used different hydrolysis conditions during methylation analysis of water insoluble glucan, dextran, and levan in the course of methylation analysis. The resulting portions of the glycosidic linkages are shown in Fig. 3.

3.2.1. Water insoluble glucan and dextran

The results clearly demonstrate that 2 M TFA is necessary to sufficiently hydrolyze water insoluble glucan and dextran. Here, high portions of terminal units were found after hydrolysis in 1 M TFA for 90 min at 121 °C, whereas no PMAAs were detected after mild hydrolysis with 1 M TFA for 30 min at 70 °C. Thus, it can be hypothesized that terminal units are most susceptible to hydrolysis. A kinetic study on the acid hydrolysis of dextran also showed that small molecules are preferably released, because glycosidic bonds near the ends of the polysaccharides have a higher reactivity than those in the center (Basedow et al., 1978). However, the increased portions of terminal units at mild hydrolysis
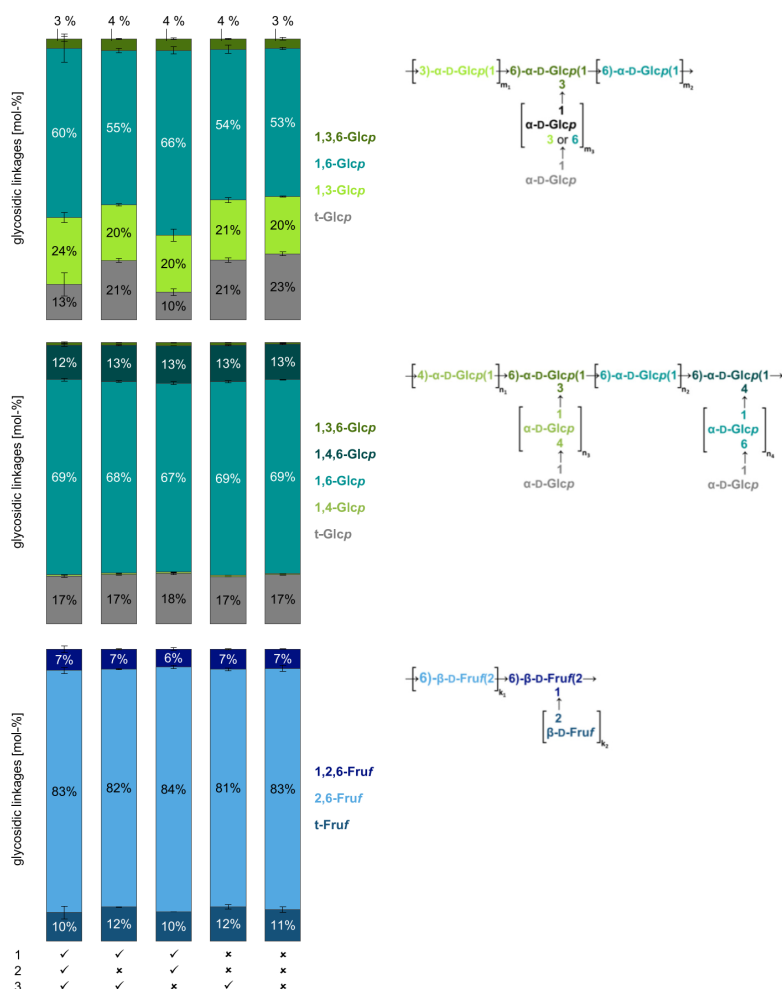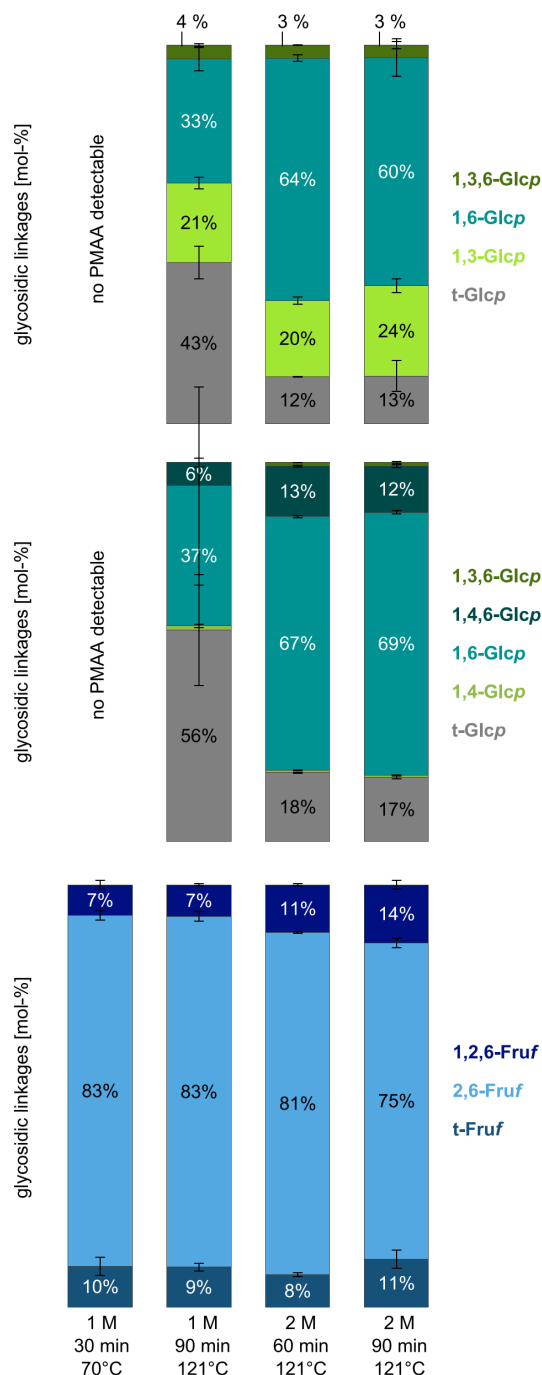
Publikation: *Carbohydrate Polymers*, 308, 120643

Fig. 3. Glycosidic linkages (mol-%) of levan (bottom), dextran (center) and water insoluble glucan (top) determined by methylation analysis. The application of different TFA concentrations (M), durations (min), and temperatures (°C) during hydrolysis is indicated below the bars. All analyses were performed in duplicate and mean values with half range uncertainties are shown. t: terminal, Glc*p*: glucopyranose, Fru*f*: fructofuranose, Numbers indicate the position of substitution in the monosaccharide unit.

conditions may also result from the hydrolysis of low molecular weight compounds.

When 2 M TFA was used, a higher portion of 1,3-linkages is observed in water insoluble glucan after 90 min instead of 60 min. This could be explained by a higher resistance of 1,3-linkages compared to 1,6-linkages, but this remains speculation at this point. For dextran, the application of 2 M TFA yields almost the same portions of glycosidic linkages for both durations of hydrolysis which indicates that degradation of the liberated partially methylated alditol acetates does not influence the results.

3.2.2. Levan

Because their glycosidic bonds are less stable, fructans are usually hydrolyzed by using milder conditions to avoid destruction of liberated fructose units (Biermann, 1988; Carpita et al., 1991). However, in expectation of glucose residues in inulin or levan, harsher conditions, e. g. 2 M TFA for 2 h at 110 °C, are sometimes used (Zhang et al., 2013). In our study, portions of the glycosidic linkages and reproducibility remained unchanged after application of 1 M TFA for 30 min at 70 °C or 90 min at 121 °C. However, increasing the TFA concentration to 2 M caused increased portions of branched units which were even higher than the portions of terminal fructose units. This ratio cannot result from the polysaccharide structure (every ramification needs to end with a terminal unit), thus, our results show that the PMAAs representing terminal fructose units are lost when harsh hydrolysis conditions are applied. This could result from a preferred hydrolysis (also indicated by our results for glucans) and a subsequent degradation of the liberated partially methylated monosaccharides. This assumption is supported by the detection of additional peaks in the GC chromatogram after hydrolysis with 2 M TFA for 90 min at 121 °C (and by the results reported in the following section). However, to obtain information about the polysaccharide structure, the ratio between 2,6-Fru*f* and 1,2,6-Fru*f* is more important than the portion of terminal units. Because it is unclear whether the levan backbone is completely hydrolyzed with 1 M or 2 M TFA, we analyzed methylated and hydrolyzed levan by HPSEC-UV-RI.

3.2.2.1. HPSEC-UV-RI of methylated and hydrolyzed levan.

To analyze the degree of hydrolysis and degradation reactions, levan was methylated and hydrolyzed by using 1 M TFA at 70 °C (for 10 min, 20 min and 30 min) and 2 M TFA at 121 °C (for 30 min, 60 min and 90 min). Furthermore, fructose was methylated and treated with 1 M TFA at 70 °C for 30 min to gain information about the elution pattern derived from degradation of methylated fructose. Untreated fructose and levan were analyzed as elution time standards.

The samples were optically different when dissolved in DMSO for HPSEC analysis: Solutions were colorless after mild hydrolysis with 1 M TFA at 70 °C, whereas beige to brown solutions were obtained when TFA concentration, duration, and temperature increased. Therefore, UV detection was used to specifically detect chromophoric reaction products besides the universal RI detection. It was expected that incomplete hydrolysis leads to residual early-eluting high molecular weight compounds whereas complete hydrolysis leads to later-eluting low molecular weight compounds.

The results of the HPSEC-UV-RI analysis are shown in Fig. 4. Methylated, acid-treated fructose yielded a rather broad RI elution pattern at a similar retention volume than untreated fructose. As expected for hydrolyzed polysaccharides, all samples contained compounds eluting at this volume while early eluting compounds were absent or of low abundance. Although slight variations can be seen in the intensity of the earlier-eluting peaks, these results indicate that the high molecular weight part of levan is hydrolyzed in all samples.

However, although it was expected that increases in TFA concentration, duration, and temperature lead to reduced/increased intensities for the polysaccharide/monosaccharide peaks in the RI elugrams, harsher hydrolysis conditions (2 M TFA and 121 °C) led to a higher
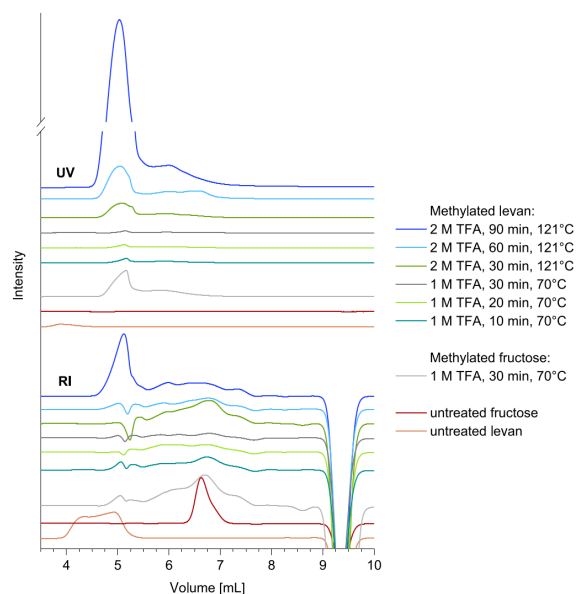
5

Publikation: *Carbohydrate Polymers*, 308, 120643

L. Ernst et al.

Fig. 4. HPSEC-UV-RI elugrams of levan and fructose (not methylated and hydrolyzed) and of methylated fructose and methylated levan after different hydrolysis procedures (TFA concentration, duration and temperature). UV detection was carried out at 420 nm. RI: refractive index, UV: ultraviolet, TFA: trifluoroacetic acid.

portion of polymeric material. This suggests the occurrence of a polymerization reaction. The UV elugrams at 420 nm confirmed that its products are responsible for the brown color observed when dissolving the samples. Furthermore, significant portions of these chromophoric compounds can be detected in all levan samples hydrolyzed with 2 M TFA at 121 °C, although the peak intensity increases with the incubation time. In contrast, levan samples hydrolyzed at mild conditions contain clearly less of these UV-absorbing products than those hydrolyzed at harsh conditions. Notably, some high molecular weight products are also observed after methylation of fructose and subsequent treatment with 1 M TFA for 30 min at 70 °C (RI and UV signal). This demonstrates that the formation of these compounds is not specific for harsh conditions, but for the exposure of (partially) methylated monosaccharides to acid and high temperatures. The formation of UV-absorbing, polymeric compounds is most likely the result of condensation and dehydration (Kent, 1953; Krol, 1978; Silberman, 1961). However, reaction products of methylated fructans/methylated fructose in acidic environments have not been described in the literature yet. Therefore, the polymerization reaction occurring during TFA hydrolysis of methylated levan could be subject of future research.

Our results confirm that levan is effectively hydrolyzed by the acid treatments used and that partially methylated fructose which is liberated during hydrolysis contributes to the formation of high molecular weight products. Therefore, these compounds cannot be avoided during acid hydrolysis. Hydrolysis with 1 M TFA at 70 °C for 20 or 30 min is well suited for levan analysis, because only low amounts of polymeric material were detected by RI and UV. An approach to avoid decomposition of liberated partially methylated monosaccharides could be to hydrolyze under reductive conditions. This approach is supposed to reduce liberated partially methylated monosaccharides to their corresponding alditols which are more stable in the acidic environment. To evaluate if this approach yields improved results for methylated levan, we used the reductive hydrolysis procedure described by Stevenson and Furneaux (1991).

3.2.2.2. Reductive hydrolysis in methylation analysis of levan. The formation of polymeric products could be hindered by immediate reduction of the anomeric carbon of liberated permethylated fructose which results in a stabilization. Therefore, this approach could also reduce overestimation of branched units after hydrolysis with 2 M TFA. Reduction during acid hydrolysis in situ can be achieved by MMB (Garegg et al., 1988; Stevenson & Furneaux, 1991). Based on the previously described protocol, different conditions were selected for reductive hydrolysis of levan (0.5 M final TFA concentration at 70 °C for 30 and 60 min and at 121 °C for 90 min as well as 1 M final TFA concentration at 70 °C for 30 and 60 min). However, initial experiments showed that the MMB treatments applied did not result in a complete reduction of partially methylated monosaccharides. Therefore, the hydrolyzed samples were subsequently treated with $NaBD_4$ to achieve complete reduction. By using this approach, deuteration can be used to differentiate between PMAAs resulting from MMB reduction and those reduced by $NaBD_4$. The results obtained from the application of reductive hydrolysis with subsequent $NaBD_4$ reduction are shown in Fig. 5.

After hydrolysis with 0.5 M TFA for 30 min at 70 °C, a clearly elevated portion of terminal units is observed which is most likely the result of incomplete hydrolysis. Hydrolysis of levan with 0.5 M TFA for 60 min at 70 °C resulted in portions of glycosidic linkages similar to those obtained with 1 M TFA for 30 min at 70 °C without using MMB (Fig. 3). In contrast, samples hydrolyzed with 1 M TFA for 30 or 60 min at 70 °C and with 0.5 M TFA for 90 min at 121 °C show higher portions for branched than for terminal units. These results suggest that reductive hydrolysis does not stabilize liberated terminal units sufficiently when harsher conditions are used. This observation is supported by the high portion of monosaccharides which are reduced by deuteride and not by MMB (Fig. S1). The low degree of MMB reduction could be the result of degradation of MMB in aqueous acid and/or of the reduction potential of MMB being too weak for partially methylated fructose (Stevenson & Furneaux, 1991). However, Garegg et al. (1988) reported that reduction of fructose was complete during hydrolysis of sucrose in 0.5 M TFA with
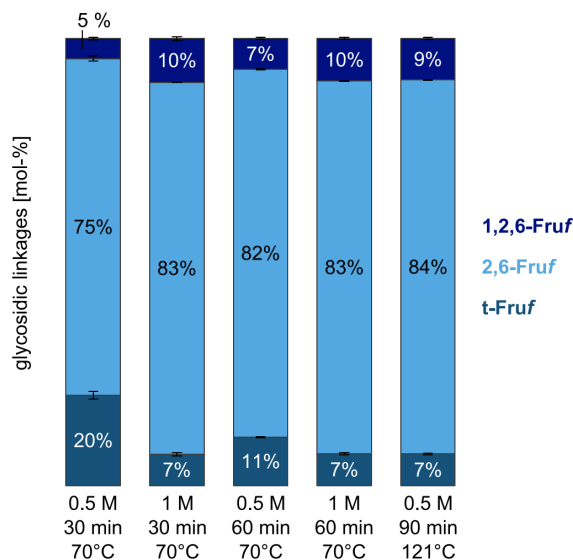
Fig. 5. Glycosidic linkages (mol-%) of levan determined by methylation analysis. The application of different TFA concentrations (M), durations (min), and temperatures (°C) during reductive hydrolysis with MMB (4-methylmorpholine-borane) is indicated below the bars. All analyses were performed in duplicate and mean values with half range uncertainties are shown. t: terminal, Fru*f*: fructofuranose, Numbers indicate the position of substitution in the monosaccharide unit.

Publikation: *Carbohydrate Polymers*, 308, 120643

L. Ernst et al.

MMB for 15 h at room temperature whereas glucose reduction was incomplete. Besides factors such as monosaccharide identity, temperature, and acid concentration (Garegg et al., 1988), permethylation is likely to influence reductions with MMB. Overall, application of reductive hydrolysis is not improving results in methylation analysis of levan under the conditions used.

3.2.3. Methylation analysis of a mixture of levan and dextran

Mixtures of dextrans and fructans may occur in exopolysaccharide isolates from some lactic acid bacteria. This complicates structural analysis because the polysaccharides require different conditions during acid hydrolysis, as seen in Sections 3.2.1 and 3.2.2. Separation of dextran and fructan would be an option, however, this step is quite work-intensive. Therefore, we analyzed a 50:50 (w/w)-mixture of levan and dextran by using methylation analysis with different hydrolysis conditions. With this approach we aimed to evaluate if the same results are obtained in the presence of another polysaccharide and if the glycosidic linkage portions resemble the overall monosaccharide composition of the mixture. Methylation analysis was performed by using 1 M TFA for 30 min at 70 °C and for 90 min at 121 °C as well as 2 M TFA at 121 °C for 60 and 90 min and 3 M TFA at 121 °C for 90 min. The comparably mild hydrolysis with 1 M TFA proved to be suitable for levan analysis (Section 3.2.2) whereas the application of 2 M TFA at 121 °C for 60/90 min was suitable for dextran (Section 3.2.1). The harsh hydrolysis conditions with 3 M TFA were applied to elucidate if glucan can be determined without detection of levan PMAAs.

Fig. 6 shows the portions of PMAAs derived from dextran and levan after methylation analysis of the mixture with different hydrolysis conditions. As expected from our previous results, only PMAAs derived from levan can be detected when mild hydrolysis conditions (1 M TFA, 30 min, 70 °C) are used. With increasing TFA concentration, duration, and temperature, increasing amounts of dextran and decreasing amounts of levan are found. At harsh conditions (2 and 3 M TFA, 90 min, 121 °C), dextrans are clearly predominant. However, low amounts of levan PMAAs can still be detected, although harsh conditions also led to the formation of detectable amounts of levan-derived degradation products.

Consequently, even harsh hydrolysis conditions can be used to

qualitatively assess fructans by methylation analysis which is in good agreement with the literature. For example, van Geel-Schutten et al. examined the exopolysaccharides of *Limosilactobacillus reuteri* LB121 by using 2 M TFA for 2 h at 120 °C in methylation analysis. In combination with monosaccharide analysis, they were able to identify levan and a branched glucan simultaneously. However, the relative amounts of glucan linkages were assessed semiquantitatively, whereas fructan was only assessed qualitatively (van Geel-Schutten et al., 1999). Ravenscroft et al. (2009) analyzed a fructan oligosaccharide with single glucosyl units in the main chain by methylation analysis with varying hydrolysis temperatures. The methylated oligosaccharides were hydrolyzed in 2 M TFA for 40 min at 60, 100 and 125 °C prior to derivatization to alditol acetates and GC–MS analysis. An increasing amount of glucose derived PMAAs was detected with increasing temperature which is in good agreement with our results.

To evaluate if the different hydrolysis procedures can be used for semiquantitative analysis, the portions of the individual glycosidic linkages were calculated for levan and dextran (Fig. 7). The results were compared to the individually analyzed polysaccharides (Fig. 3).

Levan glycosidic linkage portions determined after analysis of the mixture and hydrolysis with 1 M TFA at 70 °C for 30 min and at 121 °C for 90 min, as well as with 2 M TFA for 60 min at 121 °C were comparable to those obtained for pure levan. However, an increased portion of terminal units was observed, whereas 1,2,6-linked units were of lower abundance. Thus, the presence of dextran may slightly impede fructan hydrolysis. Nevertheless, results after hydrolysis with mild conditions still yield valuable information on levan composition. Harsher conditions (2 M TFA and 3 M TFA at 121 °C for 90 min) led to incorrect results for levan especially due to a partial coelution of PMAAs derived from 1,2,6-Fru*f* and 1,3,6-Glc*p*. Nevertheless, levan can be unambiguously identified after harsher hydrolysis conditions.

For dextran, comparable portions of glycosidic linkages are obtained for the mixture and for the pure polysaccharide when 2 M TFA at 121 °C is used for hydrolysis. Slight variations are observed when samples were hydrolyzed for 60 min, whereas the application of 90 min yielded almost identical portions of glycosidic linkages. Hydrolysis with 3 M TFA does only have a minor influence on the portions of dextran PMAAs. After milder hydrolysis conditions (1 M TFA, 121 °C for 90 min) terminal, 1,4-linked and 1,4,6-linked units are overestimated and after 1 M TFA at 70 °C for 30 min no glucan derived PMAA was detectable. This is in good agreement with the results described in Section 3.2.1. Thus, the presence of fructan only has a minor influence on the hydrolysis of dextrans.

Overall, PMAAs derived from levan can be detected together with PMAAs derived from glucan because levan is stable enough to yield some PMAAs at high TFA concentrations, durations, and temperatures. Although monosaccharide analysis after complete acid hydrolysis also yields information about the polysaccharides in the sample, methylation analysis additionally provides information about the linkage types of the monosaccharides. Thus, this method also allows for conclusions on the type of glucan or fructan. Nevertheless, monosaccharide analysis after complete hydrolysis should be performed complementary to unambiguously identify glucose and fructose and to assess their portions. Semiquantitative analysis of linkage types in each polysaccharide can be carried out by using appropriate hydrolysis conditions (2 M TFA, 60 min at 121 °C). Alternatively, glycosidic linkages can be analyzed after separation of the polysaccharides. This can for example be achieved by selective enzymatic degradation with *endo*-dextranase or *endo*-levanase, followed by dialysis of the sample.

4. Conclusion

Our results clearly confirm our hypothesis and demonstrate that sonication and hydrolysis are critical steps in the derivatization procedure of methylation analysis of bacterial HoEPS. While dextran and levan proved to be unaffected by ultrasonic treatments, sonication was crucial for water insoluble glucans to swell and deprotonate the

Fig. 6. Portions of the sum of partially methylated alditol acetates derived from dextran (terminal, 1,4-, 1,6- and 1,4,6- linked glucopyranose) and levan (terminal and 2,6-linked fructofuranose) after methylation analysis of a 50:50 (w/w) mixture of the two polysaccharides. Portions of 1,2,6-fructofuranose and 1,3,6-glucospyranose were not incorporated due to ambiguous assignment because of partial peak overlap. The application of different TFA concentrations (M), durations (min) and temperatures (°C) is indicated below the bars.
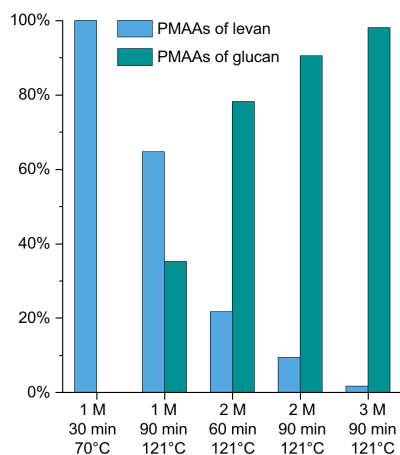
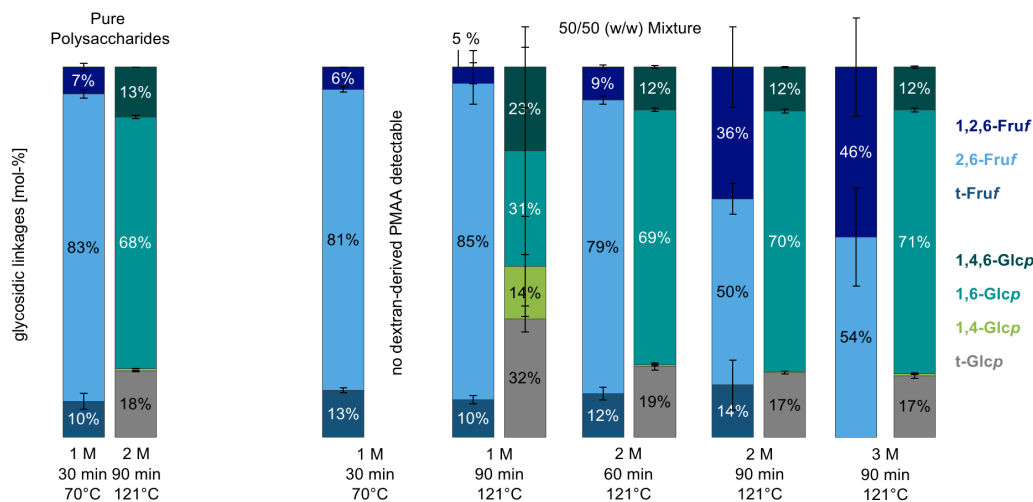Publikation: *Carbohydrate Polymers*, 308, 120643

Fig. 7. Glycosidic linkages (mol-%) of levan and dextran determined by methylation analysis of the two pure polysaccharides (left two columns) or the 50:50 (w/w)-mixture of both. Hydrolysis conditions TFA concentration (M), duration (min), and temperature (°C) are shown beneath the columns. The glycosidic linkage portions of the pure polysaccharides obtained after the application of other hydrolysis conditions are shown in Fig. 3. Due to partial peak overlap of PMAAs derived from 1,2,6-Fru*f* and 1,3,6-Glc*p* the letter was not included, because its portion is only 1 % in pure dextran.

polysaccharides prior to methylation. However, avoiding the sonication step after the addition of methyl iodide resulted in better reproducibility. Hydrolysis of glucans required 2 M TFA at 121 °C for complete hydrolysis. As expected, methylated levan can be hydrolyzed at milder conditions (1 M TFA, 70 °C, 30 min). Nevertheless, levan derived PMAAs were also detected when 2 M TFA was used in combination with longer heating times and higher temperature (121 °C), although branched units (1,2,6-Fru*f*) were overestimated and harsh conditions led to the formation of polymeric condensation products. The identity of these compounds remains unknown and should be investigated further. Reductive hydrolysis conditions with MMB can also be used, but no advantages arose from this procedure. When mixtures of levan and dextran are analyzed, 2 M TFA, 60 min, and 121 °C can be used for simultaneous identification of both polysaccharides in unknown HoEPS samples. However, semiquantitative estimation of glycosidic linkages should preferably be carried out by analyzing each polysaccharide separately.

Supplementary data to this article can be found online at https://doi.org/10.1016/j.carbpol.2023.120643.

CRediT authorship contribution statement

Luise Ernst: Conceptualization, Investigation, Methodology, Formal analysis, Validation, Visualization, Writing – original draft. **Annemarie Werner:** Investigation, Methodology, Formal analysis. **Daniel Wefers:** Conceptualization, Resources, Supervision, Writing – review & editing.

Declaration of competing interest

The authors declare that they have no known competing financial interests or personal relationships that could have appeared to influence the work reported in this paper.

Data availability

Data will be made available on request.

Acknowledgements

The authors are very grateful to Frank Jakob and Rudi Vogel from the

References

Albersheim, P., Nevins, D. J., English, P. D., & Karr, A. (1967). A method for the analysis of sugars in plant cell-wall polysaccharides by gas-liquid chromatography. *Carbohydrate Research, 5*, 340–345.
Basedow, A. M., & Ebert, K. H. (1975). Zum Mechanismus des Abbaus von Polymeren in Lösung durch Ultraschall. *Die Makromolekulare Chemie, 176*, 745–757.
Basedow, A. M., Ebert, K. H., & Ederer, H. J. (1978). Kinetic studies on the acid hydrolysis of dextran. *Macromolecules, 11*, 774–781.
Biermann, C. J. (1988). Hydrolysis and other cleavages of glycosidic linkages in polysaccharides. *Advances in Carbohydrate Chemistry and Biochemistry, 46*, 251–271.
Björndal, H., Lindberg, B., & Svensson, S. (1967). Mass spectrometry of partially methylated alditol acetates. *Carbohydrate Research, 5*, 433–440.
Blakeney, A. B., Harris, P. J., Henry, R. J., & Stone, B. A. (1983). A simple and rapid preparation of alditol acetates for monosaccharide analysis. *Carbohydrate Research, 113*, 291–299.
Carpita, N. C., Housley, T. L., & Hendrix, J. E. (1991). New features of plant-fructan structure revealed by methylation analysis and carbon-13 n.m.r. spectroscopy. *Carbohydrate Research, 217*, 127–136.
Carpita, N. C., Kanabus, J., & Housley, T. L. (1989). Linkage structure of fructans and fructan oligomers from *Triticum aestivum* and *Festuca arundinacea* leaves. *Journal of Plant Physiology, 134*, 162–168.
CCRC – Complex Carbohydrate Research Center. (2022). *The CCRC spectral database for PMAA's*. University of Georgia. https://glygen.ccrc.uga.edu/ccrc/specdb/ms/pmaa/pframe.html.
Ciucanu, I. (2006). Per-O-methylation reaction for structural analysis of carbohydrates by mass spectrometry. *Analytica Chimica Acta, 576*, 147–155.
Ciucanu, I., & Kerek, F. (1984). A simple and rapid method for the permethylation of carbohydrates. *Carbohydrate Research, 131*, 209–217.
Côté, G. L., & Leathers, T. D. (2009). Insoluble glucans from planktonic and biofilm cultures of *Leuconostoc mesenteroides* NRRL B-1355. *Applied Microbiology and Biotechnology, 82*, 149–154.
Cui, R., & Zhu, F. (2021). Ultrasound modified polysaccharides: A review of structure, physicochemical properties, biological activities and food applications. *Trends in Food Science & Technology, 107*, 491–508.
Fels, L., Jakob, F., Vogel, R. F., & Wefers, D. (2018). Structural characterization of the exopolysaccharides from water kefir. *Carbohydrate Polymers, 189*, 296–303.
Garegg, P. J., Lindberg, B., Konradsson, P., & Kvarnström, I. (1988). Hydrolysis of glycosides under reducing conditions. *Carbohydrate Research, 176*, 145–148.
Hakamori, S. (1964). A rapid permethylation of glycolipid, and polysaccharide catalyzed by methylsulfinyl carbanion in dimethyl sulfoxide. *The Journal of Biochemistry, 55*, 205–208.
Hanisch, F. G. (1994). Methylation analysis of complex carbohydrates: Overview and critical comments. *Biological Mass Spectrometry, 23*, 309–312.
Harris, P. J., Henry, R. J., Blakeney, A. B., & Stone, B. A. (1984). An improved procedure for the methylation analysis of oligosaccharides and polysaccharides. *Carbohydrate Research, 127*, 59–73.

Publikation: *Carbohydrate Polymers*, 308, 120643

Haworth, W. N. (1915). III. A new method of preparing alkylated sugars. *Journal of the Chemical Society, Transactions, 107*, 8–16.

Huang, C., Miao, M., Jiang, B., Cui, S. W., Jia, X., & Zhang, T. (2015). Polysaccharides modification through green technology: Role of ultrasonication towards improving physicochemical properties of 1,3/1,6-α-D-glucans. *Food Hydrocolloids, 50*, 166–173.

Hundschell, C. S., Braun, A., Wefers, D., Vogel, R. F., & Jakob, F. (2020). Size-dependent variability in flow and viscoelastic behavior of Levan produced by *Gluconobacter albidus* TMW 2.1191. *Foods, 9*, 192.

Jay, A. (1996). The methylation reaction in carbohydrate analysis. *Journal of Carbohydrate Chemistry, 15*, 897–923.

Kardos, N., & Luche, J.-L. (2001). Sonochemistry of carbohydrate compounds. *Carbohydrate Research, 332*, 115–131.

Kent, P. W. (1953). Chemical synthesis of hexose polymers. *The Biochemical Journal, 55*, 361–365.

Kralj, S., van Geel-Schutten, G. H., Dondorff, M. M. G., Kirsanovs, S., van der Maarel, M. J. E. C., & Dijkhuizen, L. (2004). Glucan synthesis in the genus lactobacillus: Isolation and characterization of glucansucrase genes, enzymes and glucan products from six different strains. *Microbiology, 150*, 3681–3690.

Krol, B. (1978). Condensation of fructose in acid water-solutions. *Acta Alimentaria Polonica, 04*, 287–296.

Leemhuis, H., Pijning, T., Dobruchowska, J. M., van Leeuwen, S. S., Kralj, S., Dijkstra, B. W., & Dijkhuizen, L. (2013). Glucansucrases: Three-dimensional structures, reactions, mechanism, α-glucan analysis and their implications in biotechnology and food applications. *Journal of Biotechnology, 163*, 250–272.

Lindberg, B., Lönngren, J., & Thompson, J. L. (1973). Methylation studies on levans. *Acta Chemica Scandinavica, 27*, 1819–1821.

Maina, N. H., Virkki, L., Pynnönen, H., Maaheimo, H., & Tenkanen, M. (2011). Structural analysis of enzyme-resistant isomaltooligosaccharides reveals the elongation of α-1,3-linked branches in *Weissella confusa* dextran. *Biomacromolecules, 12*, 409–418.

Meng, X., Gangoiti, J., Bai, Y., Pijning, T., van Leeuwen, S. S., & Dijkhuizen, L. (2016). Structure-function relationships of family GH70 glucansucrase and 4,6-α-glucanotransferase enzymes, and their evolutionary relationships with family GH13 enzymes. *Cellular and Molecular Life Sciences, 73*, 2681–2706.

Monsan, P., Bozonnet, S., Albenne, C., Joucla, G., Willemot, R.-M., & Remaud-Siméon, M. (2001). Homopolysaccharides from lactic acid bacteria. *International Dairy Journal, 11*, 675–685.

Münkel, F., Bechtner, J., Eckel, V., Fischer, A., Herbi, F., Jakob, F., & Wefers, D. (2019). Detailed structural characterization of glucans produced by glucansucrases from *Leuconostoc citreum* TMW 2.1194. *Journal of Agricultural and Food Chemistry, 67*, 6856–6866.

Münkel, F., Fischer, A., & Wefers, D. (2020). Structural characterization of mixed-linkage α-glucans produced by mutants of *Lactobacillus reuteri* TMW 1.106 dextransucrase. *Carbohydrate Polymers, 231*, Article 115697.

Needs, P. W., & Selvendran, R. R. (1993). An improved methylation procedure for the analysis of complex polysaccharides including resistant starch and a critique of the factors which lead to undermethylation. *Phytochemical Analysis, 4*, 210–216.

Nunes, F. M., & Coimbra, M. A. (2001). Chemical characterization of the high molecular weight material extracted with hot water from green and roasted arabica coffee. *Journal of Agricultural and Food Chemistry, 49*, 1773–1782.

Padmanabhan, P. A., Kim, D.-S., Pak, D., & Sim, S. J. (2003). Rheology and gelation of water-insoluble dextran from *Leuconostoc mesenteroides* NRRL B-523. *Carbohydrate Polymers, 53*, 459–468.

Pettolino, F. A., Walsh, C., Fincher, G. B., & Bacic, A. (2012). Determining the polysaccharide composition of plant cell walls. *Nature Protocols, 7*, 1590–1607.

Pittrof, S. L., Kaufhold, L., Fischer, A., & Wefers, D. (2021). Products released from structurally different dextrans by bacterial and fungal dextranases. *Foods, 10*, 244.

Pollock, C. J., Hall, M. A., & Roberts, D. P. (1979). Structural analysis of fructose polymers by gas-liquid chromatography and gel filtration. *Journal of Chromatography A, 171*, 411–415.

Purdie, T., & Irvine, J. C. (1903). C. The alkylation of sugars. *Journal of the Chemical Society, Transactions, 83*, 1021–1037.

Ravenscroft, N., Cescutti, P., Hearshaw, M. A., Ramsout, R., Rizzo, R., & Timme, E. M. (2009). Structural analysis of fructans from *Agave americana* grown in South Africa for spirit production. *Journal of Agricultural and Food Chemistry, 57*, 3995–4003.

Sassaki, G. L., Gorin, P. A. J., Souza, L. M., Czelusniak, P. A., & Iacomini, M. (2005). Rapid synthesis of partially *O*-methylated alditol acetate standards for GC-MS: Some relative activities of hydroxyl groups of methyl glycopyranosides on purdie methylation. *Carbohydrate Research, 340*, 731–739.

Sassaki, G. L., & Souza, L. M.d. (2013). Mass spectrometry strategies for structural analysis of carbohydrates and glycoconjugates. In A. V. Coelho, & C. de Matos Ferraz Franco (Eds.), *Tandem mass spectrometry - molecular characterization* (pp. 81–115). Croatia: InTech.

Silberman, H. C. (1961). Reactions of sugars in the presence of acids: A paper chromatographic study. *The Journal of Organic Chemistry, 26*, 1967–1969.

Sims, I. M., Carnachan, S. M., Bell, T. J., & Hinkley, S. F. R. (2018). Methylation analysis of polysaccharides: Technical advice. *Carbohydrate Polymers, 188*, 1–7.

Stevenson, T. T., & Furneaux, R. H. (1991). Chemical methods for the analysis of sulphated galactans from red algae. *Carbohydrate Research, 210*, 277–298.

Sweet, D. P., Shapiro, R. H., & Albersheim, P. (1975). Quantitative analysis by various G. L.C. Response-factor theories for partially methylated and partially ethylated alditol acetates. *Carbohydrate Research, 40*, 217–225.

van Geel-Schutten, G. H., Faber, E. J., Smit, E., Bonting, K., Smith, M. R., ten Brink, B., ... Dijkhuizen, L. (1999). Biochemical and structural characterization of the glucan and fructan exopolysaccharides synthesized by the *Lactobacillus reuteri* wild-type strain and by mutant strains. *Applied and Environmental Microbiology, 65*, 3008–3014.

van Hijum, S. A. F. T., Kralj, S., Ozimek, L. K., Dijkhuizen, L., & van Geel-Schutten, I. G. H. (2006). Structure-function relationships of glucansucrase and fructansucrase enzymes from lactic acid bacteria. *Microbiology and Molecular Biology Reviews, 70*, 157–176.

Wangpaiboon, K., Padungros, P., Nakapong, S., Charoenwongpaiboon, T., Rejzek, M., Field, R. A., & Pichyangkura, R. (2018). An α-1,6-and α-1,3-linked glucan produced by *Leuconostoc citreum* ABK-1 alternansucrase with nanoparticle and film-forming properties. *Scientific Reports, 8*, 8340.

Wangpaiboon, K., Waiyaseesang, N., Panpetch, P., Charoenwongpaiboon, T., Nepogodiev, S. A., Ekgasit, S., ... Pichayangkura, R. (2020). Characterisation of insoluble α-1,3-/α-1,6 mixed linkage glucan produced in addition to soluble α-1,6-linked dextran by glucansucrase (DEX-N) from *Leuconostoc citreum* ABK-1. *International Journal of Biological Macromolecules, 152*, 473–482.

Xu, W., Ni, D., Zhang, W., Guang, C., Zhang, T., & Mu, W. (2019). Recent advances in levansucrase and inulosucrase: Evolution, characteristics, and application. *Critical Reviews in Food Science and Nutrition, 59*, 3630–3647.

Zannini, E., Waters, D. M., Coffey, A., & Arendt, E. K. (2016). Production, properties, and industrial food application of lactic acid bacteria-derived exopolysaccharides. *Applied Microbiology and Biotechnology, 100*, 1121–1135.

Zhang, A., Zhang, Y., Yang, J., Jiang, J., Huang, F., & Sun, P. (2013). Structural elucidation of a novel water-soluble fructan isolated from *Wedelia prostrata*. *Carbohydrate Research, 376*, 24–28.

Publikation: *Carbohydrate Polymers*, 308, 120643

Supplementary
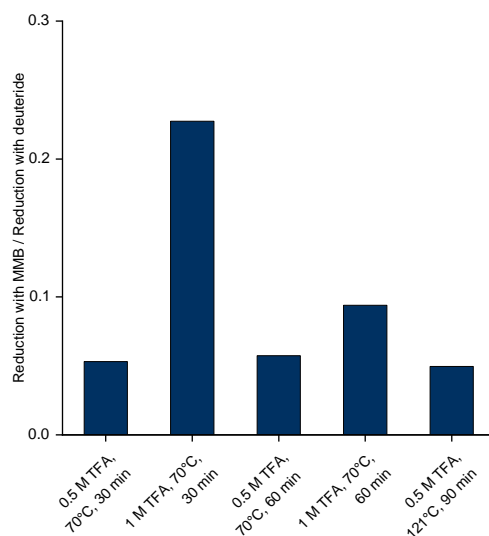
Fig. S1: Ratio of PMAAs reduced by MMB (4-methylmorpholine-borane) and by deuteride in methylation analysis of levan with reductive hydrolysis using MMB and subsequent reduction with NaBD$_4$. The values were calculated using the intensities of the fragments *m/z* 161 (reduced with MMB) and 162 (reduced with deuteride) in the spectra of PMAA peaks derived from 2,6-fructofuranose.

Publikation: *Carbohydrate Polymers*, 337, 122164

Detailed structural characterization of five water-insoluble α-glucans produced by glucansucrases from *Streptococcus* spp.

Luise Ernst [a], Celine Schulz [a], Albrecht Petzold [b], Thomas Thurn-Albrecht [b], Kay Saalwächter [c], Daniel Wefers [a,*]

[a] *Institute of Chemistry, Food Chemistry, Martin Luther University Halle-Wittenberg, 06120 Halle (Saale), Germany*
[b] *Institute of Physics, Experimental Polymer Physics, Martin Luther University Halle-Wittenberg, 06120 Halle (Saale), Germany*
[c] *Institute of Physics, NMR, Martin Luther University Halle-Wittenberg, 06120 Halle (Saale), Germany*

ARTICLE INFO

ABSTRACT

Water-insoluble α-glucans synthesized from sucrose by glucansucrases from *Streptococcus* spp. are essential in dental plaque and caries formation. Because limited information is available on the fine structure of these biopolymers, we analyzed the structures of unmodified glucans produced by five recombinant *Streptococcus* (*S.*) *mutans* DSM 20523 and *S. salivarius* DSM 20560 glucansucrases in detail. A combination of methylation analysis, *endo*-dextranase and *endo*-mutanase hydrolyses, and HPSEC-RI was used. Furthermore, crystal-like regions were analyzed by using XRD and ^{13}C MAS NMR spectroscopy. Our results showed that the glucan structures were highly diverse: Two glucans with 1,3- and 1,6-linkages were characterized in detail besides an almost exclusively 1,3-linked and a linear 1,6-linked glucan. Furthermore, one glucan contained 1,3-, 1,4-, and 1,6-linkages and thus had an unusual, not yet described structure. It was demonstrated that the glucans had a varying structural architecture by using partial enzymatic hydrolyses. Furthermore, crystal-like regions formed by 1,3-glucopyranose units were observed for the two 1,3- and 1,6-linked glucans and the linear 1,3-linked glucan. 1,6-linked regions were mobile and not involved in the crystal-like areas. Altogether, our results broaden the knowledge of the structure of water-insoluble α-glucans from *Streptococcus* spp.

1. Introduction

The structure of bacterial α-glucans is highly complex because they are composed of different backbone linkages (1,3-, 1,4-, and 1,6-linked D-glucopyranoses (Glc*p*)) as well as side chains at positions *O*2, *O*3, *O*4, or *O*6 (depending on the backbone). α-Glucans are often grouped into dextrans, which contain >50 % of 1,6-linkages, and mutans, which contain >50 % of 1,3-linkages (Li, Wang, Meng, Dijkhuizen, & Liu, 2020; Monsan et al., 2001). Mutans are usually considered to be water-insoluble polysaccharides, which is most likely caused by consecutive α-1,3-linkages (Aires, Koo, Sassaki, Iacomini, & Cury, 2010; Ernst, Offermann, Werner, & Wefers, 2024; Hare, Svensson, & Walker, 1978; Inoue, Yakushiji, Katsuki, Kudo, & Koga, 1988; Inoue, Yakushiji, &

Takehara, 1982). However, completely linear 1,6-linked α-glucans may be water-insoluble, too (He et al., 2020; Padmanabhan, Kim, Pak, & Sim, 2003; Pittrof, Kaufhold, Fischer, & Wefers, 2021). Furthermore, α-glucans with a high portion of 1,6-linkages and only minor amounts of 1,3-linkages can be insoluble in water (Ernst et al., 2024; Fels, Jakob, Vogel, & Wefers, 2018). Consequently, water-insoluble α-glucans are a group of polysaccharides with a high structural heterogeneity.

α-Glucans are synthesized from sucrose by glucansucrases (glycoside hydrolase family 70). These homologous enzymes are secreted by several lactic acid bacteria from the genera *Streptococcus* (*S.*), *Lactobacillus, Weissella,* and *Leuconostoc* and use the glucose moiety from sucrose to form polymeric glucans (Hoshino, Fujiwara, & Kawabata, 2012; Leemhuis et al., 2013; Meng et al., 2016; Xu, Yang, Niu, Wang, & Wang,

Publikation: *Carbohydrate Polymers*, 337, 122164

2018; Yu, Qian, Ge, & Du, 2022). In the mouth cavity, *S. mutans* and *S. salivarius* are of particular importance, because these organisms are involved in caries formation (Bowen & Koo, 2011; Drucker, Shakespeare, & Green, 1984; Takahashi & Nyvad, 2008). Sucrose, which naturally occurs in our diet, is known to be a virulence factor for dental caries. This is based not only on the fermentation of sucrose to lactic acid, but also on its utilization for α-glucan synthesis (Forssten, Björklund, & Ouwehand, 2010; Leme, Koo, Bellato, Bedi, & Cury, 2006; Minah & Loesche, 1977). In particular, water-insoluble α-glucans enhance adherence and accumulation of acidogenic bacteria and are an essential component of the dental biofilm (plaque), which allows bacteria to establish an acidic environment resulting in tooth enamel demineralization (Koo, Falsetta, & Klein, 2013). To understand the role of water-insoluble α-glucans in dental caries promotion and in developing prevention methods, a detailed investigation of the molecular structure of these polysaccharides is crucial.

The important structural characteristics of glucans include the linkage types, side chain positions, and side chain lengths. Furthermore, some water-insoluble α-glucans form crystalline regions. Crystallinity can influence enzyme accessibility and thus impede enzymatic hydrolysis which is a tool considered for caries prevention. Ogawa, Yui, Okamura, and Misaki (1994) analyzed the 1,3-linked sections of two α-glucans of *S. salivarius* and *mutans* which were prepared by mild Smith degradation or dextranase hydrolysis. They found that the two glucans contained two different crystal polymorphs, one of them included one water molecule per glucose unit. This water molecule was removed by drying which resulted in the other polymorph.

S. salivarius ATCC 25975 is known to encode two glucansucrases, glucosyltransferase J (GTF-J) and GTF-L, which produce water-insoluble glucans. The glucans of GTF-J were described as mainly 1,3-linked, whereas 1,3- and 1,6-linkages were observed for the glucans produced by GTF-L (Kusumi et al., 2023; Simpson, Cheetham, Giffard, & Jacques, 1995). Kobayashi et al. (2017) investigated the solely α-1,3-linked glucans formed by glucansucrase GTF-J. They confirmed different crystallinity of the hydrated and dehydrated glucans and the existence of one water molecule per glucose unit in the hydrated form. Furthermore, they found a decrease in crystallinity due to drying. Generally, dehydration and hydration are known to induce crystal transitions in polysaccharides (Kobayashi, Kimura, Heux, & Wada, 2013; Kobayashi, Kimura, Togawa, Wada, & Kuga, 2010). *S. salivarius* also encodes for other glucansucrases such as GTF-K, but these enzymes were described to produce water-soluble glucans (Simpson et al., 1995). The cariogenic potential, glucansucrases, and glucans of *S. mutans* were extensively studied in the past (Bowen & Koo, 2011; Hare et al., 1978; Hayacibara et al., 2004; Kopec, Vacca-Smith, & Bowen, 1997; Kuramitsu & Wondrack, 1983; Lin, Chen, Zhou, & Li, 2021; Wiater, Pleszczyńska, Próchniak, & Szczodrak, 2012). This organism was described to produce glucansucrases GTF-I (GTF-B) and GTF-SI (GTF-C) which synthesize (partially) water-insoluble glucans as well as GTF-S (GTF-D) which synthesizes water-soluble glucans (Hanada & Kuramitsu, 1988, 1989). Glucans of GTF-I were described as mainly 1,3-linked, whereas 1,3- and 1,6-linkages were described for glucans of GTF-SI (Hare et al., 1978; Hayacibara et al., 2004; Kopec et al., 1997). However, glucan structures were mostly only investigated by using methylation analysis and by comparing dextranase and mutanase susceptibility. Data on the crystallinity of mixed-linkage α-glucans from *Streptococcus* spp. are not available.

Consequently, a study on the comparative analysis of the fine structures and crystallinity of different water-insoluble α-glucans produced by glucansucrases from *Streptococcus* spp. is not available, despite the important role of these glucans in the human mouth cavity. Therefore, we selected five homologous glucansucrases with different amino acid sequences from *S. mutans* DSM 20523 (NCTC 10449) and *S. salivarius* DSM 20560 (NCTC 8618) for the production and subsequent characterization of glucans. Our hypothesis was that water-insoluble, native α-glucans produced by these five glucansucrases vary in terms

of their structural architecture and crystallinity. Thus, glucans were investigated by using methylation analysis, different chromatographic approaches in combination with partial enzymatic hydrolyses, X-ray diffraction (XRD), and ^{13}C magic angle spinning nuclear magnetic resonance (MAS NMR) spectroscopy.

2. Experimental

2.1. Materials

If not stated otherwise, all chemicals used were of "p.a." grade or better and were purchased from Carl Roth (Karlsruhe, Germany), Merck (Darmstadt, Germany), Thermo Fisher Scientific (Waltham, MA USA), VWR (Darmstadt, Germany), and Grüssing GmbH (Filsum, Germany). *Endo*-dextranase (EC 3.2.1.11) from *Chaetomium* sp., 8000 U/mL, was purchased from Megazyme (Bray, Ireland) and *endo*-mutanase SSAL4105 (EC 3.2.1.59) from *S. salivarius* was recombinantly produced as described by Ernst et al. (2024). Genomic DNA of *S. mutans* DSM 20523 and *S. salivarius* DSM 20560 was purchased from DSMZ (German Collection of Microorganisms and Cell Cultures GmbH, Braunschweig, Germany).

2.2. Production of recombinant glucansucrases

Molecular cloning, heterologous expression, and protein isolation of glucansucrases (SMUT1101 and SMUT1102 from *S. mutans* DSM 20523 as well as SSAL4540, SSAL4545, and SSAL4550 from *S. salivarius* DSM 20560) were performed as described previously (Ernst et al., 2024; Münkel et al., 2019). Briefly, encoding genes were amplified from genomic DNA by polymerase chain reaction (PCR) using a Phusion High-Fidelity PCR kit (Thermo Fisher Scientific, Waltham, USA). The primer pairs shown in Table 1 (synthesized by Integrated DNA Technologies (Coralville, IA, USA)) were used. Signal peptides (predicted by using the SignalP 5.0 web tool) were not amplified. Specific overhangs were inserted at both ends of the genes to allow ligase-independent cloning into the pLIC-SGC1 vector (Addgene plasmid no. 39187). For ligation independent cloning, the vector and PCR products were digested with T4 DNA polymerase (Thermo Fisher Scientific), and vector-gene adducts were transformed to 5α-competent *E. coli* cells (High efficiency, NEB, USA). The correct plasmid sequence was confirmed by Sanger sequencing (Eurofins GATC Biotech, Konstanz, Germany). For gene expression, the plasmids were transformed into One Shot BL21 Star *E. coli* (DE3, Invitrogen, USA) and cells were grown in LB medium supplemented with 100 μg ampicillin/L overnight at 37 °C and 225 rpm. The protein production was induced by the addition of isopropyl-β-D-thiogalactopyranoside (final concentration 0.1 mM). After cell lysis by sonication, cell debris was removed by centrifugation (30 min, 4 °C, 14,000 g), and recombinant proteins were isolated by immobilized metal affinity chromatography using a HisPur Ni-NTA resin (Thermo Fisher Scientific). Proteins were eluted with elution buffer (50 mM sodium phosphate, 300 mM NaCl, 100 mM imidazole, pH 7.5) and the protein concentration was calculated by absorption measurement at 280 nm (calculation of the extinction coefficient by using the amino acid sequence and the ProtParam tool). The obtained solutions were used for glucan synthesis. Sequence comparison of glucansucrases with previously described glucansucrases (Table S1) was performed with the multiple sequence alignment tools Clustal Omega and ESPript 3.0 (Robert & Gouet, 2014; Sievers & Higgins, 2014).

2.3. Glucan synthesis and monosaccharide analysis

For glucan synthesis, appropriate volumes of glucansucrase solutions (Section 2.2) containing 5 mg of protein were added to 100 mL of a 0.5 M sucrose solution (including 10 mM CaCl$_2$ and 0.05 vol-% ProClin, pH 5.9). After static incubation at 37 °C for 48 h, glucans were recovered by centrifugation at 4 °C (30 min at 10595 rcf). Subsequently, glucans were

Publikation: *Carbohydrate Polymers*, 337, 122164

L. Ernst et al.

Table 1
Genomic DNA and PCR primers used for molecular cloning of glucansucrases.

Genomic DNA	Locus tag	Primer sequence forward (5′ to 3′)	Primer sequence reverse (5′ to 3′)
S. mutans DSM 20523 (NCTC 10449)	SMUT1102	TACTTCCAATCCATGGATTCTAATGAATCGAAATCCCAAATTTCTAATGATTCTAATAC	TATCCACCTTTACTGTTAGTTAATCGGAACTCGTTCTCCAGAG
	SMUT1101	TACTTCCAATCCATGGATTCCACTGACGACCGTCAACAGG	TATCCACCTTTACTGTTAAAATCTAAAGAAATTGTCAAAGAAATCCATTACGAGAGTGTC
S. salivarius DSM 20560 (NCTC 8618)	SSAL4550	TACTTCCAATCCATGGAAGAAATAAATAAATAATATAATGGATCACCTTCAACAACTACAGTC	TATCCACCTTTACTGTTAATTTGACACGTATCCTTTCCTTGAGCG
	SSAL4545	TACTTCCAATCCATGGATGAAACTCAAGATAAGATAGATAGTAACTCAACCAAATTTAGATAC	TATCCACCTTTACTGTTAGTTTAGCACTCTAGGTGGGTAAGC
	SSAL4540	TACTTCCAATCCATGGATGAAACAACTCAACCAGTGCCTCTACG	TATCCACCTTTACTGTTATTTATCAAAATCAGCATAAACCATTTTCATCGAAGAAGACAG

resuspended in ultrapure water (100 mL) and centrifuged (30 min at 10595 rcf). This washing step was repeated twice and wet (paste-like) glucans were preserved by adding 10 μL of a 50 mg/mL NaN$_3$ solution (final concentration 0.5 mg/mL). Partial enzymatic hydrolyses (Section 2.4), XRD (Section 2.7), and ^{13}C MAS NMR spectroscopy (Section 2.8) were performed by using the undried polysaccharides, whereas an aliquot was lyophilized for methylation analysis (Section 2.6), HPSEC-RI (Section 2.5), and monosaccharide analysis. The latter was performed as described by Ernst et al. (2024) for water-insoluble homoex-opolysaccharides. In brief, glucans were hydrolyzed by using trifluoro-acetic acid (TFA) in two batches with two different conditions (2 M TFA, 60 min, 121 °C; 1 M TFA, 30 min, 70 °C), and the released mono-saccharides were analyzed by high-performance anion exchange chro-matography with pulsed amperometric detection (HPAEC-PAD).

2.4. Partial enzymatic hydrolyses and oligosaccharide analysis

About 1 mg of undried glucans was suspended in 500 μL of ultrapure water and used for *endo*-dextranase hydrolysis. After the addition of *endo*-dextranase (5 U/mg glucans), the mixture was incubated for 24 h at 40 °C and 200 rpm. For *endo*-mutanase hydrolysis, 90 μg of protein were added to 1 mg of undried glucans in 100 μL ultrapure water and incubated for 24 h at 37 °C and 200 rpm. Dextranase and mutanase were inactivated by heating to 95 °C for 10 min. Insoluble material was removed by centrifugation and lyophilized. The supernatant was used for HPAEC-PAD coupled with mass spectrometric detection (HPAEC-PAD/MS) on an ICS-6000 system equipped with a LTQ XL linear ion trap mass spectrometer (Thermo Fisher Scientific). Separation was achieved by using a CarboPac PA200 column (250 × 3 mm i.d., 5.5 μm particle size, Thermo Fisher Scientific). The column temperature was 30 °C and the PAD temperature was 25 °C. For separation, the following gradient composed of four eluents (A: ultrapure water, B: 10 mM NaOH, C: 200 mM NaOH, D: 200 mM NaOH +500 mM sodium acetate) was used at a flow rate of 0.4 mL/min: column equilibration with 100 % B 20 min before injection; 0–10 min: Isocratic 100 % B; 10–20 min: Linear gradient to 50 % C + 50 % A; 20–45 min: Linear gradient to 50 % A, 30 % C + 20 % D; 45–55 min: Linear gradient to 50 % A + 50 % D; 55–65 min: Linear gradient to 100 % D; 65–80 min: Isocratic 100 % D; 80–95 min: Isocratic 100 % C. A post column split allowed simultaneous PAD and MS analysis. Prior to MS analysis, desalting of the eluent was ach-ieved by an AERS 500e suppressor (4 mm, Thermo Fisher Scientific). To facilitate ionization by electrospray ionization, 500 μM LiCl was added at a flow rate of 0.05 mL/min (AXP-MS pump, Thermo Fisher Scientific). The source temperature was 300 °C and lithium adducts of oligosac-charides were detected in positive mode. Peaks in the chromatograms of dextranase hydrolysates were assigned by using the oligosaccharides characterized by Münkel and Wefers (2019).

2.5. High-performance size exclusion chromatography coupled with refractive index detection (HPSEC-RI)

For HPSEC-RI analysis of glucans and water-insoluble residues after *endo*-dextranase and *endo*-mutanase hydrolyses (Section 2.4), the lyophilized samples were solubilized by adding 300 μL of dimethyl sulfoxide (DMSO). After shaking at ambient temperature overnight, about 2 mg of LiCl$_{(s)}$ were added (resulting LiCl concentration: 100 mM) and the samples were again shaken overnight (60 °C, 1500 rpm). Glu-cans and water-insoluble hydrolysis products of SSAL4545, SMUT1101, and SMUT1102 were dissolved by this procedure and analyzed. SSAL4540 and SSAL4550 were not solubilized, even after a second addition of LiCl$_{(s)}$ and shaking. For chromatographic analysis, DMSO with 100 mM LiCl was used as eluent at a flow rate of 0.2 mL/min on an HPLC-RI system (P6.1L, AS6.1 L, RID 2.1 L, Knauer, Germany) equipped with a GRAM column (300 × 8 mm, particle size 10 μm) (PSS, Ger-many). Column temperature was 80 °C and RI temperature was 35 °C. The molecular weight of the glucan samples was estimated by using

3

Publikation: *Carbohydrate Polymers*, 337, 122164

L. Ernst et al.

standard dextrans with known molecular weight (dextran blue ($\sim$ 2000 kDa), 670 kDa, 270 kDa and 12 kDa, Sigma Aldrich, Germany; 64.3 kDa, PSS, Germany).

2.6. Glycosidic linkage analysis

Analysis of glycosidic linkages was carried out by methylation analysis: Lyophilized glucans were derivatized and analyzed as described in detail by Ernst, Werner, and Wefers (2023). Briefly, samples were swollen in DMSO overnight followed by an ultrasonic treatment. NaOH$_{(s)}$ was added, and the samples were again sonicated before adding methyl iodide. Methylation was repeated once, and the partially methylated polysaccharides were hydrolyzed by 2 M TFA for 90 min at 121 °C. Partially methylated monosaccharides were reduced with NaBD$_4$ and acetylated by using 1-methylimidazole and acetic anhydride. Partially methylated alditol acetates were separated by gas chromatography, identified by their mass spectra (Fig. S4), and quantified by flame ionization detection by using the response factors described by Sweet, Shapiro, and Albersheim (1975).

2.7. Wide angle X-ray diffraction (XRD)

Undried glucans were prepared on a sample holder covered with amorphous tape. This setting allowed keeping a relative humidity of 100 % for at least 16 h. A spatula tip of each sample was used; however, the exact glucan amount is unknown due to the wet state of the samples. An EMPYREAN (Malvern Panalytical) diffractometer operating in Bragg–Brentano geometry using a programmable divergence slit and Cu-Kα-radiation was used for diffraction measurements.

2.8. ^{13}C Magic angle spinning nuclear magnetic resonance (MAS NMR) spectroscopy

The ^{13}C cross-polarization (CP) and direct polarization (DP) MAS spectra of undried glucans were obtained on a Bruker Avance spectrometer with the proton resonance frequency 400 MHz. The samples were packed in 4 mm rotors and span at a MAS rate of 10 kHz and at ambient temperature. The experimental parameters were: CP contact time 1.5 ms, ^{1}H 90-degree pulse 3.6 μs, ^{13}C 90-degree pulse 4 μs. The ^{13}C signal was recorded during 35 ms with 65 kHz SPINAL proton decoupling. Repetition delay was 3 s and 10 s for CP and DP spectra, respectively. The number of signal accumulations for different samples was 10,000 to 40,000.

3. Results and discussion

For comparative investigation of fine structures and crystallinity of different water-insoluble α-glucans, five homologous glucansucrases from *Streptococcus* spp. were cloned and heterologously expressed: SMUT1101 and SMUT1102 from *S. mutans* DSM 20523 as well as SSAL4540, SSAL4545, and SSAL4550 from *S. salivarius* DSM 20560. Glucansucrases SMUT1101 and SMUT1102 showed high sequence identities (>95 %) to the two *S. mutans* glucansucrases which produce insoluble glucans, GTF-I and GTF-SI (Table S1, Fig. S1 & S2). Furthermore, glucansucrases SSAL4545 (GTF-J) and SSAL4550 (GTF-K) from *S. salivarius* were selected for comparison because they were described to produce linear 1,3- and 1,6-linked glucans, respectively. Whereas linear 1,3-linked glucans are water-insoluble and may be crystalline, 1,6-linked glucans can at least in part be water-insoluble. Furthermore, glucansucrase SSAL4540 was investigated because its amino acid sequence showed similar conserved regions to those of known, water-insoluble glucan synthesizing glucansucrases of *S. salivarius* and *mutans*, but only shared a low degree of identity (< 60 %) with the other enzymes. Consequently, this enzyme may synthesize glucans with an unusual structure. Water-insoluble polysaccharides were successfully synthesized from sucrose by using the five recombinant glucansucrases.

The paste-like undried polysaccharides were recovered by centrifugation and used for further analysis (after drying for some analyses, see Sections 2.4–2.8). Monosaccharide analysis of the obtained polysaccharides confirmed that they were solely composed of glucose. In addition, glucansucrases SSAL4540 and SSAL4550 synthesized in part water-soluble glucans resulting in lower yields of water-insoluble glucans. However, the water-soluble fraction was not of interest in this study.

3.1. Glycosidic linkages

The portions of glycosidic linkages in the water-insoluble glucans were determined by methylation analysis (Fig. 1). Low portions of artifacts from the sample workup such as fully substituted glucopyranose were detected in some chromatograms (Fig. S3). The formation of these compounds is caused by solubilization issues of the water-insoluble glucans in DMSO. Partial undermethylation may have some influence on the portions of the glycosidic linkages, however, due to the low abundance of the artifacts, the results can still be used to assess the structural composition. The glucans showed varying backbone linkages, but all samples contained 1,3,6-linked Glc*p* units which correspond to branched backbone units. Glucans produced by SMUT1101 and SMUT1102 were composed of 1,3- and 1,6-linked Glc*p* units in comparable portions: SMUT1101 glucans contained 55 % 1,3-linkages and 32 % 1,6-linkages, while SMUT1102 glucans contained 48 % 1,3-linkages and 38 % 1,6-linkages. Glucans containing mainly 1,3- and 1,6-linkages in different portions have also been described for GTF-I (GTF-B) and GTF-SI (GTF-C) of *S. mutans* GS-5 (Aires et al., 2010; Hayacibara et al., 2004; Kopec et al., 1997).

Glucans produced by SSAL4545 were mainly 1,3-linked with minor portions of 1,6-linkages (< 1 %), whereas glucans produced by SSAL4550 were mainly 1,6-linked with minor portions of 1,3-linkages (< 5 %). Simpson et al. (1995) found that GTF-J (97 % identity to SSAL4545) synthesized 1,3-linked glucans and GTF-K (96 % identity to SSAL4550) synthesized 1,6-linked glucans. However, it cannot be excluded that the minor portions of 1,3,6-linkages (and 1,6-/1,3-linkages) are artifacts which were formed during the sample workup. Furthermore, Simpson et al. (1995) described the 1,6-linked glucans of
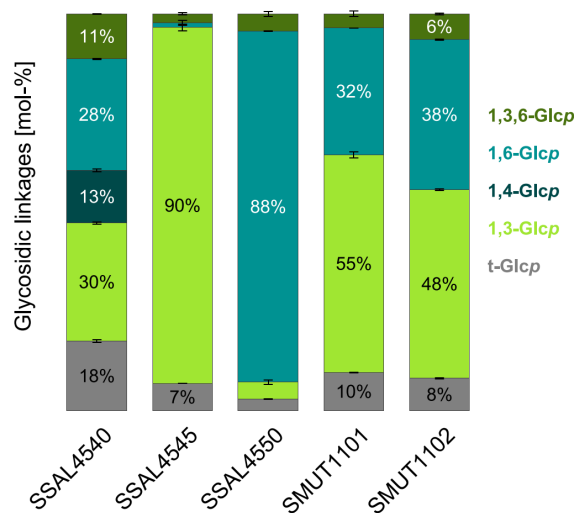

Fig. 1. Glycosidic linkages of glucans produced by glucansucrases SSAL4540, SSAL4545, SSAL4550, SMUT1101, and SMUT1102. Glycosidic linkages were determined by methylation analysis and all analyses were performed in duplicate. t: terminal, Glc*p*: glucopyranose, numbers indicate the position of substitution in the monosaccharide unit.

4

Publikation: *Carbohydrate Polymers*, 337, 122164

L. Ernst et al.

GTF-K to be water-soluble, but (partial) water-insolubility of the 1,6-linked glucans from SSAL4550 could be a result of higher linearity and/or higher molecular weight.

Linkages of SSAL4540 glucans were very diverse: Besides 30 % 1,3-linkages, 13 % 1,4- and 28 % 1,6-linkages were present. A few studies found low portions (< 5 %) of 1,4-linked Glc*p* units in glucans from *Streptococcus* spp. (Kopec et al., 1997; Tsumuraya & Misaki, 1979). However, these low amounts might be due to artifacts in methylation analysis and Smith degradation. Only Hayacibara et al. (2004) found a high portion of 1,4-linkages (16–25 %) in glucan produced by glucansucrase GTF-C from *S. mutans* WHB410. There is no previous report of mixed-linkage glucans containing a relevant portion of 1,4-linkages produced by glucansucrases of *S. salivarius*. Overall, the results indicated a high structural diversity of water-insoluble glucans produced by the five glucansucrases.

3.2. Partial enzymatic hydrolyses

To obtain information on fine structures, glucans were hydrolyzed by *endo*-mutanase and *endo*-mutanase. The resulting water-soluble products were analyzed by HPAEC-PAD/MS. The chromatograms obtained from *endo*-dextranase hydrolyses are shown in Fig. 2. *Endo*-dextranase hydrolyzes sections of linear, α-1,6-linked Glc*p* units and liberates glucose, isomaltose as well as previously described branched isomalto-oligosaccharides (Münkel et al., 2019; Pittrof et al., 2021). The chromatogram of the *endo*-dextranase hydrolysate of glucans produced by SSAL4550 contained three peaks which resulted from glucose, isomaltose, and isomaltotriose. These results suggested that SSAL4550 glucans were solely 1,6-linked because no branched oligosaccharides were detected. Consequently, the small portions of 1,3- and 1,3,6-linkages detected by methylation analysis (Section 3.1) were most likely artifacts from the sample workup. *Endo*-dextranase did not liberate any products from the glucans of SSAL4540 and SSAL4545. This supported the finding that glucans produced by SSAL4545 were exclusively 1,3-linked and that minor portions of 1,6-linkages determined by methylation analysis were artifacts (Section 3.1). In contrast, some hydrolysis could have been expected from glucans produced by SSAL4540, because they contained about 30 % 1,6-linkages (Section 3.1). The fact that these polysaccharides were not digested by *endo*-dextranase indicated that 1,6-linked Glc*p* units were not present in consecutive blocks. Chromatograms of *endo*-dextranase hydrolysates of glucans produced by SMUT1101 and SMUT1102 contained peaks resulting from isomaltose, isomaltotriose, and O3-branched isomalto-oligosaccharides. The released oligosaccharides demonstrated that SMUT1101 and SMUT1102 glucans contained consecutive 1,6-linked sections which were branched

with mono-, di-, and oligomeric side chains at position O3. Relative peak intensities of SMUT1101 and SMUT1102 glucan hydrolysates varied, indicating a varying structural architecture.

A recombinant *endo*-mutanase was used to hydrolyze sections of α-1,3-linked Glc*p* units. The chromatogram of the *endo*-mutanase hydrolysate of glucans produced by SSAL4550 (Fig. 3) did not contain any peaks which indicated that these glucans cannot be hydrolyzed by *endo*-mutanase. This result was in accordance with the observation that these glucans were exclusively composed of 1,6-linkages. The chromatograms of the four remaining glucans produced by SSAL4540, SSAL4545, SMUT1101, and SMUT1102 showed peaks resulting from linear, 1,3-linked di−/oligosaccharides (nigerose, nigerotriose and nigerotetraose) which were identified by using standard compounds. The detection of these oligosaccharides confirmed the occurrence of consecutive α-1,3-linkages. Furthermore, unknown oligosaccharides which showed an *m/z* corresponding to gluco-oligosaccharides with a degree of polymerization from 3 to 7 were detected. The presence of gluco-oligosaccharides was also confirmed by analyzing the monosaccharide composition of the oligosaccharide-containing supernatant by HPAEC-PAD after TFA hydrolysis. Because the retention times of these compounds did not correspond to α-1,3-, α-1,4-, or α-1,6-linked standard oligosaccharides, the detected peaks can be assigned to mixed-linkage or branched gluco-oligosaccharides. Furthermore, the oligosaccharide profiles (the occurrence and relative intensities of the oligosaccharide-derived peaks) suggested structural differences between the analyzed glucans. For example, the hydrolysate of glucans produced by SSAL4540 showed several different pentasaccharides which were not present in the other samples. The liberation of these oligosaccharides could be a result of the 1,3-, 1,4-, and 1,6-linkages present in these glucans. SSAL4545, SMUT1101, and SMUT1102 glucans showed comparable oligosaccharide profiles, however, different relative peak intensities indicated varying portions of oligosaccharides for glucans produced by SMUT1101 and SMUT1102. This again confirmed the different fine structures of these two polysaccharides. The liberation of mixed-linkage or branched oligosaccharides from SSAL4545 glucans confirmed the presence of 1,3,6-linked Glc*p* units in these glucans (Section 3.1).

Enzymatic hydrolysis was used to investigate structures of water-insoluble glucans produced by different glucansucrases from *Streptococcus* spp. in previous studies (Hare et al., 1978; Kopec et al., 1997; Pearce, Walker, Slodki, & Schuerch, 1990; Vacca-Smith, Venkitaraman, Quivey Jr, & Bowen, 1996). However, merely Hare et al. (1978) found unknown, presumably mixed-linkage oligosaccharides in addition to isomalto- and nigero-oligosaccharides after *endo*-dextranase as well as simultaneous *endo*-dextranase and *endo*-mutanase hydrolysis of
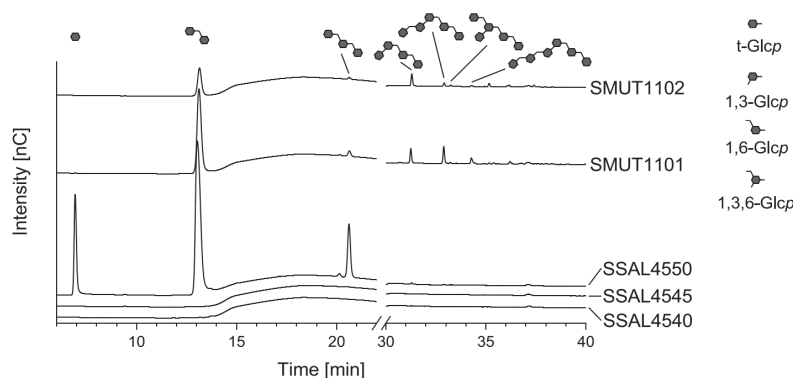
Fig. 2. HPAEC-PAD chromatograms of oligosaccharides released from glucans synthesized by glucansucrases SSAL4540, SSAL4545, SSAL4550, SMUT1101 and SMUT1102 by using *endo*-dextranase. Chromatograms are shown in stacked format and peaks were assigned according to Münkel et al. (2019) and Münkel and Wefers (2019).

5

Publikation: *Carbohydrate Polymers*, 337, 122164
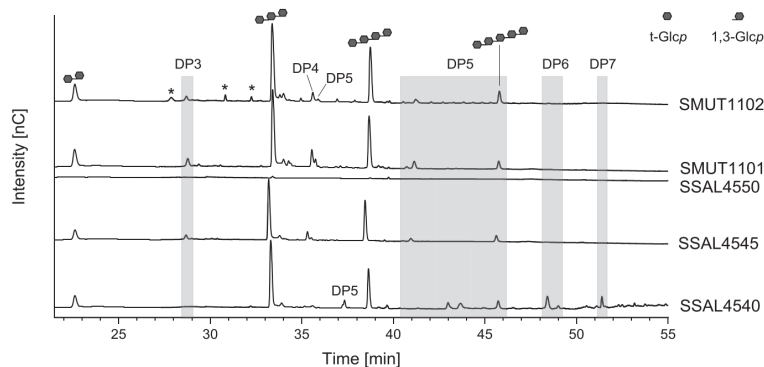
Fig. 3. HPAEC-PAD chromatograms of oligosaccharides released from glucans synthesized by glucansucrases SSAL4540, SSAL4545, SSAL4550, SMUT1101 and SMUT1102 by using *endo*-mutanase. Chromatograms are shown in stacked format and peak assignment resulted from standard compounds (nigero-oligosaccharides). The degree of polymerization (DP) of the unknown oligosaccharides was determined by mass spectrometry. Peaks marked with asterisks (*) are isomalto-oligosaccharides and were also present in SMUT1102 glucans without enzyme addition. Slight retention time shifts between 30 and 40 min were caused by different concentrations of buffer salts from mutanase solutions.

enzymatically synthesized glucans from *Streptococcus* spp. Nevertheless, their paper chromatographic approach could not provide further information on the identity of these oligosaccharides. The identification of *O3*-branched isomalto-oligosaccharides released by *endo*-dextranase hydrolysis and the release of different mixed-linkage or branched oligosaccharides by *endo*-mutanase hydrolysis from water-insoluble glucans from *Streptococcus* spp. is first reported herein.

3.3. High-performance size exclusion chromatography

Water-insoluble glucans produced by SSAL4545, SMUT1101, and SMUT1102 as well as their water-insoluble residues after *endo*-dextranase and *endo*-mutanase hydrolyses were analyzed by HPSEC-RI (Fig. 4). Glucans produced by SSAL4540 and SSAL4550 could not be

dissolved in DMSO/100 mM LiCl, so size exclusion chromatography was not possible.

The elugram of untreated glucans produced by SMUT1102 showed an intense peak at low elution volumes, indicating that these polysaccharides had a high molecular weight of at least 2000 kDa (dextran blue). *Endo*-dextranase hydrolysis reduced the elution volume of the SMUT1102 glucans significantly and the main fraction of the insoluble residue eluted between 64.3 and 12 kDa. *Endo*-mutanase hydrolysis led to water-insoluble products with a broad molecular weight distribution: The high molecular weight fraction was reduced in size and a new fraction with a lower molecular weight (between 64.3 and 12 kDa) was formed. Therefore, *endo*-mutanase hydrolysis not only resulted in water-soluble oligosaccharides (Section 3.2) but also in water-insoluble glucans with a lower molecular weight. The incomplete hydrolysis might be
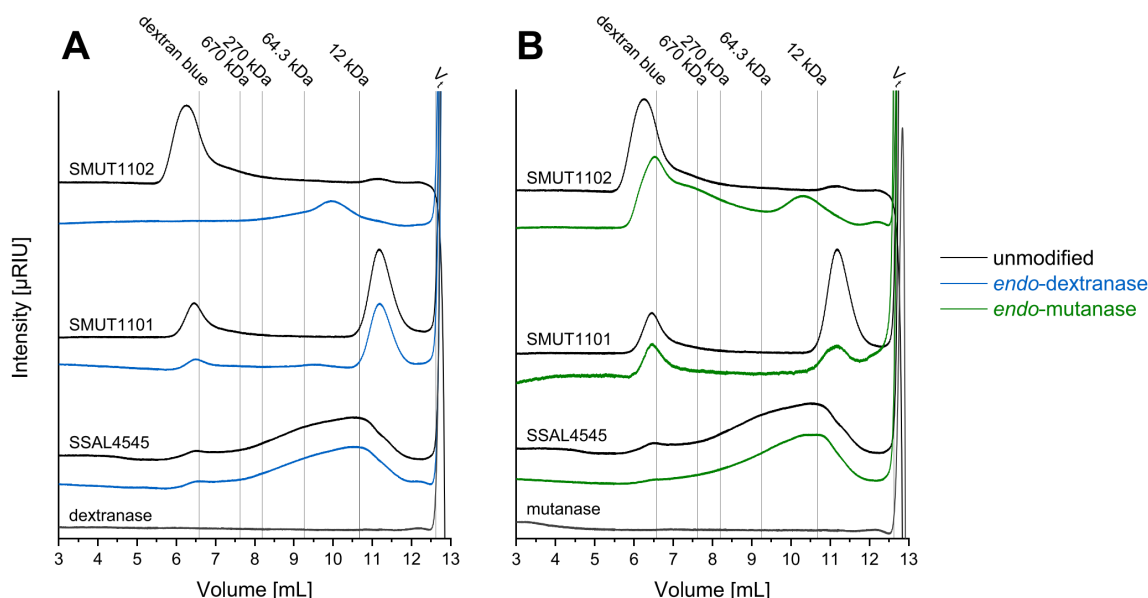
Fig. 4. HPSEC-RI elugrams of glucans produced by SSAL4545, SMUT1101, and SMUT1102 as well as their water-insoluble residues after *endo*-dextranase (A) and *endo*-mutanase (B) hydrolyses. Elugrams are shown in stacked format and peak maxima of size standards with known molecular weight are indicated by reference lines (V_t was determined by using glucose). The concentrations of injected samples differed because varying amounts of undried glucans were used for enzymatic hydrolyses (Section 2.4). Elugrams of both enzymes without glucan are displayed for comparison.

Publikation: *Carbohydrate Polymers*, 337, 122164

L. Ernst et al.

a result of branched 1,3-linked areas. However, the comparably small molecular weight shift after *endo*-mutanase hydrolysis as well as the elugrams from *endo*-dextranase hydrolysis suggested that 1,6-linked blocks had a high molecular weight, whereas 1,3-linked blocks were rather small. Therefore, our results allowed the conclusion that glucans of SMUT1102 were most likely block copolymers of 1,3- and 1,6-linked blocks.

Glucans produced by SMUT1101 contained two fractions, one at low elution volumes (below 12 kDa) and one at high elution volumes (ca. 2000 kDa). Hydrolysis with *endo*-dextranase reduced the intensity of the early-eluting peak and led to the occurrence of a peak resulting from smaller products (between 670 kDa and 12 kDa). The incomplete hydrolysis of the early-eluting, high molecular weight fraction demonstrated that SMUT1101 and SMUT1102 had different fine structures which was in good agreement with the results from the other analyses. *Endo*-mutanase hydrolyzed the low molecular weight fraction because its peak intensity decreased relative to the high molecular weight fraction. In conclusion, the high molecular weight fraction of SMUT1101 glucans contained a high portion of consecutive 1,6-linkages and the low molecular weight fraction contained a high portion of consecutive 1,3-linkages. However, both glucan molecular weight fractions were incompletely hydrolyzed, indicating that both also contained other backbone linkages or were branched.

Glucans produced by SSAL4545 exhibited a broad size distribution (ranging from ca. 2000 kDa to lower than 12 kDa) with the highest intensity at 12 kDa. Neither *endo*-dextranase nor *endo*-mutanase hydrolysis changed the elution pattern which indicated that the release of water-soluble products by *endo*-mutanase (Section 3.2) did not influence the molecular weight of the remaining water-insoluble fractions and only a small part of the glucans was hydrolyzed. Because the SSAL4545 glucans were (almost) exclusively 1,3-linked, this result was quite surprising. However, the incomplete hydrolysis could also result from limited enzymatic accessibility of the glucans.

Overall, glucans of glucansucrases SMUT1102, SMUT1101, and SSAL4545 showed varying molecular sizes and size distributions. Despite high portions of 1,3- and partly 1,6-linkages, glucans were not completely hydrolyzed to oligosaccharides by *endo*-mutanase or *endo*-dextranase. This might be due to low enzymatic accessibility, small sizes of the differently linked blocks and/or due to ramifications within the blocks of consecutive 1,3- or 1,6-linkages.

3.4. X-ray diffraction of undried glucans

For information on crystalline areas of the native glucans, they were used in an undried state to avoid changes in the crystalline structure during drying. Undried glucans were prepared on a sample holder covered with tape to avoid drying during the XRD measurement. Resulting diffractograms (Fig. 5) were compared with regards to peaks emerging from the amorphous background/halo, which indicate crystalline structures, and diffraction angles which depend on the unit cell structure. The diffractograms of glucans produced by SMUT1102 and SSAL4550 showed no peaks which indicated that these polysaccharides were largely amorphous or at least did not contain large enough ordered crystalline regions. Diffractograms of glucans produced by SSAL4540, SSAL4545, and SMUT1101 exhibited several peaks. Peak positions of glucans SMUT1101 and SSAL4545 were comparable to those described by Kobayashi et al. (2017) for the linear 1,3-linked glucans produced by GTF-J of *S. salivarius* ATCC25975. In contrast, glucans produced by SSAL4540 exhibited peaks at different angles, thus this sample contained another crystal polymorph than glucans produced by SMUT1101 and SSAL4545. This indicated that SSAL4540 glucans were structurally different from SMUT1101 and SSAL4545 glucans. However, the signals observed for SMUT1101 and SSAL4540 glucans indicated that mixed-linkage glucans from *Streptococcus* spp. may also contain crystalline areas. This finding was confirmed by ^{13}C MAS NMR spectroscopy for SMUT1101 glucans but not for SSAL4540 glucans (see Section 3.5). In
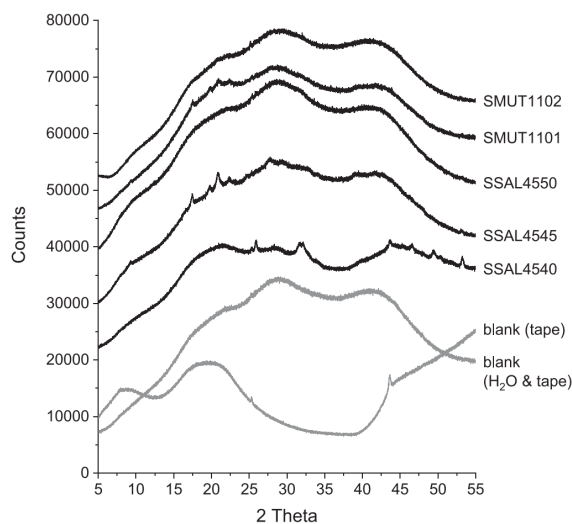
Fig. 5. X-ray diffractograms of glucans produced by SSAL4540, SAL4545, SSAL4550, SMUT1101, and SMUT1102 in an undried state (never dried or frozen). Sample diffractograms are shown in stacked format (+15,000 counts shift for SSAL4540; + 8000 counts shift for all other glucans) together with unshifted blank measurements (sample holder with tape as well as sample holder with tape and water, prepared as for the samples).

the literature, indications of crystallinity in mixed-linkage glucans have only been found for water-insoluble glucans produced by a glucansucrase from *Leuconostoc citreum* (Wangpaiboon et al., 2020). The crystal structures of the polymorphs remain to be elucidated.

3.5. ^{13}C MAS NMR spectroscopy

In addition to XRD, ^{13}C MAS NMR spectra of the undried glucans were recorded to obtain information on potentially crystalline regions. The short-CP spectra (contact time 1.5 ms) of glucans produced by SSAL4545, SMUT1102, and SMUT1101 are shown in Fig. 6. The signals observed in the spectrum of glucans produced by SSAL4545 were assigned to 1,3-linked Glc*p* units by comparing their chemical shifts to literature data (Kobayashi et al., 2010; Kobayashi et al., 2017; Poulhazan, Arnold, Warschawski, & Marcotte, 2018). The rather sharp peaks
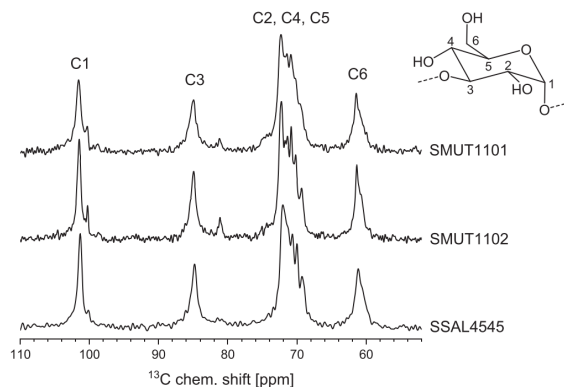
Fig. 6. ^{13}C MAS CP NMR spectra of undried glucans produced by glucansucrases SSAL4545, SMUT1101, and SMUT1102. Spectra are shown in stacked format. Peaks were assigned by comparison to literature (Kobayashi et al., 2010; Kobayashi et al., 2017; Poulhazan et al., 2018).

7

Publikation: *Carbohydrate Polymers*, 337, 122164

confirmed that 1,3-linked Glc*p* units form at least crystal-like (rather than glassy amorphous) regions. The spectra of glucans produced by SMUT1101 and SMUT1102 showed additional peaks at 81.1 ppm and 100.3 ppm which might arise from 1,3,6-Glc*p* units within the 1,3-linked sections. Both glucans contained 1,6-Glc*p* units in addition to 1,3-Glc*p* units, but no signal resulting from 1,6-Glc*p* units was found in the spectra (C6: ∼ 65 ppm, C3: ∼ 74 ppm; McIntyre & Vogel, 1991; Pidoux, Brooker, Colquhoun, & Morris, 1990). However, peaks of 1,6-Glc*p* units appeared in the corresponding DP spectra. Exemplarily, the CP and DP spectra of glucans from SMUT1101 are depicted in Fig. 7. This confirmed that 1,6-Glc*p* units were located in the mobile regions of the glucans. Overall, SMUT1101 and SMUT1102 glucans formed crystalline and/or crystal-like regions. These regions were exclusively formed by consecutive 1,3-linkages while 1,6-linked, dextran-like blocks remained mobile. The absence of peaks in the X-ray diffractogram of glucans produced by SMUT1102 might be due to small size crystal-like regions. To the best of our knowledge, mixed-linkage α-glucans have not been analyzed by ^{13}C MAS NMR spectroscopy before.

In contrast to DP spectra, CP NMR spectra of SSAL4540 glucans contained no peak which indicated, that these glucans had only mobile, hydrated residues and did not have sections with well-defined, crystal-like local packing environments. This was in contrast to the diffractograms from XRD analysis showing peaks that presumably resulted from crystalline glucan structures. This result suggested that the peaks observed in the X-ray diffractograms might not originate from glucans but from impurities. However, crystallization of glucansucrases was unlikely, as these large enzymes are difficult to crystallize (Molina, Cioci, Moulis, Séverac, & Remaud-Siméon, 2021). Here, further studies on the crystalline structure of mixed-linkage water-insoluble glucans should be performed. Spectra of SSAL4550 glucans did not show signals resulting from polysaccharides which is presumably due to low yields. However, no crystallinity is expected in the 1,6-linked SSAL4550 glucans because this linkage type was not found in the crystal-like regions of glucans SMUT1101 and SMUT1102.

3.6. Overall structure of the individual glucans

The overall structures of glucans are shown schematically in Fig. S5.
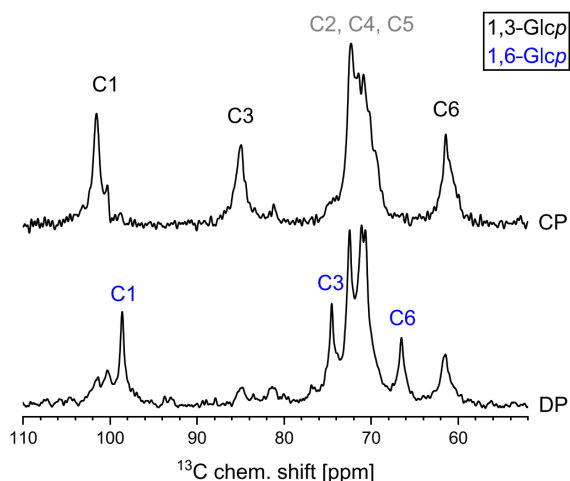
Fig. 7. ^{13}C MAS CP and DP NMR spectra of undried glucans produced by glucansucrase SMUT1101. Peaks were assigned to carbon atoms of Glc*p* units by comparison to literature (McIntyre & Vogel, 1991; Pidoux, Ruiter, Brooker, Colquhoun, & Morris, 1990; Kobayashi et al., 2010; Kobayashi et al., 2017; Poulhazan et al., 2018). Spectra are shown in stacked format. CP: cross polarization, DP: direct polarization, Glc*p*: glucopyranose.

Glucans produced by SMUT1101 and SMUT1102 contained comparable portions of 1,3- and 1,6-linked Glc*p* units as well as 1,3,6-linked Glc*p* units. Nevertheless, *endo*-dextranase and *endo*-mutanase hydrolyses revealed different fine structures: SMUT1101 glucans contained a high molecular weight fraction with high portions of consecutive α-1,6-linkages and a comparatively low molecular weight fraction with a high portion of consecutive 1,3-linkages. The results from XRD and ^{13}C MAS NMR spectroscopy indicated crystalline regions of 1,3-linked Glc*p* units. Partial enzymatic hydrolyses showed that SMUT1102 glucans contained long consecutive α-1,6-linked blocks and short α-1,3-linked blocks. The X-ray diffractogram of these high molecular weight glucans did not show any peaks, thus, large crystalline regions were absent. However, ^{13}C MAS NMR spectra demonstrated that 1,3-linked Glc*p* units were part of crystal-like regions while 1,6-linked areas were mobile.

Glucans produced by SSAL4550 were identified as linear dextrans which were water-insoluble but showed no indications of crystallinity.

Glucans produced by SSAL4545 were almost exclusively composed of 1,3-linked Glc*p* units, which formed crystalline regions according to XRD and ^{13}C MAS NMR spectroscopy.

SSAL4540 synthesized glucans which contained 1,3-, 1,4- and 1,6-linkages. Larger blocks with consecutive 1,6-linkages were most likely absent, because *endo*-dextranase did not release any oligosaccharides. Analogously, there were no consecutive 1,4-linkages because α-amylase did not hydrolyze the glucans (data not shown). However, *endo*-mutanase demonstrated that some consecutive 1,3-linkages were present. The X-ray diffractogram yielded some peaks which differed from those observed in the diffractograms of SSAL4545 and SMUT1101 glucans and the literature. However, the absence of signals in the CP ^{13}C MAS NMR spectrum indicated that the signals might not originate from the polysaccharides. Furthermore, SSAL4540 glucans were not solubilized in DMSO/100 mM LiCl. Therefore, the unusual structural composition led to varying physicochemical properties.

4. Conclusion

Our results demonstrated that the water-insoluble glucans formed by the five glucansucrases from *S. mutans* DSM 20523 and *S. salivarius* DSM 20560 have a high structural diversity and, thus, confirm our hypothesis. Glucans produced by glucansucrases SMUT1101 and SMUT1102 contained similar portions of 1,6- and 1,3-linkages, but clearly differed in their fine structure (distribution of linkage types, oligosaccharide profile, molecular weight). Both polymers showed crystal-like regions which are formed by consecutive 1,3-linkages. To our knowledge, there has been no literature report on the crystal-like structural elements in mixed-linkage water-insoluble α-glucans produced by glucansucrases from *Streptococcus* spp. In addition, completely linear, non-crystalline dextrans and mainly 1,3-linked mutans were produced by using the glucansucrases SSAL4550 and SSAL4545, respectively. The latter glucans were (in part) crystalline, which was in accordance with previously described linear 1,3-linked glucans (Kobayashi et al., 2017; Ogawa et al., 1994). The existence of water-insoluble α-glucans (glucansucrase SSAL4540) with 1,6-, 1,3-, and 1,4-linkages within the backbone was also demonstrated for the first time. Furthermore, we can conclude that the fine structures of the mixed-linkage glucans are very diverse and that the formation of crystalline or crystal-like areas is dependent on the molecular structure. Altogether, the combination of several analytical methods yielded detailed information on the fine structures of the glucans investigated.

CRediT authorship contribution statement

Luise Ernst: Writing – original draft, Visualization, Methodology, Investigation, Formal analysis, Conceptualization. **Celine Schulz:** Investigation. **Albrecht Petzold:** Writing – review & editing, Investigation, Formal analysis. **Thomas Thurn-Albrecht:** Writing – review & editing, Resources. **Kay Saalwächter:** Writing – review & editing,

Publikation: *Carbohydrate Polymers*, 337, 122164

Resources. **Daniel Wefers:** Writing – review & editing, Supervision, Resources, Conceptualization.

Declaration of competing interest

The authors declare that they have no known competing financial interests or personal relationships that could have appeared to influence the work reported in this paper.

Data availability

Data will be made available on request.

Acknowledgement

The authors are very grateful to Alexey Krushelnitsky (Institute of Physics, NMR, Martin Luther University Halle-Wittenberg) for NMR measurements and technical support.

Appendix A. Supplementary data

Supplementary data to this article can be found online at https://doi.org/10.1016/j.carbpol.2024.122164.

References

Aires, C. P., Koo, H., Sassaki, G. L., Iacomini, M., & Cury, J. A. (2010). A procedure for characterizing glucans synthesized by purified enzymes of cariogenic *Streptococcus mutans*. *International Journal of Biological Macromolecules, 46*, 551–554.

Bowen, W. H., & Koo, H. (2011). Biology of *Streptococcus mutans*-derived glucosyltransferases: Role in extracellular matrix formation of cariogenic biofilms. *Caries Research, 45*, 69–86.

Drucker, D. B., Shakespeare, A. P., & Green, R. M. (1984). The production of dental plaque and caries by the bacterium *Streptococcus salivarius* in gnotobiotic WAG/RIJ rats. *Archives of Oral Biology, 29*, 437–443.

Ernst, L., Offermann, H., Werner, A., & Wefers, D. (2024). Comprehensive structural characterization of water-soluble and water-insoluble homoexopolysaccharides from seven lactic acid bacteria. *Carbohydrate Polymers, 323*, Article 121417.

Ernst, L., Werner, A., & Wefers, D. (2023). Influence of ultrasonication and hydrolysis conditions in methylation analysis of bacterial homoexopolysaccharides. *Carbohydrate Polymers, 308*, Article 120643.

Fels, L., Jakob, F., Vogel, R. F., & Wefers, D. (2018). Structural characterization of the exopolysaccharides from water kefir. *Carbohydrate Polymers, 189*, 296–303.

Forssten, S. D., Björklund, M., & Ouwehand, A. C. (2010). *Streptococcus mutans*, caries and simulation models. *Nutrients, 2*, 290–298.

Hanada, N., & Kuramitsu, H. K. (1988). Isolation and characterization of the *Streptococcus mutans* gtfC gene, coding for synthesis of both soluble and insoluble glucans. *Infection and Immunity, 56*, 1999–2005.

Hanada, N., & Kuramitsu, H. K. (1989). Isolation and characterization of the *Streptococcus mutans* gtfD gene, coding for primer-dependent soluble glucan synthesis. *Infection and Immunity, 57*, 2079–2085.

Hare, M. D., Svensson, S., & Walker, G. J. (1978). Characterization of the extracellular, water-insoluble α-D-glucans of oral *streptococci* by methylation analysis, and by enzymic synthesis and degradation. *Carbohydrate Research, 66*, 245–264.

Hayacibara, M. F., Koo, H., Vacca-Smith, A. M., Kopec, L. K., Scott-Anne, K., Cury, J. A., & Bowen, W. H. (2004). The influence of mutanase and dextranase on the production and structure of glucans synthesized by streptococcal glucosyltransferases. *Carbohydrate Research, 339*, 2127–2137.

He, Q., Kobayashi, K., Kusumi, R., Kimura, S., Enomoto, Y., Yoshida, M., … Wada, M. (2020). In vitro synthesis of branchless linear (1→6)-α-D-glucan by glucosyltransferase K: Mechanical and swelling properties of its hydrogels crosslinked with diglycidyl ethers. *ACS Omega, 5*, 31272–31280.

Hoshino, T., Fujiwara, T., & Kawabata, S. (2012). Evolution of cariogenic character in *Streptococcus mutans*: Horizontal transmission of glycosyl hydrolase family 70 genes. *Scientific Reports, 2*, 518.

Inoue, M., Yakushiji, T., Katsuki, M., Kudo, N., & Koga, T. (1988). Reduction of the adherence of *Streptococcus sobrinus* insoluble alpha-D-glucan by *endo*-(1,3)- α -D-glucanase. *Carbohydrate Research, 182*, 277–286.

Inoue, M., Yakushiji, T., & Takehara, T. (1982). Ultrastructural changes produced in the oral bacterium *Streptococcus mutans* glucans by the action of *endo*- α −1,3-glucanase. *Archives of Oral Biology, 27*, 753–757.

Kobayashi, K., Hasegawa, T., Kusumi, R., Kimura, S., Yoshida, M., Sugiyama, J., & Wada, M. (2017). Characterization of crystalline linear (1→3)-α-d-glucan synthesized in vitro. *Carbohydrate Polymers, 177*, 341–346.

Kobayashi, K., Kimura, S., Heux, L., & Wada, M. (2013). Crystal transition between hydrate and anhydrous (1→3)-β-D-xylan from *Penicillus dumetosus*. *Carbohydrate Polymers, 97*, 105–110.

Kobayashi, K., Kimura, S., Togawa, E., Wada, M., & Kuga, S. (2010). Crystal transition of paramylon with dehydration and hydration. *Carbohydrate Polymers, 80*, 491–497.

Koo, H., Falsetta, M. L., & Klein, M. I. (2013). The exopolysaccharide matrix: A virulence determinant of cariogenic biofilm. *Journal of Dental Research, 92*, 1065–1073.

Kopec, L. K., Vacca-Smith, A. M., & Bowen, W. H. (1997). Structural aspects of glucans formed in solution and on the surface of hydroxyapatite. *Glycobiology, 7*, 929–934.

Kuramitsu, H. K., & Wondrack, L. (1983). Insoluble glucan synthesis by *Streptococcus mutans* serotype c strains. *Infection and Immunity, 42*, 763–770.

Kusumi, R., Asai, S., He, Q., Kobayashi, K., Kimura, S., Yoshida, M., & Wada, M. (2023). α-D-(1→ 3)-graft-(1→ 6)-glucan: Comb-like polysaccharide synthesized *in vitro* with α-1, 3/1, 6-glucosyltransferase L from *Streptococcus salivarius*. *Carbohydrate Research, 534*, Article 108969.

Leemhuis, H., Pijning, T., Dobruchowska, J. M., van Leeuwen, S. S., Kralj, S., Dijkstra, B. W., & Dijkhuizen, L. (2013). Glucansucrases: Three-dimensional structures, reactions, mechanism, α-glucan analysis and their implications in biotechnology and food applications. *Journal of Biotechnology, 163*, 250–272.

Lene, A. P., Koo, H., Bellato, C. M., Bedi, G., & Cury, J. A. (2006). The role of sucrose in cariogenic dental biofilm formation - new insight. *Journal of Dental Research, 85*, 878–887.

Li, X., Wang, X., Meng, X., Dijkhuizen, L., & Liu, W. (2020). Structures, physico-chemical properties, production and (potential) applications of sucrose-derived α-D-glucans synthesized by glucansucrases. *Carbohydrate Polymers, 249*, Article 116818.

Lin, Y., Chen, J., Zhou, X., & Li, Y. (2021). Inhibition of *Streptococcus mutans* biofilm formation by strategies targeting the metabolism of exopolysaccharides. *Critical Reviews in Microbiology, 47*, 667–677.

McIntyre, D. D., & Vogel, H. J. (1991). Nuclear magnetic resonance studies of homopolysaccharides related to starch. *Starch-Starke, 43*, 69–76.

Meng, X., Gangoiti, J., Bai, Y., Pijning, T., Van Leeuwen, S. S., & Dijkhuizen, L. (2016). Structure-function relationships of family GH70 glucansucrase and 4,6-a-glucano-transferase enzymes, and their evolutionary relationships with family GH13 enzymes. *Cellular and Molecular Life Sciences, 73*, 2681–2706.

Minah, G. E., & Loesche, W. J. (1977). Sucrose metabolism by prominent members of the flora isolated from cariogenic and non-cariogenic dental plaques. *Infection and Immunity, 17*, 55–61.

Molina, M., Cioci, G., Moulis, C., Séverac, E., & Remaud-Siméon, M. (2021). Bacterial α-glucan and branching sucrases from GH70 family: Discovery, structure–function relationship studies and engineering. *Microorganisms, 9*, 1607.

Monsan, P., Bozonnet, S., Albenne, C., Joucla, G., Willemot, R.-M., & Remaud-Sinéon, M. (2001). Homopolysaccharides from lactic acid bacteria. *International Dairy Journal, 11*, 675–685.

Münkel, F., Bechtner, J., Eckel, V., Fischer, A., Herbi, F., Jakob, F., & Wefers, D. (2019). Detailed structural characterization of glucans produced by glucansucrases from *Leuconostoc citreum* TMW 2.1194. *Journal of Agricultural and Food Chemistry, 67*, 6856–6866.

Münkel, F., & Wefers, D. (2019). Fine structures of different dextrans assessed by isolation and characterization of endo-dextranase liberated isomalto-oligosaccharides. *Carbohydrate Polymers, 215*, 296–306.

Ogawa, K., Yui, T., Okamura, K., & Misaki, A. (1994). Crystalline features of streptococcal (l→3)- α -D-glucans of human saliva. *Bioscience, Biotechnology, and Biochemistry, 58*, 1326–1327.

Padmanabhan, P. A., Kim, D.-S., Pak, D., & Sim, S. J. (2003). Rheology and gelation of water-insoluble dextran from *Leuconostoc mesenteroides* NRRL B-523. *Carbohydrate Polymers, 53*, 459–468.

Pearce, B. J., Walker, G. J., Slodki, M. E., & Schuerch, C. (1990). Enzymic and methylation analysis of dextrans and 1,3-a-D-glucans. *Carbohydrate Research, 203*, 229–246.

Pidoux, M., Ruiter, G. A. de, Brooker, B. E., Colquhoun, I. J., & Morris, V. J. (1990). Microscopic and chemical studies of a gelling polysaccharide from *Lactobacillus hilgardii*. Carbohydrate Polymers, 13, 351–362.

Pittrof, S. L., Kaufhold, L., Fischer, A., & Wefers, D. (2021). Products released from structurally different dextrans by bacterial and fungal dextranases. *Foods, 10*.

Poulhazan, A., Arnold, A. A., Warschawski, D. E., & Marcotte, I. (2018). Unambiguous ex situ and in cell 2D ^{13}C solid-state NMR characterization of starch and its constituents. *International Journal of Molecular Sciences, 19*, 3817.

Robert, X., & Gouet, P. (2014). Deciphering key features in protein structures with the new ENDscript server. *Nucleic Acids Research, 42*, W320–W324.

Sievers, F., & Higgins, D. G. (2014). Clustal omega. *Current Protocols in Bioinformatics, 48*, 3–13.

Simpson, C. L., Cheetham, N. W. H., Giffard, P. M., & Jacques, N. A. (1995). Four glucosyltransferases, GtfJ, GtfK, GtfL and GtfM, from *Streptococcus salivarius* ATCC 25975. *Microbiology, 141*, 1451–1460.

Sweet, D. P., Shapiro, R. H., & Albersheim, P. (1975). Quantitative analysis by various g. l.c. response-factor theories for partially methylated and partially ethylated alditol acetates. *Carbohydrate Research, 40*, 217–225.

Takahashi, N., & Nyvad, B. (2008). Caries ecology revisited: Microbial dynamics and the caries process. *Caries Research, 42*, 409–418.

Tsunuraya, Y., & Misaki, A. (1979). Structure of the water-insoluble α-D-glucan of *Streptococcus salivarius* HHT. *Carbohydrate Research, 74*, 217–225.

Vacca-Smith, A. M., Venkitaraman, A. R., Quivey, R. G., Jr., & Bowen, W. H. (1996). Interactions of streptococcal glucosyltransferases with α-amylase and starch on the surface of saliva-coated hydroxyapatite. *Archives of Oral Biology, 41*, 291–298.

Wangpaiboon, K., Waiyaseesang, N., Panpetch, P., Charoenwongpaiboon, T., Nepogodiev, S. A., Ekgasit, S., … Pichayangkura, R. (2020). Characterisation of insoluble α-1,3-/α-1,6 mixed linkage glucan produced in addition to soluble α-1,6-linked dextran by glucansucrase (DEX-N) from *Leuconostoc citreum* ABK-1. *International Journal of Biological Macromolecules, 152*, 473–482.

Publikation: *Carbohydrate Polymers*, 337, 122164

Wiater, A., Pleszczyńska, M., Próchniak, K., & Szczodrak, J. (2012). Structural diversity of streptococcal mutans synthesized under different culture and environmental conditions and its effect on mutanase synthesis. *Molecules, 17*, 11800–11815.

Xu, R. R., Yang, W. D., Niu, K. X., Wang, B., & Wang, W. M. (2018). An update on the evolution of glucosyltransferase (Gtf) genes in *Streptococcus*. *Frontiers in Microbiology, 9*, 2979.

Yu, L., Qian, Z., Ge, J., & Du, R. (2022). Glucansucrase produced by lactic acid bacteria: Structure, properties, and applications. *Fermentation, 8*, 629.

Detailed structural characterization of five water-insoluble α-glucans

produced by glucansucrases from *Streptococcus* spp.

<u>Supplementary</u>

Tab. S1. Previously described glucansucrases used for amino acid sequence alignment (Fig. S1) with glucansucrases used for glucan synthesis in this study (SMUT1101, SMUT1102, SSAL4540, SSAL4545 and SSAL4550). The assignment of glucansucrases was based on the results from Fig. S1. GTF: glucosyltransferase.

Glucansucrase	Protein Accession Number	Strain	Glucansucrase of this study
GTF-I (GTF-B)	AFM81411.1	*Streptococcus mutans* GS-5	SMUT1102
GTF-SI (GTF-C)	AFM81412.1		SMUT1101
GTF-K	CAA77898.1	*Streptococcus salivarius* (ATCC 25975)	SSAL4550
GTF-J	AAA26896.1		SSAL4545
GTF-L	AAC41412.1		-
GTF-M	AAC41413.1		-

	SMUT1102	GTF-I	SMUT1101	GTF-SI	SSAL4550	GTF-K	GTF-M	GTF-L	SSAL4545	GTF-J	SSAL4540
SMUT1102	100.00	**99.10**	76.61	75.90	46.77	47.06	49.86	49.85	47.78	47.85	49.51
GTF-I	99.10	100.00	76.18	76.76	46.77	47.38	50.14	49.63	47.78	47.94	49.74
SMUT1101	76.61	76.18	100.00	**98.66**	44.58	44.80	48.20	47.92	46.70	46.78	47.72
GTF-SI	75.90	76.76	98.66	100.00	44.77	45.16	48.84	47.94	46.66	46.71	48.15
SSAL4550	46.77	46.77	44.58	44.77	100.00	**96.47**	46.38	45.88	51.17	50.89	54.40
GTF-K	47.06	47.38	44.80	45.16	96.47	100.00	46.86	46.23	51.53	51.97	54.33
GTF-M	49.86	50.14	48.20	48.84	46.38	46.86	100.00	53.36	44.18	44.74	48.61
GTF-L	49.85	49.63	47.92	47.94	45.88	46.23	53.36	100.00	44.73	45.20	47.71
SSAL4545	47.78	47.78	46.70	46.66	51.17	51.53	44.18	44.73	100.00	**97.22**	58.81
GTF-J	47.85	47.94	46.78	46.71	50.89	51.97	44.74	45.20	97.22	100.00	58.88
SSAL4540	49.51	49.74	47.72	48.15	54.40	54.33	48.61	47.71	58.81	58.88	100.00

Fig. S1. Percent identity matrix of glucansucrases used for amino acid sequence alignment (Tab. S1) and glucansucrases SMUT1101, SMUT1102, SSAL4545, SSAL4550 and SSAL4540. GTF: glucosyltransferase.

Fig. S2. Sequence alignment of glucansucrases SMUT1101, SMUT1102, SSAL4540, SSAL4545 and SSAL4550 with sequences of glucansucrases GTF-K, GTF-J, GTF-L and GTF-M from *Streptococcus salivarius* as well as GTF-I and GTF-SI from *Streptococcus mutans*. Conserved regions II, III and IV harboring the three catalytic amino acids are shown. Nu: nucleophile, A/B: acid/base, TS: transition state stabilizer.
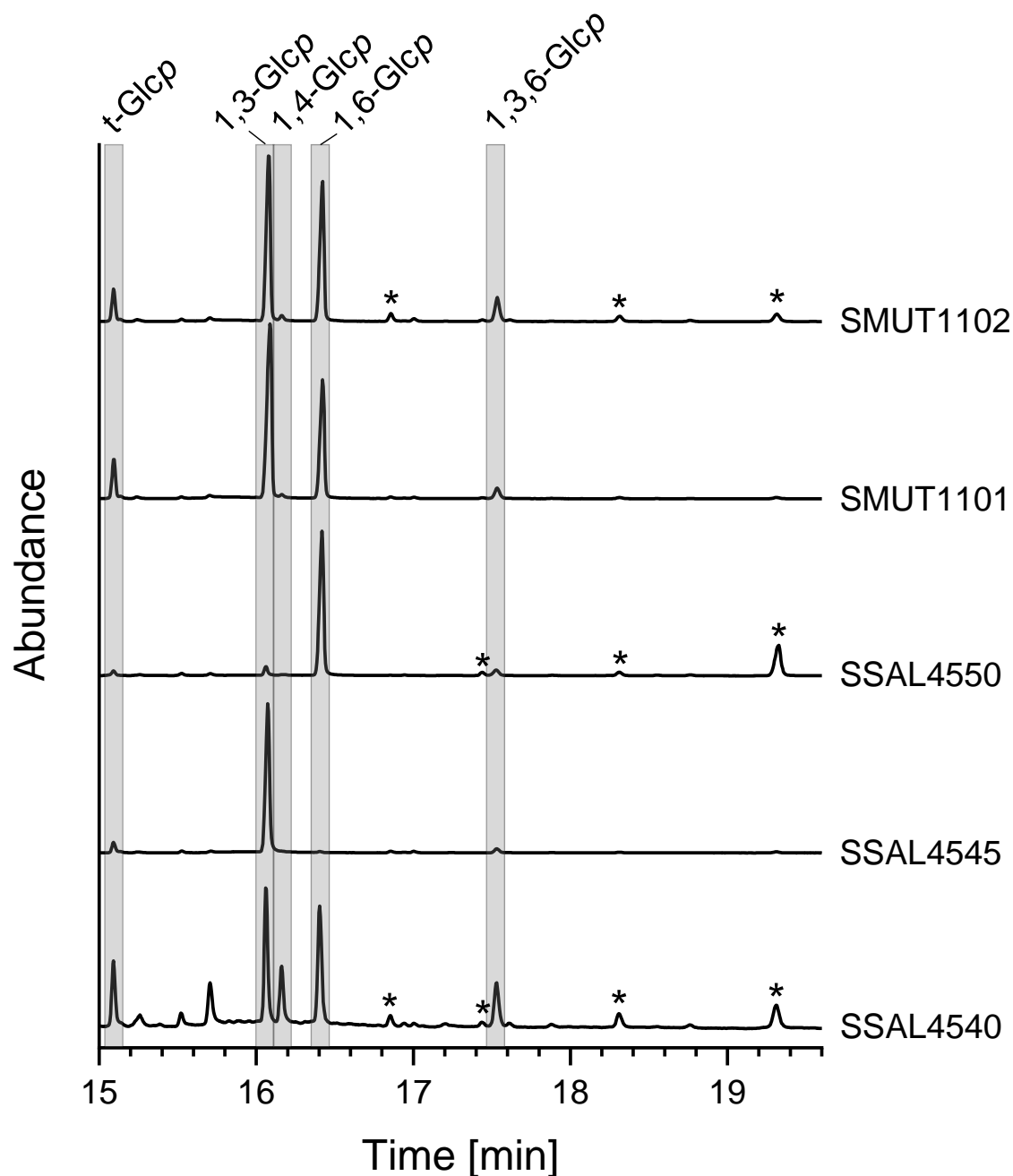
Fig. S3. GC-MS chromatograms of partially methylated alditol acetates (PMAA) derived from glucans produced by glucansucrases SMUT1101, SMUT1102, SSAL4545, SSAL4550 and SSAL4540. Peaks were identified by their mass spectra (Fig. S4) and assigned with the corresponding glycosidic linkages of glucopyranose (Glc*p*) units. Peaks marked with an asterisk are artifacts which are derived from the sample workup. Unassigned artifacts did not contain typical PMAA-derived fragments. t: terminal, the numbers indicate the position of substitution.
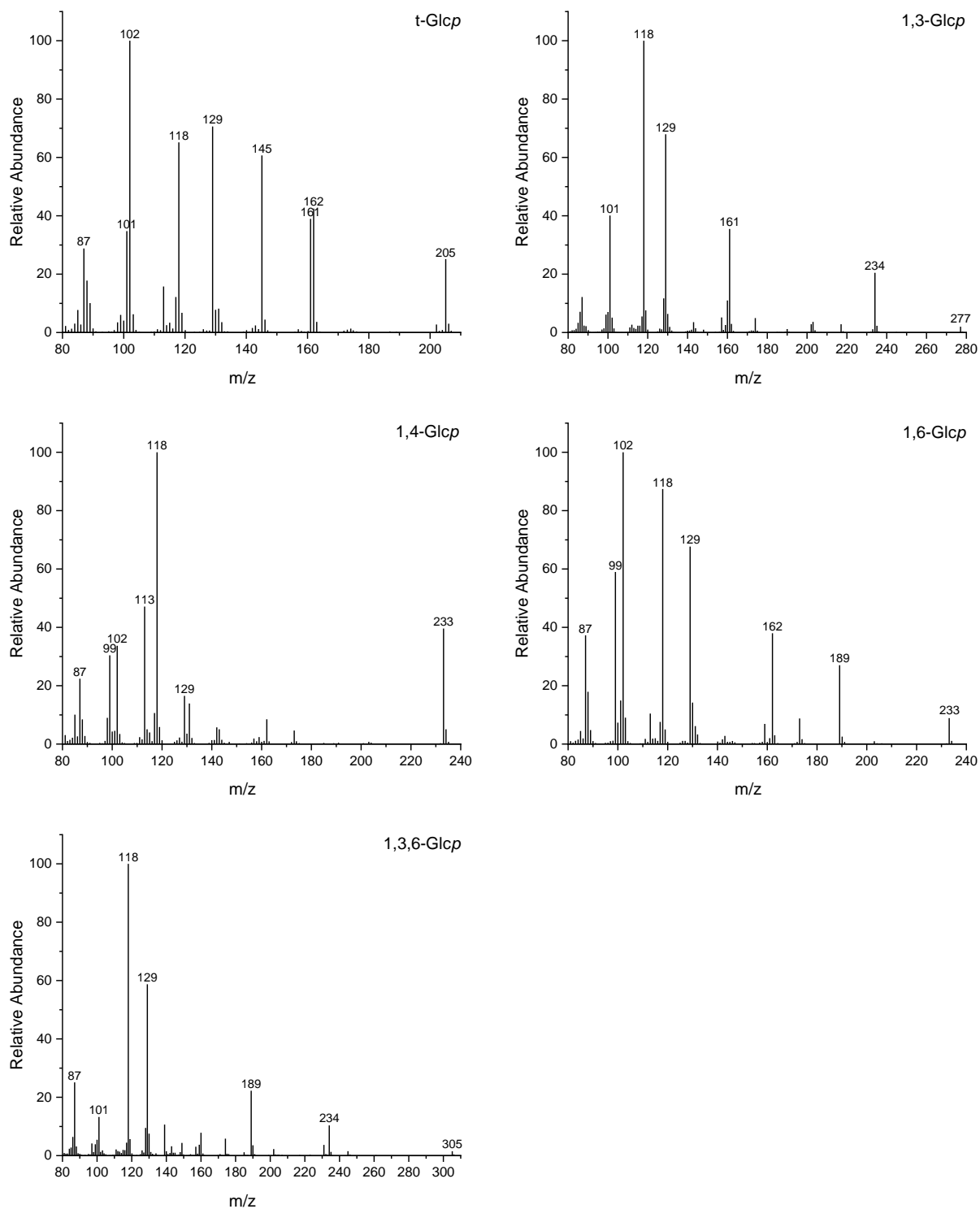
Fig. S4. EI mass spectra of partially methylated alditol acetates (PMAA) derived from variously linked glucopyranose (Glc*p*) units. t: terminal, the numbers indicate the position of substitution.
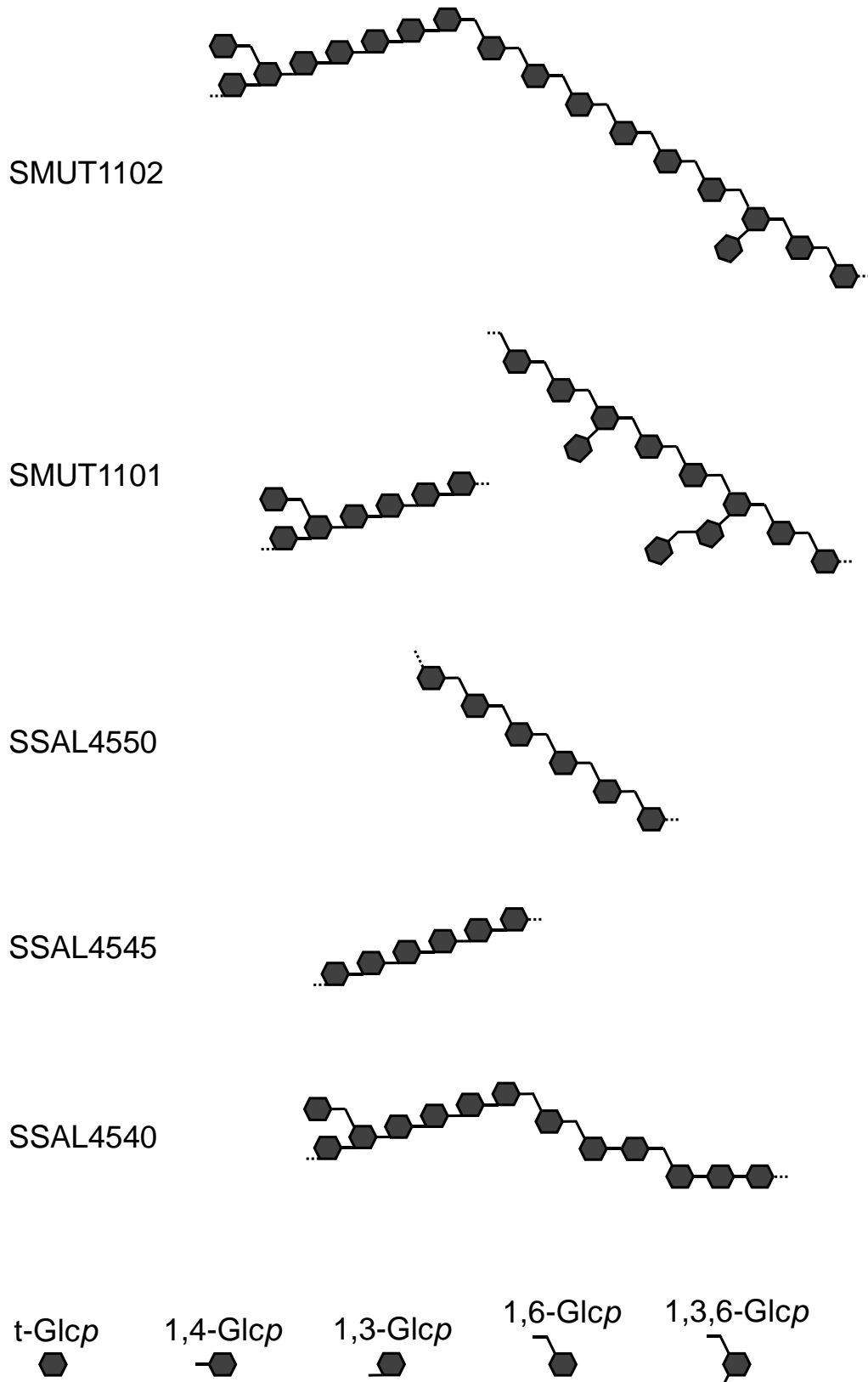
Fig. S5. Schematic segments of glucans produced by glucansucrases SMUT1101, SMUT1102, SSAL4545, SSAL4550 and SSAL4540 based on the structural analysis conducted in this study. Glc*p*: glucopyranose, t: terminal, the numbers indicate the position of substitution.

Publikation: *Carbohydrate Polymers*, 323, 121417

Comprehensive structural characterization of water-soluble and water-insoluble homoexopolysaccharides from seven lactic acid bacteria

Luise Ernst, Hanna Offermann, Annemarie Werner, Daniel Wefers[*]

Institute of Chemistry, Food Chemistry, Martin Luther University Halle-Wittenberg, 06120 Halle (Saale), Germany

ABSTRACT

Several lactic acid bacteria are able to produce water-soluble and water-insoluble homoexopolysaccharides (HoEPS) from sucrose. In this study, structures of all HoEPS which were fermentatively produced by *Leuconostoc mesenteroides* subsp. *dextranicum* NRRL B-1121 and B-1144, *Leuconostoc mesenteroides* subsp. *mesenteroides* NRRL B-1149, B-1438 and B-1118, *Leuconostoc suionicum* DSM 20241, and *Liquorilactobacillus satsumensis* DSM 16230 were systematically analyzed. Monosaccharide analysis, methylation analysis, NMR spectroscopy, size-exclusion chromatography, and different enzymatic fingerprinting methods were used to obtain detailed structural information. All strains produced water-soluble dextrans and/or levans as well as water-insoluble glucans. Levans showed different degrees of branching and high molecular weights, whereas dextrans had comparable structures and broader size distributions. Fine structures of water-soluble HoEPS were analyzed after *endo*-dextranase and *endo*-levanase hydrolysis. Water-insoluble glucans were composed of different portions of 1,3-linkages (5 to 40 %). Hydrolysis with *endo*-dextranase and *endo*-mutanase yielded further information on block sizes and varying fine structures. Overall, clear differences between HoEPS yields and structures were observed.

1. Introduction

Several lactic acid bacteria produce exopolysaccharides (EPS) with different structural characteristics and physicochemical properties. These exopolysaccharides are of particular interest, because lactic acid bacteria are widely spread, considered safe, and used by humans to produce fermented foods. Apart from potential health promoting properties, exopolysaccharides have different potential applications as hydrocolloids and dietary fiber in foods (Monsan et al., 2001; Zannini, Waters, Coffey, & Arendt, 2016). Because their applicability depends on the chemical structure, elucidation of monosaccharide compositions, molecular weights and linkage types as well as fine structures of exopolysaccharides is important.

Although some lactic acid bacteria synthesize heteroexopolysaccharides (HeEPS), the formation of homoexopolysaccharides (HoEPS) from sucrose by extracellular glucan- und fructansucrases is most common. These enzymes belong to glycoside hydrolase (GH)

families 70 and 68 and synthesize α-glucans and β-fructans, respectively (van Hijum, Kralj, Ozimek, Dijkhuizen, & van Geel-Schutten, 2006).

β-fructans can be classified into inulins, which are composed of β-1,2-linked fructofuranoses (Fru*f*) with ramifications at position *O*6, and levans, which are composed of β-2,6-linked Fru*f* with ramifications at position *O*2 (Monsan et al., 2001; van Hijum et al., 2006). Structure elucidation of selected bacterial fructans was performed in several studies (Bouallegue et al., 2020; Haddar et al., 2021; Han & Clarke, 1990; Hancock, Marshall, & Weigel, 1976; Pei, Ma, Chen, & Liu, 2020; Shi, Hou, Xu, Mørkeberg Krogh, & Tenkanen, 2019; Simms, Boyko, & Edwards, 1990).

Generally, bacterial α-glucans have a high structural diversity: They are composed of glucopyranoses (Glc*p*) which form a backbone with 1,3-, 1,4-, or 1,6-linkages. This backbone can be branched at different positions and to varying extents, whereas monomeric as well as di- and oligomeric side chains may occur (Ebisu, Misaki, Kato, & Kotani, 1974; Hare, Svensson, & Walker, 1978; Inoue, Yakushiji, Katsuki, Kudo, &

Publikation: *Carbohydrate Polymers*, 323, 121417

L. Ernst et al.

Koga, 1988; Münkel et al., 2019; Münkel & Wefers, 2019; Wiater, Choma, & Szczodrak, 1999). Glucans with a 1,6-linked backbone are referred to as dextrans, whereas glucans which contain mainly 1,3-linked Glc*p* backbone units are often called mutans. The backbone structure significantly influences water solubility: while dextrans are water-soluble, a certain amount and distribution of α-1,3-linkages leads to water-insoluble glucans. Although the exact criteria are not yet fully understood, sections with consecutive 1,3-linkages seem to be an important aspect for water-insolubility (Côté, Ahlgren, & Smith, 1999; Côté & Leathers, 2009; Hare et al., 1978; Tsumuraya & Misaki, 1979; Wiater et al., 1999; Wiater, Pleszczyńska, Próchniak, & Szczodrak, 2012). A first comprehensive attempt to analyze and compare structures of water-soluble and water-insoluble glucans from multiple bacterial strains was performed by Jeanes et al. (1954). Later on, several comparative studies regarding the structure of different glucans were published (Jeanes, Haynes, & Wilham, 1955; Pearce, Walker, Slodki, & Schuerch, 1990; Slodki, England, Plattner, & Dick, 1986). However, these investigations were based on only one or two analytical methods, such as methylation analysis, appearance, viscosity, and the amount of main enzymatically released products. Nevertheless, details on the molecular structure were not obtained by using these methods. In particular, detailed structural characterization of water-insoluble glucans was only performed for a small number of selected strains and enzymes (Côté et al., 1999; Côté & Leathers, 2009; Côté & Skory, 2012; Ebisu et al., 1974; Funane et al., 2001; Hare et al., 1978; Inoue et al., 1988; Tsumuraya & Misaki, 1979; Wangpaiboon et al., 2020; Wiater et al., 1999).

Strains of the genera *Streptococcus*, *Lactobacillus*, and *Leuconostoc* produce water-insoluble α-glucans as well as water-soluble dextrans and/or fructans (Díaz-Montes, 2021; Hare et al., 1978; Korakli & Vogel, 2006; Kralj et al., 2004; Monsan et al., 2001; Morales-Arrieta, Rodríguez, Segovia, López-Munguía, & Olvera-Carranza, 2006; Münkel & Wefers, 2019; Zahnley & Smith, 1995). Thus, to understand the overall production of HoEPS by a single bacterial strain, investigations on glucan and fructan yields and structures are crucial. Birkhed, Rosell, and Granath (1979) for example investigated the water-soluble HoEPS from several *Streptococcus* strains. They analyzed monosaccharide compositions and glycosidic linkages by methylation analysis as well as

molecular weight distributions by gel chromatography. They found both inulin-type and levan-type fructans as well as dextrans with different molecular weights. For HoEPS of *Lactobacillus* and *Leuconostoc* strains, comprehensive studies have not been conducted, yet. Therefore, the aim of this study was to extend our knowledge of the compositions and fine structures of water-soluble and water-insoluble HoEPS synthesized by different strains of *Lactobacillus* and *Leuconostoc*. Our hypothesis was that *Leuconostoc mesenteroides* subsp. *mesenteroides* and subsp. *dextranicum* as well as *Leuconostoc suionicum* and *Liquorilactobacillus satsumensis* produce different amounts of water-soluble and water-insoluble HoEPS which differ in their linkage compositions as well as their fine structures. We selected seven strains for which only limited information on HoEPS composition and structure has been published (reviewed in Table 1). For structural characterization, several analytical approaches, including enzymatic hydrolysis, mono- and oligosaccharide analysis, high performance size exclusion chromatography and methylation analysis were used. From the application and combination of these methods we obtained detailed and comprehensive information on the polysaccharide structures.

2. Experimental

2.1. Materials

The bacteria used in this study were obtained from two culture collections: Agricultural Research Service Culture Collection (NRRL), Peoria, IL, USA and German Collection of Microorganisms and Cell Cultures (DSMZ) GmbH, Braunschweig, Germany. If not stated otherwise, all chemicals used were of "p.a." grade or better and were purchased from Carl Roth (Karlsruhe, Germany), Merck (Darmstadt, Germany), Thermo Fisher Scientific (Waltham, MA USA), VWR (Darmstadt, Germany) and Grüssing GmbH (Filsum, Germany). *Endo*-dextranase (EC 3.2.1.11) from *Chaetomium* sp., 8000 U/mL was purchased from Megazyme (Bray, Ireland). *Endo*-levanase BT1760 (EC 3.2.1.65, accession number AAO76867.1) from *Bacteroides thetaiotaomicron* DSM 2079 (Mardo et al., 2017) and *endo*-mutanase SSAL4105 (EC 3.2.1.59, accession number AIY20934.1) from *Streptococcus salivarius* DSM 20560 were obtained by amplification of the corresponding

Table 1
Strains used in this study and literature data on their HoEPS. NRRL: Agricultural research service collection, DSM: German Collection of Microorganisms and Cell Cultures GmbH, Glc*p*: Glucopyranose, GH: Glycoside hydrolase.

Leuconostoc mesenteroides subsp. *dextranicum*		
NRRL B-1121	Glucans: 20–30 % 1,3-linked, water-insoluble, 50 % is solubilized by mutanase	(Jeanes et al., 1954; Pearce et al., 1990)
NRRL B-1144	Glucans: 5 % 1,3-linkages, water-soluble	(Jeanes et al., 1954)

Leuconostoc mesenteroides subsp. *mesenteroides*		
NRRL B-1149	Active glucan- and fructansucrase (identity of fructans unknown); water-insoluble glucans: 40 % 1,3-linkages, incompletely solubilized by mutanase (80 %), no 1,3,6-linked branched units, long sequences of 1,3-Glc*p*	(Jeanes et al., 1954; Pearce et al., 1990; Seymour & Knapp, 1980; Shukla et al., 2011; Shukla & Goyal, 2013; Slodki et al., 1986)
NRRL B-1438	Glucans: 10–20 % 1,3-linkages, water-insoluble & water-soluble, completely solubilized by mutanase	(Jeanes et al., 1954; Jeanes et al., 1955; Pearce et al., 1990)
NRRL B-1118	More water-insoluble than water-soluble glucans; water-insoluble glucans: 10–20 % 1,3-linkages, completely solubilized by mutanase; recombinant glucansucrase: water-insoluble glucans with equal amounts of 1,3 and 1,6-linkages, probably both in long sequences; recombinant levansucrase: levans (molecular weight: 10^6 Da)	(Côté & Skory, 2012, 2016; Côté, Skory, Unser, & Rich, 2013; Jeanes et al., 1954; Olvera, Centeno-Leija, & López-Munguía, 2007; Pearce et al., 1990; Slodki et al., 1986)

Leuconostoc suionicum		
DSM 20241	Active dextransucrase (products unknown)	(Chun, Lee, Jeon, Kim, & Jeon, 2017; Nolte, Kempa, Schlockermann, Hochgürtel, & Schörken, 2019)

Liquorilactobacillus satsumensis		
DSM 16230	Produces water-insoluble polysaccharide from sucrose; Encodes for GH70, GH13 enzymes, but no GH68 enzyme	(Côté et al., 2013; Sun et al., 2015)

2

Publikation: *Carbohydrate Polymers*, 323, 121417

L. Ernst et al.

genes by PCR (genomic DNA was purchased from DSMZ), molecular cloning of the genes, and heterologous expression of the recombinant proteins in *E. coli*. A detailed description of the protocol is given by Münkel et al. (2019). Only minor modifications were applied in this study. The annealed gene-vector product of the *endo*-levanase encoding gene was transformed to 5α-competent *E. coli* cells (High efficiency, NEB, USA), cell lysis was performed using a sonifier (SFX250, Branson Ultrasonics Corporation USA), and proteins were purified with HisPur Ni-NTA resin (Thermo Fisher Scientific).

2.2. Exopolysaccharide synthesis and isolation

Lactic acid bacteria were cultured in MRS medium (10 g/L soy peptone, 10 g/L meat extract, 5 g/L yeast extract, 1 g/L Tween80, 2 g/L dipotassium phosphate, 5 g/L sodium acetate, 2 g/L diammonium citrate, 0.2 g/L magnesium sulfate, 0.05 g/L manganese sulfate, pH 6.2) as described by Münkel et al. (2019). An overnight preculture was grown statically at 30 °C in MRS4 medium (MRS supplemented with 5 g/L glucose, 5 g/L fructose and 10 g/L maltose). HoEPS production was achieved by inoculating MRSSuc medium (MRS supplemented with 80 g/L sucrose) with 10 mL of the preculture in a 1 L Schott flask, filling up to the lip with MRSSuc, sealing, and incubating for 30 h at 30 °C and shaking at 70 rpm.

For HoEPS isolation, cultures were first centrifuged for 10 min at 3328 rcf. The resulting residues (containing water-insoluble HoEPS and cells) were washed with ultrapure water until the supernatants were colorless and clear. To precipitate water-soluble HoEPS from the combined supernatants two volumes of ethanol (96 % v/v) were added, the mixture was cooled to 4 °C and incubated overnight. Precipitated water-soluble HoEPS were collected by centrifugation as described above, redissolved in 1 M NaOH, and centrifuged to remove the water-insoluble residue. The supernatant was neutralized with HCl, dialyzed against water for 48 h (molecular weight cut off: 14 kDa) and lyophilized to obtain the water-soluble HoEPS fractions.

HoEPS in the water-insoluble residue containing cells obtained from the first centrifugation step were dissolved in 1 M NaOH and cell debris were removed by centrifugation (30 min, 3328 rcf). The supernatants were neutralized with HCl and precipitated as described above. Precipitates were recovered by centrifugation, dialyzed against water for 48 h (molecular weight cut off: 14 kDa), and lyophilized to obtain the water-insoluble HoEPS fractions. Yields of water-soluble and water-insoluble fractions were quantified by weighing the dried HoEPS.

2.3. Monosaccharide composition analysis

The monosaccharide composition of the isolated HoEPS was determined after two different trifluoroacetic acid (TFA) hydrolyses. In the case of water-soluble HoEPS, an aliquot (containing 20 µg polysaccharide) of an aqueous solution was dried prior to TFA hydrolysis. For water-insoluble HoEPS about 1 mg of the dried sample was directly hydrolyzed. The samples were hydrolyzed with 500 µL of 2 M TFA for 60 min at 121 °C for glucose determination and with 500 µL of 1 M TFA for 30 min at 70 °C for fructose determination. In both cases, TFA was removed by evaporation and subsequent co-evaporation with ethanol. The dried samples were redissolved in ultrapure water and analyzed by high performance anion exchange chromatography with pulsed amperometric detection (HPAEC-PAD) on an ICS-3000 system (Thermo Fisher Scientific, Sunnyvale, CA, USA). Separation was achieved by using a CarboPac PA20 column (150 mm × 3 mm i.d., 6.5 µm particle size, Thermo Fisher Scientific) and quantification was performed by using an external calibration. The column temperature was 30 °C and the detector temperature was 25 °C. The following gradient with a flow rate of 0.4 mL/min was used: column equilibration with 10 mM NaOH for 15 min prior to every run; 0–20 min: Isocratic 10 mM NaOH; 20–30 min: Linear gradient from 10 mM NaOH to 200 mM NaOH; 30–40 min: Isocratic 200 mM NaOH + 200 mM sodium acetate; 40–50 min: Isocratic

200 mM NaOH.

2.4. Enzymatic hydrolyses and oligosaccharide analysis

2.4.1. Endo-dextranase hydrolysis

Small amounts (1 mg) of water-soluble HoEPS were hydrolyzed, whereas water-insoluble HoEPS were hydrolyzed on a larger scale (200 mg). This was necessary because the residue obtained from the hydrolysis of water-insoluble glucans was further investigated (see below). For the hydrolysis a 1 mg/mL sample solution/dispersion was incubated with *endo*-dextranase (5 U/mg sample) for 24 h at 40 °C and shaken at 400 rpm (small scale) or 150 rpm (large scale). The enzyme was inactivated by heating to 95 °C for 15 min. Samples were centrifuged and the supernatant was analyzed by HPAEC-PAD as described in Section 2.4.4. The water-insoluble residue after hydrolysis of the water-insoluble HoEPS was washed with ultrapure water, an aliquot was hydrolyzed with *endo*-mutanase (Section 2.4.2), and the remaining water-insoluble residue was lyophilized and weighed for semiquantification.

2.4.2. Endo-mutanase hydrolysis of water-insoluble products after endo-dextranase hydrolysis of water-insoluble HoEPS

About 1 mg of wet, water-insoluble residue from *endo*-dextranase treatment was suspended in 100 µL of ultrapure water and incubated with 60 µg of *endo*-mutanase (obtained from heterologous expression) for 24 h at 37 °C and 200 rpm. The enzyme was inactivated by the addition of two volumes of ethanol. Ethanol was evaporated for 2 h at 45 °C under vacuum and the sample was resuspended in 100 µL of ultrapure water. After centrifugation the supernatant was analyzed by HPAEC-PAD/mass spectrometry (MS) as described in Section 2.4.4.

2.4.3. Endo-levanase hydrolysis of water-soluble HoEPS

300 µL of a 3 mg/mL aqueous solution of water-soluble HoEPS was incubated with 40 µg of *endo*-levanase (obtained from heterologous expression) for 24 h at 40 °C and 400 rpm. Inactivation was achieved by heating to 95 °C for 15 min and protein was removed by centrifugation. The supernatant was analyzed by HPAEC-PAD/MS (Section 2.4.4).

2.4.4. Analysis of enzymatically liberated oligosaccharides

Enzymatically hydrolyzed samples were analyzed by HPAEC-PAD on an ICS-6000 system (Thermo Fisher Scientific) equipped with a Carbo-Pac PA200 column (250 × 3 mm i.d., 5.5 µm particle size, Thermo Fisher Scientific). Temperatures and flow rate are described in Section 2.3. The following gradient composed of four eluents (A: ultrapure water, B: 10 mM NaOH, C: 200 mM NaOH, D: 200 mM NaOH + 500 mM sodium acetate) was used for separation: column equilibration with 100 % B for 20 min prior to every run; 0–10 min: Isocratic 100 % B; 10–20 min: Linear gradient to 50 % C + 50 % A; 20–45 min: Linear gradient to 50 % A, 30 % C + 20 % D; 45–55 min: Linear gradient to 50 % A + 50 % D; 55–65 min: Linear gradient to 100 % D; 65–80 min: Isocratic 100 % D; 80–95 min: Isocratic 100 % C.

Oligosaccharides from dextranase hydrolysis were identified via comparison of their retention times to the oligosaccharides described by Münkel et al. (2019). To identify unknown oligosaccharides released by mutanase and levanase, HPAEC-PAD was coupled to an LTQ-XL linear ion trap mass spectrometer (Thermo Fisher Scientific). A post column split allowed simultaneous PAD and MS analysis. Prior to MS analysis, desalting of the eluent was achieved by an AERS 500e suppressor (4 mm, Thermo Fisher Scientific). To facilitate ionization by electrospray ionization (ESI), 500 µM LiCl was added at a flow rate of 0.05 mL/min (AXP-MS pump, Thermo Fisher Scientific). The source temperature was 300 °C and lithium adducts of oligosaccharides were detected in positive mode.

2.5. Methylation analysis

Methylation analysis of water-soluble and water-insoluble fractions as well as water-insoluble residues after *endo*-dextranase hydrolysis of

Publikation: *Carbohydrate Polymers*, 323, 121417

L. Ernst et al.

water-insoluble glucans was carried out as described in detail by Ernst, Werner, and Wefers (2023). In brief, all samples were methylated by methyl iodide in dimethyl sulfoxide (DMSO)/NaOH(s). An ultrasonic treatment was used to dissolve/swell the sample in DMSO and a second ultrasonication was carried out after addition of NaOH. Methylation was repeated once and different hydrolysis procedures were used for the HoEPS fractions. Water-insoluble samples were hydrolyzed with 2 M TFA for 60 min at 121 °C and water-soluble HoEPS were methylated and hydrolyzed in two batches: One batch was hydrolyzed with 1 M TFA for 30 min at 70 °C to analyze partially methylated alditol acetates (PMAAs) derived from fructans. The second batch was hydrolyzed with 3 M TFA for 90 min at 121 °C to obtain information on glucans. Partially methylated monosaccharides were reduced by using $NaBD_4$ and acetylated by using acetic anhydride and 1-methylimidazole. PMAAs were separated by gas chromatography (GC), identified by their mass spectra and quantified by flame ionization detection (FID). The molar response factors described by Sweet, Shapiro, and Albersheim (1975) were used.

2.6. High performance size exclusion chromatography with refractive index detection (HPSEC-RI)

HPSEC-RI analysis of water-insoluble HoEPS and the water-insoluble residues, which resulted from *endo*-dextranase hydrolysis, was conducted on an HPLC-RI system (P6.1L, AS6.1L, RID 2.1L, Knauer, Germany) equipped with a GRAM column (300 × 8 mm, particle size 10 μm) (PSS, Germany). DMSO with 100 mM LiCl was used as eluent at a flow rate of 0.2 mL/min. Column temperature was 80 °C and RI temperature was 35 °C. Samples were solubilized as follows: 1 mg of lyophilized water-insoluble glucans and water-insoluble residues were swollen in 500 μL of DMSO by shaking overnight at 60 °C and 1500 rpm. Subsequently, 2 mg of LiCl(s) were added (resulting concentration: 100 mM LiCl) and the samples were shaken overnight (60 °C, 1500 rpm). A second LiCl(s) addition (2 mg) was conducted, the samples were again shaken overnight at 60 °C and 1500 rpm and finally 500 μL of DMSO was added to obtain a concentration of 100 mM LiCl. This procedure allowed for the dissolution of all water-insoluble glucans. The molecular weight of the glucan samples was estimated by using standard dextrans with known molecular weight (dextran blue, 670 kDa, 270 kDa and 12 kDa, Sigma Aldrich, Germany; 64.3 kDa, PSS, Germany).

For HPSEC-RI analysis of water-soluble HoEPS, an Agilent 1100 Series HPLC equipped with a 1260 Infinity II refractive index detector and a TSKgel G5000 PW_{XL} column (300 × 7.8 mm, particle size 10 μm; TOSOH, Japan) was used. Water-soluble HoEPS were dissolved in ultrapure water (final concentration: 1 mg/mL) and filtered (syringe filter 0,45 μm, Nylon). Ultrapure water supplemented with 0.5 g/L NaN_3 as preservative was used as eluent at a flow rate of 0.4 mL/min at 40 °C. RI detector temperature was 35 °C.

2.7. ^1H NMR spectroscopy

Water-soluble HoEPS were analyzed by ^1H NMR spectroscopy on a 400 MHz VNMRS or a 500 MHz DD2 spectrometer (Agilent, Santa Clara, CA, USA). Freeze-dried samples were solubilized in D_2O (10–20 mg/mL) and acetone was added as reference (referenced to 2.22 ppm according to Gottlieb, Kotlyar, and Nudelman (1997)).

3. Results and discussion

Seven lactic acid bacteria strains were selected for the production of water-soluble and water-insoluble HoEPS (Table 1). HoEPS synthesis was performed under identical conditions and absolute yields of water-soluble and water-insoluble HoEPS fractions varied from 0.2 to 15.5 g/L culture (Fig. 1). Total HoEPS yields varied from 5 to 22 g/L, which was equivalent to 13–55 % of the maximum yield of 40 g/L (calculated from the amount of available sucrose in the cultures). Jeanes et al. (1954 and 1955) described yields of up to 10 % of the available sucrose for strains
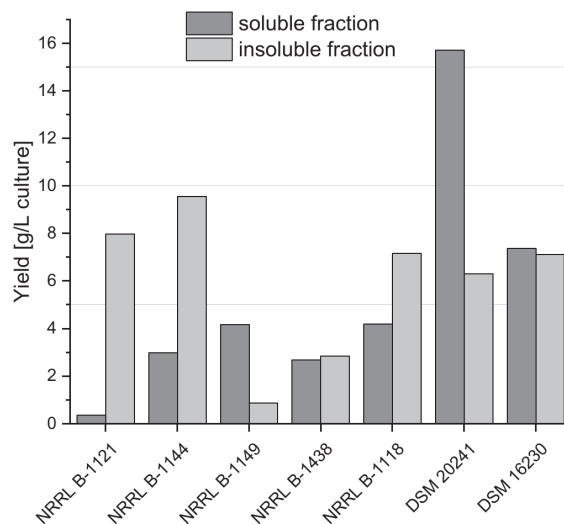
Fig. 1. Absolute yields of isolated water-soluble and water-insoluble HoEPS fractions obtained from 1 L of culture of the seven lactic acid bacteria strains used in this study (Table 1). Yields were determined gravimetrically.

NRRL B-1121, B-1144, B-1149, B-1438, and B-1118, whereas other strains used up to 30 % of the available sucrose for dextran synthesis. However, it must also be considered that HoEPS yields may vary considerably when the incubation conditions are modified. Nevertheless, high yields are a basic requirement for applications as hydrocolloids or dietary fiber. In this regard, strains NRRL B-1144, B-1118, DSM 20241, and DSM 16230 which in total used at least 25 % of the available sucrose for HoEPS production are promising candidates for HoEPS yield optimization.

Notably, varying relative yields of water-soluble and water-insoluble HoEPS were obtained for individual strains. NRRL B-1149 and DSM 20241 synthesized mainly water-soluble HoEPS. NRRL B-1438 and DSM 16230 produced equal amounts of water-soluble and water-insoluble HoEPS, whereas higher portions of water-insoluble HoEPS were obtained from NRRL B-1121, B-1144, and B-1118. For NRRL B-1118, Côté et al. (2013) also described the production of more water-insoluble than water-soluble glucans and for NRRL B-1438, Jeanes et al. (1955) found more water-insoluble than water-soluble dextrans. As described above, differences may occur due to different culture conditions. For the other strains used in this study, relative yields have not been described previously. However, water-soluble HoEPS production was known for NRRL B-1144, and water-insoluble HoEPS production has been described for NRRL B-1121, B-1149, B-1438, B-1118 and DSM 16230 (see Table 1). In this study, all strains produced water-soluble and water-insoluble HoEPS, and thus several HoEPS fractions have not been considered yet. Therefore, the water-soluble as well as the water-insoluble HoEPS were analyzed separately for their monosaccharide composition, linkage types, enzymatically released oligosaccharides, and molecular sizes.

3.1. Water-soluble HoEPS

3.1.1. Monosaccharide composition of water-soluble HoEPS

To obtain basic information on the identity of the water-soluble HoEPS, the monosaccharide compositions were analyzed by HPAEC-PAD after TFA hydrolysis. The results are shown in Fig. 2. All HoEPS were composed of glucose and/or fructose which demonstrated that water-soluble glucans and/or fructans were present. All detected monosaccharides were released from polysaccharides because no free

Publikation: *Carbohydrate Polymers*, 323, 121417

L. Ernst et al.
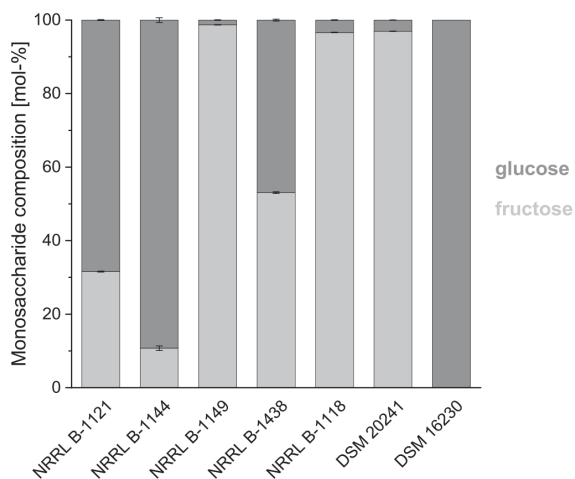
Fig. 2. Monosaccharide composition of water-soluble HoEPS obtained from the seven lactic acid bacteria strains used in this study (Table 1). Monosaccharides were analyzed by HPAEC-PAD after two TFA hydrolyses (glucose: 2 M TFA, 121 °C, 60 min; fructose: 1 M TFA, 70 °C, 30 min). All analyses were performed in duplicate.

monosaccharides or oligosaccharides were detected when the untreated HoEPS were analyzed by HPAEC-PAD. Galactose and mannose were only detected in trace amounts which demonstrates that media components were efficiently removed.

From the portions of the corresponding monosaccharides, it was concluded that glucans, fructans, and mixtures of both polysaccharides were present: Water-soluble HoEPS from strains NRRL B-1149, B-1118, and DSM 20241 consisted mainly of fructans, whereas HoEPS of DSM 16230 were glucans. Strains NRRL B-1121, B-1144 and B-1438 synthesized both, water-soluble glucans and fructans.

The expression of levansucrases is known for NRRL B-1149, and B-1118 (Table 1), but synthesis of fructans by strains NRRL B-1121, B-1144, B-1438, and DSM 20241 was not expected. According to the

literature in Table 1, all seven strains were expected to synthesize water-soluble or water-insoluble glucans. While all strains indeed formed water-insoluble glucans (Section 3.2), water-soluble glucans were solely described for NRRL B-1144, B-1438, and B-1118. In particular, DSM 16230 produced high amounts of water-soluble glucans, whereas DSM 20241 produced high amounts of fructans (Figs. 1 and 2).

3.1.2. Methylation analysis of water-soluble HoEPS

Methylation analysis was carried out to obtain information on the glycosidic linkages of water-soluble HoEPS. Different conditions were used to analyze the individual HoEPS (see Section 2.5), because glucans, fructans, and mixtures of both polysaccharides were obtained. In a previous study, we showed that the applied hydrolysis conditions are suitable to determine the linkage composition of each HoEPS individually and in a mixture of both (Ernst et al., 2023). PMAAs derived from fructans were detected in all samples except for the water-soluble fraction of DSM 16230, which was in good agreement with the results from monosaccharide analysis (see Section 3.1.1). All fructans were composed of 2,6-linked, 1,2,6-linked, and terminal Fru$f$ units which demonstrated that levan-type fructans were present. However, the portions of the individual PMAAs varied considerably. To describe the overall structure of the levans, the degree of branching was calculated from the ratio of branched backbone units (1,2,6-Fru$f$) and total backbone units (2,6-Fru$f$ + 1,2,6-Fru$f$). The degree of branching varied between 7 % and 24 % which demonstrated considerable structural differences between levans (Fig. 3A).

The results for water-soluble glucans produced by NRRL B-1121, B-1144, B-1438, and DSM 16230 showed that all glucans were composed of comparable portions of 1,6-linked Glc$p$ units and 1,3,6-linked Glc$p$ units (Fig. 3B). Furthermore, small portions (about 5 %) of 1,3-linked Glc$p$ units were detected. Thus, all water-soluble glucans were dextrans with side chains at position $O3$ and small portions of 1,3-linked units. ^{1}H NMR spectra (Fig. S1) also confirmed the presence of dextrans and levans in water-soluble HoEPS fractions. The linkage type composition of dextrans is comparable to that of many other dextrans from *Leuconostoc* and *Lactobacillus* (Coté et al., 2013; Jeanes et al., 1954; Monsan et al., 2001; Pearce et al., 1990; Slodki et al., 1986), wheares levans possessing high portions of branch points up to 24 % are rather rare (Bouallegue et al., 2020; Haddar et al., 2021; Han & Clarke, 1990;
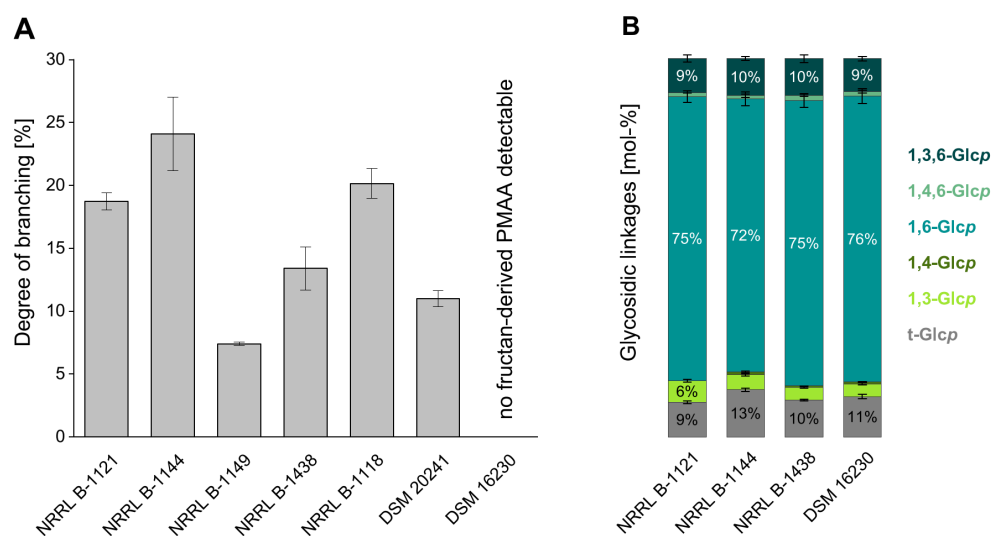
Fig. 3. Glycosidic linkages (determined by methylation analysis) of water-soluble HoEPS from seven lactic acid bacteria strains (see Table 1). A: Degree of branching of levans (calculated by dividing branched units (1,2,6-Fru$f$) by all backbone units (1,2,6-Fru$f$ and 2,6-Fru$f$)). B: Portions of glucose glycosidic linkages. t: terminal, Glc$p$: glucopyranose, numbers indicate the position of substitution in the monosaccharide unit. All analyses were performed in duplicate.

5

Publikation: *Carbohydrate Polymers*, 323, 121417

Hancock et al., 1976; Simms et al., 1990). Thus, investigation of their physiochemical properties could improve the understanding of the effect of side chains in levans.

3.1.3. Endo-dextranase and endo-levanase hydrolysis of water-soluble HoEPS

To obtain information on the dextran and levan fine structures, HoEPS were hydrolyzed with *endo*-dextranase and *endo*-levanase, respectively. Released oligosaccharides were analyzed by HPAEC-PAD and identified by reference standard oligosaccharides in the case of gluco-oligosaccharides (Münkel et al., 2019; Münkel & Wefers, 2019) or by mass spectrometry in case of fructo-oligosaccharides. *Endo*-dextranase cleaves α-1,6-linked Glc*p* units which leads to the liberation of isomaltose and branched isomalto-oligosaccharides from dextrans (Münkel & Wefers, 2019; Pittrof, Kaufhold, Fischer, & Wefers, 2021). Isomaltose and *O*3-branched isomalto-oligosaccharides were liberated from all glucan containing water-soluble HoEPS (Fig. S2). This was in good agreement with the results from methylation analysis. However, the liberated oligosaccharides also demonstrated that monomeric, dimeric as well as oligomeric side chains were present in all glucans. The oligosaccharide pattern obtained was comparable to the ones obtained from other dextrans from *Leuconostoc* or *Lactobacillus* (Münkel et al., 2019; Münkel & Wefers, 2019).

The HPAEC-PAD chromatograms of *endo*-levanase hydrolysates of water-soluble HoEPS are shown in Fig. 4. The chromatograms of the HoEPS hydrolysates from NRRL B-1149, B-1438, B-1118, and DSM 20241 contained several peaks, whereas the chromatograms of NRRL B-1121 and B-1144 had low peak intensities and no peaks were detected for DSM 16230. Thus, significant amounts of oligosaccharides were only liberated from HoEPS fractions which contained high portions of levans. Among the liberated fructo-oligosaccharides, two disaccharides as well as two tri-, tetra-, penta- and hexasaccharides were identified by using MS. In addition, several oligosaccharides with higher molecular weights were detected between 50 and 65 min. Different elution times indicated that oligosaccharides with the same degree of polymerization had varying structures. Therefore, linear 2,6-linked oligosaccharides as well as fructo-oligosaccharides resulting from ramifications were present.

3.1.4. HPSEC-RI analysis of water-soluble HoEPS

For comparison of molecular weights, water-soluble HoEPS were analyzed by HPSEC-RI (Fig. 5). HoEPS from DSM 16230, NRRL B-1144, and B-1121 showed a rather broad RI elution pattern and thus a broad size distribution. However, the early eluting peak (~6 mL) in the elugram of dextrans from DSM 16230 indicated that these dextrans contained a fraction with a very high molecular weight. HoEPS from NRRL
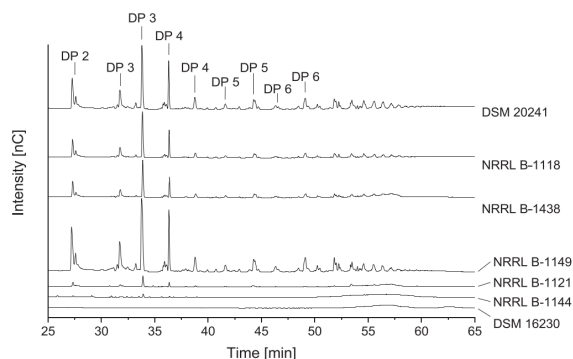
Fig. 5. HPSEC-RI elugrams of water-soluble HoEPS (black) obtained from seven lactic acid bacteria strains (Table 1) and their *endo*-dextranase hydrolysates (green). Peak maxima of size standards with known molecular masses are indicated by reference lines (V_t was determined by using glucose) and the elugram of *endo*-dextranase is given for comparison.

B-1149, B-1438, B-1118, and DSM 20241 showed an intense peak at elution volumes between 6 and 8 mL. Thus, these HoEPS were mainly composed of a high molecular weight fraction which is larger than 670 kDa. Notably, all of these HoEPS contained at least 50 % levans (see Section 3.1.1), whereas the HoEPS with a broader molecular weight distribution contained at least 50 % dextrans.

Endo-dextranase was used to identify which polysaccharide fractions can be assigned to dextrans. HoEPS from NRRL B-1121, B-1144 and DSM 16230 were hydrolyzed to a significant extent which led to the disappearance of early-eluting, high molecular weight material and to the formation of low molecular weight compounds. The elution profiles of HoEPS from NRRL B-1149, B-1118 and DSM 20241 after *endo*-dextranase hydrolysis were unchanged compared to untreated HoEPS, whereas a slight reduction in size was observed for NRRL B-1438. Minor variations in the peak intensities between the unmodified and hydrolyzed samples are most likely caused by slight variations in polysaccharide solubility before and after enzymatic hydrolysis. Altogether, the dextrans in the samples had a broad molecular weight distribution, and their size was reduced by *endo*-dextranase hydrolysis. Furthermore, the molecular sizes of levans from NRRL B-1149, B-1118 and DSM 20241 were in the range from 670 kDa to 2 million Da (dextran blue).

The estimated molecular weights of the levans were in accordance with the molecular weights of other microbial levans (Srikanth, Reddy,

Fig. 4. HPAEC-PAD chromatograms of *endo*-levanase hydrolysates of water-soluble HoEPS from seven lactic acid bacteria strains (Table 1). Degree of polymerization (DP) of the individual oligosaccharides was determined by mass spectrometry and is given above the peaks.

Publikation: *Carbohydrate Polymers*, 323, 121417

L. Ernst et al.

Siddartha, Ramaiah, & Uppuluri, 2015), wheareas most fermentatively synthesized dextrans of *Leuconostoc* and *Lactobacillus* strains showed higher molecular weights than the dextrans in this study (Díaz-Montes, 2021).

It is worth noting that in the characterized mixtures of levans and dextrans, levans showed higher molecular weights. Comparisons of fermentatively synthesized dextrans and levans molecular sizes have sparsely been found in literature. For *Lactobacillus reuteri* HoEPS, van Geel-Schutten et al. (1999) found α-glucans which showed a higher molecular weight than the levans produced by this strain. In contrast, levans from water kefir showed a higher molecular weight than dextrans (Fels, Jakob, Vogel, & Wefers, 2018).

3.1.5. Overall structure of water-soluble HoEPS

Water-soluble HoEPS synthesized by the seven lactic acid bacteria strains were obtained in yields ranging from 0.2 to 15.5 g/L culture. They consisted of dextrans and levans in different portions. Dextran structures were similar and all dextrans were hydrolyzed with *endo*-dextranase to isomaltose and isomalto-oligosaccharides with monomeric, dimeric as well as oligomeric side chains at position *O*3. Therefore, all dextrans had a comparable structure which was also comparable to other *O*3-branched dextrans. However, dextrans showed a broad size distribution ranging from 12 kDa to about 2 million Da (dextran blue) or more, whereas most dextrans in the literature show higher molecular weights. Apart from the molecular weight, the degree of branching and side chain length of dextrans are known to influence their physicochemical characteristics (Nachtigall, Hassler, Wefers, Rohm, & Jaros, 2023; Tirtaatmadja, Dunstan, & Boger, 2001). Despite the comparable degree of branching of the obtained dextrans, their broad size distribution may result in varying viscosities particularly when compared to dextrans with more narrow size distributions.

Levans showed different degrees of branching (7 % to 24 %) and *endo*-levanase hydrolysis released different, presumably linear and branched oligosaccharides from levans. This indicated a complex structural architecture. The impact of degrees and distributions of branching on the physicochemical properties of levans is unknown and should be subject of further investigations. Furthermore, levans had rather high molecular weights and narrow size distributions in the range of 670 kDa to 2 million Da (dextran blue).

3.2. Water-insoluble HoEPS

Only glucose was detected by monosaccharide analysis after TFA hydrolysis of the seven water-insoluble HoEPS, thus all water-insoluble HoEPS were glucans.

3.2.1. Methylation analysis of water-insoluble glucans

Water-insoluble glucans were analyzed by methylation analysis to obtain information on their glycosidic linkages. Results are shown in Fig. 6 and revealed that water-insoluble glucans were composed of 1,6-, 1,3- and 1,3,6-linked Glc*p* units (besides terminal units). Clear variations were observed for portions of 1,6-linkages (36 to 68 %) and 1,3-linkages (5 to 40 %). Strains NRRL B-1149 and DSM 20241 synthesized water-insoluble glucans with approximately equal portions of 1,6-linked and 1,3-linked Glc*p* units. For glucans of NRRL B-1121, B-1438, and B-1118 about 60 % 1,6-linkages and 20 % 1,3-linkages were determined. However, while the mentioned glucans all showed comparably high portions of 1,3-linkages, glucans from NRRL B-1144 and DSM 16230 were mainly 1,6-linked with 1,3-linkages accounting for less than 10 %. The portions of 1,3,6-linked Glc*p* units varied between 3 % and 12 % which demonstrated that all of the analyzed glucans are branched, but to a rather low extent. Notably, the portions of terminal glucans were higher than it would be expected from the portions of 1,3,6-linked Glc*p* units. However, this is most likely caused by residual sucrose or low molecular weight compounds which are embedded within the water-insoluble glucans and solubilized during methylation analysis (Münkel et al., 2019). Glycosidic linkages of water-insoluble glucans of NRRL B-1121, B-1149, B-1438 were in accordance with the literature (Jeanes et al., 1954; Jeanes et al., 1955; Pearce et al., 1990; Slodki et al., 1986). For strain NRRL B-1118 only the glucans synthesized by DsrI glucansucrase were described by Côté and Skory (2012) and for strains NRRL B-1144, DSM 20241, and 16230 water-insoluble glucans have not been described yet. Altogether, all water-insoluble glucans of this study were complex copolymers and contained significant portions of 1,6-linkages.

Therefore, *endo*-dextranase hydrolysis was applied to obtain more information about the different structural elements. Released isomalto-oligosaccharides in the supernatants were analyzed by HPAEC-PAD as described in Section 3.1.3 and results are shown in Fig. S2. Isomaltose and several branched isomalto-oligosaccharides were released by *endo*-dextranase. This clearly demonstrated that the 1,6-linked dextran blocks of the water-insoluble glucans were branched. Notably, comparable portions of the same compounds were detected in the water-soluble glucans. Therefore, the dextran blocks within the water-insoluble glucans contained a comparable structural architecture. However, water-insoluble glucans were incompletely hydrolyzed with *endo*-dextranase. The proportions of water-insoluble residues ranged from about 45–85 % and water-insoluble residues were additionally analyzed by methylation analysis (Fig. 6). Water-insoluble residues after *endo*-dextranase hydrolysis were mainly composed of 1,3-Glc*p* units with less than 10 % of 1,6-linkages. Thus, *endo*-dextranase efficiently hydrolyzed 1,6-linkages
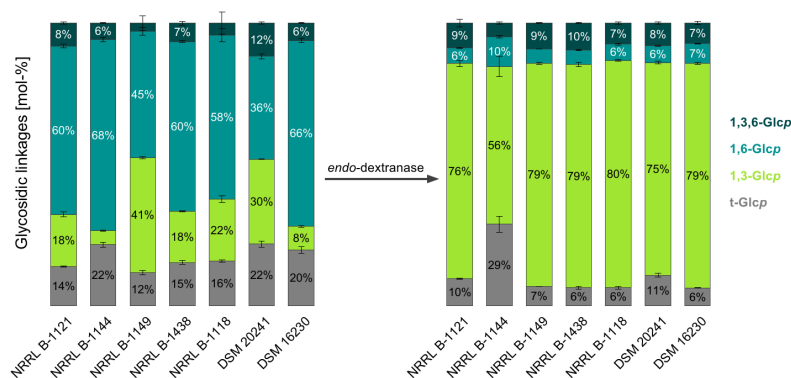
Fig. 6. Glycosidic linkages of water-insoluble glucans (left) obtained from seven lactic acid bacteria strains (Table 1) and their water-insoluble residues after *endo*-dextranase hydrolysis (right). Glycosidic linkages were determined by methylation analysis and all analyses were performed in duplicate. t: terminal, Glc*p*: glucopyranose, numbers indicate the position of substitution in the monosaccharide unit.

Publikation: *Carbohydrate Polymers*, 323, 121417

and the residue was mostly composed of the 1,3-linked blocks which render insolubility in water. Notably, the glucan residue of NRRL B-1144 showed an unusually high portion of terminal units. Although the exact portion was most likely overestimated due to methodological limitations (a tetrasaccharide would not be insoluble), these results indicated that the obtained 1,3-linked structural elements may have a lower molecular weight. All samples contained significant portions of 1,3,6-linked Glc*p* units which suggested that ramifications were also present in the 1,3-linked areas. Seymour and Knapp (1980) supposed a structure with segments of 1,3-linked Glc*p* units for water-insoluble glucans of NRRL B-1149, which was confirmed by the findings in this study.

3.2.2. Endo-mutanase hydrolysis

To obtain further information on the fine structures of the water-insoluble, mainly 1,3-linked residues from *endo*-dextranase hydrolysis, they were hydrolyzed with *endo*-mutanase. The enzymatically liberated oligosaccharides were analyzed by HPAEC-PAD/MS and the chromatograms are shown in Fig. 7. *Endo*-mutanase liberated oligosaccharides from all seven water-insoluble glucan residues, although they were not hydrolyzed completely. This confirmed that water-insoluble glucans contain α-1,3-linked Glc*p* units. In addition to linear nigero-oligosaccharides ([α-1,3-D-Glc*p*]$_n$), different unknown oligosaccharides were released which were presumably branched: By using mass spectrometric detection we were able to identify two pentasaccharides. Different portions of these compounds were present in all hydrolysates, but the highest portions were released from glucan of NRRL B-1149. Therefore, the 1,3-linked areas could also show a varying structural architecture. The release of linear nigero-oligosaccharides by *endo*-mutanase was described for glucans from *Streptococcus* bacteria (Pleszczyńska, Boguszewska, Tchórzewski, Wiater, & Szczodrak, 2012; Tsumori, Shimamura, Sakurai, & Yamakami, 2011).

3.2.3. HPSEC-RI analysis of water-insoluble glucans

HPSEC-RI analysis was performed to analyze the molecular weight distribution of water-insoluble glucans. To enable HPSEC analysis, water-insoluble glucans were dissolved in DMSO with 100 mM LiCl and this solvent was also used as eluent. To gain information about the size of the 1,3-linked areas, the water-insoluble residues after *endo*-dextranase hydrolysis were also analyzed. Fig. 8 shows the elugrams of the water-insoluble glucans as well as the elugrams of the water-insoluble residues after *endo*-dextranase hydrolysis. All water-insoluble
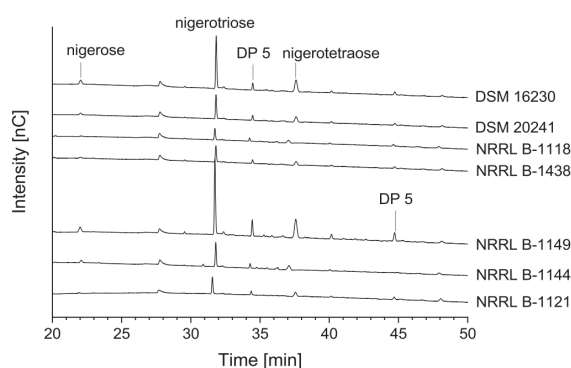
Fig. 7. HPAEC-PAD chromatograms of oligosaccharides liberated by *endo*-mutanase from water-insoluble residues after *endo*-dextranase hydrolysis of water-insoluble glucans from seven lactic acid bacteria strains (Table 1). Nigero-oligosaccharides were identified by external standard oligosaccharides and the degree of polymerization (DP) of some unknown oligosaccharides was determined by mass spectrometry. Slight retention time shifts in the area of 30–40 min were caused by different impurities as confirmed by standard compounds.
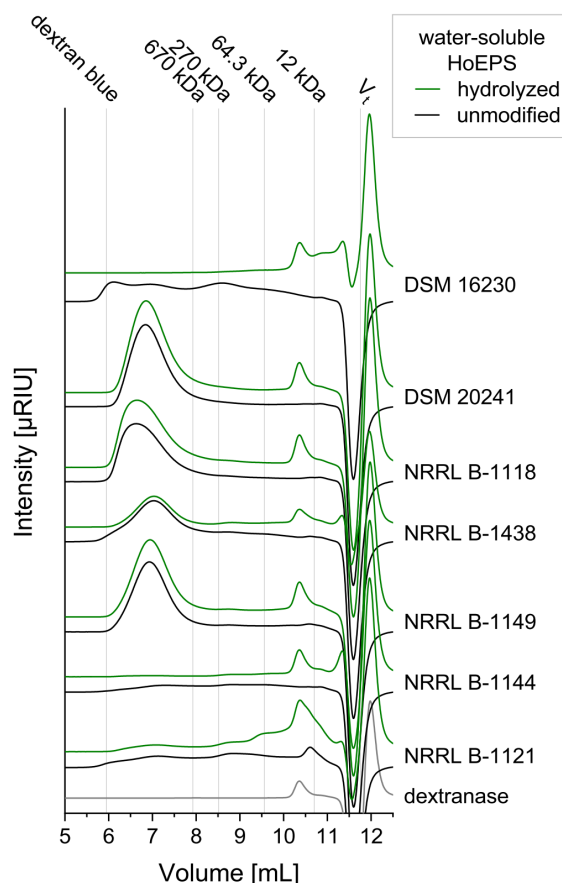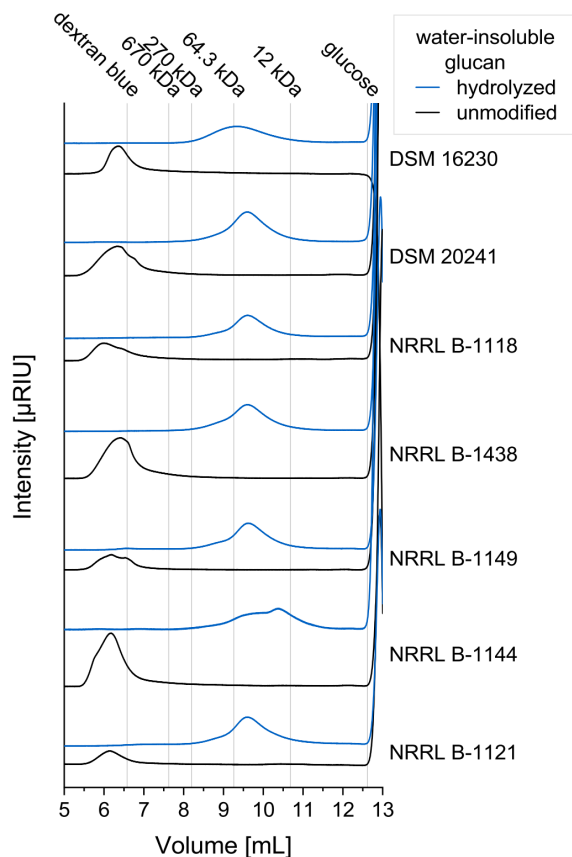

Fig. 8. HPSEC-RI elugrams of water-insoluble glucans (black) obtained from seven lactic acid bacteria strains (Table 1) and their water-insoluble residues after *endo*-dextranase hydrolysis (blue). Peak maxima of size standards with known molecular masses are indicated by reference lines. The elugram of the hydrolyzed glucans from NRRL B-1144 is enhanced by factor 3.5.

glucans eluted at comparable elution volumes than dextran blue (2 million Da) which indicated comparably high molecular weights. However, elugrams of water-insoluble glucans showed different size distributions. Notably, the early eluting peaks disappeared after *endo*-dextranase hydrolysis and the water-insoluble residues eluted between the standard compounds with 270 kDa and 12 kDa (peak maximum at about 50–60 kDa). Some differences between the individual glucans could be observed: The residue of glucans from DSM 16230 showed a peak maximum at about 64.3 kDa, and the residue of glucans from NRRL B-1144 showed a broader and flat size distribution with slightly smaller sizes than the other residues. This was in good agreement with the detection of higher portions of terminal Glc*p* units in the water-insoluble residue of NRRL B-1144 glucans (Section 3.2.1). Furthermore, these results confirmed that terminal units were overestimated for this sample. Notably, glucans from DSM 16230 and NRRL B-1144 contained high portions of 1,6-linked Glc*p* units and a different linkage distribution could be the reason for the different elution profiles. However, the overall results of this analysis suggested that all 1,3-linked areas were rather small and continuously interrupted by dextran structural elements. A block-wise structure was previously suggested for several water-insoluble glucans (Côté et al., 1999; Tsumuraya & Misaki, 1979; Wangpaiboon et al., 2020).

8

3.2.4. Overall structure of water-insoluble HoEPS

Water-insoluble HoEPS were glucans with different portions of 1,3-, 1,6-, and 1,3,6-linkages. Portions of 1,3-linked Glc*p* units ranged from 5 to 40 %. The products of *endo*-dextranase hydrolysis demonstrated that all glucans contained dextran blocks with mono-, di-, and oligomeric side chains. Methylation analysis, high performance size exclusion chromatography, and *endo*-mutanase hydrolysis of the water-insoluble products after *endo*-dextranase hydrolysis showed that water-insoluble glucans contained α-1,3-linked blocks of varying sizes and structural composition. Most likely, 1,3,6-linked units were also present in the 1,3-linked areas. Water-insoluble glucans had a high molecular weight in the range of dextran blue (about 2 million Da). Altogether, water-insoluble glucans contained 1,3-linked blocks which were interrupted by 1,6-linked blocks. For applications of water-insoluble α-glucans, the effect of these structural elements on their physicochemical properties remains to be elucidated.

4. Conclusion

The systematic and comparative characterization of the water-soluble and water-insoluble HoEPS of seven lactic acid bacteria yielded detailed information on the HoEPS production of the respective strains and on the fine structure of the individual polysaccharides. All bacteria used produced significant amounts of water-soluble HoEPS. Pure dextrans or levans as well as mixtures of both polysaccharides were identified and differences in the size distribution were observed: Levans showed a rather high molecular weight, whereas dextrans had a broad size distribution. Furthermore, differences in the structural variation between water-soluble HoEPS were observed: Dextrans showed similar linkage type portions and degrees of branching, whereas levans differed in their degree of branching which ranged from 7 to 24 %. By using *endo*-dextranase and *endo*-levanase hydrolysis, various oligosaccharides were released from all dextrans and levans. The elution patterns suggested that the different HoEPS had comparable fine structures. Furthermore, all seven strains produced water-insoluble glucans showing different portions of 1,3-linkages (5–40 %) and of 1,6-linkages (36–68 %). In addition to water-soluble, linear and branched isomalto-oligosaccharides, *endo*-dextranase hydrolysis released water-insoluble 1,3-linked polysaccharide blocks, which showed varying molecular weights. Furthermore, it is likely that the 1,3-linked blocks contain ramifications. Altogether, our results broaden the knowledge on α-glucan and levan structures and allow selection of appropriate HoEPS for further research and/or application.

CRediT authorship contribution statement

Luise Ernst: Conceptualization, Investigation, Methodology, Formal analysis, Validation, Visualization, Writing – original draft. **Hanna Offermann:** Investigation, Methodology, Formal analysis. **Annemarie Werner:** Investigation. **Daniel Wefers:** Conceptualization, Resources, Supervision, Writing – review & editing.

Declaration of competing interest

The authors declare that they have no known competing financial interests or personal relationships that could have appeared to influence the work reported in this paper.

Data availability

Data will be made available on request.

Appendix A. Supplementary data

Supplementary data to this article can be found online at https://doi.org/10.1016/j.carbpol.2023.121417.

References

Birkhed, D., Rosell, K. G., & Granath, K. (1979). Structure of extracellular water-soluble polysaccharides synthesized from sucrose by oral strains of *Streptococcus mutans, Streptococcus salivarius, Streptococcus sanguis* and *Actinomyces viscosus. Archives of Oral Biology, 24*, 53–61.

Bouallegue, A., Casillo, A., Chaari, F., La Gatta, A., Lanzetta, R., Corsaro, M. M., … Ellouz-Chaabouni, S. (2020). Levan from a new isolated *Bacillus subtilis* AF17: Purification, structural analysis and antioxidant activities. *International Journal of Biological Macromolecules, 144*, 316–324.

Chun, B. H., Lee, S. H., Jeon, H. H., Kim, D.-W., & Jeon, C. O. (2017). Complete genome sequence of *Leuconostoc suionicum* DSM 20241 provides insights into its functional and metabolic features. *Standards in Genomic Sciences, 12*, 38.

Côté, G. L., Ahlgren, J. A., & Smith, M. R. (1999). Some structural features of an insoluble α-D-glucan from a mutant strain of *Leuconostoc mesenteroides* NRRL B-1355. *Journal of Industrial Microbiology and Biotechnology, 23*, 656–660.

Côté, G. L., & Leathers, T. D. (2009). Insoluble glucans from planktonic and biofilm cultures of mutants of *Leuconostoc mesenteroides* NRRL B-1355. *Applied Microbiology and Biotechnology, 82*, 149–154.

Côté, G. L., & Skory, C. D. (2012). Cloning, expression, and characterization of an insoluble glucan-producing glucansucrase from *Leuconostoc mesenteroides* NRRL B-1118. *Applied Microbiology and Biotechnology, 93*, 2387–2394.

Côté, G. L., & Skory, C. D. (2016). Effect of a single point mutation on the interaction of glucans with a glucansucrase from *Leuconostoc mesenteroides* NRRL B-1118. *Carbohydrate Research, 428*, 57–61.

Côté, G. L., Skory, C. D., Unser, S. M., & Rich, J. O. (2013). The production of glucans via glucansucrases from *Lactobacillus satsumensis* isolated from a fermented beverage starter culture. *Applied Microbiology and Biotechnology, 97*, 7265–7273.

Díaz-Montes, E. (2021). Dextran: Sources, structures, and properties. *Polysaccharides, 2*, 554–565.

Ebisu, S., Misaki, A., Kato, K., & Kotani, S. (1974). The structure of water-insoluble glucans of cariogenic *Streptococcus mutans*, formed in the absence and presence of dextranase. *Carbohydrate Research, 38*, 374–381.

Ernst, L., Werner, A., & Wefers, D. (2023). Influence of ultrasonication and hydrolysis conditions in methylation analysis of bacterial homoexopolysaccharides. *Carbohydrate Polymers, 308*, 120643.

Fels, L., Jakob, F., Vogel, R. F., & Wefers, D. (2018). Structural characterization of the exopolysaccharides from water kefir. *Carbohydrate Polymers, 189*, 296–303.

Funane, K., Ishii, T., Matsushita, M., Hori, K., Mizuno, K., Takahara, H., Kitamura, Y., & Kobayashi, M. (2001). Water-soluble and water-insoluble glucans produced by *Escherichia coli* recombinant dextransucrases from *Leuconostoc mesenteroides* NRRL B-512F. *Carbohydrate Research, 334*, 19–25.

Gottlieb, H. E., Kotlyar, V., & Nudelman, A. (1997). NMR chemical shifts of common laboratory solvents as trace impurities. *The Journal of Organic Chemistry, 62*, 7512–7515.

Haddar, A., Hamed, M., Bouallegue, A., Bastos, R., Coelho, E., & Coimbra, M. A. (2021). Structural elucidation and interfacial properties of a levan isolated from *Bacillus mojavensis. Food Chemistry, 343*, 128456.

Han, Y. W., & Clarke, M. A. (1990). Production and characterization of microbial levan. *Journal of Agricultural and Food Chemistry, 38*, 393–396.

Hancock, R. A., Marshall, K., & Weigel, H. (1976). Structure of the levan elaborated by *Streptococcus salivarius* strain 51: An application of chemical-ionisation mass-spectrometry. *Carbohydrate Research, 49*, 351–360.

Hare, M. D., Svensson, S., & Walker, G. J. (1978). Characterization of the extracellular, water-insoluble α-D-glucans of oral *streptococci* by methylation analysis, and by enzymic synthesis and degradation. *Carbohydrate Research, 66*, 245–264.

Inoue, M., Yakushiji, T., Katsuki, M., Kudo, N., & Koga, T. (1988). Reduction of the adherence of *Streptococcus sobrinus* insoluble α-D-glucan by *endo*-1,3-α-D-glucanase. *Carbohydrate Research, 182*, 277–286.

Jeanes, A., Haynes, W. C., & Wilham, C. (1955). Characterization of dextrans from four types of *Leuconostoc mesenteroides. Journal of Bacteriology, 71*.

Jeanes, A., Haynes, W. C., Wilham, C., Rankin, J. C., Melvin, E. H., Austin, M. J., … Rist, C. E. (1954). Characterization and classification of dextrans from ninety-six strains of bacteria. *Journal of the American Chemical Society, 76*, 5041–5052.

Korakli, M., & Vogel, R. F. (2006). Structure/function relationship of homopolysaccharide producing glycansucrases and therapeutic potential of their synthesised glycans. *Applied Microbiology and Biotechnology, 71*, 790–803.

Kralj, S., van Geel-Schutten, G. H., Dondorff, M. M. G., Kirsanovs, S., van der Maarel, M. J. E. C., & Dijkhuizen, L. (2004). Glucan synthesis in the genus *Lactobacillus*: Isolation and characterization of glucansucrase genes, enzymes and glucan products from six different strains. *Microbiology, 150*, 3681–3690.

Mardo, K., Visnapuu, T., Vija, H., Aasamets, A., Viigand, K., & Alamäe, T. (2017). A highly active *endo*-levanase BT1760 of a dominant mammalian gut commensal *Bacteroides thetaiotaomicron* cleaves not only various bacterial levans, but also levan of timothy grass. *PLoS One, 12*, Article e0169989.

Monsan, P., Bozonnet, S., Albenne, C., Joucla, G., Willemot, R.-M., & Remaud-Siméon, M. (2001). Homopolysaccharides from lactic acid bacteria. *International Dairy Journal, 11*, 675–685.

Morales-Arrieta, S., Rodríguez, M. E., Segovia, L., López-Munguía, A., & Olvera-Carranza, C. (2006). Identification and functional characterization of levS, a gene encoding for a levansucrase from *Leuconostoc mesenteroides* NRRL B-512 F. *Gene, 376*, 59–67.

Münkel, F., Bechtner, J., Eckel, V., Fischer, A., Herbi, F., Jakob, F., & Wefers, D. (2019). Detailed structural characterization of glucans produced by glucansucrases from *Leuconostoc citreum* TMW 2.1194. *Journal of Agricultural and Food Chemistry, 67*, 6856–6866.

Publikation: *Carbohydrate Polymers*, 323, 121417

Münkel, F., & Wefers, D. (2019). Fine structures of different dextrans assessed by isolation and characterization of *endo*-dextranase liberated isomalto-oligosaccharides. *Carbohydrate Polymers, 215*, 296–306.

Nachtigall, C., Hassler, V., Wefers, D., Rohm, H., & Jaros, D. (2023). Dextrans of *Weissella cibaria* DSM 14295: Mircobial production, structure and functionality. *International Journal of Biological Macromolecules, 246*, 125631.

Nolte, J., Kempa, A., Schlockermann, A., Hochgürtel, M., & Schörken, U. (2019). Glycosylation of caffeic acid and structural analogues catalyzed by novel glucansucrases from *Leuconostoc* and *Weissella* species. *Biocatalysis and Agricultural Biotechnology, 19*, 101114.

Olvera, C., Centeno-Leija, S., & López-Munguía, A. (2007). Structural and functional features of fructansucrases present in *Leuconostoc mesenteroides* ATCC 8293. *Antonie van Leeuwenhoek, 92*, 11–20.

Pearce, B. J., Walker, G. J., Slodki, M. E., & Schuerch, C. (1990). Enzymic and methylation analysis of dextrans and 1,3-α-D-glucans. *Carbohydrate Research, 203*, 229–246.

Pei, F., Ma, Y., Chen, X., & Liu, H. (2020). Purification and structural characterization and antioxidant activity of levan from *Bacillus megaterium* PFY-147. *International Journal of Biological Macromolecules, 161*, 1181–1188.

Pittrof, S. L., Kaufhold, L., Fischer, A., & Wefers, D. (2021). Products released from structurally different dextrans by bacterial and fungal dextranases. *Foods, 10*, 244.

Pleszczyńska, M., Boguszewska, A., Tchórzewski, M., Wiater, A., & Szczodrak, J. (2012). Gene cloning, expression, and characterization of mutanase from *Paenibacillus curdlanolyticus* MP-1. *Protein Expression and Purification, 86*, 68–74.

Seymour, F. R., & Knapp, R. D. (1980). Structural analysis of dextrans, from strains of *leuconostoc* and related genera, that contain 3-*O*-α-D-glucosylated α-D-glucopyranosyl residues at the branch points, or in consecutive, linear positions. *Carbohydrate Research, 81*, 105–129.

Shi, Q., Hou, Y., Xu, Y., Mørkeberg Krogh, K. B. R., & Tenkanen, M. (2019). Enzymatic analysis of levan produced by lactic acid bacteria in fermented doughs. *Carbohydrate Polymers, 208*, 285–293.

Shukla, R., & Goyal, A. (2013). Elucidation of structure and biocompatibility of levan from *Leuconostoc mesenteroides* NRRL B-1149. *Current Trends in Biotechnology and Pharmacy, 7*, 635–643.

Shukla, R., Shukla, S., Bivolarski, V., Iliev, I., Ivanova, I., & Goyal, A. (2011). Structural characterization of insoluble dextran produced by *Leuconostoc mesenteroides* NRRL B-1149 in the presence of maltose. *Food Technology and Biotechnology, 49*, 291–296.

Simms, P. J., Boyko, W. J., & Edwards, J. R. (1990). The structural analysis of a levan produced by *Streptococcus salivarius* SS2. *Carbohydrate Research, 208*, 193–198.

Slodki, M. E., England, R. E., Plattner, R. D., & Dick, W. E. (1986). Methylation analyses of NRRL dextrans by capillary gas-liquid chromatography. *Carbohydrate Research, 156*, 199–206.

Srikanth, R., Reddy, C. H. S. S. S., Siddartha, G., Ramaiah, M. J., & Uppuluri, K. B. (2015). Review on production, characterization and applications of microbial levan. *Carbohydrate Polymers, 120*, 102–114.

Sun, Z., Harris, H. M. B., McCann, A., Guo, C., Argimón, S., Zhang, W., … O'Toole, P. W. (2015). Expanding the biotechnology potential of *lactobacilli* through comparative genomics of 213 strains and associated genera. *Nature Communications, 6*, 8322.

Sweet, D. P., Shapiro, R. H., & Albersheim, P. (1975). Quantitative analysis by various gas-liquid chromatography response-factor theories for partially methylated and partially ethylated alditol acetates. *Carbohydrate Research, 40*, 217–225.

Tirtaatmadja, V., Dunstan, D. E., & Boger, D. V. (2001). Rheology of dextran solutions. *Journal of Non-Newtonian Fluid Mechanics, 97*, 295–301.

Tsumori, H., Shimamura, A., Sakurai, Y., & Yamakami, K. (2011). Substrate specificity of mutanase of *Paenibacillus humicus* from fermented food. *Journal of Health Science, 57*, 78–81.

Tsumuraya, Y., & Misaki, A. (1979). Structure of the water-insoluble α-D-glucan of *Streptococcus salivarius* HHT. *Carbohydrate Research, 74*, 217–225.

van Geel-Schutten, G. H., Faber, E. J., Smit, E., Bonting, K., Smith, ten Brink, B., … Dijkhuizen, L. (1999). Biochemical and structural characterization of the glucan and fructan exopolysaccharides synthesized by the *lactobacillus reuteri* wild-type strain and by mutant strains. *Applied and Environmental Microbiology, 65*, 3008–3014.

van Hijum, S. A. F. T., Kralj, S., Ozimek, L. K., Dijkhuizen, L., & van Geel-Schutten, I. G. H. (2006). Structure-function relationships of glucansucrase and fructansucrase enzymes from lactic acid bacteria. *Microbiology and Molecular Biology Reviews, 70*, 157–176.

Wangpaiboon, K., Waiyaseesang, N., Panpetch, P., Charoenwongpaiboon, T., Nepogodiev, S. A., Ekgasit, S., … Pichayangkura, R. (2020). Characterisation of insoluble α-1,3-/α-1,6 mixed linkage glucan produced in addition to soluble α-1,6-linked dextran by glucansucrase (DEX-N) from *Leuconostoc citreum* ABK-1. *International Journal of Biological Macromolecules, 152*, 473–482.

Wiater, A., Choma, A., & Szczodrak, J. (1999). Insoluble glucans synthesized by cariogenic *streptococci*: A structural study. *Journal of Basic Microbiology, 39*, 265–273.

Wiater, A., Pleszczyńska, M., Próchniak, K., & Szczodrak, J. (2012). Structural diversity of *streptococcal* mutans synthesized under different culture and environmental conditions and its effect on mutanase synthesis. *Molecules, 17*, 11800–11815.

Zahnley, J. C., & Smith, M. R. (1995). Insoluble glucan formation by *Leuconostoc mesenteroides* B-1355. *Applied and Environmental Microbiology, 61*, 1120–1123.

Zannini, E., Waters, D. M., Coffey, A., & Arendt, E. K. (2016). Production, properties, and industrial food application of lactic acid bacteria-derived exopolysaccharides. *Applied Microbiology and Biotechnology, 100*, 1121–1135.

Comprehensive structural characterization of water-soluble and water-insoluble homoexopolysaccharides from seven lactic acid bacteria

Supplementary
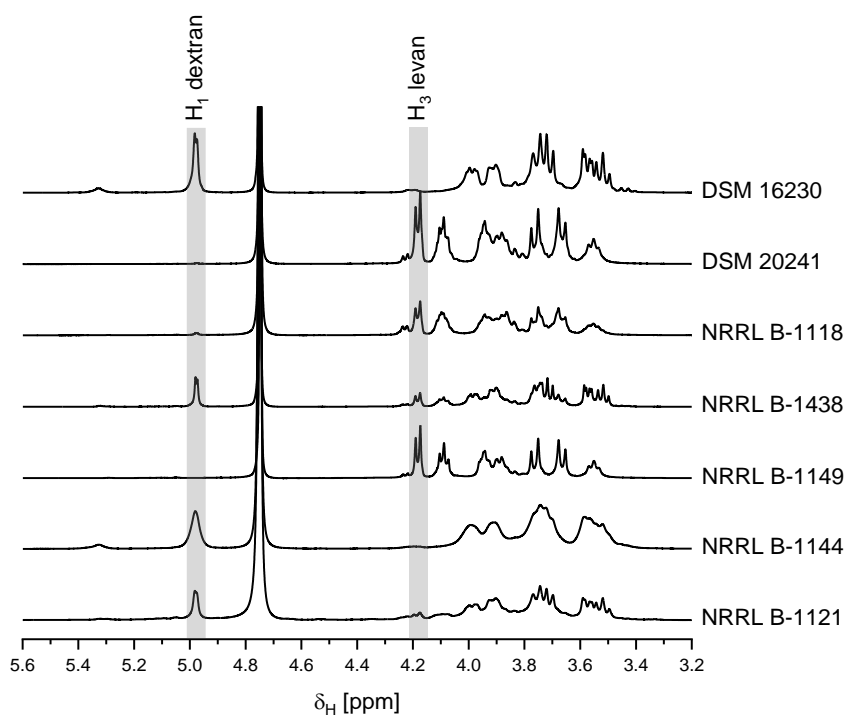
Fig. S1: ^{1}H-NMR spectra of water-soluble homoexopolysaccharides (HoEPS) obtained from seven lactic acid bacteria used in this study (Tab. 1). HoEPS were dissolved in D_2O and acetone was used as reference (2.22 ppm). Characteristic signals for dextran and levan are marked.

Publikation: *Carbohydrate Polymers*, 323, 121417
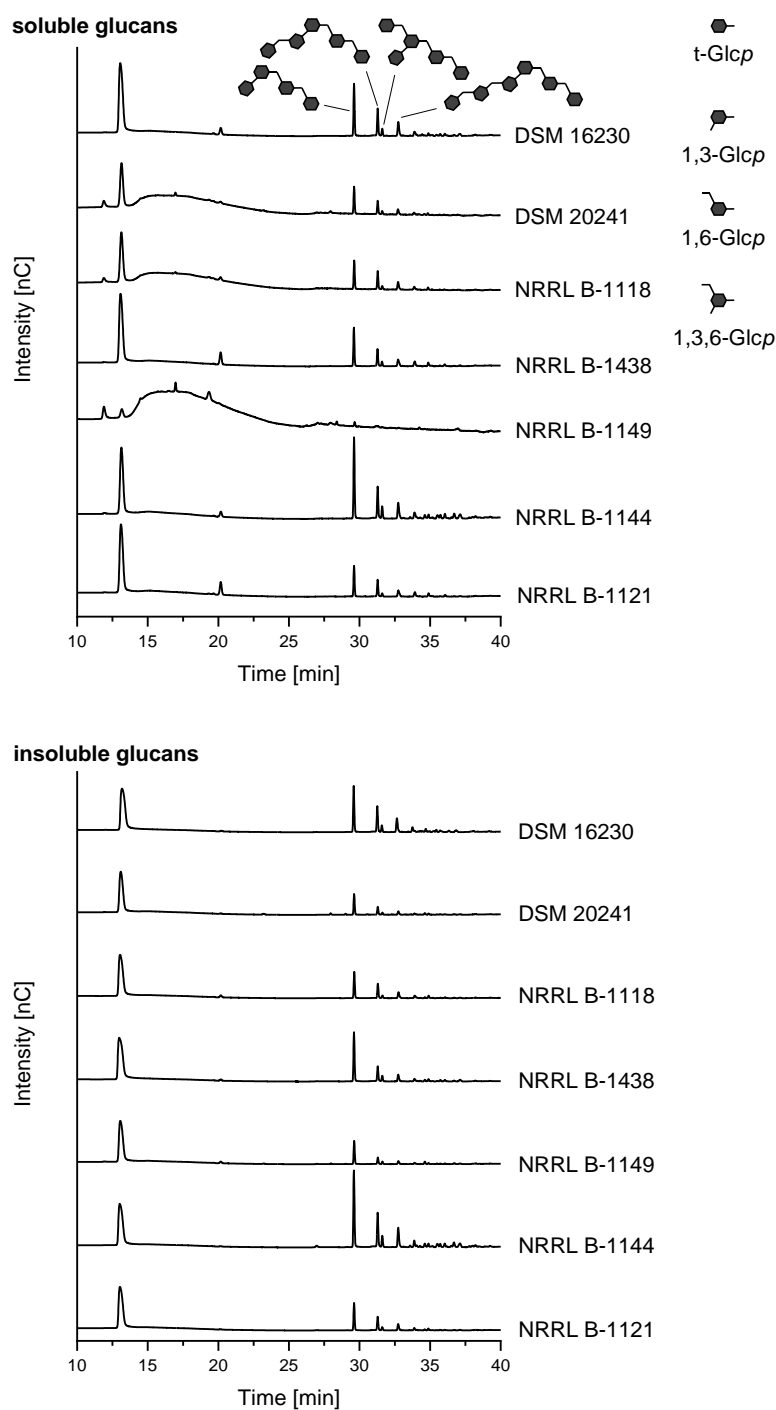
Fig. S2: HPAEC-PAD chromatograms of *endo*-dextranase hydrolysates of water-soluble glucans (top) and water-insoluble glucans (bottom) from seven lactic acid bacteria strains (Tab. 1). In all chromatograms of water-insoluble glucans the peak maximum of isomaltose was standardized to the value of 1.0, and for water-soluble glucans different concentrations were injected due to varying intensities. Peaks were assigned by comparison with standard compounds previously described (Münkel et al., 2019; Münkel & Wefers, 2019).

Publikation: _Food Chemistry_, 453, 139597
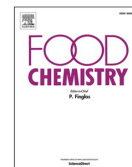
Short communication

Characterization of a novel inulosucrase from _Lactiplantibacillus plantarum_

Sahara Sarang [a], Luise Ernst [b], Daniel Wefers [b], Ram Kulkarni [a,*]

[a] _Symbiosis School of Biological Sciences, Symbiosis International (Deemed University), Pune 412115, India_
[b] _Martin Luther University Halle-Wittenberg, Kurt-Mothes-Str. 2, 06120 Halle (Saale), Germany_

ABSTRACT

Fructansucrases produce fructans by polymerizing the fructose moiety released from sucrose. Here, we describe the recombinant expression and characterization of a unique fructansucrase from _Lactiplantibacillus plantarum_ DKL3 that showed low sequence similarity with previously characterized fructansucrases. The optimum pH and temperature of fructansucrase were found to be 4.0 and 35 °C, respectively. Enzyme activity increased in presence of Ca^{2+} and distinctly in presence of Mn^{2+}. The enzyme was characterized as an inulosucrase (LpInu), based on the production of an inulin-type fructan as assessed by NMR spectroscopy and methylation analysis. In addition to β-2,1-linkages, the inulin contained a few β-2,1,6-linked branchpoints. High-performance size exclusion chromatography with refractive index detection (HPSEC-RI) revealed the production of inulin with a lower molecular weight compared to other characterized bacterial inulin. LpInu and its inulin product represent novel candidates to be explored for possible food and biomedical applications.

1. Introduction

Lactic acid bacteria (LAB) are mostly found in fermented foods and in association with animals. LAB synthesize exopolysaccharides (EPS) which influence the texture of the fermented foods and possibly contribute to the probiotic nature of LAB (Rana & Upadhyay, 2020). Although LAB produce both, homopolysaccharides (HoPS) and hetero-polysaccharides (HePS) in their extracellular environments, HoPS are synthesized at higher concentrations (Zeidan et al., 2017). Biosynthesis of the two types of HoPS – fructan and glucan from sucrose is governed by fructansucrases and glucansucrases which belong to the glycoside hydrolase (GH) 68 and GH70 families, respectively. Based on the type of linkage between the fructose residues in the fructan, fructansucrases are classified into two types. Levansucrases synthesize β-2,6-linked levan while inulosucrases generate inulin wherein fructose units are β-2,1-linked (van Hijum, Kralj, Ozimek, Dijkhuizen, & van Geel-Schutten, 2006).

The functional properties of EPS are dictated by their structural features. For example, the _in vivo_ prebiotic properties of inulin-type fructans depended on the degree of polymerization (Ito et al., 2011). Similarly, the thickening ability of EPS from _Lactococcus lactis_ subsp. _cremoris_ was altered upon altering the chemical side groups (Tuinier et al., 2001). As the native properties of HoPS such as molecular weight and branching are dictated by the activity of a single enzyme (glu-cansucrase or fructansucrase), characterizing novel enzymes and the HoPS made by them can reveal biotechnologically important candidates.

Although many bacterial fructansucrases have been cloned and enzymatically characterized, majority of them (42) are levansucrases while only five are inulosucrases (https://www.cazy.org/GH68_char acterized.html). The inulosucrases originated predominantly from LAB, viz., _Lactobacillus johnsonii_ NCC 533 (Anwar, Kralj, van der Maarel, & Dijkhuizen, 2008), _Lactobacillus gasseri_ DSM 20243 and 20604 (Anwar et al., 2010), _Limosilactobacillus reuteri_ 121 (van Hijum, van Geel-Schutten, Rahaoui, van der Maarel, & Dijkhuizen, 2002), and _Leuco-nostoc citreum_ (Olivares-Illana, López-Munguía, & Olvera, 2003). Pre-viously, we reported the rare occurrence of GH68 in _Lactiplantibacillus plantarum_ and the presence in _L. plantarum_ DKL3 of a unique GH68 which showed low sequence similarity to the previously characterized fructansucrase (Surve, Shinde, & Kulkarni, 2022). Here, we describe enzymatic properties of fructansucrase and its characterization as an inulosucrase (LpInu) along with the structural analysis of the inulin made by this enzyme.

Publikation: *Food Chemistry*, 453, 139597

S. Sarang et al.

2. Material and methods

2.1. Assessment of amino acid sequence of L. plantarum DKL3 inulosucrase (LpInu)

The complete open reading frame of inulosucrase was identified by predicting the CDS in the contigs of *L. plantarum* DKL3 (Surve et al., 2022) using ORF finder tool of NCBI (https://www.ncbi.nlm.nih.gov/orffinder/) followed by annotation using dbCAN2.0 database (Zhang et al., 2018). The nucleotide sequence has been submitted to GenBank (accession no. PP768656). Multiple sequence alignments of inulosucrase from *L. plantarum* DKL3 (LpInu) with other inulosucrases were made using CLUSTAL O (1.2.4) (https://www.ebi.ac.uk/Tools/msa/clustalo/). Characteristics features and core regions were determined by InterPro (https://www.ebi.ac.uk/interpro/). BLASTp (https://blast.ncbi.nlm.nih.gov/Blast.cgi?PAGE = Proteins) was used to assess the unique stretches of amino acid sequences in LpInu. Prediction of the signal peptide was carried out using SignalP 5.0 (https://services.healthtech.dtu.dk/services/SignalP-5.0/).

2.2. Recombinant expression and purification of LpInu

E. coli BL21(DE3) was transformed with the recombinant plasmid carrying the gene encoding LpInu from *L. plantarum* DKL3 cloned in pET30b (Surve et al., 2022). This plasmid carried the truncated version of LpInu lacking the cell-wall anchoring motif (Fig. 1) which is known to interfere with the heterologous expression of fructansucrases in *E. coli* (Anwar et al., 2008; van Hijum et al., 2002). Pre-culture was made from a transformed colony and was added (2 %) to the LB medium with 50 μg/mL kanamycin. Induction of recombinant protein expression was achieved by adding 1 mM IPTG at the $O.D._{600}$ of 0.5–0.6. After incubation at 18 °C at 150 rpm for 15–18 h, cells were lysed by ultra-sonication on ice (60 % amplitude, 10-*sec* on/off, 20 min), and cell debris removed by centrifugation (12,000 *g*, 15 min, 4 °C). The recombinant LpInu carried 6xHis-tag and was thus isolated from the mixture by Ni^{2+}-nitrilotriacetic acid (Ni-NTA) affinity chromatography and analyzed by SDS-PAGE. The protein concentrations were determined using bicinchoninic acid (BCA) protein assay kit (Thermo Fisher Scientific) while using BSA as the standard.

2.3. Biochemical characterization of recombinant LpInu

The standard activity assay was carried out in 1 mL reaction volume containing 20 mM sodium acetate buffer (pH 4.0), 9 μg/mL enzyme, 100 mM sucrose and 1 mM $CaCl_2$ at 37 °C for 1 h followed by measuring the total reducing sugars by DNSA method. One unit of LpInu enzyme activity was defined as the amount of enzyme that releases 1 μmol of monosaccharide per min from sucrose. All the enzymatic assays were carried out in triplicates.

2.3.1. Effects of pH, temperature, and chemicals

The influence of pH on LpInu's activity was assessed by using different buffers (20 mM) at pH close to their pKa (citrate-phosphate buffer, pH 2.5–6; phosphate buffer, pH 7–8; and NaOH-glycine buffer, pH 9–10). The effect of temperature was assessed in citrate–phosphate buffer (20 mM, pH 3.5) at the temperatures from 20 to 60 °C with increments of 5 °C. The rest of the experimental conditions for determining optimum pH and temperature were the same as detailed above in the standard assay except for the assay volume which was 250 μl. The initial velocity was determined by estimating the reducing sugars by 3,5-dinitrosalicylic acid (DNSA) assay (Sumner & Graham, 1921). For each varying pH and temperature, controls without any enzyme were set-up and used as spectrophotometric blanks. Overall activity (amount of glucose), hydrolytic activity (amount of fructose) and trans-fructosylation activity (amount of glucose − amount of fructose) of LpInu in presence of $CaCl_2$ were determined using high performance anion exchange chromatography coupled to pulsed amperometric detection (HPAEC-PAD) as detailed before (Ernst, Offermann, Werner, & Wefers, 2024) with minor modifications. Mono-, di- and oligosaccharides were separated on a CarboPac PA200 column using the following gradient containing of four components (A: ultrapure water, B: 10 mM NaOH, C: 200 mM NaOH, D: 200 mM NaOH + 500 mM sodium acetate) with a flow rate of 0.45 mL/min: column equilibration with 100 % B for 15 min prior to every run; 0–5 min: Isocratic 100 % B; 8 min linear gradient to 75 % B + 25 % C; 8–11 min linear gradient to 45 % A + 50 % B + 5 % D; 11–72 min linear gradient to 10 % A + 90 % B; 72–78 min isocratic 100 % D; 78–89 min isocratic 100 % B. Quantification of glucose, fructose and sucrose was performed by using an external calibration. For assessing the effects of various chemicals on enzyme activity, the reaction mixtures were separately supplemented with 10 mM each of $CaCl_2$, $CoCl_2$, $FeSO_4$, $MnSO_4$, $MgSO_4$, $ZnSO_4$, KCl, NaCl, EDTA, or 25 % SDS, and contained citrate–phosphate buffer (20 mM, pH 3.5), 100 mM sucrose, and 1 mM $CaCl_2$ at 30 °C in presence of 45 μg/mL of purified enzyme.

2.3.2. Thermostability

The enzyme (75 μg/mL) was incubated with 8.3 mM $CaCl_2$ at 4 °C and in the range from 20 to 70 °C with increments of 10 °C in the enzyme samples were aliquoted at a time interval of 1 hr for a total duration of 8 h and was used for enzymatic assay consisting of citrate–phosphate buffer (20 mM, pH 3.5) and 100 mM sucrose.

2.4. Production and structural characterization of fructan

For assessing the possible production of fructan, the purified enzyme (9 μg/ml) was incubated in citrate–phosphate buffer (20 mM, pH 3.5) with 0.5 M sucrose and 1 mM $CaCl_2$ at 30 °C for 72 h. Chilled absolute ethanol (40 ml) was added for precipitating the polysaccharide for 15–18 h at 4 °C. The precipitate was separated by centrifugation (12,000 *g*, 15 min, 4 °C). Deionized water (5 ml) was added and the resuspension was dialyzed against deionised water in the refrigerator for 24 h using cellulose membrane (cut-off, 14,000 Da) (Sigma-Aldrich). The dialyzed fraction was re-precipitated by using ethanol and the product was harvested as described above.

2.4.1. ^{1}H NMR spectroscopy of polysaccharides

About 15 mg of dried polysaccharide samples were dissolved in D_2O (1 mL) by shaking at 60 °C for 2 h. Subsequently, acetone was added as reference (2.22 ppm, Gottlieb, Kotlyar, & Nudelman, 1997). ^{1}H NMR analyses were carried out using 400 MHz VNMRS spectrometer (Agilent, Santa Clara, CA, USA). For comparison, plant inulin from a local supplier and from Fisher Scientific as well as levan produced by *Gluconobacter albidus* TMW 2.1191 (Ernst et al., 2023) were analyzed.

2.4.2. Methylation analysis of polysaccharides

For the analysis of glycosidic linkages, methylation analysis was performed as explained before (Ernst et al., 2023). Briefly, dry DMSO was used for dissolving the samples, followed by deprotonation using NaOH, and methylation using methyl iodide. Methylated polysaccharides were extracted by dichloromethane and hydrolyzed by 1 M trifluoroacetic acid at 70 °C for 30 min. Prior to gas chromatographic (GC) analysis, reduction of the partially methylated monosaccharides was carried out using sodium borodeuteride followed by acetylation using acetic anhydride and 1-methylimidazole. GC coupled to mass spectrometry was used for identification of partially methylated alditol acetates (PMAA) and flame ionization detection was used for quantification. Molar response factors described earlier (Sweet, Shapiro, & Albersheim, 1975), were applied.

2.4.3. HPSEC-RI analysis of polysaccharides

HPSEC-RI was used to obtain more information about the approximate molecular weight of the polysaccharides as explained before (Ernst

Publikation: *Food Chemistry*, 453, 139597

```
LpInu MLRNNYFGETKTHYKLYKCGKNWAVMGISLFSLGLGMLVTSQPVSADVTATSTSSSAVRTDAISESSSSAAKAETTSE-SSSSAVKAETTSASSSSA--VKAETTSA---SSSSAVKAET 114
LmU   --------MNKKFKK-------AAVGLATLAATTVLSVSLNQRT-------------VSADALNQADG--------QKDTNNSTIDNTQ----IVKDKVAEAKQTIENAQTPEEAAKAQQ 80
Lr1   ------MLERKEHKKMYKSGKNWAVVTLSTAALVFGATTVNASA-------------DTNIENNDSSTVQVTTGD--NDIAVKSVTLGSG---QVSAASDTTIRTSANANSASSAANTQ- 95
LrT   ------MLERKEHKKMYKSGKNWAVVTLSTAALVFGATTVNASA-------------DTNTENNDSSTVHVTTGD--NDIAVKSAILGSG---QVSAASDATIKNSANANSASSAANTQ- 95
LjN   ------MLENKNHKKISLSGKSLLMGTLSTAAIVLSASTANAAT-------------INADNVNENQTVEVTASSVNN-ENNKQVTEKDSADKSTSDVAEDANTKKSNENTETTEKNTQT 100
Lg2   ------MLENKNHKKMSLSGKSLLMGTLSTAAIVLSASTVNAAT-------------TNADNVNENKTVAVSTTTSANNKNNNQVNSSS--EKSVDTKAEKATTVTS---AATKEVKADA 96
Lg6   ------MLENKNHKKMSLSGKSLLMGTLSTAAIVLSASTVNAAT-------------TNADNVTKNQTVAVSATTT-NNETNNQVSSSS--EKTADSKTEKDTNLTS---AATKEVKADA 95
                                                                  .    .                 ..  .            :   :       :::

LpInu TS-ASSSSAVKAETTSASSSSAVKAKTTSASSSSAAKAETAAITTAGVANADSQTSAEVTADSTSTSQVVTNNSNNQNNTAQPAGNSTSTTQSTNQANSQISNQGQLNQFATGFVNRAIS 233
LmU   VVVQSKVALT----TLN-------A----LNSINSTSASTPDEN----PND--GS-LAPAN----------------------H-PIS---AGDPSTYDADGLKP-----EAAQAV 143
Lr1   -NSNSQVAS---SAAIT------SSTSSAASSNNTDSKAAQENTNTAKNDDTQK-AAPANESSE----AKNEPAVNVNDSSAAK-NDD------QQSSKKNTTAKLNK-----DAENVV 187
LrT   -NSNSQVAS---SAAIT------SSTSSAASSNNTDSKAAQENANTAKNDDTQK-AAPANESSE----AKNEPAVNVNDSSAAK-NDD------QQSSKKNTTAKLNK-----DAENVV 187
LjN   VVTNAPVSDVKTNTVT-------AETPVDKVVNNSDQKTTNAATTDTKKDDVKQ-VEKK-----------DSVDKTN-AEENK-DSS------VKPAENATKAELKG-----QVKDIV 187
Lg2   V-NTSPVNNVKAATTST-------TT--TKETVDGTEKTPVNSSADVKKNDAVKQ-DEKA------------ATSFKTNTEEKAN-ETS------TKTASNDNKAELKG-----QIKDIV 181
Lg6   AKTTSPVNNVKTVADTT-------TT--TKETTDNTEKSPVNFSADVKKNDAVKQ-DEKA------------ATAVKANTEVKAN-ETS------TKSASKDNKAELKG-----QIKDIV 181
        :                :       . :.       :                  .     .            *:

LpInu EGANVDPNNFTQAQIDALNKLEKYSTTKKNTDTTQFTYYQFQQTADKLAEVDPQYAIPYFKADQIQNLPAATAKDGQTGKVANMDIWDSWPVQDPTTGEIANWNGKQLVIAMMGTPNANS 353
LmU   KNAGINPKTLTDEQKLALNRVDYSHK--DETGATKMTYSDFQKIAETLVTKDSRYAIPYFNAKEIKNMPAAYTKDAQTGKIEHLDVWDSWPIQESKIGYVANWNGYQLAVAMMGMPGYND 261
Lr1   KKAGIDPNSLTDDQIKALNKMNXXKA--AKS-GTQMTYNDFQKIADTLIKQDGRYTVPFFKASEIKNMPAATTKDAQTNTIEPLDVWDSWPVQDVRTGQVANWNGYQLVIAMMGIPNQND 304
LrT   KKAGIDPNSLTDDQIKALNKMMNXXKA--AKX-GTQMTYNDFQKXADTLIKQDGRYTVPFFKASEIKNMPAATTKDAQTNTIEPLDVWDSWPVQDVRTGQVANWNGYQLVIAMMGIPNQND 304
LjN   EESGVDTSKLTNDQINELNKINFSKE--AKS-GTQLTYNDFKKIAKTLIEQDARYAIPFFNASKIKNMPAAKTLDAQSGKVEDLEIWDSWPVQDAKTGYVSNWNGYQLVIGMMGVPNVND 304
Lg2   KESDVDTSKLTNDQINELNKINFSKE--AKS-GTQLTYSDFKKIAKTLIEQDARYAIPFFNASKIKNMPAAKTMDAQTGKVEDLEIWDSWPVQDAKTGYVSNWNGYQLVGMMGVPNTND 298
Lg6   KESGVDTSKLTDDQINELNKISFSKE--AKS-GTQLTYSDFKKIAKTLIEQDARYAVPFFNASKIKNMPAAKTLDAQTGKVEDLEIWDSWPVQDAKTGYVSNWNGYQLVIGMMGVPNTND 298
        : :.::  ..:*:.*   **::.    :    *:.:** :*:: *..* :*  * :*::*:*:*.:*:*:*** : *.*:..:  :::*****:*:  *  ::**** **.:.*** *.  *.

LpInu NHLYLLYNDYGGDNFAGWKNAGDIFAGYRGDKKTGLEIFGDQEWSGSAYPLDDGSIQLFYTHSKYETKTINHQNHQRIATANLKMKLN-ADGTISIASVDNDHTLFKGKDNASANGTHYQ 472
LmU   NHIYLLYNKYGDNNLANWKNAGPIFGYNAT--------DLLQQWSGSAIVNKDGSIQLFYTKVDTSD---K-TNNQKIASATLYLTI--ENGEVKISKIANDHVVFEG------DGINYQ 361
Lr1   NHIYLLYNKYGDNELSHWKNVGPIFGYNST--------AVSQEWSGSAVLNSDNSIQLFYTRVDTSD---NNTNHQKIASATLYLTD--NNGNVSLAQVANDHIVFEG------DGYYYQ 405
LrT   NHIYLLYNKYGDNELSHWKNAGPIFGYNST--------AVSQEWSGSAVLNSDNSIQLFYTRVDTSD---NNTNHQKIASATLYLTD--NNGNVSLAQVANDHIVFEG------DGYYYQ 405
LjN   NHIYLLYNKYGDNFNHWKNAGPIFGLGT---------PVIQQWSGSATLNKDGSIQLYYTKVDTSD---NNTNHQKLASATVYLNLEKDQDKISIAHVDNDHIVFEG------DGYHYQ 406
Lg2   NHIYLLYNKYGDNNFNNWKNAGPIFGLGT---------PVIQQWSGSATLNKDGSIQLYYTKVDTSD---NNTNHQKIASATVYLNLEKDQDKISIAHVDNDHIVFEG------DGYHYQ 400
Lg6   NHIYLLYNKYGDNNFNNWKNAGPIFGLGT---------PVIQQWSGSATLNKDGSIQLYYTKVDTSD---NNTNHQKIASATVYLNLEKNQDKISIAHVDNDHIVFEG------DGYHYQ 400
        **:*:*****.**.::: ***.*.**.         *:.***  :*:*.*..*  * :.*****:*** :  . .  ::*.::*::.:.:.     ::*.    *  ::**** **.:.*** *.  *.

LpInu TFDQWAHNVTMFDGHKEDFGGADNFAMRDPPHIVKDSQGNRYLVFEASTGDDDYQSEDQIYDLRNYGGNAKFQLESLFNLINNDYSVKDKVTGKMIKIGRDMRVRASQANAAIGILGGT 592
LmU   TYEQWHK----------TNTGADNVAMRDAHVIEDEAGNRYLIFEASTGKQEYQGLDQIYNWNNYGGDDAYKIKSLFRLLAN---------------HDMESRASWANAAIGILRLDNN 455
Lr1   TYDQWKA----------TNKGADNIAMRDAHVIEDDNGDRYLVFEASTGLENYQGDDQIYNWLNYGGDDAFNIKSLFRILSN---------------DDIKSRATWANAAIGILKLNKD 499
LrT   TYDQWKA----------TNKGADNIAMRDAHVIEDDNGDRYLVFEASTGLENYQGENQIYNWLNYGGDDAFNIKSLFRILSN---------------DDIKSRATWANAAIGILKLNKD 499
LjN   TYDQWKE----------TNKGADNIAMRDAHVIDDDNGNRYLVFEASTGTENYQGDDQIYQWLNYGGTNKDNLGDFFQILSN---------------SDIKDRAKWSNAAIGIIKLNDD 500
Lg2   TYNQWKK----------TNKGADNIAMRDAHVIDDKDGNRYLVFEASTGTENYQGADQIYQWLNYGGTNKDNLGDFFQILSN---------------SDIKDRAKWSNAAIGIIKLNND 494
Lg6   TYNQWKK----------TNKGADNIAMRDAHVIDDKDGNRYLVFEASTGTENYQGADQIYQWLNYGGTNKDNLGDFLQILSN---------------SDIKDRAKWSNAAIGIIKLNND 494
        *::**            ****.**** *::.*. *:***:***** ::**:.****:   ****.  :: .::.* *.    *:. **.:*******:.*.

LpInu ENNPTVAEVYDPIIISAVMVSDEIERPDVKIGDTYYLFAASRLNRGTNDAAWRKANDKVGDNVVTLGWYSKDLTKGFKFLNGNGVVLTSTVPANWRTATYSYYAVPTRSTDPRFKNTVLI 712
LmU   ETNPQVAQVYKPLLTANMVSDEIERPDIVKLGDKYYLFAATRLNRGSNDDAWMAADKAVGDNVAMIGYVSESLTGGFKPLNESGVVLTASVPANWRTATYSYYAVPIQGQS----DKVLI 571
Lr1   EKNPKVAELYSPLISAPMVSDEIERPNVVKLGNKYYLFAATRLNRGSNDDAWMNANYAVGDNVAMVGYVADSLTGSYKPLNDSGVVLTASVPANWRTATYSYYAVPVAGKD----DQVLV 615
LrT   EKNPKVAELYSPLISAPMVSDEIERPNVVKLGNKYYLFAATRLNRGSNDDTWMNANYAVGDNVAMVGYVADSLTGSYKPLNDSGVVLTASVPANWRTATYSYYAVPVAGKD----DQVLV 615
LjN   VKNPSVAKVYSPLISAPMVSDEIERPDVVKLGNKYYLFAATRLNRGSNDDAWMATNKAVGDNVAMIGYVSDNLTHGYVPLNESGVVLTASVPANWRTATYSYYAVPVEGRD----DQLLI 616
Lg2   TKNPGVEKVYTPFISSPMVSDEIERPDVVKLGNKYYLFAATRLNRGSNDDAWMAANKAVGDNVAMIGYVSDNLTHGYVPLNESGVVLTASVPANWRTATYSYYAVPVEGRD----DQLLI 610
Lg6   TKNPGVEKVYTPLISAPMVSDEIERPDVVRLGNKYYLFAATRLNRGSNDDAWMAANKAVGDNVAMIGYVSDNLTHGYVPLNESGVVLTASVPANWRTATYSYYAVPVEGRD----DQLLI 610
        .** * ::* *:::: *********:::**:*.*******:*****:** :*  ::  *****. :*: :..** .: *** .*****:::**************** .   . ::*:

LpInu TAYMTNRNRVADYRRNKDGKAVLDPDFIQENNGEHNSTWAPSFLLRVNPDGTTRRVLPYVTNQGVWDFNNATKLNTNIM---TAKADEAYLPWEKGVPFDNGSILGSGQDWVDSMPSDPYTP 829
LmU   TSYITNRNHVAGN------------------DYESTWAPSFLLQINPDGTTKVLAKTTNQGDWIDETSENDNMLGDET-----TAALPGEKNKPINWDLIGYGHNGSYGYKYDYDLGP 667
Lr1   TSYMTNRNGVAGK---------------GMDSTWAPSFLLQINPDNTTTVLAKMTNQGDWIWDDSSENLDMIGDLD-----SAALPGERDKPVDWDLI-G-----YGLKPHDPATP 705
LrT   TSYMTNRNGVAGK---------------GMDSTWAPSFLLQINPDNTTTVLAKMTNQGDWIWDDSSENLDMIGDLD-----SAALPGERDKPVDWDLI-G-----YGLKPHDPATP 705
LjN   TSYITNRGEVAGK---------------GMHATWAPSFLLQINPDNTTTVLAKMTNQGDWIWDDSSENDMMGVLEKDAPNSAALPGEWGKPVDWDLIGG-----YNLKPHQPVTP 712
Lg2   TSYITNRGEVAGK---------------GMHATWAPSFLLQINPDNTTTVLAKMTNQGDWIWDDSSENDDMMGVLKKDAPNSAALPGEWGKPVDWDLIGG-----YNLKPHQPVTP 705
Lg6   TSYITNRGEVAGK---------------GMHATWAPSFLLQINPDNTTTVLAKMTNQGDWIWDDSSENADMMGVLEKDAPNSAALPGEWGKPVDWDLIGG-----YNLKPHQPVTP 706
        *:*:***. **.                .:*********::* *.** **  ** * * :::::::   :            * ** * . *.:. *       .  *

LpInu TAPTAPTAPTAPTAPTAPTAPTAPTAPTAPTAPTAPTAPTAPTAPTAPTAPTAPTAPINPSQPTTPTKPVQAGQAAATNFVDQRLPQTGETDQQHMTLSGLLLLAMSSLLGLFG 949
LmU   ALYNE--DPKNSYDLGPALY------NEDPKSNQDSTL---PQDTKTPEKT--TFKPESKKGAYPKRIN------------KNNSAKKLPQTGESSQVAV------LAGLSAIIASVM 754
Lr1   N-----------DPETPTT------PETPETPNTPKTPKTPENPGTPQTPNTPNTPEIPLTPETPKQP--------------ETQTNRLPQTGNNANKAM----IG-LGMGTLLSMFG 788
LrT   N-----------DPETPTT------PETPETPNTPKTPKTPENPGTPQTPNTPNTPEIPLTPETPKQP--------------ETQTNNRLPQTGNNANKAM----IG-LGMGTLLSMFG 788
LjN   I-----------PNVPTT-------PETPTTPDKPEVPTTPEVPTTPETP----TPEAPKNPVK------------------KTSQSKLPKAGDKNSFAA----VVLGAVSSILGAVG 786
Lg2   I-----------PNVPTT-------PEKPNTPTTPNTPDTPHNPTKPT------SEVPTTSVK------------------KTTQSELPKAGAKNGIVA----AIVGAVSSMLGVIG 776
Lg6   I-----------PNVPTT------PEKPENPTTPNTPDTPHTPTTPNTPDTPRTPEVPTTPVK------------------KTTQSELRS---------------------------- 761
                    *          *        *      * *                    .  ..*

LpInu MTKRQ-RKE-- 957
LmU   VALGLKRKEN- 764
Lr1   LAEINKRRFN- 798
LrT   LAGINKRRFN- 798
LjN   LTGVSKRRNN  797
Lg2   LAGVSKRKNN  787
Lg6   ---------- 761
```

Fig. 1. Multiple sequence alignment of inulosucrase (LpInu) from *L. plantarum* DKL3 with the characterized inulosucrase from other lactobacilli. LmU, *L. mulieris* UMB7800 inulosucrase (WP_167802005.1, Zhang et al., 2023); Lr1, *L. reuteri* 121 inulosucrase (AAN05575.1, van Hijum et al., 2002); LrT, *L reuteri* TMW 1.106 inulosucrase (CAL25302.1, Schwab & Gänzle, 2006); LjN, *L. johnsonii* NCC 533 inulosucrase (AAS08734.1, Anwar et al., 2008); Lg2, *L. gasseri* DSM 20243 inulo-sucrase (BK006921.1, Anwar et al., 2010); and Lg6, *L. gasseri* DSM 20604 inulosucrase (ACZ67286.1, Anwar et al., 2010). The GH68 conserved domain identified in LpInu using InterPro has been indicated with solid line above the sequence (residues 262–776) with the key residues indicated in bold. The residues involved in product specificity of inulosucrase are highlighted in grey and among these, residues different in LpInu are indicated in red (residue P502 and Q579). Amino acid stretches which were not found in the characterized inulosucrases but were similar to other fructansucrases (Table S1) are indicated in bold and underlined letters. The cleavage site identified in LpInu using SignalP 5.0 is indicated by vertical line above sequence (residues 46–47), and PXX motif is indicated by a dashed line above the sequence (residues 823–861). The truncated site at the C-terminal has been indicated by a vertical arrow. LPXTG or LPXAG motif are indicated in blue and positively charged KRR or KRK residues in green in the reference sequences. The alignment was generated using CLUSTAL O (1.2.4). (For interpretation of the references to colour in this figure legend, the reader is referred to the web version of this article.)

Publikation: *Food Chemistry*, 453, 139597

et al., 2024) with some changes. Fructan samples (1 mg/mL), dissolved in ultrapure water was filtered using syringe filter (0.45 μm, Nylon). For HPSEC-RI analysis, an HPLC (Agilent 1100 Series) having a 1260 Infinity II RI detector and a TSKgel G5000 PW$_{XL}$ column (300 × 7.8 mm, particle size 10 μm; TOSOH, Japan) was used. Elution was carried out using ultrapure water supplemented with 0.5 g/L NaN$_3$ at a flow rate of 0.35 mL/min at 60 °C. The temperature of RI detector was 35 °C and standard dextran of known molecular weight was used to estimate the molecular weight of the products (dextran blue, 670 kDa, 270 kDa and 12 kDa, Sigma Aldrich, Germany; 64.3 kDa, PSS, Germany).

2.5. Characterization of fructooligosaccharides (FOS) production by LpInu

For assessing the possible production of FOS, an assay similar to above described for fructan was set up. FOS production in the assay reactions was directly analysed by HPAEC-PAD by the method detailed above (Section 2.3.1). Plant inulin as well as kestose, nystose, and fructosylnystose from Megazyme (Bray, Ireland) were used for peak identification.

3. Results

3.1. Assessment of amino acid sequence of L. plantarum DKL3 inulosucrase (LpInu)

L. plantarum DKL3 LpInu with 957 amino acids and predicted molecular weight of 102.46 kDa revealed the presence of most of the conserved residues found in earlier reported inulosucrases as described below. The core region of 515 amino acids (residues 262 to 776), belonged to GH68 family (Fig. 1). Two residues, P502 and Q579, differed from the conserved residues in the core region of other inulosucrases (A and W, respectively). LpInu had a few unique stretches of amino acids which were not found in other inulosucrases. Some of these sequences (residues 45 to 57, 131 to 137, 480 to 489 and 726 to 744) were found to be similar to other fructansucrases upon independently subjecting them to BLASTp (Table S1, Supplementary data). LpInu was predicted to be a secretory protein with a 45 residue long signal peptide on the *N*-terminus. (Fig. 1).

3.2. Biochemical characterization of LpInu

3.2.1. Effects of pH, temperature, and chemicals

Recombinant expression of the truncated LpInu (Fig. 1) in *E. coli* BL21(DE3) followed by purification by affinity chromatography was achieved (Fig. 2A). The purity of the recombinant proteins as
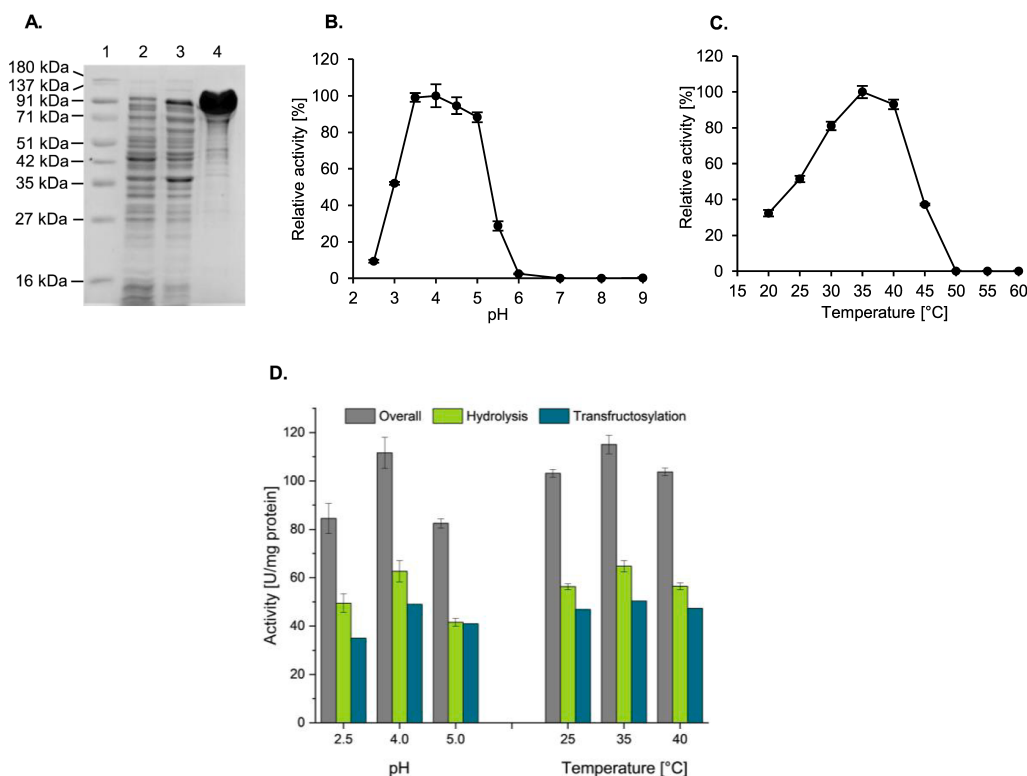
Fig. 2. Recombinant expression and enzymatic characterization of inulosucrase (LpInu) from *L. plantarum* DKL3. (A) SDS-PAGE analysis of the crude and purified LpInu. Lane 1, protein ladder (180 kDa); lane 2, crude lysate of pET30b-transformed *E. coli* BL21(DE3); lane 3, crude lysate from *E. coli* BL21(DE3) carrying LpInu-encoding construct; lane 4, purified fraction. (B) Influence of pH on the activity of LpInu. The specific activity determined using DNSA method at optimum pH (4) was calculated to be 13.4 U/mg. (C) Influence of temperature on the activity of LpInu. The specific activity determined using DNSA method at optimum temperature (35 °C) was calculated to be 17.5 U/mg. (D) Overall, hydrolysis and transfructosylation acitivity of LpInu at different pH and temperatures. Overall activity was calculated from glucose release, hydrolysis activity from fructose release and transfructosylation activity from overall activity minus hydrolytic activity. Monosaccharides were quantified using HPAEC-PAD.

Publikation: *Food Chemistry*, 453, 139597

S. Sarang et al.

determined by the densitometric analysis of the SDS-PAGE gel was approximately 90 % (Table S2, Supplementary data). This fraction of the purified protein was used for all the enzymatic assays. When the activity was assessed under varying pH, >80 % activity was found in the pH range of 3.5–5, with the highest activity at pH 4.0. The enzyme activity decreased drastically below pH 3.5 (more than 50 % reduction) and beyond pH 5.5 (more than 95 % reduction) (Fig. 2B). The enzyme showed maximum activity at 35 °C with a gradual decrease in the activity at lower temperature and a drastic reduction in the enzyme activity above 40 °C (more than 60 % reduction) (Fig. 2C). The maximum overall activity was 115 U/mg protein of which the hydrolytic activity was 65 U/mg protein and the transfructosylation activity was 50 U/mg protein. For most of the conditions used, the hydrolytic activity was higher than the transfructosylation activity, however, at pH 5.0 the relative transfructosylation activity was 50 % (Fig. 2D).

Activity of LpInu was further assessed in the presence of various chemicals. The enzyme activity in the presence of 10 mM Ca^{2+} was 10-times higher than in the control without any salt. The presence of Mn^{2+} or Mg^{2+} also boosted the activity of LpInu though to a lower extent than that by Ca^{2+}. Reactions containing Fe^{2+} and K^+ also showed increase in enzyme activity, whereas EDTA and SDS completely inactivated the enzyme (Fig. 3A).

3.2.2. Thermostability

The thermostability of LpInu was determined at varying temperatures for 8 h. The enzyme incubated at ≤ 20 °C retained more than 80 % of its activity even after 8 h (Fig. 3B). The enzyme incubated at ≥ 30 °C showed decrease in the enzyme activity within 1 h.

3.3. Structural characterization of fructan

Apart from release of reducing sugars, the enzyme assays carrying LpInu also showed slimy consistency after 72 h suggesting production of polysaccharides. The isolated polysaccharides were analyzed by various analytical approaches to obtain information on their identity and structure. ^{1}H NMR spectra showed signals characteristic for β-fructans (Fig. 4A). Comparison of the obtained spectra with literature data (Kralj et al., 2018; Yokoi et al., 2021) as well as spectra of plant inulin and levan allowed for the identification of the LpInu fructans as inulins: the ^{1}H chemicals shifts of the LpInu fructans, especially those of H_3 protons (~4.2 ppm), were similar to those of plant inulin and not to those of levan. Thus, LpInu was characterized as inulosucrase. Notably, anomeric signals of glucose units (5.41 ppm) which are present at the reducing end of plant inulin were not detected which indicated a higher molecular weight of the LpInu inulins. To analyze the molecular weight distribution of the inulins, HPSEC-RI analysis was performed (Fig. 4B). A broad elution pattern was obtained and by using dextran standards, it was estimated that the size of the analyzed inulin was below dextran blue (2,000 kDa) and ranged down to 12 kDa.

To gain additional information on the polysaccharide structure, methylation analysis was performed. Terminal, 2,1-linked, and 2,1,6-linked fructofuranose (Fru*f*) units were detected (Fig. 4C, Fig. S1), which confirms the presence of inulin. Notably, about 8 % of branched backbone units were present. Overall, the polysaccharides are branched inulins with a broad size distribution.

3.4. Fructooligosaccharide (FOS) production by LpInu

LpInu also synthesized several different oligosaccharides from sucrose (Fig. 5). Compared to plant inulin, oligosaccharides of LpInu were rather small which is indicated by their early retention times. In addition to kestose, nystose and fructosylnystose, LpInu synthesized unknown oligosaccharides which may be composed of 2,1-linked or 2,1- and 2,1,6-linked fructofuranose units.

4. Discussion

The inulosucrase gene encoded by *L. plantarum* DKL3 shows only 41.7 % identity to an inulosucrase from *Limosilactobacillus reuteri* and even lower identity to the other characterized fructosyltransferases (Surve et al., 2022). This prompted us to undertake biochemically characterization of the enzyme and structural analysis of its product.

In comparison to the other enzymes, LpInu's optimal pH was slightly lower (3.5–5). The optimum pH of other fructansucrases previously described were 7 for an inulosucrase from *Lactobacillus johnsonii* NCC 533 (Anwar et al., 2008), 4.5 to 5.5 for a levansucrase from *L. reuteri* (van Hijum, Szalowska, van der Maarel, & Dijkhuizen, 2004) and 5.4 for a fructansucrase from *Fructilactobacillus sanfranciscensis* (Tieking, Ehrmann, Vogel, & Gänzle, 2005). Since the optimum pH is dictated by enzyme pI, we compared the estimated pI of LpInu with the other enzymes and it (5.35) was not different from the reported pI of the above-mentioned fructansucrases (4.7–5.4). The optimum temperature of LpInu (35 °C) was similar to those of fructansucrases from other LAB (Dutta, Das, & Goyal, 2012), (Iliev et al., 2018), (Kang et al., 2005).

LpInu's overall (115 U/mg), hydrolytic (65 U/mg), and transfructosylation activities (50 U/mg) were lower than those for the enzymes from *L. johnsonii* and *L. gasseri* DSM 20243. The overall, hydrolytic, and transfructosylations activities for these enzymes were in
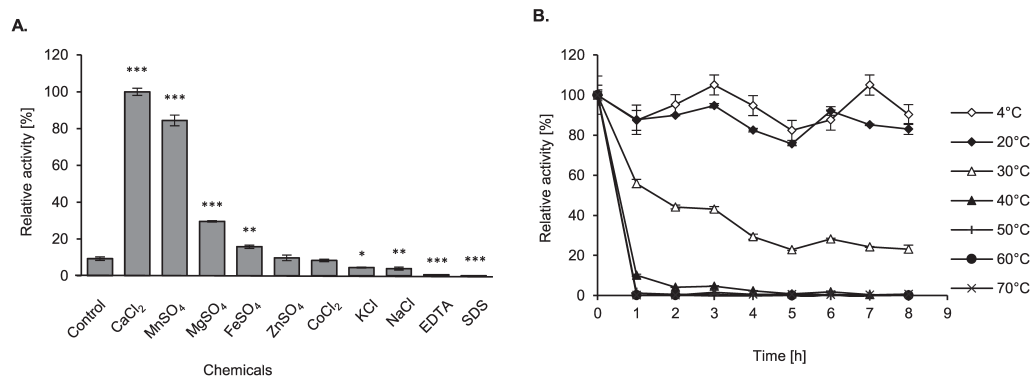
Fig. 3. Effects of various chemicals and thermal stability of inulosucrase (LpInu) from *L. plantarum* DKL3. (A) The effect of various chemicals on the activity of LpInu was accessed at 10 mM concentrations except for SDS which was used at 10 % w/v concentration. *, $p \leq 0.05$; **, $p \leq 0.01$; ***, $p \leq 0.001$ (one-way ANOVA with Tukey's test). (B) Thermostability of purified LpInu assessed by exposing the enzyme to the respective temperatures for 8 h followed by determination of the residual activity.

Publikation: *Food Chemistry*, 453, 139597
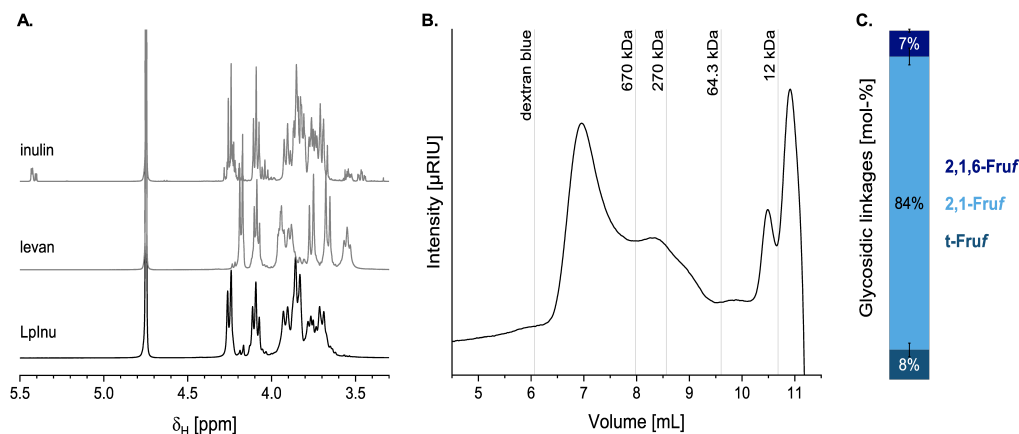
Fig. 4. Structural analysis of the polysaccharide made by LpInu. (A) ^{1}H NMR spectrum of LpInu polysaccharide in D_2O (plant inulin and levan spectra are shown for comparison). (B) HPSEC-RI elugrams of LpInu polysaccharide (reference lines of elution volumes of dextran size standards are shown). (C) Glycosidic linkage types of LpInu polysaccharide (determined in duplicate by methylation analysis (Fig. S1); numbers indicate the position of substitution in the fructofuranosyl (Fru*f*) units; t: terminal).
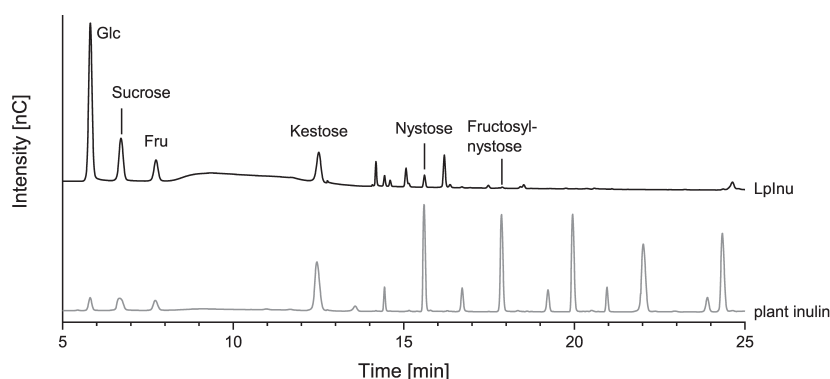
Fig. 5. Fructooligosaccharides produced by LpInu. HPAEC-PAD chromatogram of a 500 mM sucrose solution which was incubated with LpInu for 72 h at 30 °C. The chromatogram of plant inulin is shown for comparison and peaks were identified by using standard compounds.

the range of 316–378 U/mg, 88–178 U/mg, and 187–291 U/mg, respectively (Anwar et al., 2008, Anwar et al., 2010). Anwar et al. (2012) found reduction in the overall, hydrolytic and transglycosylation activities of *L. reuteri* 121 inulosucrase upon replacing A425 residue with proline. Interestingly, the residue homologous to A425 in LpInu was proline (Fig. 1). This could be a reason for lower enzymatic activities of LpInu.

Increase in the LpInu's activity in the presence of Ca^{2+} is consistent with earlier reports (Anwar et al., 2008, 2010; Ozimek, Euverink, van der Maarel, & Dijkhuizen, 2005). LpInu's lower activity observed without providing exogenous Ca^{2+} could be because of Ca^{2+} already bound to the recombinant enzyme purified from *E. coli* (Anwar et al., 2008). Enhancement of LpInu's activity by Mn^{2+} is a unique feature. None of the previously characterized inulosucrases have been shown to have activity in the presence of Mn^{2+} (Ni, Chen, Xu, Zhang, & Mu, 2020; Zhang, Ni, Xu, Zhang, & Mu, 2023).

The thermostability of LpInu was lesser than a few other enzymes reported earlier. Inulosucrase from *Lactobacillus jensenii* and *Lactobacillus mulieris* retained more than 70 % activity at 60 °C and 45 °C, respectively, after 10 h of incubation (Ni et al., 2020; S. Zhang et al., 2023).

^{1}H NMR and methylation analyses revealed the existence of more than 80 % β-2,1-linked, 7 % β-2,1,6-linked and 8 % terminal Fru*f* units which demonstrates the presence of branched inulin. The glycosidic linkages obtained for inulin are similar to inulin synthesized by inulosucrase of *Limosilactobacillus reuteri* 121 (van Hijum et al., 2002) and inulin synthesized by inulosucrase of *Leuconostoc citreum* CW28 (Olivares-Illana et al., 2003). Recombinant LpInu synthesized inulin of broad size distribution which was determined using HPSEC-RI. The highest molecular weight compounds eluted after dextran blue (~2 × 10^6 Da). Thus, the molecular weight is most likely lower than that of other characterized microbial fructans, viz., synthesized by inulosucrase from *Lactobacillus johnsonii* NCC 533 (4 × 10^7 Da) (Anwar et al., 2008) and inulosucrase from *Limosilactobacillus reuteri* 121 (>10^7 Da) (van Hijum et al., 2002). The possible contribution of unique features in the primary structure of LpInu to the lower molecular weight of its inulin product needs to be examined. Production of kestose and nystose by LpInu is similar to that reported for most of inulosucrases reported earlier (Anwar et al., 2008, 2010; van Hijum et al., 2002). While the production of unknown FOS by LpInu is also similar to that by the enzymes from *L. johnsonii* NCC 533, *L. gasseri* DSM 20243, and *L. gasseri* DSM 20604 (Anwar et al., 2008, 2010), whereas the enzyme from

6

Publikation: *Food Chemistry*, 453, 139597

L. reuteri 121 does not produce such additional FOS (van Hijum et al., 2002).

5. Conclusion

Inulins are well known to have prebiotic effects and to be useful as food texturizers. Recently, they have also been tested as biomaterials for tissue-engineering applications (Kalirajan, Behera, Selvaraj, & Palanisamy, 2022). We provide new information on an active inulosucrase from *L. plantarum*, a LAB species which has never been characterized for the presence of functional fructansucrases or glucansucrases. The unique biochemicals features of LpInu (lower optimum pH, lower specific activity, activation by Mn^{2+}, and lower molecular weight of the inulin) could be correlated to some of the unique sequence features (larger size, presence of extra amino acid stretches, amino acid substitutions, etc.) that would demand further experimental validation. The experiments ongoing in our laboratory would shed more light on the possible plethora of applications of inulin produced by recombinant LpInu.

Funding details

CRediT authorship contribution statement

Sahara Sarang: Writing – original draft, Visualization, Validation, Methodology, Investigation, Formal analysis. **Luise Ernst:** Writing – original draft, Visualization, Methodology, Investigation, Formal analysis. **Daniel Wefers:** Writing – review & editing. **Ram Kulkarni:** Writing – review & editing, Supervision, Project administration, Methodology, Conceptualization.

Declaration of competing interest

The authors declare that they have no known competing financial interests or personal relationships that could have appeared to influence the work reported in this paper.

Data availability

No data was used for the research described in the article.

Appendix A. Supplementary data

Supplementary data to this article can be found online at https://doi.org/10.1016/j.foodchem.2024.139597.

References

Anwar, M. A., Kralj, S., Piqué, A. V., Leemhuis, H., van der Maarel, M. J. E. C., & Dijkhuizen, L. (2010). Inulin and levan synthesis by probiotic *Lactobacillus gasseri* strains: Characterization of three novel fructansucrase enzymes and their fructan products. *Microbiology, 156*(4), 1264–1274. https://doi.org/10.1099/mic.0.036616-0

Anwar, M. A., Kralj, S., van der Maarel, M. J. E. C., & Dijkhuizen, L. (2008). The probiotic *lactobacillus johnsonii* ncc 533 produces high-molecular-mass inulin from sucrose by using an inulosucrase enzyme. *Applied and Environmental Microbiology, 74*(11), 3426–3433. https://doi.org/10.1128/AEM.00377-08

Anwar, M. A., Leemhuis, H., Pijning, T., Kralj, S., Dijkstra, B. W., & Dijkhuizen, L. (2012). The role of conserved inulosucrase residues in the reaction and product specificity of *Lactobacillus reuteri* inulosucrase. *The FEBS Journal, 279*(19), 3612–3621. https://doi.org/10.1111/j.1742-4658.2012.08721.x

Dutta, A., Das, D., & Goyal, A. (2012). Purification and characterization of fructan and fructansucrase from *Lactobacillus fermentum* AKJ15 isolated from Kodo ko jaanr, a fermented beverage from north-eastern Himalayas. *International Journal of Food Sciences and Nutrition, 63*(2), 216–224. https://doi.org/10.3109/09637486.2011.618826

Ernst, L., Offermann, H., Werner, A., & Wefers, D. (2024). Comprehensive structural characterization of water-soluble and water-insoluble homoexopolysaccharides from seven lactic acid bacteria. *Carbohydrate Polymers, 121417*. https://doi.org/10.1016/j.carbpol.2023.121417

Ernst, L., Werner, A., & Wefers, D. (2023). Influence of ultrasonication and hydrolysis conditions in methylation analysis of bacterial homoexopolysaccharides. *Carbohydrate Polymers, 308*, Article 120643. https://doi.org/10.1016/j.carbpol.2023.120643

Gottlieb, H. E., Kotlyar, V., & Nudelman, A. (1997). NMR chemical shifts of common laboratory solvents as trace impurities. *The Journal of Organic Chemistry, 62*(21), 7512–7515. https://doi.org/10.1021/jo971176v

Iliev, I., Vasileva, T., Bivolarski, V., Salim, A., Morel, S., Rabier, P., & Gabriel, V. (2018). Optimization of the expression of levansucrase L17 in recombinant *E. coli*. *Biotechnology & Biotechnological Equipment, 32*(2), 477–486. https://doi.org/10.1080/13102818.2018.1431056

Ito, H., Takemura, N., Sonoyama, K., Kawagishi, H., Topping, D. L., Conlon, M. A., & Morita, T. (2011). Degree of polymerization of inulin-type fructans differentially affects number of lactic acid bacteria, intestinal immune functions, and immunoglobulin a secretion in the rat cecum. *Journal of Agricultural and Food Chemistry, 59*(10), 5771–5778. https://doi.org/10.1021/jf200859z

Kalirajan, C., Behera, H., Selvaraj, V., & Palanisamy, T. (2022). In vitro probing of oxidized inulin cross-linked collagen-ZrO2 hybrid scaffolds for tissue engineering applications. *Carbohydrate Polymers, 289*, Article 119458. https://doi.org/10.1016/j.carbpol.2022.119458

Kang, H. K., Seo, M. Y., Seo, E. S., Kim, D., Chung, S. Y., Kimura, A., Day, D. F., & Robyt, J. F. (2005). Cloning and expression of levansucrase from *Leuconostoc mesenteroides* B-512 FMC in *Escherichia coli*. *Biochimica et Biophysica Acta (BBA) - Gene Structure and Expression, 1727*(1), 5–15. https://doi.org/10.1016/j.bbaexp.2004.10.012

Kralj, S., Leeflang, C., Sierra, E. I., Kempiński, B., Alkan, V., & Kolkman, M. (2018). Synthesis of fructooligosaccharides (FosA) and inulin (InuO) by GH68 fructosyltransferases from *Bacillus agaradhaerens* strain WDG185. *Carbohydrate Polymers, 179*, 350–359. https://doi.org/10.1016/j.carbpol.2017.09.069

Ni, D., Chen, Z., Xu, W., Zhang, W., & Mu, W. (2020). Efficient production of inulin and oligosaccharides using thermostable inulosucrase from *Lactobacillus jensenii*. *International Journal of Biological Macromolecules, 165*, 1250–1257. https://doi.org/10.1016/j.ijbiomac.2020.10.003

Olivares-Illana, V., López-Munguía, A., & Olvera, C. (2003). Molecular Characterization of inulosucrase from *leuconostoc citreum* : A fructosyltransferase within a glucosyltransferase. *Journal of Bacteriology, 185*(12), 3606–3612. https://doi.org/10.1128/JB.185.12.3606-3612.2003

Ozimek, L. K., Euverink, G. J. W., van der Maarel, M. J. E. C., & Dijkhuizen, L. (2005). Mutational analysis of the role of calcium ions in the *Lactobacillus reuteri* strain 121 fructosyltransferase (levansucrase and inulosucrase) enzymes. *FEBS Letters, 579*(5), 1124–1128. https://doi.org/10.1016/j.febslet.2004.11.113

Rana, S., & Upadhyay, L. S. B. (2020). Microbial exopolysaccharides: Synthesis pathways, types and their commercial applications. *International Journal of Biological Macromolecules, 157*, 577–583. https://doi.org/10.1016/j.ijbiomac.2020.04.084

Schwab, C., & Gänzle, M. G. (2006). Effect of membrane lateral pressure on the expression of fructosyltransferases in *Lactobacillus reuteri*. *Systematic and Applied Microbiology, 29*(2), 89–99. https://doi.org/10.1016/j.syapm.2005.09.005

Sumner, J. B., & Graham, V. A. (1921). Dinitrosalicylic acid: A reagent for the estimation of sugar in normal and diabetic urine. *Journal of Biological Chemistry, 47*(1), 5–9. https://doi.org/10.1016/S0021-9258(18)86093-8

Surve, S., Shinde, D. B., & Kulkarni, R. (2022). Isolation, characterization and comparative genomics of potentially probiotic *Lactiplantibacillus plantarum* strains from Indian foods. *Scientific Reports, 12*(1), 1940. https://doi.org/10.1038/s41598-022-05850-3

Sweet, D. P., Shapiro, R. H., & Albersheim, P. (1975). Quantitative analysis by various g.l.c. response-factor theories for partially methylated and partially ethylated alditol acetates. *Carbohydrate Research, 40*(2), 217–225. https://doi.org/10.1016/S0008-6215(00)82604-X

Tieking, M., Ehrmann, M. A., Vogel, R. F., & Gänzle, M. G. (2005). Molecular and functional characterization of a levansucrase from the sourdough isolate *Lactobacillus sanfranciscensis* TMW 1.392. *Applied Microbiology and Biotechnology, 66*(6), 655–663. https://doi.org/10.1007/s00253-004-1773-5

Tuinier, R., van Casteren, W. H. M., Looijesteijn, P. J., Schols, H. A., Voragen, A. G. J., & Zoon, P. (2001). Effects of structural modifications on some physical characteristics of exopolysaccharides from *Lactococcus lactis*. *Biopolymers, 59*(3), 160–166. https://doi.org/10.1002/1097-0282(200109)59:3<160::AID-BIP1015>3.0.CO;2-V

van Hijum, S. A. F. T., Kralj, S., Ozimek, L. K., Dijkhuizen, L., & van Geel-Schutten, I. G. H. (2006). Structure-function relationships of glucansucrase and fructansucrase enzymes from lactic acid bacteria. *Microbiology and Molecular Biology Reviews, 70*(1), 157–176. https://doi.org/10.1128/MMBR.70.1.157-176.2006

van Hijum, S. A. F. T., Szalowska, E., van der Maarel, M. J. E. C., & Dijkhuizen, L. (2004). Biochemical and molecular characterization of a levansucrase from *Lactobacillus reuteri*. *Microbiology, 150*(3), 621–630. https://doi.org/10.1099/mic.0.26671-0

van Hijum, S. A. F. T., van Geel-Schutten, G. H., Rahaoui, H., van der Maarel, M. J. E. C., & Dijkhuizen, L. (2002). Characterization of a novel fructosyltransferase from *lactobacillus reuteri* that synthesizes high-molecular-weight inulin and inulin oligosaccharides. *Applied and Environmental Microbiology, 68*(9), 4390–4398. https://doi.org/10.1128/AEM.68.9.4390-4398.2002

7

Publikation: *Food Chemistry*, 453, 139597

S. Sarang et al.

Yokoi, K., Tsutsui, S., Arakawa, G., Takaba, M., Fujii, K., & Kaneko, S. (2021). Molecular and biochemical characteristics of inulosucrase InuBK from *Alkalihalobacillus krulwichiae* JCM 11691. *Bioscience, Biotechnology, and Biochemistry, 85*(8), 1830–1838. https://doi.org/10.1093/bbb/zbab094

Zeidan, A. A., Poulsen, V. K., Janzen, T., Buldo, P., Derkx, P. M. F., Øregaard, G., & Neves, A. R. (2017). Polysaccharide production by lactic acid bacteria: From genes to industrial applications. *FEMS Microbiology Reviews, 41*(Supp_1), S168–S200. https://doi.org/10.1093/femsre/fux017

Zhang, H., Yohe, T., Huang, L., Entwistle, S., Wu, P., Yang, Z., & Yin, Y. (2018). dbCAN2: A meta server for automated carbohydrate-active enzyme annotation. *Nucleic Acids Research, 46*(W1), W95–W101. https://doi.org/10.1093/nar/gky418

Zhang, S., Ni, D., Xu, W., Zhang, W., & Mu, W. (2023). Characterization of a processive inulosucrase from *Lactobacillus mulieris* for efficient biosynthesis of high-molecular-weight inulin. *Enzyme and Microbial Technology, 164*, Article 110186. https://doi.org/10.1016/j.enzmictec.2022.110186

8

Supplementary Material

Characterization of a novel inulosucrase from *Lactiplantibacillus plantarum*
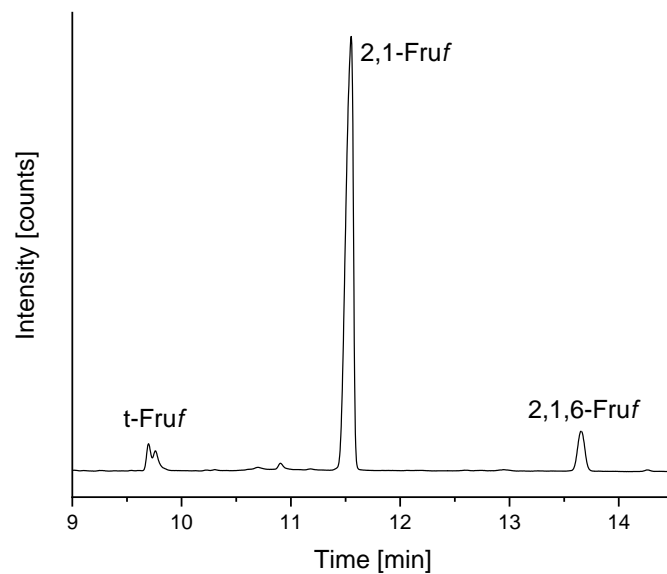
Figure S1: GC-FID chromatogram of partially methylated alditol acetates (PMAA) derived from LpInu polysaccharide. PMAA were identified by mass spectrometry and peaks were assigned with the corresponding glycosidic linkages of fructofuranose units. t: terminal, Fru*f*: fructofuranose, the numbers indicate the position of substitution.

Publikation: *Food Chemistry*, 453, 139597

Table S1: Unique amino acid stretches in L. plantarum inulosucrase (LpInu) and their similarity with other fructansucrases as determined by BLASTp

SADVTATSTSSSA (residues 45-57)

Description	Accession	Per. Ident	Query Cover	E value	Max Score	Total Score	Acc. Len
fructansucrase [Weissella confusa]	ADB27748.1	100%	100%	1.00E-08	38.8	81.2	900

SSSSAVK (residues 131-137)

Description	Accession	Per. Ident	Query Cover	E value	Max Score	Total Score	Acc. Len
fructansucrase [Weissella confusa]	ADB27748.1	100%	100%	0.004	21.8	96.9	900
fructosyltransferase [Streptococcus mutans GS-5]	AAA88584.1	100%	100%	5.9	13.4	22.9	797

NVTMFDGHKE (residues 480-489)

Description	Accession	Per. Ident	Query Cover	E value	Max Score	Total Score	Acc. Len
fructansucrase [Weissella confusa]	ADB27748.1	90%	100%	9.00E-07	32.9	32.9	900

RNKDGKAVLDPDFIQENNG (residues 726-744)

Description	Accession	Per. Ident	Query Cover	E value	Max Score	Total Score	Acc. Len
fructansucrase [Weissella confusa]	ADB27748.1	100%	100%	6.00E-17	63.8	63.8	900
levansucrase [Lactobacillus gasseri]	ACZ67287.1	100%	100%	6.4	15.5	30.5	768

Publikation: *Food Chemistry*, 453, 139597

	Table S2: Densitometric analysis of the SDS-PAGE images to determine the purity of LpInu using ImageJ		
Band No.	Relative front (Rf)	Adjusted volume	Band (%)
1	0.157	3,42,350	89.8
2	0.231	23,550	6.2
3	0.349	15,200	4.0
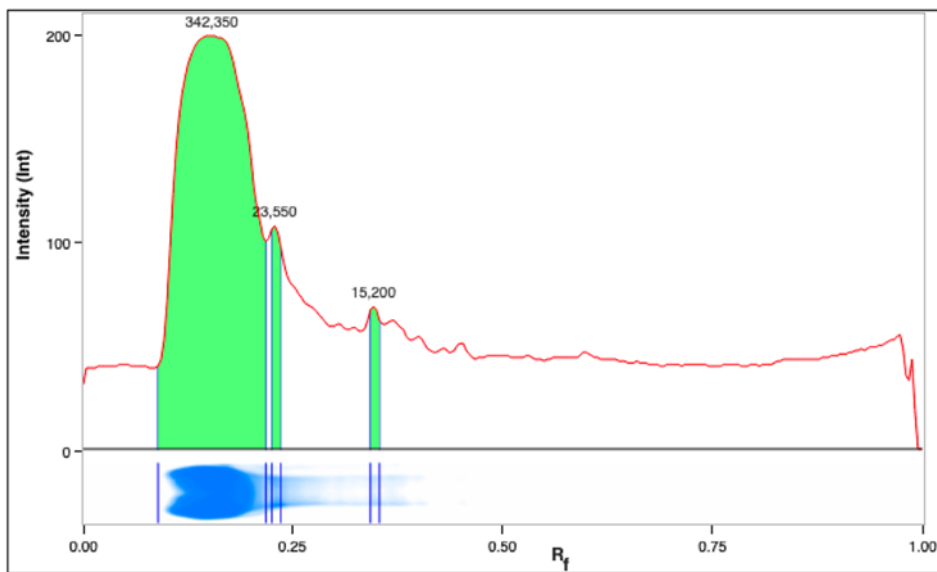
Publikation: *Journal of Applied Microbiology*, 134, lxad268

JOURNAL OF
APPLIED
MICROBIOLOGY

OXFORD
UNIVERSITY PRESS

Glycoside hydrolase family 32 enzymes from *Bombella* spp. catalyze the formation of high-molecular weight fructans from sucrose

Luca Härer [1], Luise Ernst[2], Julia Bechtner[3], Daniel Wefers[2], Matthias A. Ehrmann[1,*]

[1]Chair of Microbiology, Technical University of Munich, Gregor-Mendel-Straße 4, 85354 Freising, Germany
[2]Institute of Chemistry, Division of Food Chemistry, Martin Luther University Halle–Wittenberg, Kurt-Mothes-Straße 2, 06120 Halle (Saale), Germany
[3]Department of Food Science–Food Technology, Aarhus University, Agro Food Park 48, 8200 Aarhus N, Denmark

*Corresponding author. Chair of Microbiology, Technical University of Munich, Gregor-Mendel-Straße 4, 85354 Freising, Germany; Tel: +49(0)8161 71-3301; E-mail: matthias.ehrmann@tum.de

Abstract

Aims: Acetic acid bacteria of the genus *Bombella* have not been reported to produce exopolysaccharides (EPS). In this study, the formation of fructans by *B. apis* TMW 2.1884 and *B. mellum* TMW 2.1889 was investigated.

Methods and Results: Out of eight strains from four different *Bombella* species, only *B. apis* TMW 2.1884 and *B. mellum* TMW 2.1889 showed EPS formation with 50 g l^{-1} sucrose as substrate. Both EPS were identified as high-molecular weight (HMW) polymers (10^6–10^7 Da) by asymmetric flow field-flow fractionation coupled to multi angle laser light scattering and UV detecors (AF4-MALLS/UV) and high performance size exclusion chromatography coupled to MALLS and refractive index detectors (HPSEC-MALLS/RI) analyses. Monosaccharide analysis via trifluoroacetic acid hydrolysis showed that both EPS are fructans. Determination of glycosidic linkages by methylation analysis revealed mainly 2,6-linked fructofuranose (Fru*f*) units with additional 2,1-linked Fru*f* units (10%) and 2,1,6-Fru*f* branched units (7%). No glycoside hydrolase (GH) 68 family genes that are typically associated with the formation of HMW fructans in bacteria could be identified in the genomes. Through heterologous expression in *Escherichia coli* Top10, an enzyme of the GH32 family could be assigned to the catalysis of fructan formation. The identified fructosyltransferases could be clearly differentiated phylogenetically and structurally from other previously described bacterial fructosyltransferases.

Conclusions: The formation of HMW fructans by individual strains of the genus *Bombella* is catalyzed by enzymes of the GH32 family. Analysis of the fructans revealed an atypical structure consisting of 2,6-linked Fru*f* units as well as 2,1-linked Fru*f* units and 2,1,6-Fru*f* units.

Impact Statement

This is the first report of bacterial glycoside hydrolase 32 family enzymes involved in the formation of high-molecular weight fructans.

Abbreviations

HMW:	high-molecular weight
GH:	glycoside hydrolase
FTase:	fructosyltransferase
FOS:	fructo-oligosaccharides
Fru*f* :	fructofuranose
HPAEC-PAD:	high-performance anion exchange chromatography with pulsed amperometric detection
TFA:	trifluoroacetic acid
NMR:	nuclear magnetic resonance
AF4:	asymmetric flow field-flow fractionation
UV:	ultraviolet
MALLS:	multiangle laser light scattering
HPSEC:	high-performance size exclusion chromatography
RI:	refractive index
E. coli :	*Escherichia coli*
ORF:	open reading frame
AA:	amino acid

Introduction

Bacterial fructans are typically classified into levans and inulins. Both are exopolysaccharides (EPS) that differ in the linkage types of the fructofuranose (Fru*f*) backbone: levans have β-(2→6) linkages and inulins are composed of β-(2→1) linkages (Velázquez-Hernández et al. 2009). Inulins are common in plants, but their formation is only associated with a few Gram-positive genera (van Hijum et al. 2002, Velázquez-Hernández et al. 2009, Ni et al. 2019, Xu et al. 2019). Levans, on the other hand, are produced by a variety of prokaryotes, such as lactic acid bacteria (Ni et al. 2018), pseudomonads (Visnapuu et al. 2011), and acetic acid bacteria (Jakob et al. 2019). Bacterial fructans offer many applications, e.g. as pre-

biotics in foods (Coussement 1999, Kaur and Gupta 2002) or as emulsifiers in cosmetics (Banguela and Hernández 2006).

The extracellular formation of the two fructan types from sucrose is catalyzed by either inulosucrases (inulin; EC 2.4.1.9) or levansucrases (levan; EC 2.4.1.10). Both fructo-syltransferases (FTases) are classified as glycoside hydrolase (GH) 68 family enzymes by the "Carbohydrate Active Enzyme Database" (CAZy; http://www.cazy.org). In addition to the hydrolysis reaction, where water is the acceptor of the fructosyl unit, they catalyze the transfer of the fructosyl unit of sucrose to another saccharide, which leads to the formation of a fructan and the release of glucose (Meng and Fütterer 2003, Martínez-Fleites et al. 2005, Lammens et al. 2009, Alamäe et al. 2023). All GH68 family enzymes contain a five-bladed β-propeller structure harboring the catalytic triad, which consists of three acidic residues (Pons et al. 2004). They share this structure as well as a retaining reaction mechanism with enzymes of the GH32 family, which also belong to the GH family clan J (Pons et al. 2004, Alamäe et al. 2023). Unlike GH68 family members, enzymes belonging to the GH32 family generally have an additional C-terminal β-sandwich module (Lammens et al. 2009). Besides the differences in structure, the catalyzed reaction is also different: Most identified and characterized enzymes of the GH32 family catalyze hydrolysis reactions including a water molecule as an acceptor, e.g. the cleavage of sucrose into glucose and fructose (Liebl et al. 1998) or the degradation of levan into smaller molecules (Zhang et al. 2019).

Recently, the distribution of GH68 and GH32 family enzymes among acetic acid bacteria has been studied *in silico* (Jakob et al. 2019). For the genus *Bombella*, an acetic acid bacterium that is considered a symbiont of the honey bee *Apis mellifera* (Miller et al. 2021, Parish et al. 2022), only GH32 enzymes with *exo-β*-fructosidase activity have been identified so far (Jakob et al. 2019, Härer et al. 2022). Nevertheless, we observed slime formation by *Bombella* strains when growing on sucrose-containing medium, but not on glucose- or fructose-containing medium. Thus, in this study, the formation of high-molecular fructans by *Bombella* strains was investigated and the structures of the formed fructans were elucidated. In addition, the responsible enzyme was identified and assigned to fructan synthesis through heterologous gene expression in *Escherichia coli*. The corresponding protein sequences were analyzed phylogenetically and functionally and compared to other prokaryotic enzymes.

Materials and methods

Bacterial strains and growth conditions

Eight strains from three different species of the genus *Bombella* were used in this study: *B. apis* TMW 2.1882, *B. apis* TMW 2.1884, *B. apis* TMW 2.1886, *B. apis* TMW 2.1888, *B. apis* TMW 2.1890, *B. apis* TMW 2.1891, *B. favo-rum* TMW 2.1880, and *B. mellum* TMW 2.1889. *Bombella* spp. were cultivated in LMG 404 media (1% yeast extract; 5% glucose, pH 6.6) at 30°C and 200 rpm, if not stated otherwise.

For cloning and heterologous gene expression, *E . coli* Top10 was used. If not stated otherwise, *E. coli* was grown in Lysogeny Broth (LB, 10 g l^{-1} tryptone, 5 g l^{-1} yeast extract, 5 g l^{-1} NaCl) at 37°C. If necessary, 100 μg ml^{-1} ampicillin were added to the media.

Heterologous expression of *B. apis* TMW 2.1884 ORF DTI93_RS00530 and *B. mellum* TMW 2.1889 ORF CPA56_RS00775 in *E. coli*

For heterologous expression of the *B. apis* TMW 2.1884 ORF DTI93_RS00530 and *B. mellum* TMW 2.1889 ORF CPA56_RS00775, the pBAD/*Myc*-His A plasmid was used. Additionally, an extended version (gene sequences in Supplementary Material S2) of the *B. apis* TMW 2.1884 ORF DTI93_RS00530 was cloned. *Bombella apis* TMW 2.1884 and *B. mellum* TMW 2.1889 genomic DNA was isolated using the E.Z.N.A. Bacterial DNA Kit (Omega Bio-tek). To amplify the ORF DTI93_RS00530, the primer pair (5′-TTTCTCCATACCCGTTTTTTGGGCTAACAGGAGGAAT TAACCATGACGGACCTGTCCAATG-3′) and (5′-GCTGGAGACCGTTTAAACTCAATGATGATGATGATGA TGGCCATAATCACTTGTCGAAACGG-3′) was used. For the extended version, the primer pair (5′-TTTCTCCATACCCGTTTTTTGGGCTAACAGGAGGAAT TAACCATGGTCACGATTCTTATTTTTG-3′) and (5′-GCTGGAGACCGTTTAAACTCAATGATGATGATGATGA TGGCCATAATCACTTGTCGAAACGG-3′) was used. Accordingly, the primer pair (5′-TTTCTCCATACCCGTTTTTTGGGCTAACAGGAGGAAT TAACCATGATGGACCTGTCCAG-3′) and (5′-GCTGGAGACCGTTTAAACTCAATGATGATGATGATGA TGGCCGTAATCACTTGTAGAAACGG-3′) was used for the ORF CPA56_RS00775. A Q5 High-Fidelity DNA Polymerase [New England Biolabs (NEB), Frankfurt a. M., Germany] was used for the polymerase chain reaction (PCR) according to the manufacturer's instructions. The obtained PCR products were purified using a Monarch PCR and DNA Cleanup Kit (NEB). The unmodified pBAD/*Myc*-His A plasmid was digested using SalI-HF and NocI-HF restriction enzymes (NEB). For the integration of the amplified genes into the linearized plasmids, Gibson Assembly (Gibson Assembly Master Mix, NEB) was performed according to the manufacturer's protocol. The assembled expression plasmids were transformed into *E. coli* Top10 using heat-shock transformation (Froger and Hall 2007).

Production and recovery of fructans

For the synthesis of fructans, *Bombella* strains were plated on agar plates (pH 5) containing 10 g l^{-1} yeast extract, 50 g l^{-1} sucrose, and 15 g l^{-1} agar–agar. For this purpose, 10 μl of an overnight culture was distributed equally on the agar plates. The plates were incubated at 30°C for 4 days. Formation of slime around the cultures indicated the formation of an extracellular polysaccharide. For heterologous fructan production, transformed *E. coli* Top10 was plated on modified LB-media agar plates containing additional 2 g l^{-1} arabinose for induction of the gene expression, 36 g l^{-1} sorbitol to prevent the formation of inclusion bodies and 50 g l^{-1} sucrose as a substrate. The plates were incubated at 20°C for 2 weeks.

For the recovery of formed fructans, the bacteria and slime were washed off the plate with 1.5 ml saline (0.9% NaCl) and the solution was collected. To obtain a higher yield, 10 plates of the same strain were used and the liquids were pooled. To remove the cells, the solution was centrifuged (10 000 × *g*, 10 min, 20°C). Precipitation of the polysaccharides from the supernatant and dialysis were carried out according to Hund-schell et al. (2020). The sample was treated with two volumes of chilled ethanol (−20°C) to precipitate the polysac-

Publikation: *Journal of Applied Microbiology*, 134, lxad268

Glycoside hydrolase family 32 enzymes from *Bombella* spp. catalyze the formation of high-molecular weight fructans from sucrose **3**

charide. After centrifugation ($10\,000 \times g$, 10 min, 4°C), the supernatant was discarded, and the pellet dissolved in distilled water. Dialysis against dH_2O (MWCO: 3.5 kDa; 4°C) was performed for 48 hours with at least five water changes. The dialyzed solution was then lyophilized to obtain the purified polysaccharide.

Monosaccharide composition analysis

The monosaccharide composition of the fructans was analyzed after trifluoroacetic acid (TFA) hydrolysis. A first batch of the samples was hydrolyzed with 1 M TFA at 70°C for 30 min for fructan hydrolysis. A second batch was hydrolyzed with 2 M TFA at 121°C for 60 min to hydrolyze potentially present glucans, mannans, or galactans. In both cases, TFA was removed by evaporation and subsequent co-evaporation with ethanol. Monosaccharides were analyzed by high-performance anion exchange chromatography with pulsed amperometric detection (HPAEC-PAD) on an ICS-6000 system (Thermo Scientific Dionex, Sunnyvale, CA, USA). Separation was achieved on a CarboPac PA20 column (150 × 3 mm i.d., 6.5 μm particle size, Thermo Scientific Dionex) using a flow rate of 0.4 ml min^{-1}. Column equilibration was achieved with 10 mM NaOH for 15 min. After sample injection, the following gradient was applied: 0–20 min: 10 mM NaOH, 20–30 min: Linear gradient from 10 to 200 mM NaOH, 30–40 min: Isocratic 200 mM NaOH + 200 mM sodium acetate, 40–50 min: Isocratic 200 mM NaOH. The column temperature was 30°C and the detector temperature was 25°C. Quantification was achieved by using an external calibration.

Nuclear magnetic resonance spectroscopy

For nuclear magnetic resonance (NMR) spectroscopy, a 10 mg ml^{-1} fructan solution in D_2O was prepared and acetone was used as internal reference [^{1}H: 2.22 ppm, ^{13}C: 30.89 ppm, according to Gottlieb et al. (1997)]. Proton, H, H-correlated spectroscopy (COSY), and heteronuclear single quantum coherence (HSQC) experiments were acquired on a 500 MHz DD2 spectrometer (Agilent, Santa Clara, CA, USA).

Methylation analysis

Methylation analysis was conducted as described by Ernst et al. (2023). In brief, samples were solubilized in dimethyl sulfoxide, deprotonated with dry NaOH(s), and methylated by using methyl iodide. Permethylated fructans were hydrolyzed with 1 M TFA at 70°C for 30 min, reduced by NaBD$_4$, and acetylated by using acetic anhydride and 1-methylimidazole. The obtained permethylated alditol acetates (PMAAs) were extracted into dichloromethane and separated by gas chromatography (GC). Identification was performed by using mass spectrometry and relative quantification was performed using a flame ionization detector and the molar response factors described by Sweet et al. (1975). Because the four PMAAs derived from 2,1- and 2,6-Fru*f* units have an identical retention time (in the case of the mannitol derivatives) or partially coelute (in the case of the sorbitol derivatives), their relative amounts were calculated based on the mass spectra. For 2,1-Fru*f* units, the intensities of specific fragments with m/z 161 and 190 were used to assess their portion. In the case of 2,6-Fru*f* units, the intensities of fragments with m/z 162 and 189 were used for calculation.

Endo-levanase hydrolysis and oligosaccharide analysis

Endo-levanase (5 U mg^{-1} sample; EC 3.2.1.65 from *Bacteroides thetaiotaomicron*, purchased from Megazyme (Bray, Ireland)) was added to a 3 mg ml^{-1} solution of fructans in dH_2O and incubated for 24 h at 40°C and 400 rpm. Inactivation was achieved by heating to 95°C for 15 min and protein was removed by centrifugation. The supernatants were analyzed by HPAEC-PAD on an ICS-6000 system (Thermo Scientific Dionex) coupled to an LTQ-XL linear ion trap mass spectrometer (MS) (Thermo Scientific). A post column split allowed simultaneous PAD and MS analysis. Prior to MS analysis, desalting of the eluent was achieved by an AERS 500e suppressor (4 mm, Thermo Scientific Dionex). To facilitate ionization by electrospray ionisation (ESI), 500 μM LiCl was added at a flow rate of 0.05 ml min^{-1} (AXP-MS pump, Thermo Scientific, Waltham, MA, USA). The source temperature was 300°C and oligosaccharides were detected in positive mode as their lithium adducts. A CarboPac PA200 column (250 × 3 mm i.d., 5.5 μm particle size, Thermo Scientific Dionex) was used for oligosaccharide separation at 0.4 ml min^{-1} and 30°C. Four eluents (A: dH_2O, B: 10 mM NaOH, C: 200 mM NaOH, and D: 200 mM NaOH + 500 mM sodium acetate) were used and the column was equilibrated with 100% B during 20 min before injection. After sample injection, the following gradient was used for separation: 0–10 min: Isocratic 100% B; 10–20 min: Linear gradient to 50% C + 50% A; 20–45 min: Linear gradient to 50% A, 30% C + 20% D; 45–55 min: Linear gradient to 50% A + 50% D; 55–65 min: Linear gradient to 100% D; 65–80 min: Isocratic 100% D; and 80–95 min: Isocratic 100% C. For comparison, levan of *Gluconobacter albidus* (Hundschell et al. 2020) was also hydrolyzed and analyzed.

Molecular weight determination via asymmetric flow field-flow fractionation

The molecular weight of purified fructans was determined using asymmetric flow field-flow fractionation (AF4, Wyatt Technology, Dernbach, Germany) coupled with multiangle laser light scattering (MALLS, Dawn Heleos II, Wyatt Technology) and ultraviolet (UV) detection (Dionex Ultimate 3000, Thermo Fisher Scientific) according to Ua-Arak et al. (2016, 2017). Separation was carried out on 10 kDa regenerated cellulose membranes (Wyatt Technology) using a 50 mM NaNO$_3$ eluent solution. Purified fructans were dissolved in dH_2O (final concentration 0.1 g l^{-1}) and injected (100 μl) into the separation channel. Each sample was measured at least twice. To calculate molar masses using UV concentration signals, the specific extinction coefficients of the isolated fructans at 400 nm were determined: A concentration series (0.1–10 mg ml^{-1} in dH_2O) of the purified fructans was prepared, and the UV extinctions at 400 nm were measured using a FLOUstar Omega microplate reader (BMG Labtech, Ortenberg, Germany). The obtained values were used to calculate the specific extinction coefficients [ml (mg·cm)$^{-1}$] of the isolated levan samples. These coefficients were then used to calculate the molar mass distributions using the random coil model integrated in the ASTRA 6.1 software (Wyatt Technology), assuming a refractive index increment (dn/dc) value of 0.146 ml g^{-1} (in 50 mM NaNO$_3$) for levan (Ua-Arak et al. 2017).

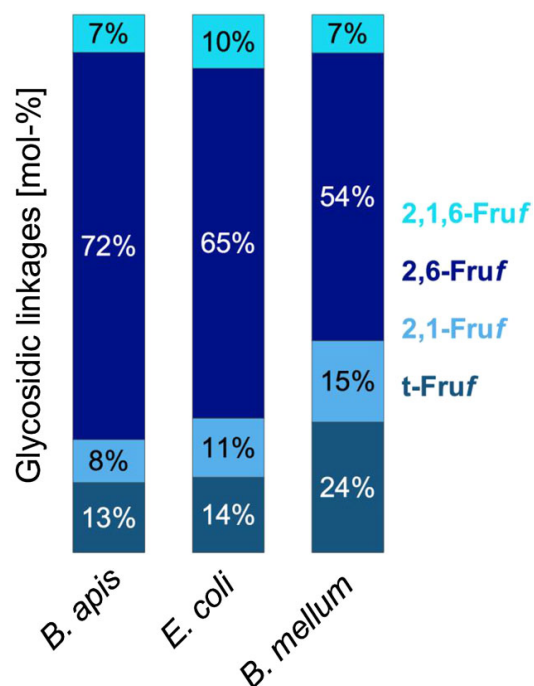Publikation: *Journal of Applied Microbiology*, 134, lxad268

Figure 1. Glycosidic linkages [mol-%] of fructans determined by methylation analysis. *Bombella apis/B. mellum:* native fructans produced by *B. apis* TMW 2.1884 or *B. mellum* TMW 2.1889 recovered from sucrose-containing agar-plates. *Escherichia coli:* fructan produced by *E. coli* Top10 strain expressing an extended version of the *B. apis* TMW 2.1884 GH32 family enzyme. All analyses were performed in duplicate and half range uncertainties were max. 4%. Fru*f*: fructofuranose, t: terminal, numbers indicate the substituted positions.

Molecular weight determination via high-performance size exclusion chromatography

In addition to AF4-UV/MALLS, fructans as well as their *endo*-levanase hydrolysates were analyzed by high-performance size exclusion chromatography coupled to MALLS and refractive index (RI) detectors (HPSEC-MALLS/RI). Analysis was performed on an Agilent 1100 Series HPLC with MALLS detector (PSS SLD7100) and RI detector (1260 Infinity II) equipped with a TSKgel PWXL 5000 column (300 × 7.8 mm i.d., 10 μm particle size, TOSOH Bioscience LLC). Water supplemented with 0.5 g l^{-1} NaN$_3$ was used as eluent at a flow rate of 0.35 ml min^{-1}, column temperature was 60°C, and RI temperature was 35°C. Samples were dissolved in ultrapure water (final concentration 1 mg ml^{-1}). Dextran size standards with known molecular weights (dextran blue, 670, 270, and 12 kDa, Sigma–Aldrich, Darmstadt, Germany; 64.3 kDa, PSS, Esslingen a. N., Germany) were used in addition to MALLS size determination using a refractive index increment (dn/dc) value of 0.146 ml g^{-1} (as for AF4-MALLS).

In-silico whole genome and sequence analysis

Whole genome data of the strains *B. apis* TMW 2.1882 (NZ_NWUT00000000), *B. apis* TMW 2.1884 (NZ_QORR01000001), *B. apis* TMW 2.1886 (QORS00000000), *B. apis* TMW 2.1888 (CP030979), *B. apis* TMW 2.1890 (NZ_NWUV00000000), *B. apis* TMW 2.1891 (NZ_QORT00000000), *B. favorum* TMW 2.1880 (NZ_NWUS00000000), and *B. mellum* TMW 2.1889 (NZ_PDLY00000000) were obtained from the National Center for Biotechnology Information (NCBI) database. For the annotation of carbohydrate active enzymes from the genome data, the DBcan webserver (Yin et al. 2012, Zhang et al. 2018) was used. Crystal structures of proteins were predicted with the SWISS-MODEL webserver (Guex et al. 2009, Bertoni et al. 2017, Bienert et al. 2017, Waterhouse et al. 2018, Studer et al. 2020). For the prediction of protein domains, the InterPro webserver (Paysan-Lafosse et al. 2023) was used. Sequence alignments were done with the Clustal Omega webtool (www.ebi.ac.uk/Tools/msa/clustalo) or the CLC Main Workbench (QIAGEN, Hilden, Germany).

For the phylogenetic analysis, protein sequences were retrieved from the NCBI database (https://www.ncbi.nlm.nih.gov). Sequence alignment was carried out with the ClustalW tool integrated in MEGA X (Kumar et al. 2018). Phylogenetic trees were calculated using the neighbor-joining method (Saitou and Nei 1987) with 1000 bootstrap replicates (Felsenstein 1985).

Results

Exopolysaccharide formation by *Bombella* spp.

The formation of extracellular polysaccharides from sugars, such as cellulose or levan, is a typical trait of acetic acid bacteria (Gullo et al. 2018, Jakob et al. 2019). The formation of such substances is typically tested by plating the strains on agar plates containing the respective sugar, which can serve as substrate for the enzymatic reaction. Slime formation around the colonies indicates the formation of exopolysaccharides. To test whether *Bombella* spp. can form EPS from sucrose, eight different strains of three different *Bombella* species (see the "Bacterial strains and growth conditions" section) were streaked onto agar plates with 50 g l^{-1} sucrose and incubated for 4 days at 30°C (see the "Production and recovery of fructans" section). Two strains were forming EPS when growing on sucrose: *B. apis* TMW 2.1884 and *B. mellum* TMW 2.1889. No slime was formed when the strains were grown on a mixture of 25 g l^{-1} glucose and 25 g l^{-1} fructose (monosaccharides of sucrose) or on 50 g l^{-1} raffinose. In other literature, EPS of acetic acid bacteria are isolated from liquid cultures (Jakob et al. 2013), since this was not possible with the *Bombella* strains, the EPS were recovered directly from the plates as described in the "Production and recovery of fructans" section.

Monosaccharide composition and glycosidic linkages

Monosaccharide analysis (see the "Monosaccharide composition analysis" section) showed that both EPS were composed of fructose. Galactose and glucose were only detected in traces (<2%). Thus, both EPS are fructans. By using NMR-spectroscopy (see the "Nuclear magnetic resonance spectroscopy" section), levan-derived signals were detected for both fructans (data not shown). In addition, determination of glycosidic linkages by methylation analysis (see the "Methylation analysis" section) provided further insights into the portions of linkages (Fig. 1) and revealed that both fructans are not solely 2,6-linked but also contain ∼10% of 2,1-

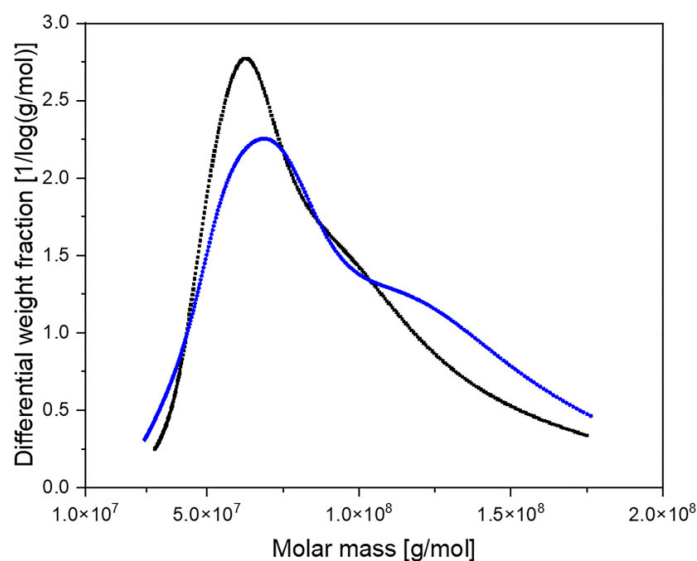Publikation: *Journal of Applied Microbiology*, 134, lxad268

Figure 2. Molecular weight distribution of native *B. apis* TMW 2.1884 (black) and *B. mellum* TMW 2.1889 (blue) fructans recovered from sucrose-containing agar-plates determined with AF4-MALLS.

linked Fru*f* units. Furthermore, both fructans contain 7% of branched units (2,1,6-Fru*f*).

Molecular weight determination

AF4-MALLS (see the "Molecular weight determination via asymmetric flow field-flow fractionation" section) was used to determine the molecular weight of the recovered fructans from *Bombella*. The average molecular weight of the *B. apis* TMW 2.1884 and *B. mellum* TMW 2.1889 fructan was 77.6 mDa (±0.2%) and 80.5 mDa (±0.5%), respectively. The molecular weight distribution is shown in Fig. 2 as the differential weight fraction.

In addition, a HPSEC-MALLS/RI analysis was performed (Fig. 3). The analysis showed that both fructans have comparable molecular weights but different size distributions. Comparison of the elugrams to standard dextrans with known molecular weights revealed that the fructans have a size between 270 kDa and several mDa. Furthermore, the calculated molecular weights from HPSEC-RI/MALLS analysis were 6 and 12 mDa for *B. apis* TMW 2.1884 and *B. mellum* TMW 2.1889, respectively. Minor variations in the obtained molecular weights result from the different analytical methods used. Nevertheless, all results clearly indicate that the fructans are high-molecular weight (HMW) polysaccharides.

Endo-levanase hydrolysis and distribution of glycosidic linkages

To obtain information on the distribution of 2,1- and 2,6-linkages in both fructans from *Bombella*, *endo*-levanase hydrolysis was performed. Subsequently, the enzymatically released oligosaccharides were analyzed by HPAEC-PAD/MS (Fig. 4). Both chromatograms showed several peaks, thus, multiple oligosaccharides were liberated by *endo*-levanase from both fructans. The oligosaccharide patterns were similar, indicating that both fructans contain similar structural elements. Oligosaccharides with identical degrees of polymer-

ization but different elution times indicate that differently linked oligosaccharides are present. For comparison, the hydrolysate of levan from *G. albidus* was analyzed. This levan is solely 2,6- and 2,1,6-linked as revealed by methylation analysis (Hundschell et al. 2020, Ernst et al. 2023). Thus, released oligosaccharides should exclusively contain these two linkage types. The chromatograms of the fructan hydrolysates from *Bombella* and *G. albidus* were comparable. Thus, 2,1-linkages of *Bombella* fructans most likely form blocks, which are not hydrolyzed by *endo*-levanase and not resolved by HPAEC-PAD.

To gain further information on the size of the obtained hydrolysis products, the *endo*-levanase hydrolysates were analyzed by HPSEC-RI and compared to the unmodified fructans from *Bombella* (Fig. 3). The peaks of the HMW fractions of both fructans disappeared after *endo*-levanase hydrolysis and intense peaks at high elution volumes appear. This indicates that HMW fractions were hydrolyzed to products with a lower molecular weight. Notably, the elugram of *B. mellum* contained hydrolysis products with a molecular weight of up to 670 kDa. Presumably, these products consist of blocks with consecutive 2,1-linkages or alternating 2,1- and 2,6-linkages, which were not hydrolyzed by *endo*-levanase.

Identification of the *Bombella* FTase

In order to identify the enzyme that catalyzes fructan synthesis, the *Bombella* genomes were analyzed *in silico* for corresponding genes. For this purpose, the genomes of all eight strains were annotated with the DBcan webserver (see the "*In silico* whole genome and sequence analysis" section), a tool that identifies all carbohydrate active enzymes in the respective genomes. Typically, levan synthesis of acetic acid bacteria is catalyzed by enzymes of the GH68 family. Since no enzymes of the GH68 family were identified, enzymes from the GH32 family were also included in the search. A GH32 fam-
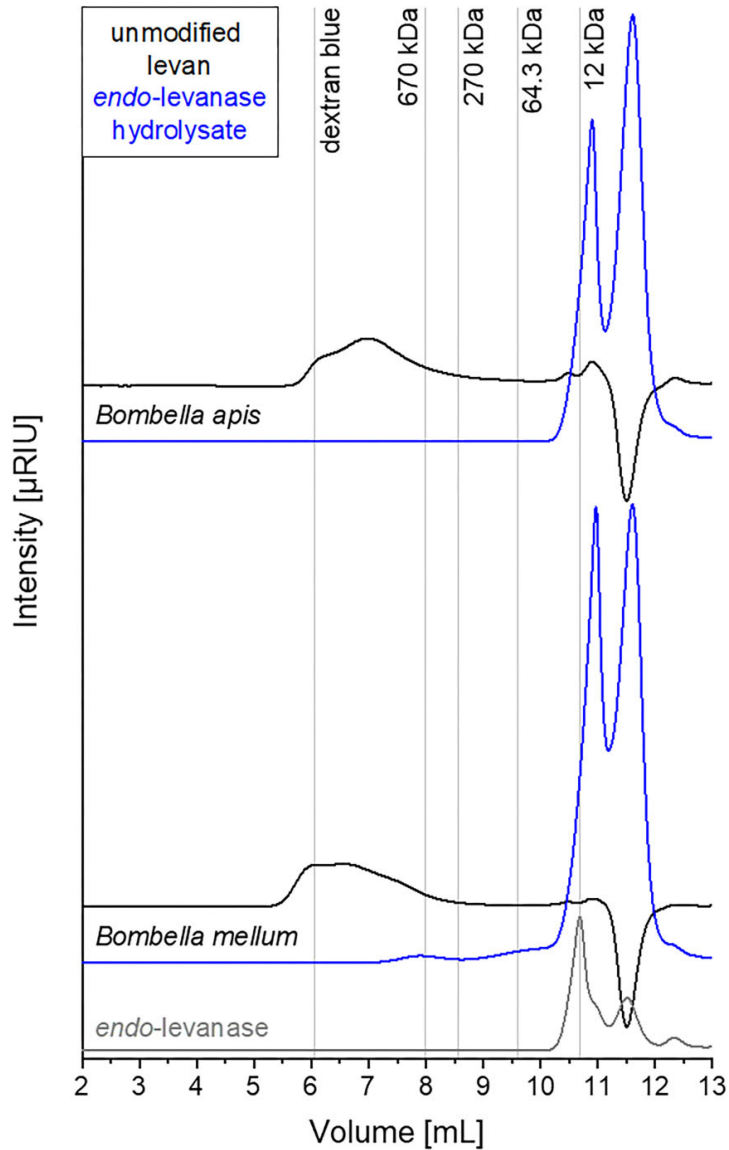
Publikation: *Journal of Applied Microbiology*, 134, lxad268

Figure 3. HPSEC-RI elugrams of native fructans from *B. apis* TMW 2.1884 and *B. mellum* TMW 2.1889 strains recovered from sucrose-containing agar-plates (black) as well as their *endo*-levanase hydrolysates (blue). The elugram of *endo*-levanase without fructan is given in gray for comparison and elution volumes of standard dextrans with known molecular weights are indicated by reference lines.

ily enzyme was identified in all genomes. However, for *B. apis* TMW 2.1884, *B. apis* TMW 2.1891, and *B. mellum* TMW 2.1889, additional GH32 family enzymes were identified with the respective locus tags DTI93_RS00530 [445 amino acids (AAs)], DTJ15_RS01635 (476 AAs), and CPA56_RS00775 (520 AAs).

The percentage identity between the three enzymes is between 87.3% and 94.7% and below 23.7% toward the other GH32 family enzymes (Table 1). In the *B. apis* TMW 2.1891 open reading frame (ORF) DTI93_RS00530, one nucleotide is missing after position C1376, which probably leads to the expression of a nonfunctioning protein due to a frameshift

(for gene alignment, see Supplementary Material S1). This mutation explains why the respective strain did not form EPS. The affected site in the *B. apis* TMW 2.1891 genome was sequenced by Eurofins Genomics (Ebersberg, Germany) for confirmation.

To demonstrate that the synthesis of *Bombella* spp. fructans is catalyzed by the identified additional GH32 family enzymes, the *B. mellum* TMW 2.1889 ORF CPA56_RS00775 as well as two versions of the *B. apis* TMW 2.1884 ORF DTI93_RS00530 were cloned and expressed in *E. coli* Top10 (see the "Heterologous expression of *B. apis* TMW 2.1884 ORF DTI93_RS00530 and *B. mellum* TMW 2.1889 ORF

Publikation: *Journal of Applied Microbiology*, 134, lxad268

Glycoside hydrolase family 32 enzymes from *Bombella* spp. catalyze the formation of high-molecular weight fructans from sucrose **7**
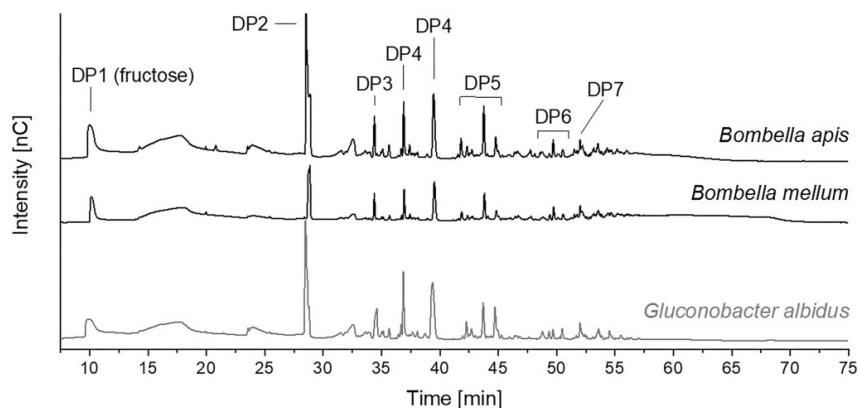

Figure 4. HPAEC-PAD chromatograms of the *endo*-levanase hydrolysates of native fructans from *B. apis* TMW 2.1884 and *B. mellum* TMW 2.1889 recovered from sucrose-containing agar-plates. The chromatogram of the hydrolysate of levan from *G. albidus* TMW 2.1191 is shown for comparison. Degrees of polymerization (DP) of the individual oligosaccharides were determined by MS and are given above the peaks.

Table 1. Percentage identity [%] of *Bombella* GH32 family enzymes calculated with Clustal Omega.

	1	2	3	4	5	6	7	8	9	10	11
1	100	91.37	90.98	90.82	90.82	90.98	90.98	90.98	23.67	22.03	22.59
2	91.37	100	92.97	92.97	92.97	93.13	93.13	93.13	22.81	21.68	21.88
3	90.98	92.97	100	99.53	99.68	99.68	99.68	99.84	22.6	21.44	21.88
4	90.82	92.97	99.53	100	99.53	99.84	99.84	99.68	22.81	21.64	22.12
5	90.82	92.97	99.68	99.53	100	99.68	99.68	99.84	22.81	21.64	22.12
6	90.98	93.13	99.68	99.84	99.68	100	100	99.84	22.81	21.64	22.12
7	90.98	93.13	99.68	99.84	99.68	100	100	99.84	22.81	21.64	22.12
8	90.98	93.13	99.84	99.68	99.84	99.84	99.84	100	22.81	21.64	22.12
9	23.67	22.81	22.6	22.81	22.81	22.81	22.81	22.81	100	90.56	87.34
10	22.03	21.68	21.44	21.64	21.64	21.64	21.64	21.64	90.56	100	94.74
11	22.59	21.88	21.88	22.12	22.12	22.12	22.12	22.12	87.34	94.74	100

1–8: GH32 family enzymes present in all *Bombella* genomes. 1 = *B. favorum* TMW 2.1880 (CPA57_RS07755), 2 = *B. mellum* TMW 2.1889 (CPA56_RS07355), 3 = *B. apis* TMW 2.1891 (DTJ15_RS07680), 4 = *B. apis* TMW 2.1888 (DTQ13_04 050), 5 = *B. apis* TMW 2.1884 (DTI93_RS04755), 6 = *B. apis* TMW 2.1882 (CO583_RS08065), 7 = *B. apis* TMW 2.1890 (CPA54_RS07155), and 8 = *B. apis* TMW 2.1886 (DTJ06_07 900). 9–11: Additional GH32 family enzymes. 9 = *B. mellum* TMW 2.1889 (CPA56_RS00775), 10 = *B. apis* TMW 2.1884 (DTI93_ RS00530), and 11 = *B. apis* TMW 2.1891 (DTJ15_RS01635). NCBI accession number are given in parentheses.

CPA56_RS00775 in *E. coli*" and "Production and recovery of fructans" sections). The first version corresponds to the original ORF, the second version is extended by 357 bases (119 AAs) because, according to the whole genome data, another ORF is also conceivable (Supplementary Material S2). An *E. coli* Top10 strain transformed with an unmodified expression plasmid was always included as a control. Purification of a useable amount of the heterologously expressed proteins by affinity chromatography failed due to poor expression and the strong tendency to form inclusion bodies. However, slime formation was observed for the *E. coli* strain expressing the extended version of the *B. apis* TMW 2.1884 protein when grown on agar plates containing the substrate sucrose, the inducer arabinose and sorbitol to facilitate correct protein folding (see the "Production and recovery of fructans" section). Formed fructans were recovered from the agar plates (see the "Production and recovery of fructans" section) and subjected to methylation analysis (see the "Methylation analysis" section). The analysis revealed that comparable portions of all three linkage types (2,6-Fru*f*, 2,1-Fru*f*, and 2,1,6-Fru*f*) occur in the fructan natively produced by *B. apis* TMW 2.1884 (see the "Exopolysaccharide formation by *Bombella* spp." section) and in the fructan produced by the *E. coli* strain expressing the

extended version of the GH32 family enzyme (Fig. 1). With a high level of confidence, it is postulated that the heterologous expressed enzyme is the FTase that catalyzes fructan formation in *B. apis* TMW 2.1884. Accordingly, it is assumed that in *B. mellum* TMW 2.1889, the ORF CPA56_RS00775 encodes for the corresponding FTase.

Sequence analysis of the *Bombella* FTase

For a phylogenetic analysis of the *Bombella* FTases, several GH32 and GH68 family enzyme sequences were obtained from the NCBI database. Actual enzymatic activity of the enzymes used was demonstrated in corresponding publications. The GH68 family was represented by levansucrases from *G. albidus* (Jakob et al. 2020), *Kozakia baliensis* (Brandt et al. 2016), *G. diazotrophicus* (Martínez-Fleites et al. 2005), *Halomonas smyrnensis* (Poli et al. 2009), *P. syringae* (Visnapuu et al. 2011), *Ba. subtilis* (Porras-Domínguez et al. 2015), *Leuconostoc mesenteroides* (Kang et al. 2005), and *Limosilactobacillus reuteri* (Ni et al. 2018). Accordingly, enzymes from *Ba. licheniformis* (Porras-Domínguez et al. 2014), *Ba. subtilis* (Jensen et al. 2016), *G. diazotrophicus* (Menéndez et al. 2004), *Microbacterium* sp. AL-210 (Cha et al. 2001), *Paenarthrobac-*
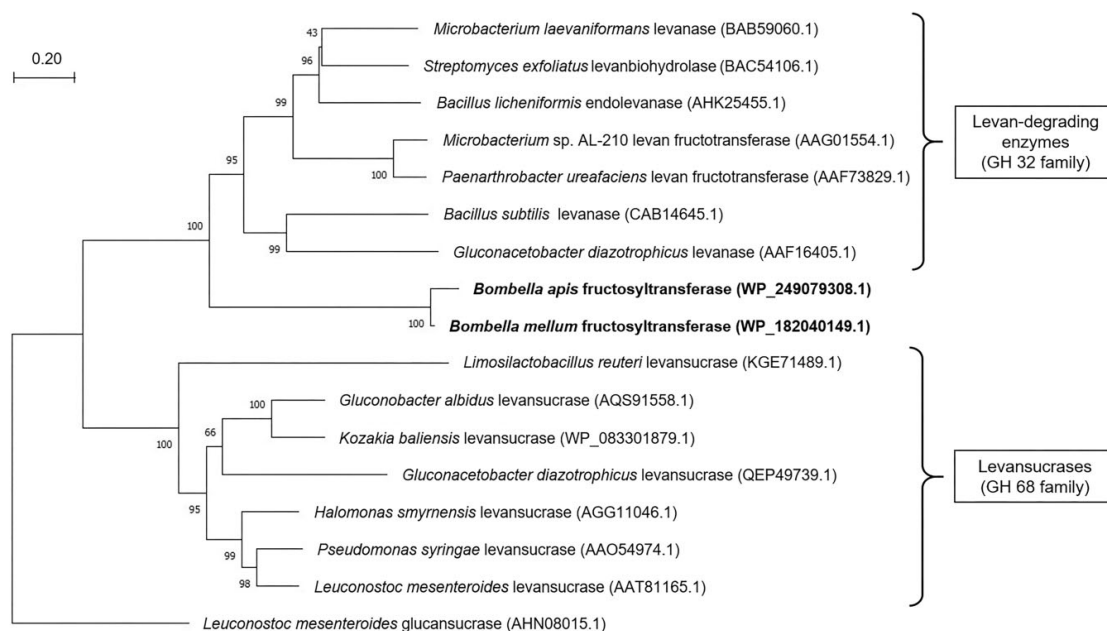
Publikation: *Journal of Applied Microbiology*, 134, lxad268

Figure 5. Phylogenetic tree of bacterial GH32 and GH68 family enzymes with *Bombella* FTases using the neighbor-joining method (Saitou and Nei 1987) in MEGA X (Kumar et al. 2018). Scale represents the number of amino acid substitutions per site. Numbers at nodes indicate bootstrap percentages using 1000 replicates. *Granulibacter bethesdensis* CGDNIH1^T was used as the outgroup. NCBI accession numbers are given in parentheses.
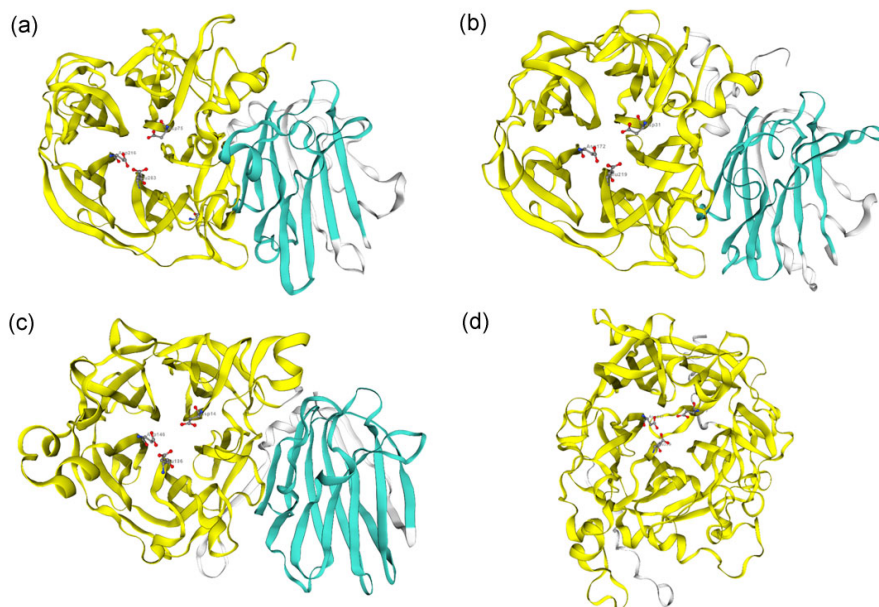

Figure 6. Protein crystal structure models of (a) *B. apis* TMW 2.1884 and (b) *B. mellum* TMW 2.1889 FTases. Models were constructed with the SWISS-MODEL (Template SMTL ID: 3rwk.1). The GH32 C-terminal domains are colored turquoise (*B. apis*: 444–551; *B. mellum*: 400–507) and N-terminal five-bladed β-propeller catalytic domains yellow (*B. apis*: 50–393; *B. mellum*: 24–351). The highlighted predicted catalytic triad consists of Asp75, Asp216, and Glu263 for *B. apis* and Asp31, Asp172, and Glu219 for *B. mellum*. For comparison, visualized crystal structures models of a (c) levan fructotransferase (GH32 family) from *Pa. ureafaciens* (SMTL ID: 4fff.1) and a (d) levansucrase (GH68 family) from *G. diazotrophicus* (SMTL ID: 1w18.1) are shown.

Glycoside hydrolase family 32 enzymes from *Bombella* spp. catalyze the formation of high-molecular weight fructans from sucrose **9**

Table 2. Conserved motifs among microbial FTase.

Motif number	Motif designation	Consensus sequence	Position*	*Bombella* sequence	Position *Bombella* (apis/mellum)	Function
I	VWDSW	(V/L)WD(T/S)(W/M)	84–8	**LWRTW**	(87–91/43–7)	Catalytic nucleophile, conserved in GH68 family
II	EWSGS	(E/Q)W(A /S)G(T/S)	162–6	**YWSGS**	(145–9/101–5)	Sucrose box I, conserved in GH68 family
III	DG	DG	172–3	RG	(160–1/116–7)	Involved in acceptor recognition
IV	LFYTD	L(F / Y)YT(D / C)	177–81	V̲YYYI	(165–9/121–5)	Sucrose box II and acceptor recognition
V	RDP	RDP	246–8	**RDC**	(215–7/171–3)	Catalytic center, stabilizes transition state and contributes to sucrose hydrolysis and fructan polymerization
VI	YLVFE	Y(M / L)VFE	258–62	F̲AF̲F̲R̲	(238–42/194–8)	Sucrose hydrolysis and transfructosylation
VII	PLI	PL(V / I)	330–2	**PLV**	(260–2/216–8)	Conserved among FTase; unknown function
VIII	DEIER	D(Q / E) (T / I)ER	339–43	L̲K(I̲/V̲)(V̲/L̲)KD	(270–4/226–30)	Catalytic center, acid–base catalyst, conserved in GH68 family
IX	YLFT	YLF(T / S)	354–7	AI̲L̲G	(285–8/241–4)	Conserved in microbial FTase
X	YKPLN	YXP(L / M)N	388–92	**YK**G̲F̲Q̲	(363–7/319–23)	Conserved in GH68 family
XI	TYS	TYS	410–2	**D**Y̲**S**	(381–3/311–13)	Orientates nucleophilic residue for transfructosylation

*Motif designation and amino acids positions are relative to *Ba. subtilis* levansucrase sequence (NCBI accession number: P05655). Modified from Velázquez-Hernández et al. (2009). Bold characters in the *Bombella* sequence indicate consensus positions, underlined characters indicate amino acids with properties similar to the consensus sequence. Functions were obtained from Meng and Fütterer (2003), Martínez-Fleites et al. (2005), and van Hijum et al. (2006).

ter ureafaciens (Song et al. 2000), *M. laevaniformans* (Song et al. 2002), and *Streptomyces exfoliatus* (Yokota et al. 1993) were used for the levan-degrading GH32 family. The corresponding phylogenetic tree with all NCBI accession numbers is shown in Fig. 5. The tree shows a clear grouping of the two GH enzyme families, independent of the taxonomic relationship of the host organisms. The uniqueness of *Bombella* FTases is shown by the formation of its own branch, which can be assigned to the GH32 family.

Crystal structure models of the *B. apis* TMW 2.1884 and *B. mellum* TMW 2.1889 FTases (Fig. 6) were constructed with the SWISS-MODEL webserver (Template SMTL ID: 3rwk.1, see the "*In-silico* whole genome and sequence analysis" section). Additionally, visualized crystal structures of a levan-sucrase (GH68 family) from *G. diazotrophicus* (SMTL ID: 1w18.1) and a levan fructotransferase (GH32 family) from *P. ureafaciens* (SMTL ID: 4fff.1) are shown for comparison. Protein domains predicted by InterPro (see the "*In-silico* whole genome and sequence analysis" section) were added manually. Five-bladed *β*-propeller catalytic domains (yellow) were detected in all enzymes. The C-terminal domains of the three GH32 enzymes form typical *β*-sandwich modules (turquoise), which clearly distinguishes them from the GH68 family enzyme. Catalytic triads are composed of Asp75, Asp216, and Glu263 for *B. apis*, Asp31, Asp172, and Glu219 for *B. mellum*, Asp73, Asp247, and Glu339 for *G. diazotrophicus* and Asp14, Asp146, and Glu196 for *P. ureafaciens*.

Both enzyme sequences of *Bombella* FTases were screened for conserved motifs of other microbial FTases (Velázquez-Hernández et al. 2009). A total of 11 motifs with different functions were analyzed. The results are shown in Table 2. All motifs were found in both enzyme sequences, but the cor-

responding regions all show differences from the consensus sequences described in literature. All identified FTase motifs are located on the N-terminal five-bladed *β*-propeller catalytic domain. In order to compare whether the motifs are more conserved in the *Bombella* FTases than in other GH32 enzymes, an alignment was made with the enzymes mentioned above and the motifs were marked (Fig. 7). Of the 11 motifs, some actually appear to be more conserved, such as motifs I, IV, and VII. Other motifs, such as V and VI, which are associated with polymerization/transfructosylation, do not show increased conservation in *Bombella* FTases.

Discussion

Fructan structure

Fructans of *Bombella* spp. are levan-type fructans, which possess 2,1-linked Fru*f* units in addition to 2,6- and 2,1,6-linked Fru*f* units. Furthermore, we demonstrated that larger blocks of 2,1-linked Fru*f* units are present in fructans from *B. mellum*. However, smaller consecutively 2,1-linked sections may also be present in *B. apis* fructans. Bacterial mixed-linkage fructans have not been described in literature yet. However, in the plant kingdom fructans containing 2,1- and 2,6-linkages, so called graminans, are known (Verspreet et al. 2014). From our data, we cannot conclude with certainty whether the fructans of *Bombella* are composed of two separate differently linked polysaccharides or whether they are copolymers. Nevertheless, it seems likely that a single enzyme forms copolymers rather than two individual polymers. Methylation analysis also demonstrated that fructans are branched by 2,1,6-Fru*f* units, which was supported by the results from *endo*-levanase hydrolysis: Several oligosaccharides were liberated,

```
                 I                                                          II
Bapi    LWRTWALGNPEWTPNSGFPTTSWISYSGPTIDAMTSDDDREPSGKDVFIDKNSSLSGTYW    146
Bmel    LWRTWALGDPEWTPDSGFPATSWISYSGPTIDAMTSDDDREPSGKDVFIDKNSSLSGTYW    102
MAL2    LYYLHSGQN--------NGPGGW--------DHATTSDGVAFTHHGTVMPL--QPDFPVW    117
Pure    LYYLHSDQN--------NGPGGW--------DHASTTDGVAFTHHGTVMPL--RPDFPVW    108
Mlae    YYYLYNADYDA--NPRANFGTEW--------RLATSADGVAFADQGVAAPKGTNANYDLW    148
Blic    YYYLYNRDYPD-----G-NGTEW--------RHAVSDDLVHWQDQGVAIPKYTNKNGDFW     85
Sexf    YYYLYNADYFT-----GVVGTAW--------RLATTKDLVSFTDRGVAVPKDTTPNGDLW    119
Bsub    LFYQYHPYGLQ------WGPMHW--------GHAVSKDLVTWEHLPVALYP--DEKGTIF    105
Gdia    LFYQYAPGSMT------WGHPSW--------GHATSTDLLHWTEHGVAIAA--TPGEEIF    113
             :             *            :  *     .          :

           II        III    IV
Bapi    SGSVWVDEEDRLGRGRGSVYYISGPAPV----------LQAIYLLVAKRLG--EVPYNL    194
Bmel    SGSVWVDEENRLGRGCGSVYYISGPAPV----------LQAIYLLVADRLG--EVPYNL    150
MAL2    SGSAVVDTANTAGFGAGAVIALATQPTD-------GIRKYQEQYLYWSTDGGYTFTALPD    170
Pure    SGSAVVGTANTAGFGAGAVVALATQPTD-------GVRKYQEQYLYWSTDGGFTFTALPD    161
Mlae    SGSAVVDHAGTAGFGPGAVVMLVTQMDHPTAAQKLDASGQQAQFLWYSVDGGRTFRPDGD    208
Blic    SGSVVVDSQNTAGFGKGAIVAINTQ-PS-------ANDGKEEQFLWYSQNGGKTFKPYGE    137
Sexf    SGSAVVDTGNTAGFGAGAVVVIVTMSPG-------GGTDHQEQFLYYSTDGGLTFTNYGT    172
Bsub    SGSAVVDKNNTSGFGTGKEKPLVAIYT-------QDREGHQVQSIAYSNDKGRTWTKYAG    158
Gdia    SGSLVPDPLNRSGLGSTDAPPLLAFHTSVFHDNPAHPDGTQAQSVSVSHDGGFTWRPYAH    173
        ***    .   .    *             :     :         :   :       *

                                        V                         VI
Bapi    G--ICCSPDL--VPESVRDEGRDFRDCRVFWDDDNSQLVMATTIGTRF--AFFRSVNGTS    248
Bmel    G--MCCSPDL--VPDSVRDGGRDFRDCRVFWDDDHSQLVMAATIGTRF--AFFRSLNGTS    204
MAL2    PVILN-TDGRTATTPAEIENAEWFRDPKIHWDALRGEWVCVIGRARYA--SFYTSTNLRD    227
Pure    PVIVN-TDGRAATTPAEIENAEWFRDPKIHWDTARGEWVCVIGRLRYA--AFYTSPNLRD    218
Mlae    EPVIP-GDGR----------RDFRDPKVVWDDERQRWVALIAERDRV--SFYTSPDLHR    254
Blic    EPVLP-NPDT----------VDFRDPKVIWDEEDDKWVMALAEGTKI--GFYESQNLKE    183
Sexf    DPVLP-NPGV----------ADFRDPKVIRDEDRGRWVMALAENDKI--GFYHSADLKS    218
Gdia    NPVLTLHPDS----------RQFRDPSVFWYQDGGCWIMTTVVGDAQLVKLYRSTDLLH    222
            :    .              ***  :          :          :: * :

                        VII       VIII            IX
Bapi    WDFLSSME-----GPGPLVECPNVMKLKIVDDHGNTLGHKWAILGAVQGDYPGGTQSHEC    303
Bmel    WEFLSSLE-----GPGPLVECPNVMKLKVLDGQGNTPGYKWAILGAVQGDYPGGTQSNEC    259
MAL2    WQWTSNFDYPN--HALGGIECPDLFEMTAGDG-----TRHWILAASMDAYG---VGLPMT    277
Pure    WTLRRNFDYPN--HALGGIECPDLFEITADDG-----TRHWILAASMDAYG---IGLPMT    268
Mlae    WTRTGEY--VN--AGIGTIECPDLFRLRADDG-----TTHWVMGVSANGYA---TNEPAT    302
Blic    WRYTSSF--QT--ENIGIIECPDLFKMRADDG-----TYKWVLGASANGKG---AGKPNT    231
Sexf    WTYVGGF--VH--DGIGVIECPDLFRITAGDG-----TVKWVLGASANGKG---SGLPNT    266
Bsub    WTYASEFGQDQ-GSHGGVWECPDLFELPVDGN---PNQKKWVMQVSVGNGA---VSGGSG    257
Gdia    WSFLSDFQPSGYRKPGMLWEMPTLVPLKLDGN---PRATRWVMIVSVNPWS---IAGGSG    276
        *             *  * :. :    ..        :*  :  :
```

Figure 7. Alignment of GH32 family enzymes. Letters with a green background correspond to the consensus sequence of conserved motifs of microbial FTases (GH68 family), red letters do not. Bapi = *B. apis* FTase, Bmel = *B. mellum* FTase, MAL2 = *M.* sp. AL-210 levan FTase, Pure = *Pa. ureafaciens* levan FTase, Mlae = *M. laevaniformans* levanase, Blic = *Ba. licheniformis* endolevanase, Sexf = *S. exfoliatus* levanbiohydrolase, Bsub = *Ba. subtilis* levanase, and Gdia = *G. diazotrophicus* levanase.

which suggests the presence of different linkage types. Overall, this reveals that fructans from *Bom bella* have highly complex molecular structures.

The molecular weight of fructans from *Bombella* is in the range of 10^6–10^7 Da as revealed by different analytical methods. Thus, the fructans are HMW polysaccharides, which are usually synthesized by GH68 enzymes (Srikanth et al. 2015, Jakob et al. 2019) and not by GH32 enzymes (Lammens et al. 2009, Alamäe et al. 2023).

Bombella FTases in comparison with other GH32 and GH68 family enzymes

The identified FTases of *B. apis* TMW 2.1884 and *B. mellum* TMW 2.1889 can be assigned to the GH32 family both phylogenetically (see the "Sequence analysis of the *Bombella* FTase" section and Fig. 5) and structurally (see the "Sequence analysis of the *Bombella* FTase" section and Fig. 6). To our knowledge, there is no other description of bacterial enzymes of the GH32 family involved in the formation of HMW fructans. In other

acetic acid bacteria, only levansucrases are known to catalyze the formation of HMW fructans (Jakob et al. 2019). The corresponding enzymes could be divided into two groups based on sequence differences, but all were assigned to the GH68 family.

All protein motifs found in the FTases of *B. apis* TMW 2.1884 and *B. mellum* TMW 2.1889 that have been associated with fructan formation (Velázquez-Hernández et al. 2009) lie in the N-terminal five-bladed β-propeller catalytic domain region shared by all GH32 and GH68 enzymes (see the "Sequence analysis of the *Bombella* FTase" section). However, since these motifs of the *Bombella* FTases do not exactly correspond to the given consensus sequences, their actual function cannot be determined with certainty. In order to clarify the actual influence of the corresponding motifs on the formation of HMW fructans, complex mutation studies would have to be carried out, as has already been done by Meng and Fütterer (2003) and Xu et al. (2022) for GH68 family enzymes.

Publikation: *Journal of Applied Microbiology*, 134, lxad268

As mentioned in the introduction, a major difference between GH68 and GH32 enzymes is the C-terminal domain of the GH32 enzymes consisting of two six-stranded β-sheets, which are composed of antiparallel β-strands forming a sandwich-like fold (Lammens et al. 2009). This structure has been linked to FTase activity in fungi, albeit only for the formation of fructo-oligosaccharides (FOS) (Trollope et al. 2015). Whether the C-terminal domains of the *Bombella* FTases play a role in the synthesis of the HMW fructans cannot be concluded with the current state of knowledge.

Future prospects

Apart from the open questions concerning fructan structures and catalysis mechanisms discussed in the previous sections, the discovery of the *Bombella* FTases has opened up numerous further research topics. A more detailed investigation of the heterologously expressed enzyme with regards to substrate specificity and enzyme kinetics could shed light on the actual function of the enzyme in *Bombella* strains possessing it. In addition, this could lead to the identification of potential applications. One application of the fructans, which can already be discussed, is the use as prebiotics in foods or in infant nutrition (Coussement 1999, Kaur and Gupta 2002). Due to the presence of three different types of glycosidic linkages (see the "Monosaccharide composition and glycosidic linkages" and "*Endo*-levanase hydrolysis and distribution of glycosidic linkages" sections) that prevent complete enzymatic hydrolysis, the *endo*-levanase hydrolysates of *Bombella* fructans contain a variety of low-molecular weight fructans and fructooligosaccharides and could therefore be particularly suitable as prebiotic food supplements.

Ethical approval

This research did not contain any studies involving animal or human participants, nor did it take place on any private or protected areas. No specific permissions were required for corresponding locations.

Supplementary data

Supplementary data is available at *JAMBIO Journal* online.

Conflict of interest: None declared.

Funding

Author contributions

Luca Härer (Conceptualization, Data curation, Investigation, Methodology, Visualization, Writing – original draft), Luise Ernst (Conceptualization, Data curation, Formal analysis, Investigation, Methodology, Visualization, Writing – original draft), Julia Bechtner (Conceptualization, Writing – review & editing), Daniel Wefers (Supervision, Writing – review & editing), and Matthias A. Ehrmann (Funding acquisition, Project administration, Supervision, Writing – review & editing)

Data availability

The data underlying this article are available in the article and in its online supplementary material.

References

Alamäe T, Ernits K, Hernández L *et al*. Chapter 4–Fructan enzymes in microbes and plants: structure, function, and product formation. In: Wimvan, EbruToksoy *The Book of Fructans*. Amsterdam, Netherlands, Elsevier Science 2023, 47–73.

Banguela A, Hernández L. Fructans: from natural sources to transgenic plants. *Biotecnología Aplicada* 2006;**23**:202–210.

Bertoni M, Kiefer F, Biasini M *et al*. Modeling protein quaternary structure of homo- and hetero-oligomers beyond binary interactions by homology. *Sci Rep* 2017;**7**:10480. https://doi.org/10.1038/s41598-017-09654-8.

Bienert S, Waterhouse A, de Beer TAP *et al*. The SWISS-MODEL Repository—new features and functionality. *Nucleic Acids Res* 2017;**45**:D313–9. https://doi.org/10.1093/nar/gkw1132.

Brandt JU, Jakob F, Behr J *et al*. Dissection of exopolysaccharide biosynthesis in *Kozakia baliensis*. *Microb Cell Fact* 2016;**15**:170. https://doi.org/10.1186/s12934-016-0572-x.

Cha J, Park NH, Yang SJ *et al*. Molecular and enzymatic characterization of a levan fructotransferase from *Microbacterium* sp. AL-210. *J Biotechnol* 2001;**91**:49–61. https://doi.org/10.1016/S0168-1656(01)00288-7.

Coussement PA. Inulin and oligofructose: safe intakes and legal status. *J Nutr* 1999;**129**:1412S–7S. https://doi.org/10.1093/jn/129.7.1412S.

Ernst L, Werner A, Wefers D. Influence of ultrasonication and hydrolysis conditions in methylation analysis of bacterial homoexopolysaccharides. *Carbohydr Polym* 2023;**308**:120643. https://doi.org/10.1016/j.carbpol.2023.120643.

Felsenstein J. Confidence limits on phylogenies: an approach using the bootstrap. *Evol* 1985;**39**:783. https://doi.org/10.2307/2408678.

Froger A, Hall JE. Transformation of plasmid DNA into *E. coli* using the heat shock method. *J Vis Exp* 2007;**6**:253.

Gottlieb HE, Kotlyar V, Nudelman A. NMR chemical shifts of common laboratory solvents as trace impurities. *J Org Chem* 1997;**62**:7512–5. https://doi.org/10.1021/jo971176v.

Guex N, Peitsch MC, Schwede T. Automated comparative protein structure modeling with SWISS-MODEL and Swiss-PdbViewer: a historical perspective. *Electrophoresis* 2009;**30**:S162–73. https://doi.org/10.1002/elps.200900140.

Gullo M, La China S, Falcone PM *et al*. Biotechnological production of cellulose by acetic acid bacteria: current state and perspectives. *Appl Microbiol Biotechnol* 2018;**102**:6885–98. https://doi.org/10.1007/s00253-018-9164-5.

Härer L, Hilgarth M, Ehrmann MA. Comparative genomics of acetic acid bacteria within the genus *Bombella* in light of beehive habitat adaptation. *Microorganisms* 2022;**10**:1058. https://doi.org/10.3390/microorganisms10051058.

Hundschell CS, Braun A, Wefers D *et al*. Size-dependent variability in flow and viscoelastic behavior of levan produced by *Gluconobacter albidus* TMW 2.1191. *Foods* 2020;**9**:192. https://doi.org/10.3390/foods9020192.

Jakob F, Gebrande C, Bichler RM *et al*. Insights into the pH-dependent, extracellular sucrose utilization and concomitant levan formation by *Gluconobacter albidus* TMW 2.1191. *Antonie Van Leeuwenhoek* 2020;**113**:863–73. https://doi.org/10.1007/s10482-020-01397-3.

Jakob F, Pfaff A, Novoa-Carballal R *et al*. Structural analysis of fructans produced by acetic acid bacteria reveals a relation to hydrocolloid function. *Carbohydr Polym* 2013;**92**:1234–42. https://doi.org/10.1016/j.carbpol.2012.10.054.

Publikation: *Journal of Applied Microbiology*, 134, lxad268

Jakob F, Quintero Y, Musacchio A *et al.* Acetic acid bacteria encode two levansucrase types of different ecological relationship. *Environ Microbiol* 2019;**21**:4151–65. https://doi.org/10.1111/1462-2920.14768.

Jensen SL, Diemer MB, Lundmark M *et al.* Levanase from *Bacillus subtilis* hydrolyses β-2,6 fructosyl bonds in bacterial levans and in grass fructans. *Int J Biol Macromol* 2016;**85**:514–21. https://doi.org/10.1016/j.ijbiomac.2016.01.008.

Kang HK, Seo MY, Seo ES *et al.* Cloning and expression of levansucrase from *Leuconostoc mesenteroides* B-512 FMC in *Escherichia coli*. *Biochim Biophys Acta* 2005;**1727**:5–15. https://doi.org/10.1016/j.bbaexp.2004.10.012.

Kaur N, Gupta AK. Applications of inulin and oligofructose in health and nutrition. *J Biosci* 2002;**27**:703–14. https://doi.org/10.1007/BF02708379.

Kumar S, Stecher G, Li M *et al.* MEGA X: molecular evolutionary genetics analysis across computing platforms. *Mol Biol Evol* 2018;**35**:1547–9. https://doi.org/10.1093/molbev/msy096.

Lammens W, Le Roy K, Schroeven L *et al.* Structural insights into glycoside hydrolase family 32 and 68 enzymes: functional implications. *J Exp Bot* 2009;**60**:727–40. https://doi.org/10.1093/jxb/ern333.

Liebl W, Brem D, Gotschlich A. Analysis of the gene for beta-fructosidase (invertase, inulinase) of the hyperthermophilic bacterium *Thermotoga maritima*, and characterisation of the enzyme expressed in *Escherichia coli*. *Appl Microbiol Biotechnol* 1998;**50**:55–64. https://doi.org/10.1007/s002530051256.

Martínez-Fleites C, Ortíz-Lombardía M, Pons T *et al.* Crystal structure of levansucrase from the Gram-negative bacterium *Gluconacetobacter diazotrophicus*. *Biochem J* 2005;**390**:19–27. https://doi.org/10.1042/BJ20050324.

Menéndez C, Hernández L, Banguela A *et al.* Functional production and secretion of the *Gluconacetobacter diazotrophicus* fructose-releasing exo-levanase (LsdB) in *Pichia pastoris*. *Enzyme Microb Technol* 2004;**34**:446–52. https://doi.org/10.1016/j.enzmictec.2003.11.018.

Meng G, Fütterer K. Structural framework of fructosyl transfer in *Bacillus subtilis* levansucrase. *Nat Struct Biol* 2003;**10**:935–41. https://doi.org/10.1038/nsb974.

Miller DL, Smith EA, Newton ILG. A bacterial symbiont protects honey bees from fungal disease. *mBio* 2021;**12**:e0050321. https://doi.org/10.1128/mBio.00503-21.

Ni D, Xu W, Bai Y *et al.* Biosynthesis of levan from sucrose using a thermostable levansucrase from *Lactobacillus reuteri* LTH5448. *Int J Biol Macromol* 2018;**113**:29–37. https://doi.org/10.1016/j.ijbiomac.2018.01.187.

Ni D, Xu W, Zhu Y *et al.* Inulin and its enzymatic production by inulosucrase: characteristics, structural features, molecular modifications and applications. *Biotechnol Adv* 2019;**37**:306–18. https://doi.org/10.1016/j.biotechadv.2019.01.002.

Parish AJ, Rice DW, Tanquary VM *et al.* Honey bee symbiont buffers larvae against nutritional stress and supplements lysine. *ISME J* 2022;**16**:2160–8. https://doi.org/10.1038/s41396-022-01268-x.

Paysan-Lafosse T, Blum M, Chuguransky S *et al.* InterPro in 2022. *Nucleic Acids Res* 2023;**51**:D418–27. https://doi.org/10.1093/nar/gkac993.

Poli A, Kazak H, Gürleyendağ B *et al.* High level synthesis of levan by a novel *Halomonas* species growing on defined media. *Carbohydr Polym* 2009;**78**:651–7. https://doi.org/10.1016/j.carbpol.2009.05.031.

Pons T, Naumoff DG, Martínez-Fleites C *et al.* Three acidic residues are at the active site of a beta-propeller architecture in glycoside hydrolase families 32, 43, 62, and 68. *Proteins* 2004;**54**:424–32. https://doi.org/10.1002/prot.10604.

Porras-Domínguez JR, Ávila-Fernández Á, Miranda-Molina A *et al.* *Bacillus subtilis* 168 levansucrase (SacB) activity affects average levan molecular weight. *Carbohydr Polym* 2015;**132**:338–44. https://doi.org/10.1016/j.carbpol.2015.06.056.

Porras-Domínguez JR, Ávila-Fernández Á, Rodríguez-Alegría ME *et al.* Levan-type FOS production using a *Bacillus licheniformis* endole-

vanase. *Process Biochem* 2014;**49**:783–90. https://doi.org/10.1016/j.procbio.2014.02.005.

Saitou N, Nei M. The neighbor-joining method: a new method for reconstructing phylogenetic trees. *Mol Biol Evol* 1987;**4**:406–25.

Song E-K, Kim H, Sung H-K *et al.* Cloning and characterization of a levanbiohydrolase from *Microbacterium laevaniformans* ATCC 15953. *Gene* 2002;**291**:45–55. https://doi.org/10.1016/S0378-1119(02)00630-3.

Song K, Bae K, Lee Y *et al.* Characteristics of levan fructotransferase from *Arthrobacter ureafaciens* K2032 and difructose anhydride IV formation from levan. *Enzyme Microb Technol* 2000;**27**:212–8. https://doi.org/10.1016/S0141-0229(00)00135-6.

Srikanth R, Reddy CHSSS, Siddartha G *et al.* Review on production, characterization and applications of microbial levan. *Carbohydr Polym* 2015;**120**:102–14. https://doi.org/10.1016/j.carbpol.2014.12.003.

Studer G, Rempfer C, Waterhouse AM *et al.* QMEAND is Co-distance constraints applied on model quality estimation. *Bioinf* 2020;**36**:1765–71.

Sweet DP, Shapiro RH, Albersheim P. Quantitative analysis by various g.l.c. response-factor theories for partially methylated and partially ethylated alditol acetates. *Carbohydr Res* 1975;**40**:217–25. https://doi.org/10.1016/S0008-6215(00)82604-X.

Trollope KM, van Wyk N, Kotjomela MA *et al.* Sequence and structure-based prediction of fructosyltransferase activity for functional sub-classification of fungal GH32 enzymes. *FEBS J* 2015;**282**:4782–96. https://doi.org/10.1111/febs.13536.

Ua-Arak T, Jakob F, Vogel RF. Characterization of growth and ex-opolysaccharide production of selected acetic acid bacteria in buckwheat sourdoughs. *Int J Food Microbiol* 2016;**239**:103–12. https://doi.org/10.1016/j.ijfoodmicro.2016.04.009.

Ua-Arak T, Jakob F, Vogel RF. Fermentation pH modulates the size distributions and functional properties of *Gluconobacter albidus* TMW 2.1191 levan. *Front Microbiol* 2017;**8**:807. https://doi.org/10.3389/fmicb.2017.00807.

van Hijum SAFT, Kralj S, Ozimek LK *et al.* Structure–function relationships of glucansucrase and fructansucrase enzymes from lactic acid bacteria. *Microbiol Mol Biol Rev* 2006;**70**:157–76. https://doi.org/10.1128/MMBR.70.1.157-176.2006.

van Hijum SAFT, van Geel-Schutten GH, Rahaoui H *et al.* Characterization of a novel fructosyltransferase from *Lactobacillus reuteri* that synthesizes high-molecular-weight inulin and inulin oligosaccharides. *Appl Environ Microb* 2002;**68**:4390–8. https://doi.org/10.1128/AEM.68.9.4390-4398.2002.

Velázquez-Hernández ML, Baizabal-Aguirre VM, Bravo-Patiño A *et al.* Microbial fructosyltransferases and the role of fructans. *J Appl Microbiol* 2009;**106**:1763–78. https://doi.org/10.1111/j.1365-2672.2008.04120.x.

Verspreet J, Holmgaard Hansen A, Dornez E *et al.* Liquid chromatography/mass spectrometry analysis of branched fructans produced in vitro with 13C-labeled substrates. *Rapid Commun Mass Spectrom* 2014;**28**:2191–200. https://doi.org/10.1002/rcm.7013.

Visnapuu T, Mardo K, Mosoarca C *et al.* Levansucrases from *Pseudomonas syringae* pv. tomato and *P. chlororaphis* subsp. *aurantiaca*: substrate specificity, polymerizing properties and usage of different acceptors for fructosylation. *J Biotechnol* 2011;**155**:338–49. https://doi.org/10.1016/j.jbiotec.2011.07.026.

Waterhouse A, Bertoni M, Bienert S *et al.* SWISS-MODEL: homology modelling of protein structures and complexes. *Nucleic Acids Res* 2018;**46**:W296–303. https://doi.org/10.1093/nar/gky427.

Xu W, Ni D, Hou X *et al.* Crystal structure of levansucrase from the Gram-negative bacterium *Brenneria* provides insights into its product size specificity. *J Agric Food Chem* 2022;**70**:5095–105. https://doi.org/10.1021/acs.jafc.2c01225.

Xu W, Ni D, Zhang W *et al.* Recent advances in levansucrase and inulosucrase: evolution, characteristics, and application. *Crit Rev Food Sci Nutr* 2019;**59**:3630–47. https://doi.org/10.1080/10408398.2018.1506421.

Publikation: *Journal of Applied Microbiology*, 134, lxad268

Glycoside hydrolase family 32 enzymes from *Bombella* spp. catalyze the formation of high-molecular weight fructans from sucrose **13**

Yin Y, Mao X, Yang J *et al*. dbCAN: a web resource for automated carbohydrate-active enzyme annotation. *Nucleic Acids Res* 2012;**40**:W445–51. https://doi.org/10.1093/nar/gks479.

Yokota A, Kondo K, Nakagawa M *et al*. Production of levanbiose by a levan-degrading enzyme from *Streptomyces exfoliatus* F3–2. *Biosci Biotechnol Biochem* 1993;**57**:745–9. https://doi.org/10.1271/bbb.57.745.

Zhang H, Yohe T, Huang L *et al*. dbCAN2: a meta server for automated carbohydrate-active enzyme annotation. *Nucleic Acids Res* 2018;**46**:W95–W101. https://doi.org/10.1093/nar/gky418.

Zhang W, Xu W, Ni D *et al*. An overview of levan-degrading enzyme from microbes. *Appl Microbiol Biotechnol* 2019;**103**:7891–902. https://doi.org/10.1007/s00253-019-10037-4.

Publikation: *Journal of Applied Microbiology*, 134, lxad268

S1:

Publikation: *Journal of Applied Microbiology*, 134, lxad268

S2: GH 32 family enzyme gene of *B. apis* TMW 2.1884 with the locus tag DTI93_RS00530 in the genome NZ_QORR01000001:

>21884_B_apis_DTI93_RS00530

ATGACGTCGGATGATGATCGTGAGCCTTCCGGCAAGGATGTCTTCATCGACAAGAATAGCAGTCTTTCCGGCACGTACTGGTCCGGAAGTGTG

TGGGTGGATGAAGAAGACAGGCTGGGCCGTGGTCGGGGCAGTGTCTATTATTACATATCTGGCCCGGCCCCTGTCTTGCAGGCCATATATCTC

CTGGTGGCGAAGAGGCTCGGCGAGGTTCCGTACAATTTGGGGATATGCTGTTCTCCTGATCTCGTGCCGGAATCCGTGCGTGATGAGGGGCG

GGACTTCAGGGACTGCCGTGTATTCTGGGATGACGATAACAGCCAGCTGGTGATGGCAACGACGATCGGAACACGATTTGCGTTCTTTCGCAG

CGTTAATGGGACGTCATGGGATTTTCTTTCCAGCATGGAAGGACCAGGACCGCTGGTGGAGTGCCCCAATGTCATGAAGCTGAAAATCGTCGA

TGATCATGGGAATACTCTGGGACATAAGTGGGCGATACTGGGAGCCGTGCAGGGTGATTATCCTGGTGGGACCCAGTCGCATGAATGCTGTGT

GGCTTGGTTGGGGGCGTGGGATGGCACGCAGTTTATTCCGGATGAGCAGGCCAAGGCCATCCCTCTGGATTACGGGCCGGATTCCTATGCGA

CCGTGGCAGGCCGCAATGGCAGGTCGACCTATGTGGGGTGCTGGCTGGGTAATTGGGATTACTCGCTTCTGCCTTCACCCTATAAGGGTTTCC

AGAACATCCAGTCCTATCCCAGGGCTTGCTGGATACAGACTGACTACAGTGGCCGGCAGAAAGTCTACACATGTCCTGTGGAAAAAGCGGATG

GTATCACTGGGATAGGGGGCCCCAGGCAGACGATAGGTGGTGAGGGCAATCCTGATTTTGCGTCAGATGAGGTAGAGACGTCGGACTGCTATC

GTCTGGATGTTGTGCTGGATCAGGTTGATGGTCACTGGCCAGAGGAAGTACGCATATCCGTCAATAAGGGCCGGGTGGAAGGCACGGAGTAC

AGTACCGACCTGATCATCTACCGGAGCGGTCAGATCACGTTTGACAGGACCAGAGCAGGCATCCTGTATCCCGGCTATCCCAATGAACCACCT

GAGGGCTGGGGAAAGACGTATTCCATTCCGGCAGGTCTGAAGAGCAATGCGACTTCCAACATGATCATCACCATCCTGATCGATACCAGCAGC

CTGGAAGTGTTCATCAATGGAGGCCAGACGTCCCTGACAGGGCTGGTCTTTCCACCGAAGGGATGTACGGGGGGTCAACATTACGTCAACGCA

GCCTGTTCATGTGTCCGTTTCGACAAGTGATTATTGA

Extended version (additional bases are marked in yellow):

>21884_B_apis_ DTI93_RS00530_extended

ATGGTCACGATTCTTATTTTTGATAATATTTGCCGTAGATGGCACAATTTTTATGGCAACGCTCTCATGAGACGGGGCCATGTGTGCCCTATCGGT

ACTGTCATCGGATTTTTTCGCGAAAGGTTTTTGTCTATGACGGACCTGTCCAATGTTTCGGTAGCGTATTATCCTAAGAGGCATCTGGCTCCTGT

ACCGGTCCCCGGCAGACACAAATGGCAGAATGACGGTCAAAACTACGTTTATGACCGGAAGGCCAGACTGTGGAGGACGTGGGCTCTGGGAA

ACCCGGAATGGACTCCTAACAGCGGTTTTCCAACGACGTCGTGGATTTCTTATAGCGGCCCTACCATCGATGCGATGACGTCGGATGATGATCG

TGAGCCTTCCGGCAAGGATGTCTTCATCGACAAGAATAGCAGTCTTTCCGGCACGTACTGGTCCGGAAGTGTGTGGGTGGATGAAGAAGACAG

GCTGGGCCGTGGTCGGGGCAGTGTCTATTATTACATATCTGGCCCGGCCCCTGTCTTGCAGGCCATATATCTCCTGGTGGCGAAGAGGCTCGG

CGAGGTTCCGTACAATTTGGGGATATGCTGTTCTCCTGATCTCGTGCCGGAATCCGTGCGTGATGAGGGGCGGGACTTCAGGGACTGCCGTG

TATTCTGGGATGACGATAACAGCCAGCTGGTGATGGCAACGACGATCGGAACACGATTTGCGTTCTTTCGCAGCGTTAATGGGACGTCATGGG

ATTTTCTTTCCAGCATGGAAGGACCAGGACCGCTGGTGGAGTGCCCCAATGTCATGAAGCTGAAAATCGTCGATGATCATGGGAATACTCTGGG

ACATAAGTGGGCGATACTGGGAGCCGTGCAGGGTGATTATCCTGGTGGGACCCAGTCGCATGAATGCTGTGTGGCTTGGTTGGGGGCGTGGG

ATGGCACGCAGTTTATTCCGGATGAGCAGGCCAAGGCCATCCCTCTGGATTACGGGCCGGATTCCTATGCGACCGTGGCAGGCCGCAATGGC

AGGTCGACCTATGTGGGGTGCTGGCTGGGTAATTGGGATTACTCGCTTCTGCCTTCACCCTATAAGGGTTTCCAGAACATCCAGTCCTATCCCA

GGGCTTGCTGGATACAGACTGACTACAGTGGCCGGCAGAAAGTCTACACATGTCCTGTGGAAAAAGCGGATGGTATCACTGGGATAGGGGGC

CCCAGGCAGACGATAGGTGGTGAGGGCAATCCTGATTTTGCGTCAGATGAGGTAGAGACGTCGGACTGCTATCGTCTGGATGTTGTGCTGGAT

CAGGTTGATGGTCACTGGCCAGAGGAAGTACGCATATCCGTCAATAAGGGCCGGGTGGAAGGCACGGAGTACAGTACCGACCTGATCATCTAC

CGGAGCGGTCAGATCACGTTTGACAGGACCAGAGCAGGCATCCTGTATCCCGGCTATCCCAATGAACCACCTGAGGGCTGGGGAAAGACGTA

TTCCATTCCGGCAGGTCTGAAGAGCAATGCGACTTCCAACATGATCATCACCATCCTGATCGATACCAGCAGCCTGGAAGTGTTCATCAATGGA

GGCCAGACGTCCCTGACAGGGCTGGTCTTTCCACCGAAGGGATGTACGGGGGGTCAACATTACGTCAACGCAGCCTGTTCATGTGTCCGTTTC

GACAAGTGATTATTGA

10 Lebenslauf

Luise Sophia Ernst

Seit 11. 2019	Promotionsstudentin und wissenschaftliche Mitarbeiterin an der Martin-Luther-Universität Halle-Wittenberg (MLU) Naturwissenschaftliche Fakultät II Institut für Chemie (Abteilung Lebensmittelchemie)
03.-10. 2019	Masterarbeit am Karlsruher Institut für Technologie (KIT), Institut für Angewandte Biowissenschaften (Abteilung für Lebensmittelchemie und Phytochemie) zum Thema: Herstellung und Verwendung rekombinanter Enzyme zur Modifikation und Analyse von Pektinen
2013-2019	Studium der Lebensmittelchemie am KIT (Abschluss: Master of Science)
2013	Abitur an der Winfriedschule Fulda

11 Danksagung